

The Synthesis of Selective Immobilized Ligands for the Extraction of Toxic Metal Ions from Water Doped with these Contaminants

by

Bernardus Francis Barnard

Dissertation presented for the degree of

Doctor of Philosophy

(Chemistry)

at

STELLENBOSCH UNIVERSITY



Promoter: Dr. Robert. C. Luckay (University of Stellenbosch)

Faculty of Science

Department of Chemistry and Polymer Science

Co-promoters: Prof. Leslie F. Petrik & Dr. Alexander Nechaev (University of the Western Cape)

Faculty of Science

Department of Chemistry

December 2014

Declaration

By submitting this dissertation electronically, I declare that the entirety of the work contained therein is my own, original work, that I am the sole author thereof (save to the extent explicitly otherwise stated), that reproduction and publication thereof by Stellenbosch University will not infringe any third party rights and that I have not previously in its entirety or in part submitted it for obtaining any qualification.

Date: 10 November 2014

Abstract

In this study, two novel ligands were synthesized and separately two crown ether derivatives were all immobilized onto four different silica substrates. These immobilized ligand systems were used to extract six different metal and metalloid ions in water. The extraction capacity of the different immobilized ligands was compared with each other to determine whether the substrates had any influence on the extraction capabilities of these ligands. After the extraction experiments, recovery of the immobilized ligands was attempted by re-protonating the ligands so as to displace the metal ions.

Two free parent ligands, 1,4,7-tris-[(*S*)-2-hydroxypropyl]-1,4,7-tri-azacyclodecane (THTD) and 1,4,8-tris-[(*S*)-2-hydroxypropyl]-1,4,8-tri-azacycloundecane (THTUD), were synthesized. Previous formation constant data indicated that THTD and THTUD form very stable complexes with Cd^{2+} which should make these ligands ideal for the extraction of Cd^{2+} . These two ligands are less symmetric due to the carbon bridges between the nitrogen atoms, which differ in length. This gives the ligands the special feature that they can form five - and six membered rings during complexation with the metal ions. The ligands were fully characterized by NMR, mass spectrometry and elemental analysis.

Characterization of the silica substrates was done using BET, low angle X-ray diffraction and FTIR. MCM-41 has the highest surface area, followed by SBA-15, Si gel (60 Å) and HMS. Although MCM-41 has the largest surface area, it was not the best support to use. HMS and Si gel (60 Å) have the smallest and almost identical surface areas. Yet, Si gel (60 Å) was a far better support to use than HMS, and even better than MCM-41. The worst supports were SBA-15 and HMS.

A spacer, 3-Glycidyloxypropyl-trimethoxysilane (glymo), was introduced to immobilize the ligands to the silica substrates. Solid state NMR and FTIR analysis confirmed that the spacer could indeed be successfully immobilized on the various silica supports.

The immobilized ligands were fully characterized with the use of solid state NMR and FTIR. The thermal stability of the immobilized ligands was determined by means of TGA. The immobilized ligands are stable up to 200°C where after they started to disintegrate.

According to literature, 15-crown-5 and 18-crown-6 are suitable ligands for the extraction of Sr^{2+} and UO_2^{2+} . Since these ligands were to be immobilized, (2-aminomethyl)-15-crown-5

and (2-aminomethyl)-18-crown-6 were used because of the amino group that can be used as an anchor for immobilization. To immobilize these ligands onto the activated silica substrates, two methods were used: 1) directly onto the substrate by using the amino groups at the end of the carbon arm and 2) by means of the glymo spacer which connects the (2-aminomethyl)-15-crown-5 and (2-aminomethyl)-18-crown-6 to the silica substrates. The immobilization was confirmed and the ligand-substrate moiety fully characterized by solid state NMR and FTIR. The thermal stability of the immobilized crown ethers was determined by means of TGA as stable up to 200°C where after they disintegrated.

Extraction experiments were conducted at 25°C and atmospheric pressure. The extractions were done at pH values of 4.5 and 5.9. The extraction capacity of the immobilized ligands was determined by ICP analysis. As expected, the extraction done at pH 5.9 was significantly better than at pH 4.5. Cr^{6+} was the best-extracted metal ion. The best extraction results were obtained with Si gel (60 Å) as support. It was also noticeable that the extraction capacity increased with a spacer added to the support, except for the extraction of UO_2^{2+} . Better extraction for the uranyl was obtained using the 15-crown-5 and 18-crown-6 immobilized directly onto the supports, rather than with a spacer added.

Recovery of the metal ions and the immobilized ligands was attempted, but without success. This aspect will be examined again in future work.

In conclusion, ligands were successfully synthesized and immobilized. These immobilized ligands produced moderate extraction results with a number of metal ions from aqueous solution.

Opsomming

Hierdie studie behels die sintetisering van 2 nuwe ligande en die immobilisering daarvan, te same met 2 kroon eters, op vier verskillende silika substrate. Die geïmmobiliseerde ligande is gebruik vir die ekstraksie van verskillende metaal - en metaloïed ione uit water. Die ekstraksie kapasiteit van die onderskeie geïmmobiliseerde ligande is vergelyk om te bepaal of die substrate 'n uitwerking op die ekstraksie vermoë van die ligande het. Herwinnings eksperimente is uitgevoer deur die verplasing van die geadsorbeerde metaal ione deur middel van reprotonasie van die ligande.

Twee nuwe azamakrosikliese basis ligande, 1,4,7-tris-[(*S*)-2-hidroksipropiel]-1,4,7-tri-azasiklodekaan (THTD) en 1,4,8-tris-[(*S*)-2-hidroksipropiel]-1,4,8-tri-azasikloundekaan (THTUD), is gesintetiseer. Vormings konstante data dui daarop dat THTD en THTUD uiters stabiele komplekse met Cd^{2+} vorm wat hierdie ligande dus geskik behoort te maak vir die ekstraksie van Cd^{2+} . Die twee ligande toon ook 'n mindere mate van simmetrie as gevolg van die verskillende lengtes van die koolstof brê tussen die stikstof atome. Hierdie eienskap verskaf aan die ligande die moontlikheid om beide vyf- en sesledige ringe vorm tydens kompleksering met die metaal ione. Die ligande is ten volle gekarakteriseer deur middel van KMR-metings, massa-spektroskopie en element analise.

Karakterisering van die silika substrate [Si gel (60 Å), MCM-41, SBA-15, and HMS] sluit in BET, lae hoek X-straaldiffraksie en FTIR. MCM-41 het die grootste oppervlakte, gevolg deur SBA-15, Si gel (60 Å) en HMS. Ten spyte van die feit dat MCM-41 die grootste oppervlakte het, was dit egter nie die beste substraat om te gebruik nie. Die interne areas van die uiters groot porie-oppervlaktes van MCM-41 is nie toeganklik vir immobilisering nie a.g.v. die uiter klein porie-openinge. Si gel (60 Å) en HMS het die kleinste oppervlak areas. Si gel (60 Å) is 'n baie beter substraat om te gebruik as HMS, en selfs ook beter as MCM-41 aangesien die totale oppervlakte van die Si gel (60 Å) gebruik kan word. Die mees ongeskikte substrate was SBA-15 en HMS. Die alreeds klein oppervlak areas word verder “verklein” a.g.v. die klein porie openinge wat die interne oppervlakte van die porieë ontoeganklik maak.

'n Verbinder, 3-Glysidieoksiopropiel-trimetoksisilaan (glymo) is gebruik om die ligande op die silika substrate te immobiliseer. Vaste toestand KMR en FTIR analise het bevestig dat die verbinder suksesvol geïmmobiliseer is op die onderskeie silika substrate. Die

geïmmobiliseerde aza makrosikliese ligande is ten volle gekarakteriseer deur vaste toestand KMR en FTIR. Die termiese stabiliteit is bepaal d.m.v. GTA en die geïmmobiliseerde ligande is stabiel tot 250°C.

Die basis ligande 15-kroon-5 en 18-kroon-6 is uiters geskik vir die ekstraksie van Sr^{2+} en UO_2^{2+} . Om hierdie kroon eters te immobiliseer, is (2-aninometiel)-15-kroon-5 en (2-aninometiel)-18-kroon-6 gebruik. Die amino groep dien as anker vir die immobilisering. Twee metodes van immobilisering op silika is gebruik: 1) direkte immobilisering op die substraat en 2) immobilisering d.m.v. die glymo verbinder. Die immobilisering is bevestig en die ligand-substraat funksionel groep is gekarakteriseer d.m.v. vaste toestand KMR en FTIR. Die termiese stabiliteit van die geïmmobiliseerde kroon eters is bepaal d.m.v. GTA en is stabiel tot 200°C.

Ekstraksie eksperimente is uitgevoer by 25°C en atmosferiese druk. Die ekstraksies is uitgevoer by pH waardes van 4.5 en 5.9. Die adsorpsie kapasiteit van die geïmmobiliseerde ligande is bepaal d.m.v. IGP analise. Soos verwag is die ekstraksie by pH 5.9 beter as by pH 4.5. Cr^{6+} ekstraksie was die hoogste met al die die ligande geïmmobiliseer op die onderskeie substrate. Si gel (60 Å) was die beste substraat om te gebruik. Die ekstraksie kapasiteit van al die metaal ione het verbeter met die toevoeging van 'n verbinder, behalwe vir UO_2^{2+} . Beter ekstraksie van die UO_2^{2+} is verkry met die gebruik van die kroon eters wat direk op die substrate geïmmobiliseer is, eerder as met 'n verbinder toegevoeg. Herwinning van die metaal ione en die ligande is probeer deur standard filtrasie. Na die filtrasie is die geïmmobiliseerde ligande en substrate met water gewas. Die filtreerpapier en ligande is met HNO_3 behandel, maar van die metaal ione het egter op die filtreer papier agter gebly en die IGP resultate het 'n hoër herwinning getoon as wat tydens die ekstraksie verkry is. Hierdie aspek sal weer in die toekoms ondersoek moet word.

Die ligande is suksesvol gesintetiseer en geïmmobiliseer. Hierdie geïmmobiliseerde ligande toon gemiddelde ekstraksie resultate met 'n aantal metaal ione uit waterige medium by 'n pH van 5.9.

To my Parents

ID & Marie Barnard

And my sisters

Alet, Esther and Annamarie

Acknowledgements

I now realized that doing a PhD is definitely not for the fainthearted or the lazy, for it is one of the hardest things I've done up to now. I am in the fortunate position to have had the opportunity to complete this PhD, but I realize that this would not have been possible without the help of colleagues, friends and family. Therefore I would like to acknowledge and thank the following people for their invaluable contribution to this thesis.

I would like to thank my supervisor, Dr R. Luckay, for giving me the opportunity to pursue my dreams, for all his support, guidance, inspiration, encouragement. What I have learned from you is much more than just how to conduct research. When there were problems, you taught me how to calmly approach, analyze and solve it. This way of doing things was not only applicable in my work, but also outside the lab.

Secondly I would like to acknowledge my co-promoters, Prof L. Petrik and Dr. A. Nechaev for all their input, support and encouragement. Thank you for your positive attitude towards me, for accepting me into your ENS groups at UWC and for supporting my work in everyway. I really enjoyed working with you and I wish that one day, we might work together again.

Thank you to the entire ENS group of the University of the Western Cape for making me feel welcome and making me one of the group. I would like to single out Dr. Zeboneni Gondongwana for synthesizing and supplying the different silica supports that was used in this study.

I would also like to express my gratitude towards CAF (the Central Analytical Facility) here at the University of Stellenbosch for the analysis that they performed (NMR, ICP-MS, BET, XRD, TGA and SEM).

I would like to thank Eric Ward for all the glassware that he made for me and also for being a very good friend.

Thank you to my family. Although they did not always understand my work, they were always encouraging and supporting me. Finally my parents can stop worrying about me, for they provided me with an excellent education.

I wish to thank Markus and Lizbé for their friendship during all my trials and tribulations. I would also like to thank all the other people (Jantjie, Liezel and Zandr ) who assisted me in one way or another.

Finally I would like to thank the NRF and UWC for financial assistance. I have no choice but to single out Prof. Leslie Petrik for supporting me financially when things were really tight. A big word of thanks must also go to Me. Erinda Cooper who worked tirelessly to make sure my bursaries were paid on time.

Presentations

Workshop on the NRF Flagship Programme: Nanotechnology for Water Treatment, Stellenbosch University, Stellenbosch, April 2011, The Synthesis of Highly Selective Immobilized Ligands for Extraction of Toxic Metal Ions from Waste Water and Brine

11th annual UNESCO / IUPAC workshop and conference on functional polymeric materials & composites, Stellenbosch University, Stellenbosch, April 2011, The Synthesis of Highly Selective Immobilized Ligands for Extraction of Toxic Metal Ions from Waste Water and Brine, BF Barnard (US), RC Luckay(US), L Petrik(UWC) and A Nechaev(UWC)

South African Chemical Institute (SACI), Cape Town, August, 2009, The Synthesis of Highly Selective Ligands, Immobilized on Si Supports, for the Selective Extraction of Toxic Metal Ions from Waste Water and Brine, BF Barnard (US), RC Luckay(US), L Petrik(UWC) and A Nechaev(UWC)

Industrial Workshop on the Treatment of Waste Water, Johannesburg, March 2010

Radiation Safety Training Course, Johannesburg, Feb 2010

Abbreviations

223	1,4,7,-triazacyclodecane
332	1,4,8,-triazacycloundecane
15-c-5	(2-aminomethyl)-15-crown-5
18-c-6	(2-aminomethyl)-18-crown-6
Å	Ångstrom (1×10^{-10} m)
APMS	3-Aminopropyltrimethoxysilane
APTES	3-Aminopropyltriethoxysilane
BAL	British anti-Lewisite
BET	Brunauer, Emmett and Teller (adsorption of gas molecules on a solid surface)
BTP	(2,6-di(5,6-dipropyl-1,2,4-triazin-3-yl)pyridine)
CAF	Central Analytical Facility
CTA	cyclamtetraacetate
CTAB	Cethyl trimethylammonium bromide
Cyclam	14-ane-N ₄
DCH18C6	dicyclohexano-18-crown-6
DCH30C10	dicyclohexano-30-crown-10
DtBuCH18C6	4,4,5-di-(t-butyl)dicyclohexo)-18-crown-6
DETA	1,4,7-triazacyclodecane-N,N',N''-triacetic acid
DEHPA	Organophosphoric acid
DNA	Deoxyribonucleic acid
EDTA	Ethylenediaminetetraacetate
Emim ⁺ Tf ₂ N ⁻	1-Methyl-3-ethylimidazolium bis(trifluoromethylsulfonyl)imide
FTIR	Fourier Transform Infra Red
Glymo	3-Glycidyloxypropyl-trimethoxysilane
HLRLW	High Level Radioactive Liquid Waste
ICP-MS	Inductively Coupled Plasma Mass Spectrometry
IL	Ionic Liquid
ISPE	Inorganic Solid-phase Extractant
MIBK	isobutylmethylketone
MRLW	Medium Radioactive Liquid Waste
NMR	Nuclear Magnetic Resonance
NOTA	1,4,7-triazacyclononane-N,N',N''-triacetic acid

Omim ⁺ Tf ₂ N ⁻	1-Methyl-3-octylimidazolium bis(trifluoromethyl-sulfonyl)imide
SEM.....	Scanning Electron Microscopy
SHAB	Soft-Hard Acid-Base
SPE	Solid phase extraction
TACN	1,4,7-triazacyclononane
TBAI.....	tetrabutylammoniumiodide
TETA.....	1,4,8,11-tetraazacyclotetradecane-N,N',N'',N'''-tetraacetic acid
TGA.....	Thermal Gravimetric Analysis
THEC	tetrakis(2-hydroxyethyl)cyclam
THETAC	1,4,7-tris-(2-hydroxyethyl)-1,4,7-triazacyclononane
THTD	1,4,7-tris-[(S)-2-hydroxypropyl]-1,4,7,-triazacyclodecane
THTUD	1,4,8-tris-[(S)-2-hydroxypropyl]-1,4,8,-triazacycloundecane
TiBOGA	N,N,N',N',-tetra-isobutyl-3-oxa-glutaramide
TMC	tetramethylcyclac
TOPO	Tri- <i>n</i> -octylphosphine oxide
TPEN.....	<i>N,N,N',N'</i> -tetrakis(2-pyridylmethyl)ethylenediamine
UWC.....	University of the Western Cape
XRD	X-Ray Diffraction

Table of Contents

Abstract	iii
Opsomming	vi
Acknowledgements	ix
Presentations	xi
Abbreviations	xii
Table of Contents	xiv
Addendums	xix
List of Figures	xix
List of Tables	xxiii
Chapter 1 <i>Introduction: Problem Statement and Aims</i>	1
1.1 Rationale	1
1.2 Problem Statement and Research Questions	1
1.3 Aims and Objectives	2
1.4 Scope & Limitations	4
1.5 Research Approach	5
Chapter 2 <i>Literature Review</i>	7
2.1 General Introduction	7
2.2 Toxic Elements in Waste Water	12
2.2.1. Chromium (Cr^{6+})	12
2.2.2. Arsenic (As^{5+})	13
2.2.3. Strontium (Sr^{2+})	13
2.2.4. Cadmium (Cd^{2+})	14
2.2.5. Mercury (Hg^{2+})	16
2.2.6. Uranium (U^{6+})	16
2.3 A Brief Overview of Macrocyclic Ligands	18
2.3.1. A short history of macrocyclic ligands	19
2.3.2. General applications of macrocyclic ligands	19
2.3.3. Selectivity of macrocyclic ligands	21
2.3.3.1. <i>Ligand design</i>	21
2.3.3.2. <i>Metal ion selectivity of crown ethers (oxygen donors)</i>	24

2.3.3.3.	<i>Metal ion selectivity of azamacrocyclic ligands (nitrogen donors)</i>	27
2.4	Stability of Metal Complexes	28
2.5	The Chelate and Macrocyclic Effect.....	31
2.6	Silica as an Immobilization Substrate	36
2.7	Conclusion	42
Chapter 3	<i>The Synthesis and Immobilisation of the Macrocyclic Ligands</i>	48
3.1.	Introduction.....	48
3.2.	Methods and Pathways of Synthesis.....	48
3.2.1.	Template synthesis	48
3.2.2.	High dilution synthesis.....	49
3.2.3.	Direct synthesis	50
3.2.4.	Silica as an immobilization substrate	50
3.2.4.1	<i>Si gel (60 Å)</i>	51
3.2.4.2	<i>MCM-41</i>	51
3.2.4.3	<i>SBA-15</i>	52
3.2.4.4	<i>HMS</i>	52
3.3.	Experimental.....	52
3.3.1.	Materials.....	52
3.3.2.	Instrumentation for analysis	53
3.3.2.1	<i>FTIR</i>	53
3.3.2.2	<i>NMR</i>	53
3.3.2.3	<i>X-ray diffraction</i>	54
3.3.2.4	<i>BET</i>	55
3.3.2.5	<i>TGA</i>	56
3.3.3.	The direct immobilization of 15-C-5 and 18-C-6 to different silica substrates	56
3.3.4.	The immobilization of the glymo spacer to different silica substrates ...	57
3.3.5.	The immobilisation of 15-c-5 and 18-c-6 to different substrates by means of the glymo spacer	58
3.3.6.	The synthesis of 223 and 332.....	58
3.3.7.	The immobilisation of 223 and 332 to different silica substrates by means of the glymo spacer	58

3.3.8.	Addition of the pendant arms to the immobilised 223 and 332 to create immobilised THTD and THTUD	59
3.4.	Results and Discussion	61
3.4.1.	Powder X-ray diffraction of the various silica supports	61
3.4.1.1	<i>MCM-41</i>	61
3.4.1.2	<i>HMS</i>	62
3.4.1.3	<i>SBA-15</i>	62
3.4.1.4	<i>Si gel (60 Å)</i>	63
3.4.2.	FTIR spectra.....	64
3.4.2.1	<i>Spectra of the direct immobilisation of the crown ethers</i>	64
3.4.2.2	<i>Spectra of the immobilized crown ethers by means of the glymo spacer</i>	65
3.4.2.3	<i>Spectra of the immobilized azamacrocycles by means of the glymo spacer</i>	66
3.4.3.	NMR.....	67
3.4.3.1	<i>The solid state NMR spectra of the crown ethers, directly immobilized on the silica supports</i>	68
3.4.3.2	<i>The solid state NMR spectrum of the glymo spacer immobilized on the silica supports</i>	69
3.4.3.3	<i>The solid state NMR spectra of the crown ethers immobilized on the silica supports with the glymo spacer</i> ...	70
3.4.3.4	<i>The solid state NMR spectra of the aza crown ethers immobilized on the silica supports with the glymo spacer</i> ...	70
3.4.4.	BET results of the silica supports.....	71
3.4.4.1	<i>Surface area determination and comparison of the four silica supports</i>	71
3.4.4.2	<i>Pore volume determination and the comparison between the four silica supports</i>	74
3.4.4.3	<i>Determination of the average pore volume of the different silica supports</i>	76
3.4.5.	TGA.....	78
3.4.5.1	<i>TGA curve of the directly immobilized crown ethers</i>	78
3.4.5.2	<i>TGA curve of the immobilized crown ethers by means of a spacer</i>	79

3.4.5.3	<i>TGA curve of the immobilized aza crown ethers by means of a spacer</i>	80
3.4.6.	Elemental Analysis.....	81
3.4.6.1	<i>The elemental analysis of the directly immobilized 15-crown-5</i>	82
3.4.6.2	<i>The elemental analysis of the directly immobilized 18-crown-6</i>	82
3.4.6.3	<i>The elemental analysis of the immobilized 15-crown-5 by means of the glymo spacer</i>	82
3.4.6.4	<i>The elemental analysis of the immobilized THTD by means of the glymo spacer</i>	83
3.4.6.5	<i>The elemental analysis of the immobilized THTUD by means of the glymo spacer</i>	83
3.5.	Conclusion	83
Chapter 4	<i>The Extraction of the Toxic Elements from Water</i>	87
4.1.	Introduction.....	87
4.2.	Extraction of the Toxic Elements	89
4.3.	Results and Discussion	90
4.3.1	Extraction of As(V) with various ligands immobilized on four different silica supports	90
4.3.2	Extraction of Cd(II) with various ligands immobilized on four different silica supports	92
4.3.3	Extraction of Cr(VI) with various ligands immobilized on four different silica supports	95
4.3.4	Extraction of Sr(II) with various ligands immobilized on four different silica supports.....	98
4.3.5	Extraction of Hg(II) with various ligands immobilized on four different silica supports	101
4.3.6	Extraction of U(VI) with various ligands immobilized on four different silica supports	101
4.3.7	Extraction of two metal ions with various ligands immobilized on four different silica supports	104
4.3.8	Extraction of four different metal ions with various ligands immobilized on four different silica supports	106

4.3.9	Extraction of various metal ions with 15-c-5 directly immobilized on different silica supports	109
4.3.10	Extraction of various metal ions with 18-c-6 directly immobilized on different silica supports	110
4.3.11	Extraction of various metal ions with 15-c-5 immobilized with a glymo spacer on different silica supports.....	111
4.3.12	Extraction of various metal ions with 18-c-6 immobilized with a glymo spacer on different silica supports.....	112
4.3.13	Extraction of various metal ions with THTD immobilized with a glymo spacer on different silica supports.....	113
4.3.14	Extraction of various metal ions with THTUD immobilized with a glymo spacer on different silica supports.....	114
4.4.	Discussion of the Protonation Constants: Influence of the pH on the Extraction	115
4.5.	Conclusion	116
Chapter 5	<i>Conclusion and Future Work</i>	119
5.1.	Conclusions.....	119
5.2.	Future work.....	120
 ADENDUMS:		
A – FTIR spectra		II
B – Solid state NMR spectra		XXX
C – Extraction data		XLV
D – Low Angle X-Ray Diffraction of the Various Silica Support.....		XC
E – BET Analysis		XCIII
F – TGA Analysis		XCIII

List of Figures

Figure 2.1	There are two possible outcomes for bifunctional alkylation. There is the cis-isomer (a) or the trans-isomer (b). ¹²	9
Figure 2.2	Alkylating agents alkylate DNA primarily at the N-7 position of guanine bases after the formation of aziridinenium ions. This is the cause of the interstrand DNA cross-link. ¹²	10
Figure 2.3	The structure of BAL (British anti-Lewisite) is shown. It is also known as Dimercaprol (C ₃ H ₈ OS ₂).....	13
Figure 2.4	The chemical structure of TPEN.	15
Figure 2.5	Examples of natural biological macrocycles: a) the porphyrin ring of the haem protein, b) the chlorin ring of chlorophyll and c) the corrin ring of vitamin B ₁₂ . ^{65,66}	20
Figure 2.6	Examples of synthetic macrocycles: phthalocyanine (a) which can be used as semi-conductors, catalysts or colouring agents and natural antibiotics such as nonactin (b) and valinomycin (c). ⁷⁴	22
Figure 2.7	Differences in formation constants for 18-crown-6 for different metal ions in MeOH medium at 25 °C.	25
Figure 2.8	Formation constants of various macrocyclic ligands for K ⁺ , Cs ⁺ and Na ⁺	26
Figure 2.9	ΔLogK ₁ values versus nitrogen donor macrocyclic ring size for Ni ²⁺ , Cd ²⁺ , Cu ²⁺ , Zn ²⁺ and Pb ²⁺	28
Figure 2.10	The schematic structure of the mixed valence binuclear Cu(II)-Cu(I) complex produced (Gagné, Koval and Smith). ⁸⁸	30
Figure 2.11	The Schwarzenbach model of the chelate effect.	34
Figure 2.12	The chair conformation and bite sizes for cyclohexane.	35
Figure 2.13	The ideal bond lengths and bond angles with five and six membered chelate rings are shown.	35
Figure 2.14	Smaller metal ions require a six-membered ring for minimum strain in the ring. For larger metal ions to maintain minimum strain energy, a five-membered ring is required.	36
Figure 2.15	A chelating molecule that is directly immobilised on the silica surface will produce steric hindrances at the silanol site. A spacer attached to the support will provide attachment for a chelating molecule which can maximise the affinity for the metal ion. ¹¹⁹	39

Figure 2.16	Schematic view of the silica support.	40
Figure 3.1	A schematic view of the cyclisation step involved in a template macrocyclic synthesis.....	49
Figure 3.2	Bis-[N,N'-ditosyl-N,N'-pentamethylene-p-phenyldiamine] as synthesised by Stetter and Roos. ¹⁸	49
Figure 3.3	A schematic view of the cyclization step involved in a non-templated macrocycle synthesis.	50
Figure 3.4	The instruments that were used for the determination of the NMR spectra of the intermediate as well as the final products. The 600MHz was used for the soluble samples and the 500MHz was used for the solid samples.	54
Figure 3.5	The low angle powder XRD that was used for the determination of the diffraction patterns to confirm that the supports were indeed correct.	55
Figure 3.6	The thermogravimetric analyser that was used in the thermogravimetric analysis for the determination of the thermal stability of the immobilized products.	56
Figure 3.7	The synthesis and immobilisation of THTD and THTUD on the silica supports are shown. The legend indicates the different bridges between the donor atoms as well as the protection group that was used.....	60
Figure 3.8	Powder X-ray diffraction pattern of MCM-41 (cubic). The hkl and d/Å values are shown and were compared to the literature.	62
Figure 3.9	Powder X-ray diffraction pattern of HMS.....	62
Figure 3.10	Powder X-ray diffraction pattern of SBA-15..	63
Figure 3.11	Powder X-ray diffraction pattern of Si gel (60 Å).....	63
Figure 3.12	The FTIR spectrum of the direct immobilisation of 18-c-6 on silica gel. This spectrum is representative of 15-c-5 and 18-c-6 on all four supports.	64
Figure 3.13	The FTIR spectrum of 15-c-5 on silica gel 60 Å by means of the glymo spacer. This spectrum is representative of 15-c-5 and 18-c-6 on all four supports.....	66
Figure 3.14	The FTIR spectrum of THTD immobilised by the glymo spacer on silica gel (60 Å). The spectrum is representative of THTUD as well. This spectrum is basically the same for the other supports that were also used.	66
Figure 3.15	The solid state ¹³ C NMR spectrum of 18-c-6 directly immobilised on a silica support. This spectrum is also representative of 15-c-5 immobilised directly onto the silica support.....	68

Figure 3.16	The solid state NMR spectrum shows the direct immobilisation of the crown ethers on the silica supports. This spectrum is representative of both crown ethers immobilized on all four supports.	69
Figure 3.17	The spectrum is a representation of the immobilized glymo spacer on the silica supports.	69
Figure 3.18	The solid state spectrum ^{13}C -NMR is representative of the immobilization of the crown ethers onto the silica supports by means of the glymo spacer.....	70
Figure 3.19	The solid state ^{13}C NMR spectrum is representative of the immobilization via the glymo spacer, of the aza-crown ethers onto the silica supports.....	71
Figure 3.20	The isotherm plot of the adsorption and desorption data to determine the surface areas of Si-gel 60 Å and MCM-41.....	72
Figure 3.21	The isotherm plot of the adsorption and desorption data to determine the surface areas of HMS and SBA-15.....	72
Figure 3.22	A comparison between surface areas of the four different silica supports.	73
Figure 3.23	BJH Adsorption cumulative Pore Volume graph of Si gel (60 Å) and MCM-41 are shown. The pore volume ($\text{cm}^3\cdot\text{g}^{-1}$) is plotted against the pore diameter (Å).....	74
Figure 3.24	BJH adsorption cumulative pore volume graph of HMS Å and SBA-15 are shown. The pore volume (cm^3/g) is plotted against the pore diameter (Å).....	75
Figure 3.25	A comparison between average pore volumes of the different supports are shown.....	76
Figure 3.26	The graphs show the cumulative pore areas of Si-gel 60 Å and MCM-41. The pore area is plotted against the pore diameter.	76
Figure 3.27	The graphs show the cumulative pore areas of HMS Å and SBA-15. The pore area is plotted against the pore diameter.	77
Figure 3.28	A comparison between average pore diameters of the different supports are shown.....	78
Figure 3.29	The curve is representative of the thermal degradation of the directly immobilized crown ethers on the silica surfaces.	79
Figure 3.30	The curve is representative of the thermal degradation of the immobilized crown ethers with the glymo spacer on the silica surfaces.....	80
Figure 3.31	The curve is representative of the thermal degradation of the immobilized crown ethers with the glymo spacer on the silica surfaces.....	81

Figure 4.1	The extraction of As(V) with various ligands immobilized on four different silica supports.	91
Figure 4.2	The extraction of Cd(II) with various ligands immobilized on four different Si supports	94
Figure 4.3	The extraction of Cr(VI) with various ligands immobilized on four different Si supports	97
Figure 4.4	The extraction of Sr(II) with various ligands immobilized on four different Si supports	100
Figure 4.5	The extraction of UO_2^{2+} with various ligands immobilized on four different Si supports	103
Figure 4.6	The extraction of 2 metal ions with various ligands immobilized on four different Si supports.....	105
Figure 4.7	The extraction of four different metal ions with various ligands immobilized on four different Si supports.	108
Figure 4.8	The extraction of various metal ions with 15-c-5, directly immobilized on different silica supports.	109
Figure 4.9	The extraction of various metal ions with 18-c-6, directly immobilized on different silica supports.	110
Figure 4.10	The extraction of various metal ions with 15-c-5, immobilized with a glymo spacer on different silica supports.	111
Figure 4.11	The extraction of various metal ions with 18-c-6, immobilized with a glymo spacer on different supports.....	112
Figure 4.12	The extraction of various metal ions with THTD, immobilized with a glymo spacer on different silica supports.	113
Figure 4.13	The extraction of various metal ions with THTUD, immobilized with a glymo spacer on different silica supports.	114
Figure 4.14	Structures of the neutral, free ligands, THTD and THTUD.	116

List of Tables

Table 2.1	The classification of ring sizes of cyclic molecules	18
Table 2.2	A comparison between the ligand field strength of unidentate ligands, open chain bidentate ligands and macrocyclic ligands. ¹⁰²	24
Table 2.3	The stability of a few complexes that are mentioned in the Irving-Williams series. ^{85,87}	29
Table 3.1	The surface areas of Si-gel 60 Å and MCM-41 are shown according to the adsorption and desorption data as shown in the graphs in figure 3.20.	71
Table 3.2	The surface areas of SBA-15 and HMS are shown according to the adsorption and desorption data as shown in the graphs in figure 3.21.	72
Table 3.3	The average size of the pore diameters and average pore volumes for MCM-41 and Si-gel (60 Å) are shown in the table below.	74
Table 3.4	The average size of the pore diameters and average pore volumes for HMS and SBA-15 are shown in the table below.	75
Table 3.5	The average pore diameter for Si-gel 60 Å and MCM-41 was determined by BET and is shown in the table below.	77
Table 3.6	The average pore diameter for HMS and SBA-15 was determined by BET and is shown in the table below.	78
Table 3.7	The calculated and the analytically found analysis (in %) of the directly immobilized 15-crown-5 on various substrates.	82
Table 3.8	The calculated and the analytically found analysis (in %) of the directly immobilized 18-crown-6 on various substrates.	82
Table 3.9	The calculated and the analytically found analysis (in %) of the directly immobilized 15-crown-5 on various substrates.	82
Table 3.10	The calculated and the analytically found analysis (in %) of the immobilized THTD on various substrates by means of the glymo spacer.	83
Table 3.11	The calculated and the analytically found analysis (in %) of the immobilized THTUD on various substrates by means of the glymo spacer.	83
Table 4.1	Formation constants of complexes of some tetraaza macrocycles.	88
Table 4.2	The metal salts that were used for the preparation of the different solutions.	89
Table 4.3	The comparison between the stability constants (log <i>K</i>) of THTD, THTUD, [10]-ane-N ₃ , THETAC and TETA are shown.	92
Table 4.4	The p <i>K</i> _a values of the two free azamacrocyclic ligands are shown.	92
Table 4.5	The log(<i>K</i>) values of ligands with similar structures as THTD and THTUD.	116

Chapter 1

Introduction: Problem Statement and Aims

1.1 Rationale

Water resources in South Africa do not exist in abundance. South Africa is a developing country and demands on water resources are increasing due to the needs of expanding industries, mining and agriculture. A large portion of the South African population depends on water for domestic use and, in rural areas, to maintain herds or crops. Migration of rural population to urban areas has led to an increasing demand for domestic water in city areas, whilst in rural areas 12% of the population have no access to piped water. This part of the population depends on water obtained from natural streams and rivers. Unfortunately, due to spillage of effluent from the heavy industries, the streams and rivers are contaminated with toxic heavy metals. This is a scenario of grave concern as it can result in health hazards and pollution of arable land, rendering it useless. This study has been undertaken to find a way to selectively remove the toxic heavy metal ions from waste water and brine.

1.2 Problem Statement and Research Questions

About 80% of the water in SA is used in mining and heavy industries for cooling, creating slurries, separations, etc. Mine dumps contain heavy metal ions such as U (in whatever form or species) which are by-products in Au mining. These heavy metal ions dissolve easily and get washed into rivers and streams. Some industries even dump untreated water directly into rivers and streams.

The toxic metal ions of concern in this study are: Cr^{6+} , As^{5+} , Sr^{2+} , Cd^{2+} , Hg^{2+} , U^{6+} .

- Cr^{6+} – carcinogenic
- As^{5+} – lethal ground water contamination
- Sr^{2+} – radioactive by-product in nuclear power plants
- Cd^{2+} – 6th most poisonous substance both for humans and animals

- Hg^{2+} – most Hg compounds are extremely toxic and can result in a perpetual destructive cycle
- U^{6+} – radioactive and extremely toxic

Although there are a number of extraction methods that produce high yields, in most cases, the ligands used, are destroyed and the metal ions cannot be recovered for re-use. This means new ligands must be produced at high cost to the companies who must also dispose of the unrecoverable toxic metal ions and ligands in a responsible way. Currently water is decontaminated by means of homogeneous extraction, a method not geared to handling huge amounts of water.

The purpose of this project is to develop a heterogeneous method which will permit the recovery of the heavy metal ions. Subsequently the metal ions can be re-used. The system must also be able to handle industrial amounts of water. Initially the cost might be perceived as expensive, but the recovery of the metal ions will in the long term make such a system more financially beneficial.

1.3 Aims & Objectives

The aim of this study is to synthesize two novel triaza-macrocycles with pendant arms for the selective extraction of Cd^{2+} . The crown ethers will be used for the selective extraction of the Sr^{2+} and the UO_2^{2+} .

The next objective can be divided into two parts:

- a) To immobilize the macrocycles onto silica supports to create an insoluble ligand system
- b) To evaluate the performance of the ligands system on the uptake of heavy metals from synthetic contaminated water.

The ligands will be immobilised either directly on to the various supports, or by means of a spacer.

A glymo spacer was introduced to establish what the effect would be on the extraction capabilities of the various ligands compared to the situation where the ligands are directly attached to the support. When there is a spacer, the influence of the support can

be considered as negligible. The longer spacer however will give more freedom to the ligands in solution which will enable the ligands to move more freely to come into contact with the metal ions, yielding a better extraction.

To immobilize the aza-macrocycle to the silica supports, an “anchor” must be used and this “anchor” must be chosen in such a way that the immobilized ligand does not deviate too much from the original ligand. The aza-crown ethers were therefore immobilized by means of a glymo spacer onto the silica supports.

The immobilization of these parent ligands on different silica substrates must be done using a glymo spacer before attaching the oxygen donating pendant arms to the aza-macrocycles. The epoxide end of the glymo spacer will be used to attach to a nitrogen atom in the ring of the aza-macrocycle. 2(*S*)-hydroxypropyl will be added to the immobilized aza-macrocycles to create the remaining pendant arms for the ligands.

The 15-crown-5 substrate-ligand system would specifically be used to see if it is selective for the extraction of Sr^{2+} . The 18-crown-6 substrate-ligand system would specifically be used to see if it is selective for the extraction of UO_2^{2+} .

Using the amino group of the two (2-aminomethyl) crown ethers as the attachment point, immobilization would be achieved by using the glymo spacer.

Another objective is to immobilize the two (2-aminomethyl) crown ethers directly on the different silica substrates. The aminomethyl group acts only as an anchor for the crown ethers to attach to the silica supports.

The extraction of the directly immobilized crown ethers will be compared to that of the crown ethers immobilized with the glymo spacer.

The extraction capabilities of the different immobilized ligands will be examined at two different pH values.

To determine the extraction capabilities of the immobilized ligands, standard solutions containing the different metal ions will be used. In the initial experiments, single metal ion solutions will be prepared to determine the extraction capabilities of the different

ligands on the various supports. Competitive extractions (with a mixture of metal ions in solution) will also be carried out in order to determine the selectivity of a specific ligand with the various metal ions. The results will be determined by ICP.

1.4 Scope & Limitations

The scope of this study was thus to synthesize selective ligands and to immobilize them on insoluble supports. This was done for the selective extraction of the metal ions as well as for the easy recovery of the ligands and metal ions. The extraction was done over a 24 h period at 25°C because equilibrium should be reached in this time period.¹ The pH of mine water can be as low as 2 or even below 2. A pH of 2 is the absolute limit of the stability of the immobilized ligands. Below this pH, the ligands break away from the supports and at even lower pH start to disintegrate. The metal ion solutions had to be buffered to protect the immobilized ligands. An acetic acid/acetate buffer was used to buffer these metal ion solutions. Two pH levels were investigated – 4.5 and 5.9 – since 5.9 is the upper limit of the acetic acid / acetate buffer and with the pK_a of acetic acid being 4.74 a pH of 4.5 is an acceptable and comfortable pH value to carry out the extraction. However, this system limits us from moving to a pH of 2.0 because of the hydrolysis of the ligand from the substrate. Furthermore, we did not envisage carrying out the extraction at any further pH values

Extraction experiments were conducted to establish whether there is selectivity between the various ligands as well as to determine whether or not the supports had any influence on the extraction capabilities of the ligands. Another factor that had to be considered was whether the spacer had any influence on the extraction when the crown ethers were used.

The mine water that was obtained did not contain any of the metal ions that were targeted, and thus no actual extraction from real mine water could be done, thus only simulated solutions were used.

The regeneration tests of the ligands require HNO_3 of a particular concentration so as to only release metal ions from the ligand and not to hydrolyse the ligand from the substrate. This aspect will not be covered in this study because low pH's reprotonates the ligand and at pH 2 hydrolysis of the ligand from the substrate occurs.

1.5 Research Approach

By investigating what industries there are as well as what types of mines there are in the different areas of the country, the types of heavy metal ions were determined. The selection of ligands depended on the toxic heavy metal ions that were identified.

There are two main research approaches:

- a) Single metal ion solutions will be made to determine the extraction capacity of the different ligands with the various metal ions.
- b) A mixture of the various metal ions will be made into a solution to determine the selectivity of the ligands.

For the extraction of Sr^{2+} and UO_2^{2+} , the 15-crown-5 ligand system and the 18-crown-6 ligand system were selected respectively (chapter 2 - section 2.2.3 & 2.2.6) for it is known that the crown ethers are selective towards these metal ions.^{2, 3} Aza-crown ethers (THTD and THTUD) were used because a previous study showed that strong complexes were obtained with these free ligands when Cd^{2+} were used.⁴ These ligands will be immobilized on the different silica supports. All the immobilized ligands will be analysed and their structures confirmed by means of NMR and FTIR analyses. Extraction of the single metal ions will be conducted to determine the extraction capacity of the various ligands. Once these experiments are completed, the selectivity of the different ligands on the different supports will also be investigated. These experiments will be the competitive extraction experiments where separately, individual ligands and supports would be used to extract metal ions from a mixture of metal ions from one solution.

All aqueous solutions will be analysed by means of ICP.

By immobilising the ligands on the various supports through different methods, it is hoped to find the best and cheapest method to clean up polluted rivers and streams so that the general population can have access to clean and safe water.

References

¹ J.Kramer in PhD thesis

² B. Grüner *et al.*, *New J. Chem.*, 2002, **26**, 867

³ G. Tian *et al.*, *Solvent Extr. Ion Exch.*, 2005, **23**, 519

⁴ B.F. Barnard in M.Sc thesis, University of Stellenbosch, pp 25 – 40

Chapter 2

Literature Review

2.1. General Introduction

Without water life cannot exist on earth. The world is currently facing a dilemma, because water is rapidly becoming a very scarce commodity, especially in developing countries such as South Africa and India. It is therefore clear that the contamination and pollution of water is one of the biggest problems facing the world's populations.

Water pollution at the local level is usually associated with climate, landform structures, industrial development etc.¹ The disposal of municipal solid waste is of great concern throughout the world, particularly in developing countries such as India and South Africa. To minimize the high cost of landfill disposal and other unacceptable disposal options, the use of bio-solids were encouraged in agriculture. Bio-solids unfortunately have relatively high concentrations of heavy metals, P and N, and the accumulation of these toxins, even at very low concentrations, can cause huge problems by contaminating the environmental food chain and the ground water that will eventually supply drinking water to the population.^{2,3}

Although South Africa is currently regarded as a developing country, it is relying heavily on its industrial and mining sectors. In order for these industries to run successfully, millions of litres of water are used for separations, cooling, making slurries, etc. This results in vast amounts of water going to waste in a country that cannot afford such a loss, since South Africa is a relatively arid country.

The industrial and mining water is contaminated with ions such as Cr^{6+} , As^{5+} , Sr^{2+} , Cd^{2+} , Hg^{2+} and UO_2^{2+} and is therefore extremely toxic. The heavy metal ion contamination of this industrial waste water, which finds its way into rivers and streams, is a threat, not only to the ecosystem, but especially to the people depending on the rivers and streams for household water. The severe toxicological effects on living organisms due to heavy metal contamination, for instance Cd^{2+} , is potentially

life threatening. Cadmium is actually regarded as one of the most toxic heavy metal elements and is listed as the sixth most poisonous substance for humans and animals.⁴ According to Patterson⁵ in 1987, Cd, Cr, and Hg were amongst the 10 basic metals that were classified as of primary importance for recovery from waste streams because of their toxicity in water.⁶

The disposal of radioactive waste is another problem that needs to be addressed. In many countries, including South Africa, the use of nuclear materials, either in the medical field or as fuel for power plants, creates disposal problems. It is also important to consider that next to such a facility, there might be an accidental release of radio nuclides into the environmental water. It is therefore important to monitor the environment in order to preserve and protect the natural surface and underground water from this type of pollution.¹

Most effluents treated by wastewater treatment plants contain high levels of pollutants including heavy metal ions such as Cd^{2+} and Pb^{2+} .⁷ It is clear that the disposal of hazardous heavy metal ions and other toxins in aqueous waste streams is a huge problem caused by heavy industries. It is necessary to find working methods for the successful removal of these problem materials from waste water before they are released into natural streams and rivers.

Hydrogels are widely used in the purification of waste water and the stabilisation of mineral sediments. Their properties include the ability to control the diffusion process, their swelling response to changes in ionic strength, pH, temperature and their capability to bind selectively to certain metal ions. They are easy to handle and are reusable.³ Unfortunately they do not extract Cd^{2+} and this leaves an opening to develop new ligands to try and extract Cd^{2+} from waste water.

The use of chelating agents, especially macrocyclic ligands, has increased dramatically over the last couple of years. The primary field of interest for macrocyclic molecules is the medical field. Weeks *et al.*⁸ stated that pendant arm poly-azamacrocycles draw attention because, amongst other applications, they have the potential to be used as biological tracers.^{9,10}

The use of polyoxa, polyaza and polyoxa-polyaza macrocycles can vary from sensors for cations and anions as well as for molecular scaffolds for materials and biological models. It is also known that mixed donor polyoxa-diaza macrocycles are very efficient in the complexation of a large number of heavy metal ions.¹¹

Parker *et al.*¹² stated that nitrogen mustards such as chlorambucil, melphalan, cyclophosphamide and ifosfamide are amongst the most useful clinical agents for the treatment of a number of cancers due to the fact that they are bi-functional alkylating agents. Figure 2.1 shows clearly that there are two ways for the pendant arms to connect to the macrocycles to form this bi-functionality.

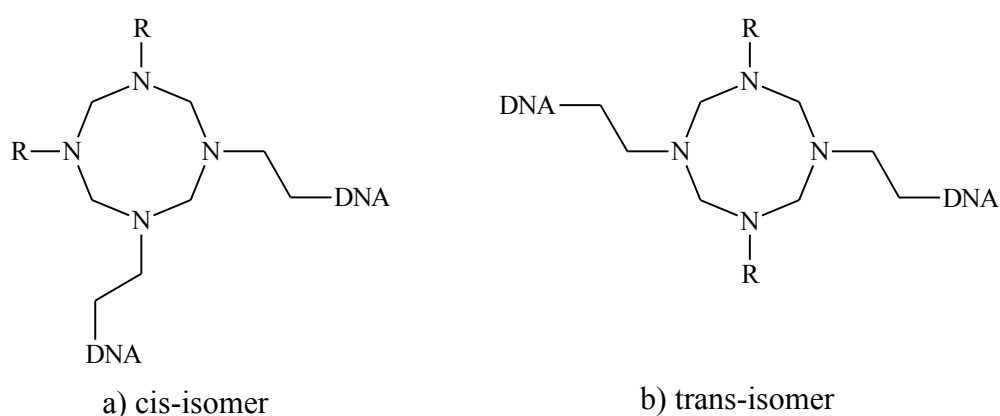


Figure 2.1 There are two possible outcomes for bi-functional alkylation. There is the (a) cis-isomer or (b) the trans-isomer.¹²

These alkylating agents alkylate the DNA primarily at the N-7 position of guanine bases (figure 2.2) in the groove after the formation of aziridinenium ions. The critical event caused by these clinical agents of this type, is the DNA interstrand cross-link.

Poly-azamacrocycles provide a possibility for two or more alkylating moieties to be present in the same molecule. Since their coordination chemistry is well documented, it provides an opportunity for pro-drug formation through complexation with metal ions.¹²

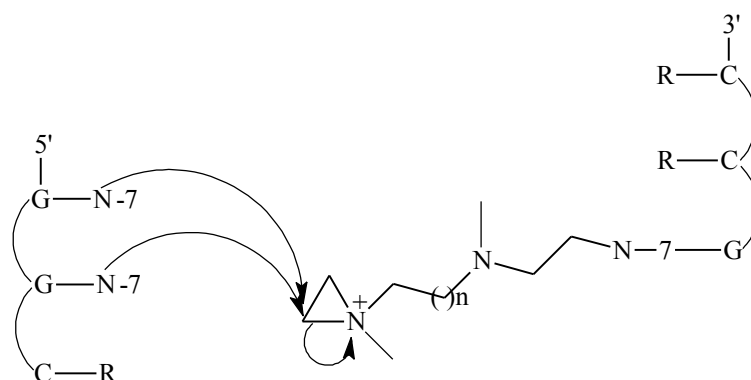


Figure 2.2 Alkylating agents alkylate DNA primarily at the N-7 position of guanine bases after the formation of aziridinenium ions. This is the cause of the interstrand DNA cross-link.¹²

Heavy metals are fairly easily absorbed in the intestinal tract to form complexes with proteins and enzymes, for example As^{3+} , Cd^{2+} and Hg^{2+} which have a high affinity for soft donors. Therefore, the removal of heavy metal ions from the body is essential and is based primarily on the concepts of soft-hard acid-base (SHAB) and the principles of coordination chemistry. The use of ligands containing N, S and/or other soft donors is very useful.¹³

Nowadays, there is growing interest in synthetic macrocycles and their metal complexes. This interest depends on the fact, firstly, that these compounds may mimic naturally occurring macrocycles in their structural and functional features and secondly, on their rich chemical behaviour. For instance, 12- to 16-membered cyclic tetra-amine ligands have a strong tendency to coordinate in a co-planar fashion with 3d transition metal ions to form strong complexes. These in-plane metal-nitrogen interactions are modulated according to the size of the ligand cavity.¹⁴

Because of the great number of selective ligands available nowadays, solvent extraction became a very useful method for the selective separation and concentration of metal ions from complex aqueous solutions. Separation by solvent extraction is generally considered to be economical for concentrations from 0.01 to 1.0 mol.dm⁻³.^{6,15} Typically, macrocycles contain a central hydrophilic cavity, ringed with either electropositive or electronegative binding atoms. The exterior framework is flexible and exhibits hydrophobic behaviour. The hydrophobic exterior allows the macrocycle to be soluble in ionic substances and in non-aqueous solvents, making it useful in a variety of media.¹⁶

Although alkali and alkali earth metal ions are “less” toxic, there is also an interest in the extraction thereof from aqueous solutions. This can be done by means of macrocycles. Another method is to make use of calixarenes, which are also a type of macrocycle. Calixarenes are bucket-shaped macrocycles containing phenol groups that form the “bottom of the bucket”. For Sr^{2+} , the best extractant up to now was shown to be calix[8]arene actamide.¹⁷ It is also shown that Sr^{2+} is extracted by dicyclohexano-18-crown-6 (DCH18C6) into ionic liquids.¹⁸

In recent years, new areas of interest opened up for the use of macrocycles.^{10, 19} One such area is the selective extraction of precious metals in hydrometallurgy. Green and Hancock²⁰ reported that extraction was done from solutions containing Cu^{2+} , Ni^{2+} , Co^{2+} , Zn^{2+} , Mn^{2+} , Fe^{2+} and U^{3+} at levels between 0.2 and 0.8 g.L⁻¹ in a sulphate medium at a pH of 2. Various macrocyclic and spherical ligands, as well as their open-chain counterparts are nowadays used in analytical detection, material preparation catalytic function, medical use and nanoscopic devices.²¹

The liquid-liquid extraction of UO_2^{2+} with organic solutions of crown ethers for example, was studied intensively by S.K. Mundra and co-workers,²² N.V. Deorkar and S.M. Kopkar²³ and M. Shamsipur and co-workers. It was found by M. Shamsipur and co-workers that the extraction properties of the ligands depended on the number of ester oxygen atoms and on the nature of the substituents present in the macrocyclic molecule. They also found that most elements were more likely to be extracted when in their highest oxidation state.²⁴ The best result for the extraction of UO_2^{2+} was obtained when complexed to DCH18C6.²⁵

The problem in using free ligands is the fact that it is very hard to recover the ligands again once they have been used. In order to reuse these ligands, it is necessary to find a suitable medium to which these ligands can anchor so that they can be recovered for reuse. Modifying polymer surfaces provide a possible way of immobilizing ligands on the surfaces for the extraction and recovery of metal ions from solutions. This will also provide a way for the recovery and reuse of the ligand. There are quite a number of synthetic routes for the chemical modification of polymer surfaces. Howarter and Youngblood²⁶ proposed a way of modifying the surface of polymers with 3-aminopropyltriethoxysilane (APTES). The reaction

proceeds by initial APTES adsorption to the substrate, lateral bonding and then multilayer formation which make this analogous to silane multilayer formation.

In conclusion, because water is such a precious and scarce commodity, the conservation of the world's water resources is of utmost importance. The immobilization of the ligands will provide us with a way of recovering the ligands as well as the heavy metal ions that were extracted. From an economical view, it is also sensible since water does not go to waste, the cost of ligand production will be cut because the ligands can be reused and the metal ions that were extracted can also be recovered for further use. Ligand selectivity thus provides a method for extracting only the metal ions that are required, either because of safety concerns, or for profit.

2.2. Toxic Elements in Waste Water

Although most of the heavy metal ions are toxic, it was decided for this study, to concentrate only on 6 of these metal ions namely Cr^{6+} , As^{5+} , Sr^{2+} , Cd^{2+} , Hg^{2+} and U^{6+} . Cr^{6+} is used in the motor industry, As^{5+} is a problem in ground water and $^{90}\text{Sr}^{2+}$ is a by-product formed during nuclear power generation. Cd rods are used in conjunction with B rods in the cooling process in nuclear power stations. Hg^{2+} accumulates in the fatty tissue of fish. U is used as fuel in nuclear power stations.

2.2.1. Chromium (Cr^{6+})

Cr^{6+} is very hazardous in cases of skin contact (it is easily absorbed through the skin), eye contact, inhalation or ingestion. Cr^{6+} is a confirmed carcinogen (tumorigenic) as well as a mutagen (genetic material). This metal ion causes damage to the kidneys, liver, gastrointestinal tract, the upper respiratory tract, skin and eyes. Other health risks include fetotoxicity or post-implantation mortality and birth defects. It dissolves easily in water and since it is used by motor manufacturers, it tends to find its way into streams and rivers.²⁷

2.2.2. Arsenic (As^{5+})

Arsenic causes many problems in many third world countries where groundwater is contaminated with arsenic derivatives. Arsenic can enter the body on dermal contact, eye contact, inhalation or ingestion. It is a confirmed carcinogen which increases the risk of cancer, especially of the bladder. It causes damage to the blood, kidneys, lungs and liver. According to the State of California, arsenic also causes birth defects and reproductive harm. Arsenic is extremely poisonous and potentially lethal. It is thus of the utmost importance to clean up mining water, since this seeps into groundwater that is used by a large portion of the human population.²⁷

In World War II, British chemists developed the ligand BAL (British anti-Lewisite – figure 2.3) in order to combat any chemical warfare coming from the Germans because the Germans used dichloro(2-chlorovinyl)arsine as part of their chemical warfare campaign against the allied forces. BAL is also known as Dimercaprol ($\text{C}_3\text{H}_8\text{OS}_2$) and is still in use even after 60 years. Nowadays BAL is used as a chelator in the treatment of poisoning from arsenic, mercury, gold and other heavy metal ions.

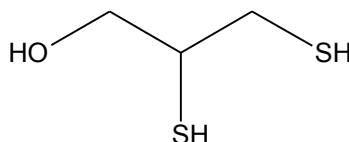


Figure 2.3 The structure of BAL (British anti-Lewisite) is shown. It is also known as Dimercaprol ($\text{C}_3\text{H}_8\text{OS}_2$).

2.2.3. Strontium (Sr^{2+})

The removal and recovery of $^{90}\text{Sr}^{2+}$ from nuclear waste has received a lot of attention since the 1940's. Since the end of the 60's and mid-70's, two kinds of extractants, crown ether derivatives and cobalta bis(dicarbollide) derivatives,²⁸ received quite a lot of attention because these derivatives showed some very promising results in the separation and recovery of $^{90}\text{Sr}^{2+}$ and $^{137}\text{Cs}^+$ from high level radioactive liquid waste (HLRLW). HLRLW has been generated from the reprocessing of spent nuclear fuel. The main

hazard of HLRLW consists of unrecovered U and Pu as well as some minor actinides. There are also some radioactive fission products such as $^{90}\text{Sr}^{2+}$.²⁹

Up to now, the recovery processes were not cost effective, as well as the fact that these extractants were very toxic and could therefore not be implemented on an industrial scale.²⁹ Other methods for the selective extraction of Sr^{2+} from aqueous solutions include the extraction into supercritical fluid CO_2 with DCH18C6 from water at pH 3, 60°C and 100 atmosphere. It was reported by Wai *et al*³⁰ that 18-membered crown ethers with cavity diameters of 2.6 – 2.8 Å are most suitable for the extraction of Sr^{2+} which has a diameter of 2.2 Å. This is one of the reasons for using the chosen ligands 18-crown-6 and 15-crown-5.

2.2.4. Cadmium (Cd^{2+})

Cadmium is mainly obtained in the metallurgical processing as a by-product of metals such as copper, lead and zinc.³¹ It is therefore important that a method is developed for the effective separation of cadmium from other metals. Liquid-liquid extraction is one convenient way of solving the problem and has been widely used for the extraction and separation of Cd. Extractants for the extraction and separation of Cd includes amines^{32, 33}, carboxylic acids³⁴, alkanes³⁵, alkyl xanthates³⁶ as well as organophosphorus extractants.³¹

Although cadmium is an extremely toxic metal, it is still used extensively as pigments, in electroplating, in metallurgical products and various other industries.³⁷ The purity of the metal is utterly important in fields such as control rods in nuclear reactors.³¹ Even at low concentration, cadmium is considered to be one of the most toxic heavy metal elements. The entry of cadmium into the body can occur through eye contact, inhalation or via ingestion. Cadmium can cause lung, blood and kidney diseases. It is also a suspected carcinogen and it is very harmful to the environment since Cd^{2+} is highly soluble in water.

Studies were carried out by Gupta and co-workers³¹ in the extraction of Cd^{2+} , along with other elements, from a hydrochloric acid medium using Cyanex 923. The extraction capacity of 91 – 92% was obtained. A recovery of 98 – 99% was achieved with Cyanex 923 and the Cyanex 923 could be used for up to 15 cycles for the extraction and stripping of Cd^{2+} . Rodríguez and co-workers³⁷ also investigated the liquid-liquid extraction of Cd^{2+} by Cyanex 923 in a solid-supported liquid membrane system, but the process is not as successful as was hoped for. As the temperature was increased, the extraction decreased because the extraction process is exothermic. It was also found that the extraction is dependent on the extractant concentration, but not upon the initial metal ion concentration. It was found in previous studies that THTD and THTUD form very stable complexes with Cd^{2+} .^{38,39}

Takeshita and co-workers⁴⁰ synthesized a hexa-nitrogen ligand, *N,N,N',N'*-tetrakis(2-pyridylmethyl)ethylenediamine (TPEN), that can coordinate and enclose metal ions (figure 2.4). They found that Cd^{2+} was selectively extracted by the semi-cyclic structure containing nitrogen donors in the BTP gel (2,6-di(5,6-dipropyl-1,2,4-triazin-3-yl)pyridine).

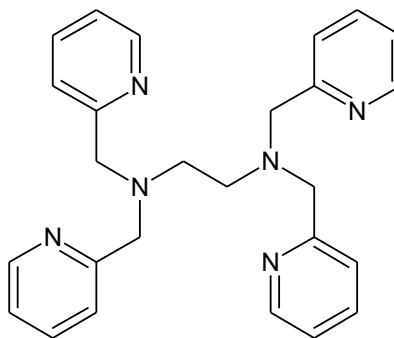


Figure 2.4 The chemical structure of TPEN.

A study was done by B. Wassink, D. Dreisinger and J. Howard,⁴¹ to separate Zn^{2+} and Cd^{2+} , from Co^{2+} and Ni^{2+} . A 30% Aliquat 336, a strong base anion exchanger, in either a chloride (R_4NCl) or thiocyanate (R_4NSCN) form was used for the separation and there appeared to be a slight advantage of Cd^{2+} over the extraction of Zn^{2+} .

Fenton and co-workers⁴² studied complexes with mixed donor atoms in the macrocyclic ring with a variety of metal ions. The transition metal ions show complexes that are six coordinate, but Cd^{2+} is an exception, being eight coordinate, so this must be kept in mind for this specific study. Hydrogels were used by Essaway and Ibrahim⁴³ for the extraction of Cu^{2+} , Ni^{2+} and Cd^{2+} . It was found that Cd^{2+} was the least extractable with these specific hydrogels.

2.2.5. Mercury (Hg^{2+})

Mercury and most of its compounds are very toxic. The route of entry into the body is the same as for all the other metal ions discussed. Mercury can also be transferred to the offspring of mammals, because it is secreted in the maternal milk of mammals.²⁷ It is toxic to the kidneys, lungs, nervous system and mucous membranes. Tremors, impaired cognitive skills and sleep disturbances occur when exposed to mercury vapours, even at very low levels. Mercury has a tendency to accumulate in fish and shellfish. Since fish is a substantial source of food in South Africa, it is important to rid streams of mercury to prevent contamination of fresh water fish, but also to prevent the mercury from reaching the ocean.

2.2.6. Uranium (U^{6+})

The concentration of uranium in seawater is approximately $3.3 \mu\text{g.L}^{-1}$, and in fresh water it is much lower.⁴⁴ The real problem arises in the industry where uranium is a by-product in gold mines, and this ends up on mine dumps and rain water then washes the uranium into the environmental water.

South Africa used to be the largest supplier of gold (Au) in the world. Uranium is a fairly mobile element in surface or near-surface environments. Not only is uranium extremely toxic and radioactive,^{45,46} it is also very precious as a fuel for nuclear power stations or nuclear power plants.

Uranyl (UO_2^{2+}) is nephrotoxic. It is also chemically toxic and carcinogenic in bone.⁴⁷ It may even cause mutagenic or teratogenic effects. There is also the danger of cumulative effects. Due to this quality, its geochemical exploration methods require the measurement of trace quantities of the metal ion in water samples, plants, soils and rocks.⁴⁸

One of the methods for the extraction of U^{6+} is known as a cloud point extraction. This process uses a mixture of the ionic surfactant, cethyl trimethylammonium bromide (CTAB) and a non-ionic surfactant, TritonX-114, for the extraction of U^{6+} from an aqueous solution. This method has a detection limit of 0.06 ng.mL^{-1} and is used for the determination of U^{6+} in tap water, waste-water and well samples. It has been reported that amongst other methods and materials, activated Si gel⁴⁹ is used for the enrichment of U^{6+} from dilute solutions. In 2009 Sadeghi and Sheikhzadeh used Murexide that was chemically bonded to silica gel immobilised by 3-aminopropyl trimethoxysilane (APMS) for the extraction of UO_2^{2+} . A maximum sorption of 1.13 mmol g^{-1} was obtained.⁵⁰ This happens prior to its determination with the use of various analytical techniques.⁴⁵ The use of poly-dentate oxygen-donating ligands are known to form high-affinity complexes with hard Lewis acids from the f-block.^{51,52} The uranyl (UO_2^{2+}) ion is known to be a hard Lewis acid and therefore will have an affinity for hard donor groups. It is thus clear that UO_2^{2+} will be oxophilic and this is one reason why crown ethers are considered as ligands for the extraction of U^{6+} .^{52,53} Because of the size of UO_2^{2+} , the ligand does not accept the uranyl into the cavity, but it would stay on the outside of the crown ether.^{52,54} M. Sakama and co-workers used diamyl amylphosphonate $(\text{C}_5\text{H}_{11}\text{O})_2\text{C}_5\text{H}_{11}\text{PO}$ for the extraction of hexavalent UO_2^{2+} from $2 \text{ mol.dm}^{-3} \text{ HNO}_3$.⁵⁵ Uranium adopts a hexavalent oxidation state that is usually linear. This linearity will be maintained as far as possible. This means that coordination can only take place in the equatorial plane that is perpendicular to the $\text{O}=\text{U}=\text{O}$ vector. The apical moieties are almost non-reactive, except with the appropriate macrocyclic ligands.^{50,56} The orientation of the chelator around the UO_2^{2+} depends very strongly on the length of the spacer that connects the ligand to the substrate. Short, flexible linkers were found to work best, and $\text{N}_{\text{amide}}-\text{H}\cdots\text{O}_{\text{phenolate}}$ hydrogen-bonding stabilized the deprotonated metal chelated

ligands.^{50,57,58} It was found that ethylsulfanyl groups disrupt the planar conjugated ligand arrangement with UO_2^{2+} introduced to the thiophene linker. The new arrangement forms a dimeric structure in which each ligand spans two uranyl centres $(\text{UO}_2)_2\text{L}_2$.⁵⁹

The reprocessing of nuclear fuel also produces medium radioactive liquid waste (MRLW). Grüner and co-workers²⁸ suggest two ways of disposing of these HLRLW and MRLW: 1) disposal or long-term interim storage after vitrification and 2) separation of long-lived elements in view of their destruction by transmutation or immobilisation in very stable matrices for the radio nuclides that cannot be transmuted. MRLW can be disposed of in surface repositories provided that the activity of long-lived elements is removed.

Not only is it necessary to protect South Africa's population from these harmful elements, it is also possible to benefit from recovering these elements. Although these elements are very harmful, they are precious commodities and it is important to recover it for reuse.

2.3. A Brief Overview of Macrocyclic Ligands

Cyclic molecules can be divided into four groups; small, normal, medium and large (table 2.1). A macrocyclic ligand is by definition a cyclic molecule with at least three potential donor atoms in a ring which contains a minimum of nine atoms.⁶⁰ This means no macrocyclic ligand can be classified as normal or small.

Table 2.1 The classification of ring sizes of cyclic molecules

Ring Size	Classification
3, 4	Small
5 – 7	Normal
8 – 11	Medium
$12 \leq$	Large

2.3.1. A short history of macrocyclic ligands

According to Pedersen and Frensdorff,⁶¹ prior to 1967, not much was known about the chemistry of macrocyclic ligands. It was only after the accidental discovery of the first macrocyclic crown compound – dibenzo[18]crown-6 – by Pedersen and Frensdorff, that the true versatility of the macrocyclic ligand came to be known. This macrocyclic ligand was an accidental by-product of the synthesis of bis[2-(*o*-hydroxyphenoxy)ethyl] ether. The crystals that were formed would not dissolve in pure methanol, but became soluble upon the addition of sodium salts, which led to the discovery of the coordination power of the crown ethers. This in turn led to the synthesis of other macrocycles containing a variety of donor atoms. In 1982 for example, Buøen *et al.*⁶² synthesized 1,4,7,10-tetrakis(2-hydroxyethyl)-1,4,7,10-tetraazacyclododecane that was used for the complexation of alkali cations.

2.3.2. General applications of macrocyclic ligands

Macrocyclic ligand transition metal complexes are involved in a number of biological systems, for instance the porphyrin ring of the haem-protein (Fe containing ring - figure 2.5 a), the chlorin ring of chlorophyll (Mg containing ring - figure 2.5 b) and the corrin ring of vitamin B₁₂ (Co containing ring - figure 2.5 c). It was in the '60s that strong complexes were observed involving Na⁺, K⁺ and other related cations, but these were limited to biological materials only.^{63,64,69}

Macrocyclic polyethers (crown ligands) have an almost unique property in their tendency to form complexes with alkali salts and other salts with similar cations. These complexes are held together by electrostatic interactions between the cation and the negative end of the C-O dipoles. Some of the cations that are of interest in this study that were observed to form stable complexes with crown ligands, are Sr²⁺, Cd²⁺ and Hg²⁺.⁶⁹

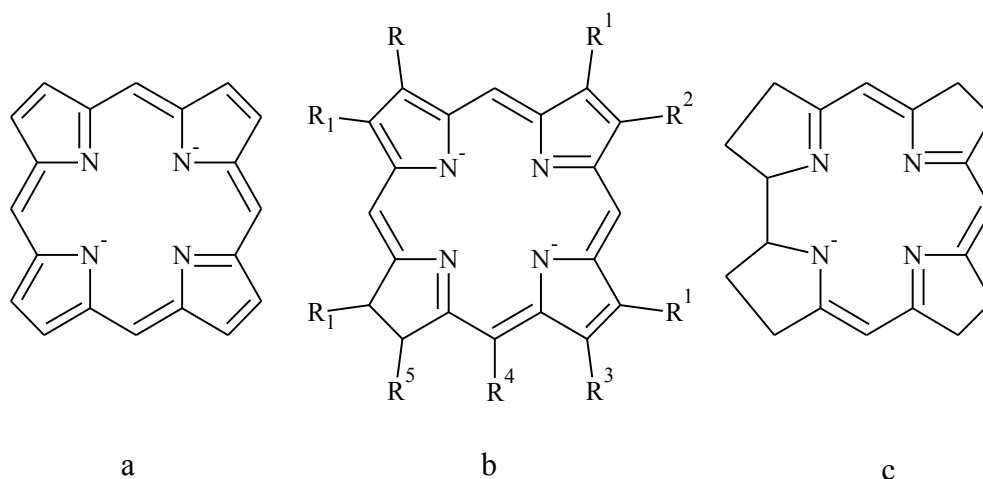


Figure 2.5 Examples of natural biological macrocycles: a) the porphyrin ring of the haem-protein, b) the chlorin ring of chlorophyll and c) the corrin ring of vitamin B₁₂.^{65,66}

Currently a large number of synthetic macrocyclic ligands have been prepared and investigated, for example phthalocyanine (figure 2.6 a), which can be used as semi-conductors, catalysts or colouring agents.^{67,68} Crown ethers react in a manner similar to that of naturally occurring antibiotics such as nonactin (figure 2.6 b) and valinomycin (figure 2.6 c).^{69,70} Macrocycles are also used extensively in the medical field. β -thalassemia, commonly known as Cooley's anaemia, is treated with desferral, a macrocyclic ligand which contains hard oxygen donors to get rid of the iron overload.¹³

Macrocyclic ligands are widely used in solvent extraction of metal salts, and more importantly, in the recovery of precious metals and the removal of toxic elements from waste water of industrial plants. Macrocyclic ligands form very stable complexes with various metal ions, but they are very selective towards certain metal ions. This attribute now opens up the possibility to selectively isolate specific metal ions from a mixture of ions by using tailor made macrocyclic ligands.^{71,72}

2.3.3. Selectivity of macrocyclic ligands

2.3.3.1 Ligand design

Much effort has been put into the design of macrocyclic ligands. One very effective method is to use the ligand as an ion size selective masking agent in the solvent extraction method. This effectively means that metal ions with a larger ionic radius, will be extracted at a higher pH. This method ensures for a selective separation of the metal ions.⁷³

There are a number of factors to consider when designing new macrocyclic ligands:¹³

- The SHAB character of the metal ion
- The metal ion radius
- The coordination number of the metal ion
- The geometry of the metal ion e.g. square planar, octahedral etc.
- The general affinity of the metal ion with a particular type of ligand e.g., OH^- , NH_3 , CH_2S^- etc.
- The ring size of the ligand
- The presence, bulkiness and density of steric groups on the ligand
- The induction effects of bridges between the donor atoms
- The chelate ring size

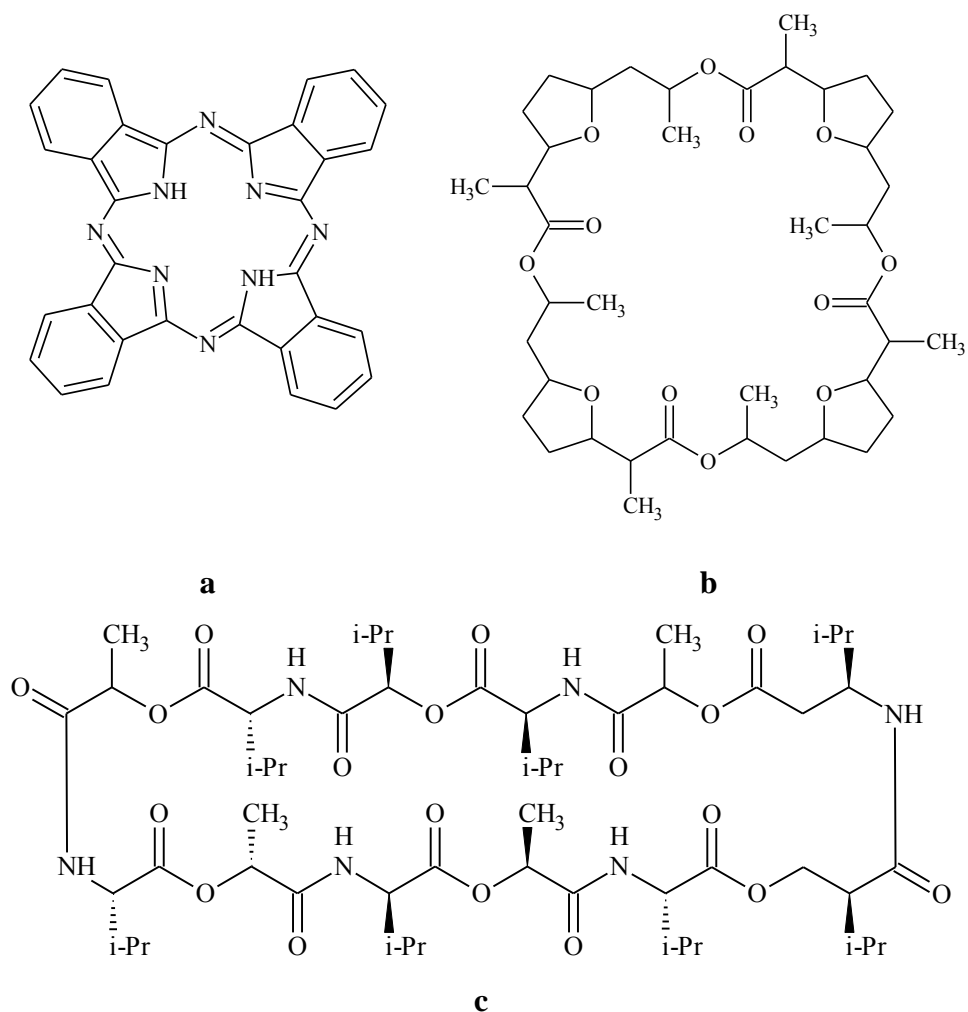


Figure 2.6 Examples of synthetic macrocycles: phthalocyanine (a) which can be used as semi-conductors, catalysts or colouring agents and natural antibiotics such as nonactin (b) and valinomycin (c).⁷⁴

“Pendant donor macrocycle” simply means that there are additional donor groups attached to the periphery of the macrocycle.⁷⁵ The reason for the use of these types of ligands is mainly to provide a set of non-labile macrocyclic donors which will serve to immobilize the metal ion along with a set of labile macrocyclic donors which can perturb the metal ions at additional coordination sites.⁷⁶ By adding pendant arms, there is double the amount of donor atoms and the donor atoms on the pendant arms can also be used as attachment points for other molecules.⁷⁶

Tri-azamacrocycles have three nitrogen atoms in the ring to which the pendant arms can attach. This gives the macrocyclic ligand the means for forming six coordinate complexes.

There are two distinct groups of facial donors: 1) the macrocyclic nitrogen donors and 2) the donor groups of the pendant arms. The pendant arms also provide the possibility of different alkylation moieties to be present in the same molecule. This addition means that the macrocyclic ligand can have hard-hard, soft-soft or hard-soft combinations in the donor atom configuration. By changing the length of the pendant arms, the coordination ring size will be altered, which means that the bite size of the ligand can be tailored to the exact size needed for the specific metal ion that needs to be accommodated. It is also possible to create 5- and 6-membered rings in the same structure, minimizing size-match selectivity.

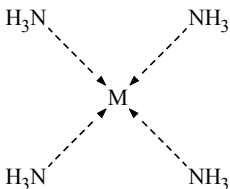
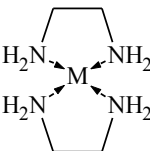
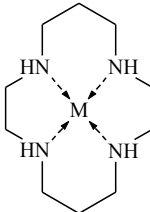
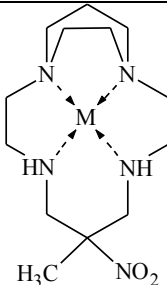
By introducing different donor atoms to the macrocycle, heterocyclic functionality gets build into the crown ring. This gives macrocycles with unsaturated nitrogen atoms a greater affinity for most transition and post-transition metal ions compared to the pure crown ethers.^{21,77,78}

A number of dual macrocyclic nitrogen/oxygen ligands have been synthesized. The complexes with these ligands were all 1:1 metal:ligand with the metal located in the cavity of the macrocycle. More specifically, when K^+ was introduced as the cation, it was found that the stability reduces as nitrogen is introduced into the ring. The stability constant decreased in the order $O > NR > NH$. With Ag^+ , the trend was completely reversed. It was therefore concluded that only electrostatic bonding is present with the potassium, whereas with silver both electrostatic and covalent bonding is present.

From table 2.2 it can be seen that the ligand field strength increases with donor atom basicity along the series $0^\circ < 1^\circ < 2^\circ < 3^\circ$ and

secondly, the increasing power of the nitrogen donor atoms of the ligands along the series $0^\circ < 1^\circ < 2^\circ < 3^\circ$. The bridges between the donor atoms produce an induction effect by “pushing” electrons towards the donor atoms and this will assist the donor atoms in donating electrons to the metal ion.¹⁰²

Table 2.2 A comparison between the ligand field strength of unidentate ligands, open chain bidentate ligands and macrocyclic ligands.¹⁰²

	0°	1°	2°	3°
				
$\Delta H[\text{Cu(II)}](\text{kcalmol}^{-1})$	-22.0	-25.5	-32.4	
$\nu(\text{d-d})(\text{cm}^{-1})\text{Cu(II)}$	17000	18300	19900	21050
$\nu(\text{d-d})(\text{cm}^{-1})\text{Ni(II)}$	~20000	21600	22470	23900

2.3.3.2 Metal ion selectivity of crown ethers (oxygen donors)

When Pedersen synthesized the first crown ethers, it was thought that the only correlation would be the size of the cation in question and the diameter of the macrocycle.⁷⁹ Hancock *et al.* pointed out that pre-organization and size-match selectivity is a total oversimplification for the complexation with metal ions.⁸⁰

It is important to note that there is considerable strain in a medium sized macrocyclic ligand.⁸¹ This strain can be problematic when smaller metal ions are targeted, since the macrocycle has a fairly rigid framework and cannot bend too much to accommodate the smaller metal ions. On the other hand, the much bigger crown ethers have much less strain in the framework and can bend and wrap themselves around smaller metal ions, or flatten out when larger metal ions need to be accommodated so that these metal ions can fit into the cavity of the crown ethers.

18-crown-6 has an estimated radius of between 1.8 – 2.2 Å. K^+ has an ionic radius of ≈ 1.96 Å.⁸² As expected, 18-crown-6 has a preference for K^+ , which might suggest some measure of size-match selectivity. Figure 2.7 shows the formation constants of 18-crown-6 plotted against different metal ion radii.

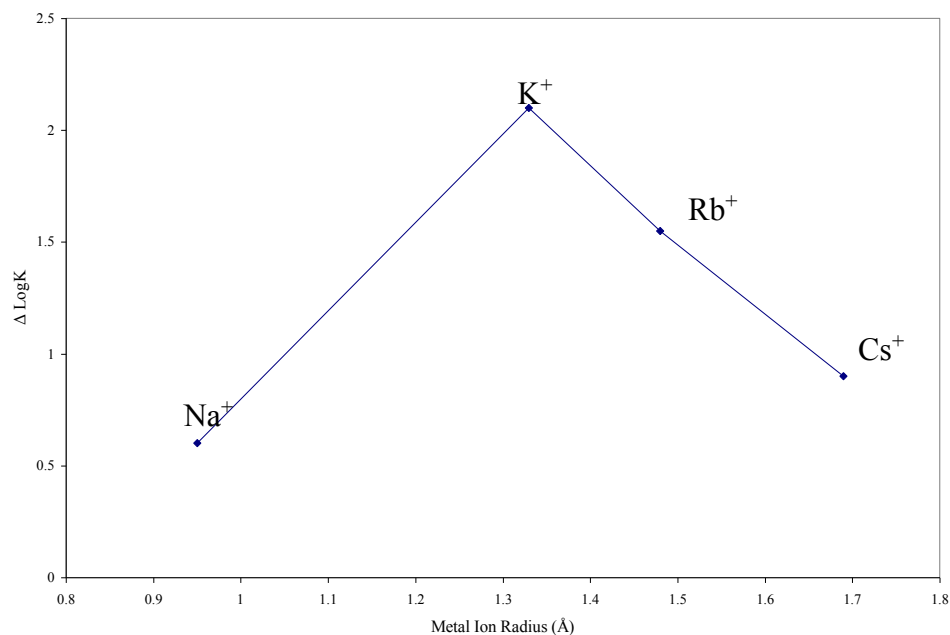


Figure 2.7 Differences in formation constants for 18-crown-6 for different metal ions in MeOH medium at 25 °C.

This idea however is not consistent over the broad spectrum of the crown ethers, for instance, 12-crown-4 is hardly influenced by the metal ion size. DCH30C10 forms a more stable complex with K^+ than with the larger Cs^+ . Large crown ethers can fold around the metal ions which create the idea that there are no real cavities and that their selectivity is mainly due to their torsional constraints. The cavities of both 12-crown-4 and 15-crown-5 are too small to allow metal ions to enter. This means that the metal ion must coordinate outside the cavity of the crown ethers. This type of coordination will influence the selectivity in much the same way as open-chain ligands. Figure 2.8 shows the formation constants of a variety of macrocyclic ligands with three different metal ions. From the data in figure 2.8 it is quite clear that there is hardly any evidence of size-match selectivity.

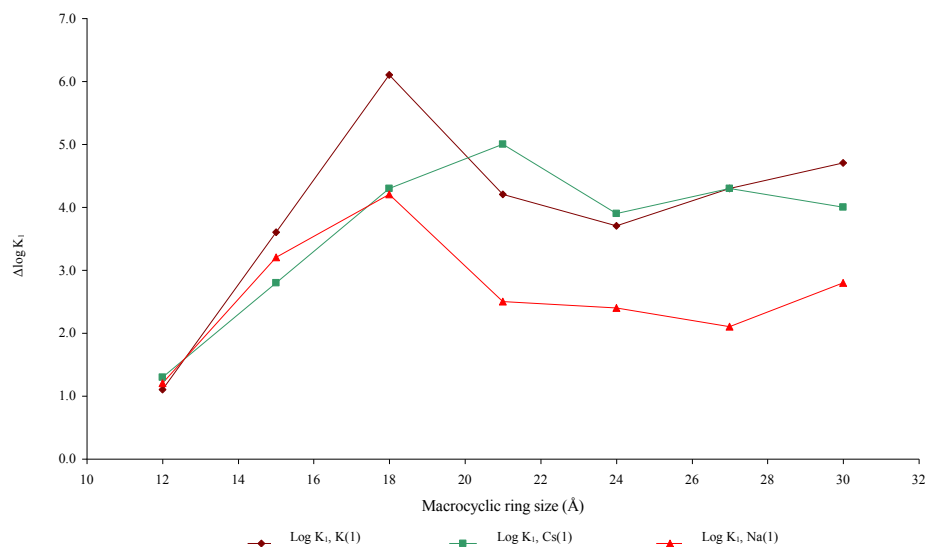


Figure 2.8 Formation constants of various macrocyclic ligands for K^+ , Cs^+ and Na^+ .

18-crown-6 is quite successful as a selective masking agent in the extraction of alkaline earth metal ions into certain organic solvents. Only 18-crown-6 shows some size match selectivity because of its preference for K^+ . This gives rise to the idea that 18-crown-6 is ion size selective, favouring the cations with a larger ionic radius. According to Gloe *et al.*, the soft metal ion, Hg^{2+} , shows a definite ring size effect. It was also found that hard metal ions such as Sr^{2+} are not, or only slightly extracted by ligands with nitrogen and oxygen donor atoms.⁸³ It is thus rather interesting then that 15-crown-5 and 18-crown-6 selectively extract Sr^{2+} from aqueous solutions as is reported in the literature.

Crown ethers are effective as masking agents in the aqueous phase, although not quite as effective when considering ion size selectivity. It must actually be emphasized that 15-crown-5 might not be so effective due to its smaller molecular weight and cavity size.⁷⁴

2.3.3.3 *Metal ion selectivity of azamacrocyclic ligands (nitrogen donors)*

Since ring-structured ligands are used, size match selectivity is a factor that must be considered. Nitrogen containing macrocycles need between 13 and 16 atoms in the ring to fully encircle a first row transition metal ion and the nitrogen donors must be situated in such a way that five-, six- or seven-membered rings will be formed on coordination.

Medium sized nitrogen donor macrocycles have cavities of a fairly fixed size⁸⁴ (0.85 Å – 0.95 Å) and should, at least in theory, display a much greater selectivity for metal ions on the basis of size-match selectivity than that of open chain polyamines.⁸⁵

Different tetra-azamacrocycles were used to investigate size match selectivity for various metal ions (figure 2.9). Pb^{2+} shows a steady decrease in the $\Delta\log(K)$ as the size of the macrocycle increases. Pb^{2+} , for instance, complexes more strongly with [12]-ane-N₄ which has a cavity much too small to accommodate Pb^{2+} . Zn^{2+} is considered a medium sized metal ion, and size match selectivity suggests that it should complex best with [15]-ane-N₄, yet it shows a weak preference for [12]-ane-N₄ which is rather small in comparison with [15]-ane-N₄. Size match selectivity would suggest that low spin Ni^{2+} would fit best in the cavity of [13]-ane-N₄, yet it complexes better with [14]-ane-N₄ which has a larger cavity than [13]-ane-N₄. Only Cu^{2+} and high spin Ni^{2+} follow the size match selectivity rule when tetra-azamacrocyclic ligands are used.

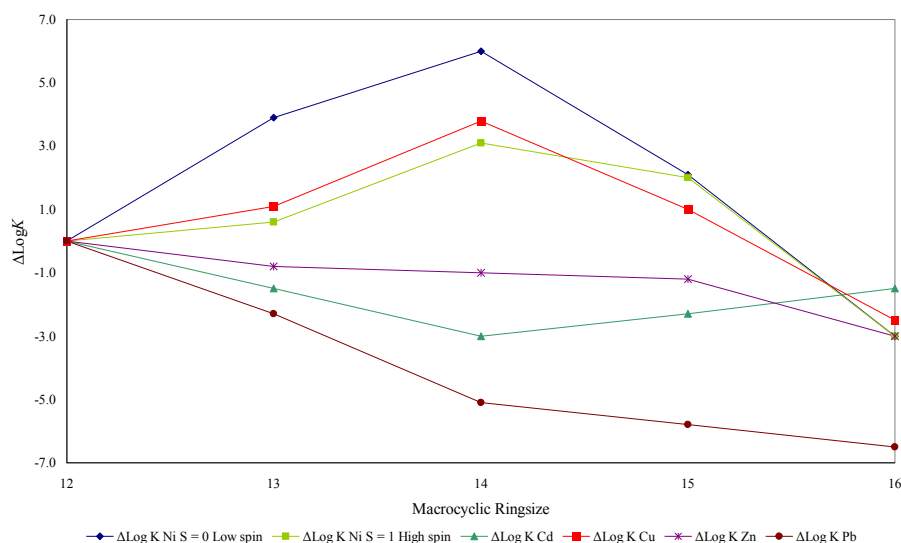


Figure 2.9 $\Delta\text{Log}K_1$ values versus nitrogen donor macrocyclic ring size for Ni^{2+} , Cd^{2+} , Cu^{2+} , Zn^{2+} and Pb^{2+} .

Tri-azamacrocycles differ from tetra-azamacrocycles in that the ligands are considered too small to have a cavity. The rings are also much more rigid than the tetra-azamacrocycles. Because the tri-azamacrocycles are so small, the metal ions do not lie in the plane of the ring, but coordinate above the ring. Therefore it is concluded that size match selectivity does not play a part when metal ions complex to tri-azamacrocycles.

2.4. Stability of Metal Complexes

The Irving-Williams series is one of the earliest correlations in the stability between metal complexes for a given ligand. The order for a given ligand is: $\text{Ba}^{2+} < \text{Sr}^{2+} < \text{Ca}^{2+} < \text{Mg}^{2+} < \text{Mn}^{2+} < \text{Fe}^{2+} < \text{Co}^{2+} < \text{Ni}^{2+} < \text{Cu}^{2+} > \text{Zn}^{2+}$. Ligands and metals were now being classified as type (a) or type (b) according to their preferential bonding (table 2.3).⁸⁶ Pearson suggested the terms hard, for type (a) and soft, for type (b).⁸⁷ Type (a) are the alkali metals, alkaline earth metals and lighter transition metals in higher oxidation states such as Ti^{4+} , Cr^{3+} , Fe^{3+} , Co^{3+} and H^+ . Type (b) metal ions are the heavier transition metals and those in lower oxidation states such as Cu^+ , Ag^+ , Hg^+ , Hg^{2+} , Pd^{2+} and Pt^{2+} . Type (a) metal ions prefer to bind to type (a) ligands and type (b) metal ions prefer to bind to type (b) ligands.⁸⁶

Table 2.3 The stability of a few complexes that are mentioned in the Irving-Williams series.^{85,87}

Tendency to complex with class (a) metal ions	Tendency to complex with class (b) metal ions
N >> P > As > Sb	N << P > As > Sb
O >> S > Se > Te	O << S < Se ~ Te
F > Cl > Br > I	F < Cl < Br < I

The strength of a metal complex is of great importance in all fields whether medical or industrial, for it is necessary to know how easy it is to break the complex again for drug release or for the recovery of precious metals. The determination of stability constants will give a very clear indication of how strong the ligand will attach itself to a specific metal ion.

Stability constants are an effective means of determining the affinity of a ligand for a specific metal ion. The determination of stepwise stability constants for monodentate ligands started with the formation of transition metal-ammonia complexes in aqueous solution. This work led to stability work on chelate compounds. (The same procedures are also used for the determination of protonation constants).

Stability constants are a quotient involving concentrations of, or activities of reacting species in solution at equilibrium.⁸⁸ The quantitative description of metal complex stabilities and equilibria are of concern in various fields such as environmental monitoring of toxic metals and medicinal agents based on metal ions.⁸⁹



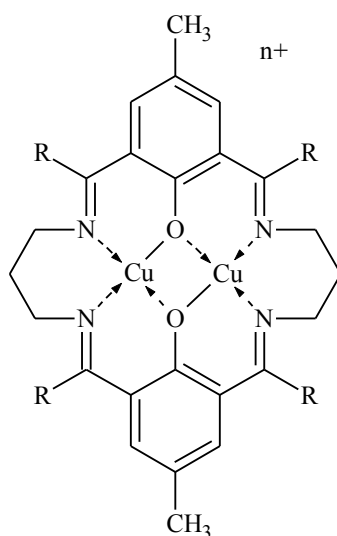
$$K_{eq} = \frac{a_C^\gamma a_D^\delta}{a_A^\alpha a_B^\beta} \quad (2.2)$$

Equation 2.1 is used for the general reaction for the determination of the stability constant. Equation 2.2 is used when concentrations or activities are being used.

It is clear that equation 2.2 is rather complicated to use, so it is common practice to measure stability constants at a constant ionic strength. This changes equation 2.2 into the simplified equation 2.3:

$$K_c = \frac{[C]^{\gamma}[D]^{\delta}}{[A]^{\alpha}[B]^{\beta}} \quad (2.3)$$

Ligand lability is lessened by the chelating effect which means that transition metal ions often experience strange environments and therefore also exhibit novel chemical properties. Another strange phenomenon is the fact that several metal ions may be held in close steric proximity within the same molecule (figure 2.10).⁹⁰



1. Cu(II)-Cu(II) $n = 2$, $R = H$
2. Cu(II)-Cu(I) $n = 1$, $R = H$
3. Cu(II)-Cu(I)(CO) $n = 1$, $R = H$
4. Cu(II)-Cu(I) $n = 1$, $R = CH_3$

Figure 2.10 The schematic structure of the mixed valence bi-nuclear Cu(II)-Cu(I) complex. (Gagné, Koval and Smith).⁸⁸

Zompa and Margulis⁹¹ found that the thermodynamic and spectroscopic properties of transition metal complexes of the cyclic tri-amine 1,4,7-triazacyclononane ([9]-ane-N₃), are quite unusual because they are far more stable than the corresponding complexes containing facially coordinated tri-amines. They also ascribed the thermodynamic stability to the cyclic nature of the ligand and its associated large configurational entropy contribution. Yang and Zompa⁹² postulated that the observed spectroscopic behaviour can be attributed to a huge trigonal distortion (elongation of the C₃ axis of symmetry from octahedral geometry), but they could

not prove this postulation. This distortion was later proven by Zompa and Margulis⁹¹ through X-ray diffraction studies.

Belal and co-workers⁹³ stated that 1,4,7-tri-azacyclononane (TACN) is too small to form equatorial complexes, unlike 14-ane-N₄ (cyclam) for instance. TACN must coordinate in a facial configuration giving *bis* complexes which have a sandwich structure⁹¹ or mono-complexes with a piano-stool structure.⁹⁴

As can be seen from the stability constants previously discussed, the addition of pendant arms produce ligands with much greater stabilization for the complexes of larger metal ions such as Cd²⁺ [radius = 0,97Å] for instance. The stability constants were determined by Sayer and co-workers⁹⁵, using glass electrode potentiometry and polarography. When compared, it is interesting to note that the stability constants of 1,4,7 tris-(2-hydroxyethyl)-1,4,7-triazacyclononane (THETAC) are just as high, or even higher than the parent macrocycle, [9]-ane-N₃, which suggests that it is hexadentately coordinated to the metal ions.⁹⁵ The complexes with the post transition heavy metal ions are held together by O...H...O hydrogen bonds.⁹⁶

2.5. The Chelate and Macrocyclic Effect

Metal chelates are defined as cyclic organo-metallic compounds in which the metal is part of one or more, five- or six-membered ring(s).⁹⁷

Macrocyclic complexes have an unusual stability and this is attributed to the fixed geometrical placement of the ligand donor atoms according to Busch and co-workers (1971).⁹⁸ This effect was first illustrated with cyclic tri-amine. Yang and Zompa⁹² presented further proof of the coordination strength of cyclic tri-dentate amines by determining formation constants of Ni²⁺, Cu²⁺ and Zn²⁺ complexes. Lindoy⁹⁹ stated three reasons why macrocyclic ligands often yield complexes with unusual properties. Firstly, on complex formation, geometrical factors, arising from the cyclic nature of the ligands, often impose additional constraints on the position of the donor atoms. Secondly, if the macrocycle is fully conjugated and incorporates $(4n+2)\pi$ electrons, then enhanced electron delocalization and ligand stability are characteristic of the resulting Hückle aromatic system. Thirdly, macrocyclic ligand

complexes are almost always found to be more stable thermodynamically and kinetically than their open chain analogues. These properties are intrinsic features related to the cyclic nature of the ligands, known as the macrocyclic effect.⁹⁹

Martell and Hancock¹⁰⁰ state four factors that play a role in the origin of the macrocyclic effect:

- Macrocyclic ligands are pre-organised whereas “chainlike” ligands have free moving ends. This means that the free macrocyclic ligand has only a limited number of conformers. Some of these conformers have structures that are similar to the conformation required to complex to the metal ion.
- Desolvation of the donor atoms in the ring of the macrocycle is easier and faster, because there are normally fewer solvent molecules accommodated in the cavity due to the confined space.
- The induction effect of the carbon bridges between the donor atoms will cause the ligand to be more basic.
- Enforced repulsion between the lone pairs of electrons of the donor atoms in the cavity of the macrocycle which is released when the metal complex is formed.¹⁰⁰

It was previously suggested that the macrocyclic and the chelate effect have a common origin. This hypothesis was later disproven for it is not possible to ascribe a single origin to the macrocyclic effect. It is therefore clear from the law of thermodynamics that there is a direct relation between K , ΔH and ΔS .¹⁰¹

$$\Delta G = \Delta H - T\Delta S \quad (1.4)$$

$$\Delta G = -RT \ln K \quad (1.5)$$

$$\frac{d(\ln K)}{dT} = \frac{\Delta H}{RT^2} \quad (1.6)$$

When a unidentate ligand (figure 2.11 A) attaches itself to a metal ion, it does not affect the second, or for that matter any of the other ligands, for they are still free to move without any restrictions throughout the entire solution.

The chelate effect was proposed by Schwarzenbach in terms of a bidentate ligand, which stated that when the first donor atom had attached itself to the metal ion, the second donor atom is now confined to move only in a restricted volume (figure 2.11 B). As can be seen from this model, the entropy of the donor atoms (of the bidentate ligand), is greatly reduced compared to that of the unidentate ligands. According to Schwarzenbach, the chelate effect would prove itself as a more favourable entropy complex forming agent than would be the case for the analogous unidentate complex forming agents. It would therefore also appear that the stability of complexes with larger chelate rings would be of lower complex stability than those of five - or six membered chelate rings due to the larger volume to which the chelate ring would be restricted when coordinated to the metal ion by only one donor atom. This might appear to be true in general, but it seems to be in disagreement with the observation that was actually made. The decrease in the formation constant that occurs as the chelate ring increases in size, is an entropy effect for ligands with a ring size of seven or more, whereas for the chelate ring sizes less than seven, it is predominantly an enthalpy effect. Considering the schematics of figure 2.11, it was tempting to think that entropy is the driving force behind the reactions concerning macrocycles.¹⁰²

This assumption was almost completely wrong. From data collected by Martell and Hancock¹⁰², it was shown that both enthalpy and entropy contribute to the macrocyclic effect.

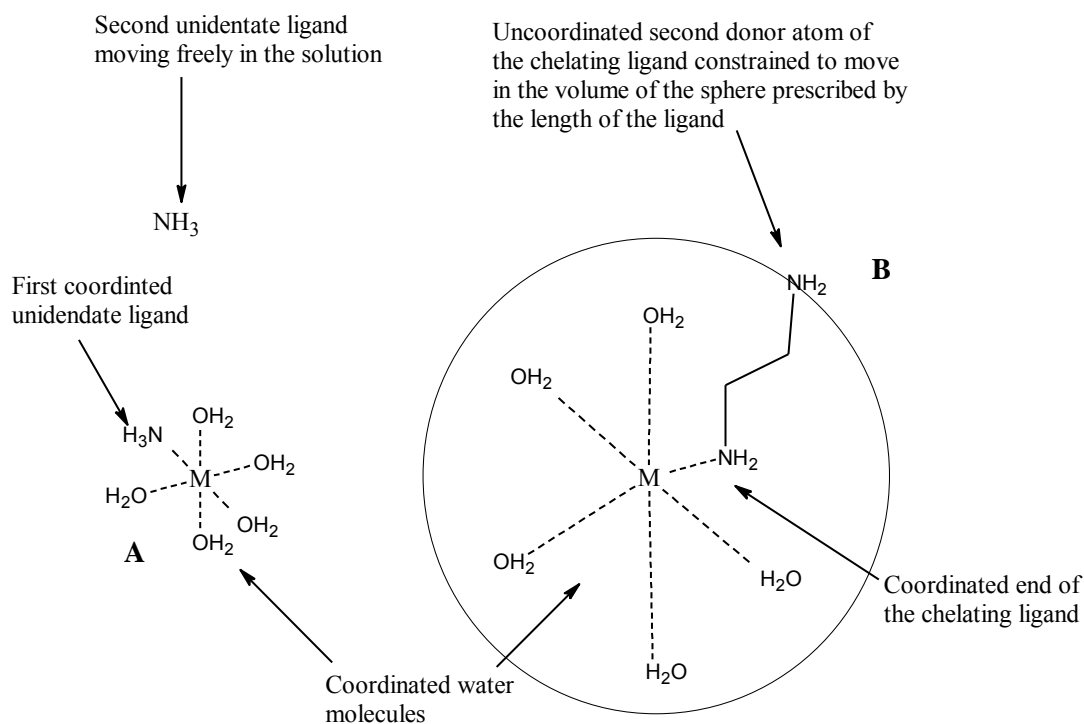


Figure 2.11 The Schwarzenbach model of the chelate effect.

Ring size and the solvation of the macrocycle must also be taken into consideration. As can be seen, this is again linked to the entropy effect.¹⁰¹ It is thus clear that a single factor cannot be considered alone when macrocyclic complexes are formed.

Size-match selectivity is an oversimplification of factors that control the selectivity of macrocycles for metal ions. Just because some metal ions have the same radius as the fixed cavity of the macrocycle, it does not necessarily mean that it will form the best or strongest complex. To form the complex, the metal ion must make either a six membered or a five membered ring to keep the strain as low as possible. It is known that five-membered chelate rings favour larger metal ions and six-membered chelate rings favour smaller metal ions with the series of tetra-azamacrocycles.^{103, 104}

The torsion angles in cyclohexane in the chair conformation are all 60° . The bond angles are all ideal at 109.5° . This is the most stable conformation because the strain energy is at a minimum. This gives the cyclohexane ring a “bite size” of 2.5 \AA when forming a six-membered ring (figure 2.12) with smaller metal ions for example. Larger metal ions prefer to form five-membered rings. Since all the bond angles and bond lengths remain unchanged, the “bite-size” is the only parameter that will change to 2.8 \AA (figure 2.12).

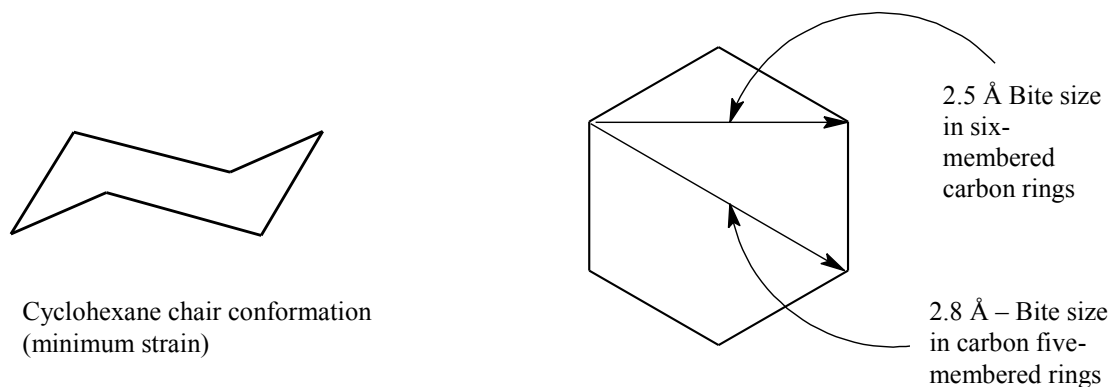


Figure 2.12 The chair conformation and bite sizes for cyclohexane.

With nitrogen donor atoms (figure 2.13), the bond lengths between the metal ions and the donor atom are 1.6 Å and 2.5 Å respectively in the six- and five-membered rings. The bond angles are 109.5 ° and 69 ° respectively in the six- and five-membered rings, which makes the geometry very favourable, keeping the strain energy at a minimum, when coordinated to the metal ions.^{13, 103}

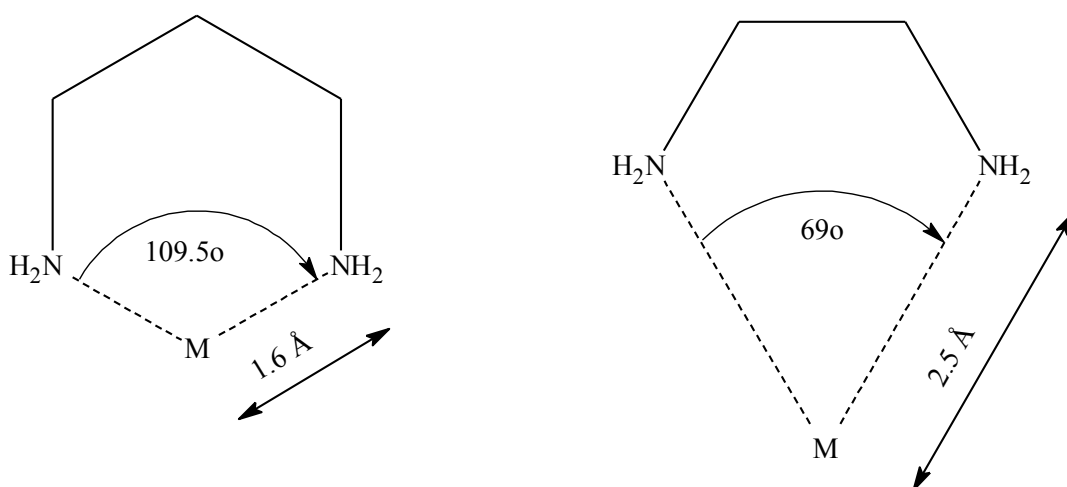


Figure 2.13 The ideal bond lengths and bond angles with five and six membered chelate rings are shown.

When the nitrogen donor atoms in the ring are exchanged with oxygen donors, the angles change considerably. In the six-membered metal coordination ring, the C-O-C angle changes from the ideal 109.5° to 126°. The bond lengths between the metal ion and the two oxygen donor atoms increase from 1.6 Å with the nitrogen donors, to 1.9 Å in the six-membered chelate ring with oxygen donors (figure 2.14). The bond lengths in the five-membered chelate ring also changed considerably when the

nitrogen atoms are changed to oxygen donors. As can be seen in figure 2.14, the bond lengths increased from 2.5 Å between the nitrogen donors and the metal ion, to more than 3.2 Å when oxygen donors are used.¹³

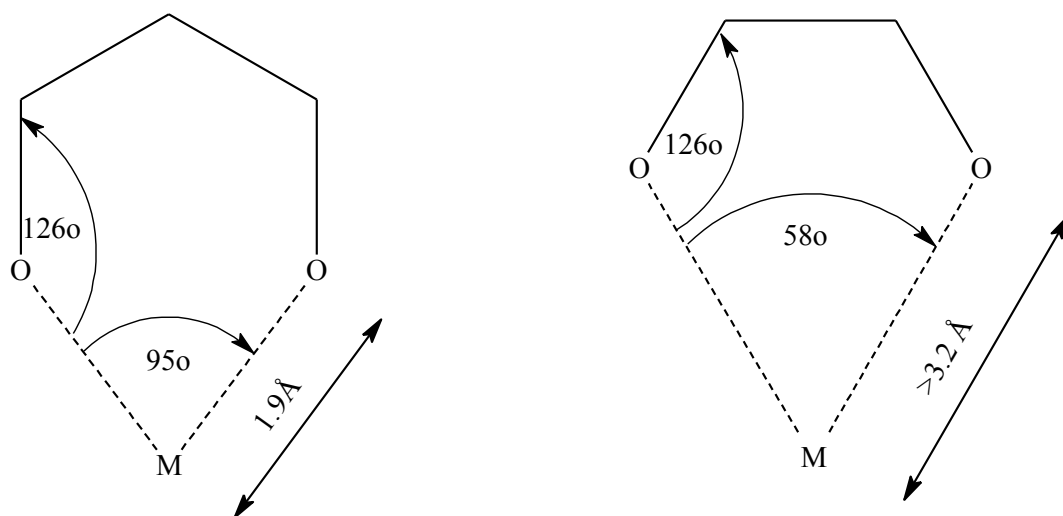


Figure 2.14 Smaller metal ions require a six-membered ring for minimum strain in the ring. For larger metal ions to maintain minimum strain energy, a five-membered ring is required.

In the five-membered ring, the M-O-C bond angle is the same as in the six-membered ring at 126°.¹³

As can be seen from the discussion above, it is clear that there are considerable differences between neutral oxygen donor ligands and neutral nitrogen donor ligands. Neutral nitrogen donor ligands tend to form as close to tetrahedral structures as possible when coordinated to a metal ion, while oxygen donor rings tend to prefer a trigonal planar geometry, most probably because oxygen has a sp^2 hybridisation, and thus very little strain in the ring.¹³

2.6 Silica as an Immobilization Substrate

The ability of porous solids is of great scientific and technological significance due to their interactions with atoms, ions and molecules. One of the most exciting discoveries in the field of material synthesis is the formation of mesoporous silicate sieves with liquid crystal templates. M41S silica was discovered in 1992 and since then has attracted much attention because of their large surface areas, well-defined pore structures, inert framework and non-toxicity. A series of inorganic silica meso-

structures such as M41's, HMS and SBA-n have been synthesized by different methods and their applications range from catalytic supports in fine chemistry and pharmaceutical chemistry to the production of special polymer products. Yu and Zhai stated (rather contradictory), that the full potential of these materials has been hampered because they are not very stable.¹⁰⁵ Zhao and co-workers¹⁰⁶ developed SBA-15 and this compound had greater thermal and chemical stability than MCM-41.

Microporous ($\leq 20 \text{ \AA}$) and mesoporous ($\sim 20 - 500 \text{ \AA}$) inorganic solids have found great use as catalysts and sorption media. MCM-41 and SBA-15 have periodically ordered structures which consist of two-dimensional arrays of uniform mesopores.¹⁰⁷ The pore size distributions for these two solids are very narrow.¹⁰⁸

M41S has large channels from 1.5 to 10 nm, ordered in hexagonal (MCM-41), cubic (MCM-48) and laminar (MCM-50) arrays. M41S has long-range order and surface areas above $700 \text{ m}^2 \cdot \text{g}^{-1}$. Of all the M41S members, MCM-41 is considered to be the most important.¹⁰⁹ It is because of these properties that mesoporous materials can be used as catalysts^{110, 111}, for adsorption^{112, 113}, separation^{114, 115} and chemical sensing.^{116, 117} The immobilization of extraction ligands on silica supports have far more advantages than immobilization on organic polymer supports. Some of the advantages are: short time for equilibration, excellent swelling resistance in different solvents and easy modification of the surfaces.¹¹⁸

There is an increasing utilisation of mechanically stable synthetic matrices as solid supports. Solvent impregnated resins and chelating polymeric resins were used for the extractive concentration of metal ions from aqueous solutions and waste water. Silica gels in particular lend themselves to be modified as such supports. The surfaces are modified either by impregnation of organic ligands directly onto the surface, or by covalent grafting through spacer units for metal ion extraction purposes.¹¹⁹ Inorganic supports have also been used successfully as stationary phases for extraction chromatographic separation.¹²⁰ Since the mid 70's, major efforts have been made to immobilise different chelating agents on silica gels by covalent bonding.^{121,122} Izatt and co-workers were some of the first groups to immobilize macrocyclic ligands onto silica gel in 1988.^{123,124,125} These studies

concentrated mainly on the immobilisation of crown ethers and not so much on aza-macrocycles.¹²⁶

The selectivity of the surface with the immobilised functional groups depends on the size of the modifier,¹²⁷ the activity of the loaded group^{128,129} and the SHAB characteristics of the donor atoms.

The immobilisation of molecules on various supports has been studied previously by Buszewski and co-workers¹³⁰ and Bermudez and co-workers.¹³¹ The preparation of modified silicas with a reagent adsorbed was found to be rather easy, and their chemical-analytical properties are not affected by the sorbent with covalent grafted reagents. These types of solid-phase reagents have huge possibilities for analytical work in varied applications.¹³² The active hydrogen atom of the silanol groups on the silica substrates has the ability to react with organosilyl groups to give some organic nature to the precursor inorganic carrier. These are covalent bonds and these bonds are resistant to removal from the surface by organic solvents or even water. The immobilisation of the desired reactive groups causes the silica gels to have a wide variety of uses. It can be used as an ion exchanger, stationary phases in chromatography, enzyme catalysts, and metal ion extractors, heterogeneous catalysts or even in the use of biotechnological processes.¹³³

To obtain a specific modified support depends on the synthetic method used. These methods can be altered to include reactive centres, for instance, oxygen, nitrogen, sulphur and phosphorus. These atoms can be disposed in the backbone chains of the silica gel supports, in order to enable the surface to be modified so that it can act in a variety of applications.¹³⁴ A huge variety of anchored molecules on the silica supports, contain oxygen and nitrogen, or a combination of the two, gives the modified silica surfaces the ability to extract cations from aqueous and non-aqueous solutions.¹³³

Packings with chemically bonded phases are obtained by substitution reactions between the modifiers and the accessible silanol groups on the surfaces of the silica supports. Stable covalent bonds are formed because of these interactions. The silanol groups can be arranged in three different ways namely, isolated, geminal or vicinal. These groups co-exist with siloxane groups on the surfaces. Different

supports have different structures. Globular is characteristic for narrow pore silica gel while macro- and gigaporous silica gels are more sponge-like. In theory, the optimal support must have a pore diameter of $12 (\pm 0.5) \text{ nm}$, a pore volume of $1.2 (\pm 0.1) \text{ cm}^3 \cdot \text{g}^{-1}$ and a surface area of $320 (\pm 20) \text{ m}^2 \cdot \text{g}^{-1}$.¹³⁵

It was found that the covalent bond attached to the surface will prevent the attached molecule from detaching itself from the support, thus providing a stable matrix (figure 2.15). It must be stressed that the chemical and analytical properties of the chelating agent, including the complex forming ability may differ from the free ligand to that of the same ligand immobilised on a solid support.¹³⁶ Another factor to remember is that, by introducing organic functional groups to the silica surface, the partial conversion of the silanol groups will be changed to a new organo-functional surface that will now possess organophilic properties. This may be the reason why the immobilized ligands and the support surface functions may be totally different from the original molecules.¹³⁷

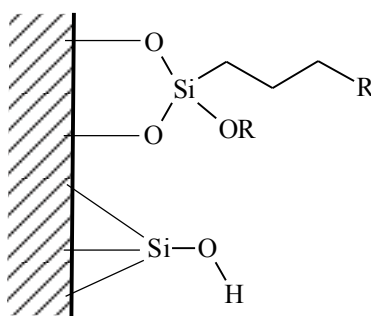


Figure 2.15 A chelating molecule that is directly immobilised on the silica surface will produce steric hindrances at the silanol site. A spacer attached to the support will provide attachment for a chelating molecule which can maximise the affinity for the metal ion.¹¹⁹

The reasons for choosing silica supports for the immobilization of tailored ligands, are:

- a great variety of silylating agents are available to allow functional groups in the inorganic framework^{130,138}
- it is easier to attach spacer molecules on silica than on organic polymeric supports¹³⁸
- it has a high specific surface area with a constant composition which makes analysis and interpretation of results easy¹³⁸

- d) silica has high mass exchange characteristics and no swelling¹³⁹
- e) silica has a great resistance to organic solvents^{138,140}
- f) silica has very high thermal stability¹⁴¹
- g) the support must be preferably mono-functional to avoid interactions of metal ions with other types of chelating groups¹⁴²
- h) fast binding kinetics as well as fast regeneration kinetics are required¹⁴²

According to Warshawsky in 1981,¹⁴³ to have high mass transfer rates, impregnated resins should have high mobility of the extractant in the resin phase, high mobility of the metal ion between the resin and the aqueous phase and a high hydrophilic balance of the resin.¹⁴⁴

There are also some disadvantages to consider when silica is used as an immobilising agent. There might be irreversible binding of metal ions as well as a lack of selectivity on repeated use.^{145,146} Silica is also not very stable toward alkaline conditions because it dissolves very easily above pH 9.¹⁴¹

Silica is a polymer of silicic acid, consisting of inter-linked SiO_4 in a tetrahedral fashion (figure 2.16). Silica gel is a porous, granular form of silica and there are three fundamental parameters in surface area characterisation:¹¹⁹

- Specific surface area ($\text{m}^2 \cdot \text{g}^{-1}$)
- Specific pore volume; distribution of pore size or pore area
- Particle size

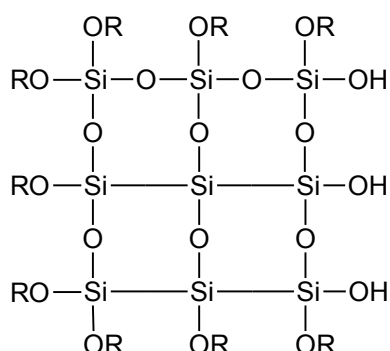


Figure 2.16 Schematic view of the silica support.

In order to use silica as a support, the surface needs to be modified. Silica surfaces can be modified in two different ways. The first process is by organo-

functionalization. This is where the modifying agent is an organic group. The second method is by inorganic-functionalization where the anchored group on the surface can be an organo-metallic composite or a metal oxide. In the conventional covalent grafting procedure, the surface hydroxyl groups are chemically reacted with commercial silane coupling reagents that will act as a precursor for further immobilisation of the organic molecules.¹¹⁹

Bradshaw *et al.*¹⁴⁷ found that the $\log K$ values for the immobilized crown ether complexes of several metal ions were almost the same as for the free macrocycle. According to this observation, the extraction of other metal ions should not be influenced in any major way when macrocyclic crown ethers are immobilised on silica surfaces.

Brunel *et al.*¹⁴⁸, and Cauvel *et al.*¹⁴⁹ managed to anchor primary and secondary amines to the surface of MCM-41. The product that was obtained was found to be active and selective for carrying out Knoevenagel condensation reactions. It is also useful for the preparation of monoglycerides, starting from 2, 3-epoxy alcohols and fatty acids.¹⁰⁹

SBA-15 can be prepared over a wide range of uniform pore sizes (up to 300 Å) and pore wall thicknesses. The thick silica walls are different from the thinner MCM-41 walls. This difference leads to greater hydrothermal stability on the part of the SBA-15 in comparison with MCM-41.

HMS also has thicker pore walls, higher thermal stability and a smaller crystallite size than MCM-41. An ordered hexagonal structure, like that of MCM-41, is almost totally absent. HMS has an exclusive wormhole channel motif instead.

Because of its large internal surface area, and relatively large external area, it was decided that these types of silica supports (Si gel (60 Å, MCM-41, SBA-15 and HMS) are well suited to be used as supports for organic ligands.

Not much is known about the behaviour of SBA-15 and HMS when used as support surfaces for immobilized ligands.

2.7. Conclusion

Three factors were taken into consideration when the silica supports were chosen: 1) the ligands that will be used, 2) the size of the cavity of the ligand and 3) the coordination-geometry.¹⁵

By attaching the ligands to the supports, it is hoped that the ligands will retain their original functionality while the supports will help with the recovery of these ligands. The use of the different supports will help to identify which of the supports will accommodate the optimal amount of ligand without interfering with the extraction capabilities of the ligands.

References

- ¹ M. Sakama *et al.*, *J. Radioanal. Nucl. Chem.*, 2007, **273**, 187
- ² T.G. Kazi *et al.*, *Anal. Bioanal. Chem.*, 2005, **383**, 297
- ³ H.A. Essaway and H.S Ibrahim, *Reactive & Functional Polymers*, 2004, **63**, 421
- ⁴ G-Z. Fang J. Tan and X-P. Yan, *Anal. Chem.*, 2005, **77**, 1734
- ⁵ J.W. Patterson in *Metal Speciation and Recovery*, Lewis Publishers, Inc.: Chelsea, MI, 1987
- ⁶ N.V. Deorkar and L.L. Tavlarides, *Ind. Eng. Chem. Res.*, 1997, **36**, 399
- ⁷ G. Guibaud, E. van Hullebusch and F. Bordas, *Chemosphere*, 2006, **64**, 1955
- ⁸ J.M. Weeks *et al.*, *J. Chem. Soc., Dalton Trans.*, 2001, 2157
- ⁹ E.Cole *et al.*, *J. Chem. Soc., Dalton Trans.*, 1994, 1619
- ¹⁰ J.Huskens and A.D. Sherry, *J. Chem. Soc., Dalton Trans.*, 1998, 177
- ¹¹ F. Li *et al.*, *J. Chem. Soc., Dalton Trans.*, 2006, 5396
- ¹² L.L. Parker *et al.*, *Bioorg. Med. Chem.*, 2005, **13**, 2389
- ¹³ A.E. Martell and R.D. Hancock in *Metal Complexes in Aqueous Solutions*, Plenum Press, New York, 1996, pp. 149 – 184
- ¹⁴ L. Sabatini and L. Fabbrizzi, *Inorg. Chem.*, 1979, **18**, 438
- ¹⁵ S. Akita and H. Takeuchi, *J. Chem. Eng. Jpn.*, 1990, **23**, 439
- ¹⁶ J.J. Christensen, D.L. Eatough and R.M. Reed, *Chem. Rev.*, 1974, **74**, 351
- ¹⁷ A. Casnati *et al.*, *J. Am. Chem. Soc.*, 2001, **123**, 12182
- ¹⁸ D.C. Stepinski *et al.*, *Green Chem.*, 2005, **7**, 151
- ¹⁹ P.D. Beer, P.K. Hopkins and J.D. McKinney, *Chem. Commun.*, 1999, 1253
- ²⁰ B.B Green and R.D Hancock, *J. S. Afr. Inst. Min. Metall.*, 1982, **82**, 303
- ²¹ K.Gloe *et al.*, *Coord. Chem. Rev.*, 2001, **222**, 103
- ²² S.K.Mundra, S.A. Pai and M.S. Subramanian, *J. Radioanal.Nucl. Chem.*, 1987, **116**, 203
- ²³ N.V. Deorkar and S.M. Kopkar, *J. Radioanal.Nucl. Chem.*, 1989, **130**, 433
- ²⁴ M. Shamsipur, A.R. Ghaisvand and Y. Yamini, *Anal. Chem.*, 1999, **71**, 4892
- ²⁵ M. Shamsipur, A.R. Ghaisvand and Y. Yamini, *Anal. Chem.*, 1999, **71**, 4892
- ²⁶ J.A. Howarter and J.P. Youngblood, *Macromolecules*, 2007, **40**, 1128
- ²⁷ All the information was obtained from the MSDS from the various suppliers
- ²⁸ B. Grüner *et al.*, *New J. Chem.*, 2002, **26**, 867
- ²⁹ G. Tian *et al.*, *Solvent Extr. Ion Exch.*, 2005, **23**, 519
- ³⁰ C.M. Wai *et al.*, *Chem. Commun.*, 1999, 2533
- ³¹ B. Gupta, A. Deep and P. Malik, *Hydrometallurgy*, 2001, **61**, 65
- ³² S. Stenstrom, *Hydrometallurgy*, 1989, **1**, 159
- ³³ J. Kalemekiewicz, M.J F. Leroy and J.P. Brunette, *Solvent Extr. Ion Exch.*, 1991, **4**, 769
- ³⁴ S.K. Gogia, O.V. Singh and S.N Tandon, *Indian J. Chem.*, 1982, **Sect. A 21**, 942
- ³⁵ T. Jiang and Y. Su, *J. East China Inst. Chem. Technol.*, 1991, **17**, 9
- ³⁶ T. Sato, *Solvent Extr. Res. Dev. Jpn.*, 1994, **1**, 73
- ³⁷ A.M. Rodrigues, D. Gómez-Limón and F.J. Alguacil, *J. Chem. Technol. Biotechnol.*, 2005, **80**, 967
- ³⁸ B.F. Barnard (MSc Thesis), University of Stellenbosch, 2008

- ³⁹ A.E. Martell and R.D. Hancock in *Metal complexes in Aqueous Solutions*, Plenum Press, New York, 1996, p. 154
- ⁴⁰ K. Takeshita *et al.*, *Hydrometallurgy*, 2003, **70**, 63
- ⁴¹ B. Wassink, D. Dreisinger and J. Howard, *Hydrometallurgy*, 2000, **57**, 235
- ⁴² R.R Fenton *et al.*, *J. Chem. Soc., Dalton trans.*, 2002, 2185
- ⁴³ H.A. Essaway and H.S. Ibrahim, *Reactive & Functional Polymers*, 2004, **61**, 421
- ⁴⁴ T. Madrakian, A. Afkhami and A. Mousavi, *Talanta*, 2007, **71**, 610
- ⁴⁵ J.L. Domingo in *M.W. Corn (Ed), Handbook of Hazardous Materials*, Academic Press, London, 1993, pp.705-711
- ⁴⁶ R.J. Lewis in *Sax's Dangerous Properties of Industrial Materials*, Van Nostrand Reinhold, New York, 1996
- ⁴⁷ A.E.V. Gorden, J. Xu and K.N. Raymond, *Chem. Rev.*, 2003, **103**, 4207
- ⁴⁸ M. Shamsipur, A.R. Ghiasvand and Y. Yamini, *Anal. Chem.*, 1999, **71**, 4892
- ⁴⁹ J. Havel, M. Vrchlabsky and Z. Kohn, *Talanta*, 1992, **39**, 795
- ⁵⁰ S.Sadeghi and E. Sheikhzadeh, *J. Hazard. Mater.*, 2009, **163**, 861
- ⁵¹ G. Szigethy and K.N. Raymond, *Inorg. Chem.*, 2009, **48**, 11489
- ⁵² A.E.V. Gorden, J. Xu and K.N. Raymond, *Chem. Rev.*, 2003, **103**, 4207
- ⁵³ N. Kaltsoyannis and P. Scott in *The f-Elements*, Oxford Univesity Press: New York, 1999
- ⁵⁴ H. Hassaballa *et al.*, *Inorg. Chem.*, 1998, **37**, 4666
- ⁵⁵ M. Sakama *et al.*, *J. Radioanalytical and Neclear Chemistry*, 2007, **273**, 187
- ⁵⁶ P.L. Arnold *et al.*, *J. Am. Chem. Soc.*, 2006, **128**, 9610
- ⁵⁷ J. Xu and K.N. Raymond, *Chem. Rev.*, 2003, **103**, 4207
- ⁵⁸ T.M. Garrett, M.E. Cass and K.N. Raymond, *J. Coord. Chem.*, 1992, **25**, 241
- ⁵⁹ G. Szgethy and K.N. Raymond, *Inorg. Chem.*, 1999, **38**, 308
- ⁶⁰ E.C. Constable in *Coordination Chemistry of Macrocyclic Compounds*, Oxford University Press, New York, 1999, p. 1, 32
- ⁶¹ C.J. Pedersen and H.K. Frensdorff, *Angew. Chem. Internat. Edit.*, 1972, **11**, 16
- ⁶² S. Buøen *et al.*, *J.Chem. Soc. Chem. Commun.*, 1982, **20**, 1172
- ⁶³ Z. Stefanac and W. Simon, *Microchem. J.* 1967, **12**, 125
- ⁶⁴ L.A.R. Pioda, H.A. Wachter, R.E. Dohner and W. Simon, *Helv. Chim. Acta*, 1967, **50**, 1373
- ⁶⁵ E.C. Constable in *Coordination Chemistry of Macrocyclic Compounds*, Oxford University Press, New York, 1999, pp. 2, 10, 11
- ⁶⁶ L.F. Lindoy in *The Chemistry of Macrocyclic Ligand Complexes*, Cambridge University Press, New York, 1989, p. 3
- ⁶⁷ E.C. Constable in *Coordination Chemistry of Macrocyclic Compounds*, Oxford University Press, New York, 1999, p. 2, 8, 10
- ⁶⁸ L.F. Lindoy in *The Chemistry of Macrocyclic Ligand Complexes*, Cambridge University Press, New York, 1989, p. 2
- ⁶⁹ R.N. Greene, *Tetrahedron Lett.*, 1972, **18**, 1793
- ⁷⁰ M. Pinkerton, L.K. Steinrauf and P.Dawkins, *Biochem. Biophys. Res. Comm.*, 1969, **35**, 512
- ⁷¹ P.A. Tasker, P.G. Plieger and L.C. West, *Comprehensive Coordination Chemistry II*, 2004, **9**, 759

- ⁷² P.A.Tasker and V. Gasperov, *Macrocyclic Chemistry*, 2005, 365
- ⁷³ S. Tsurubou *et al.*, *Anal. Chem.*, 1995, **67**, 1465
- ⁷⁴ E.C. Constable in *Coordination Chemistry of Macrocyclic Compounds*, Oxford University Press, New York, 1999, pp. 4, 8
- ⁷⁵ K.P. Wainwright, *J. Chem. Soc., Dalton Trans.* 1980, 2117
- ⁷⁶ K.P. Wainwright, *Coord. Chem. Rev.*, 1997, **166**, 35
- ⁷⁷ J.S. Bradshaw *et al.* (Eds.) in *Comprehensive Supramolecular Chemistry*, vol. 1, Elsevier, Oxford, 1996, *Chemistry of Macrocyclic Compounds*, Oxford University Press, New York, 1999, pp. 21, 22pp. 35 – 95
- ⁷⁸ T.W. Bell *et al.* (Eds.) in *Inclusion Compounds: Key Organic Host Systems*, Oxford University Press, Oxford, 1991, pp 325 – 390
- ⁷⁹ R.N. Greene, *Tetrahedr. Lett.*, 1972, 1793
- ⁸⁰ R.D. Hancock *et al.*, *Coord. Chem. Rev.*, 2007, **251**, 1678
- ⁸¹ H. Koyama and T. Yoshino, *Bull. Chem. Soc. Jpn.*, 1972, **45**, 481
- ⁸² E.C. Constable in *Coordination Chemistry of Macrocyclic Compounds*, Oxford University Press, New York, 1999, pp. 21, 22
- ⁸³ K. Gloe *et al.*, *Coord. Chem. Rev.*, 2001, **222**, 103
- ⁸⁴ D.H. Busch, *Acc. Chem. Res.*, 1978, **11**, 392
- ⁸⁵ C.M. Madeyski, J.P. Michael and R.D Hancock, *Inorg. Chem.*, 1984, **23**, 1487
- ⁸⁶ J.E. Huheey, E.A. Keiter and R.L. Keiter in *Inorganic Chemistry, Principles of Structure and Reactivity*, HarperCollins College Publishers, New York, 1993, 344-346
- ⁸⁷ R.G. Pearson, *J. Am. Chem. Soc.*, 1963, **85**, 3533
- ⁸⁸ A.E. Martell and R.J. Motekaitis in *Determination and Use of Stability Constants*, VCH Publishers, New York, 1988, pp 1-31
- ⁸⁹ K.N. Raymond and J.M. McCormick, *J. Coord. Chem.*, 1998, **46**, 51
- ⁹⁰ R.R. Gagné, C.A. Koval and T.J. Smith, *J. Am. Chem. Soc.*, 1977, **99**, 8367
- ⁹¹ L.J. Zompa and T.N. Margulis, *Inorg. Chim. Acta*, 1978, **28**, L157
- ⁹² R. Yang and L.J. Zompa, *Inorg. Chem*, 1976, **15**, 1499
- ⁹³ A.A. Belal *et al.*, *J. Chem. Soc., Dalton Trans.*, 1989, 931
- ⁹⁴ P. C. Chaudhuri *et al.*, *Inorg. Chim. Acta*, 1984, **23**, 427
- ⁹⁵ B.A. Sayer, J.P. Michael and R.D. Hancock, *Inorg. Chim. Acta*, 1983, **77**, L63
- ⁹⁶ R. Luckay *et al.*, *Inorg. Chim. Acta*, 1996, **246**, 159
- ⁹⁷ D.A. Skoog, D.M. West and F.J. Holler in *Fundamentals of Analytical Chemistry*, Saunders College Publishing, Fort Worth, 1997, p. 95
- ⁹⁸ D.H. Busch *et al.* in *Adv. Chem. Ser.*, **100**, American Chemical Society Publications, Washington D.C., 1971, pp. 44 – 78
- ⁹⁹ L.F. Lindoy, *Chem. Soc. Rev.*, 1975, **4**, 421
- ¹⁰⁰ A.E. Martell and R.D. Hancock in *Metal Complexes in Aqueous Solutions*, Plenum Press, New York, 1996, pp. 101-105
- ¹⁰¹ E.C. Constable in *Coordination Chemistry of Macrocyclic Compounds*, Oxford University Press, New York, 1999, p. 55 – 59

- ¹⁰² A.E. Martell and R.D. Hancock in *Metal Complexes in Aqueous Solutions*, Plenum Press, New York, 1996, p. 64
- ¹⁰³ R.D. Hancock *et al.*, *Coord. Chem. Rev.*, 2007, **251**, 1678
- ¹⁰⁴ A.E. Martell and R.D. Hancock in *Metal Complexes in Aqueous Solutions*, Plenum Press, New York, 1996, pp. 77 – 82, 98 – 104
- ¹⁰⁵ H. Yu and Q-Z. Zhai, *Microporous and mesoporous Materials*, 2009, **123**, 298
- ¹⁰⁶ D.Y. Zhao *et al.*, *Science*, 1998, **279**, 548
- ¹⁰⁷ C.T. Kresge *et al.*, *Nature*, 1992, **359**, 710
- ¹⁰⁸ O. González *et al.*, *Catalysis Today*, 2009, **148**, 140
- ¹⁰⁹ A. Corma, *Chem. Rev.*, 1997, **97**, 2373
- ¹¹⁰ Sujandi, E.A. Prasentyanto and S.E Park, *Appl. Catal. A: Gen.*, 2008, **350**, 244
- ¹¹¹ Y. Lou *et al.*, *J. Catal.*, 2007, **247**, 245
- ¹¹² Y. Jiang *et al.*, *Micropor. Mesopor. Mater.*, 2007, **103**, 316
- ¹¹³ T.L. Lasseter *et al.*, *J. Am. Chem. Soc.*, 2004, **126**, 10220
- ¹¹⁴ E. Kim *et al.*, *Chem. Commun.*, 2008, **33**, 3921
- ¹¹⁵ V.J. Mayani *et al.* *Chromatogr.*, 2006, **A 1135**, 186
- ¹¹⁶ M. Zhou *et al.*, *Anal. Chem.*, 2008, **80**, 4642
- ¹¹⁷ M. Guan *et al.*, *Micro and Mesoporous Materials*, 2009, **123**, 193
- ¹¹⁸ O. Zaporozhets *et al.*, *Talanta*, 1999, **49**, 899
- ¹¹⁹ P.K. Jal, S. Patel and B.K. Mishra, *Talanta*, 2004, **62**, 1005
- ¹²⁰ T. Braun and G. Ghersi, *Extraction Chromatography*, Elsevier: Amsterdam, The Netherlands, 1975
- ¹²¹ J.R. Jezorek and H. Freiser, *Anal. Chem.*, 1979, **51**, 366
- ¹²² M.A. Marshall and H.A. Mottola, *Anal. Chem.*, 1983, **55**, 2089
- ¹²³ N.E. Izatt *et al.*, *Ind. Eng. Chem. Res.*, 2000, **39**, 3405
- ¹²⁴ J.S. Bradshaw *et al.*, *J. Chem. Soc. Chem. Commun.*, 1988, **60**, 812
- ¹²⁵ R.M. Izatt *et al.*, *Anal. Chem.*, 1988, **60**, 1825
- ¹²⁶ N.V. Deorkar and L.L. Tavlarides, *Ind. Eng. Chem. Res.*, 1997, **36**, 399
- ¹²⁷ M.L. Breuning *et al.*, *Anal. Chem.*, 1991, **63**, 21
- ¹²⁸ M.E Mahmoud, *Anal. Lett.*, 1996, **29**, 1791
- ¹²⁹ M.E Mahmoud and E.M. Soliman, *Talanta* 1997, **44**, 15
- ¹³⁰ B. Buszewski *et al.*, *J. High Resolut. Chromatogr.*, 1998, **21**, 267
- ¹³¹ V.Z. Bermudez, L.D. Carlos and L. Alcácer, *Chem. Mater.*, 1999, **11**, 59
- ¹³² O. Zaporozhets *et al.*, *Talanta*, 1999, **49**, 899
- ¹³³ M.R.M.C. Santos and C. Airoidi, *Journal of Colloid and Interface Science*, 1996, **183(2)**, 416
- ¹³⁴ H.J. Kim *et al.*, *J. Mater. Chem.*, 1993, **33**, 537
- ¹³⁵ B. Buszewski *et al.*, *J. High Resol. Chromatogr.*, 1998, **21**, 267
- ¹³⁶ S.B. Savvin and A.V. Mikhoilova, *Zh. Anal. Khim.*, 1996, **51**, 49
- ¹³⁷ U. Pyell and G. Stork, *Fresenius J. Anal. Chem.*, 1992, **343**, 576
- ¹³⁸ L.N.H. Arakaki *et al.*, *J. Colloid. Interface Sci.*, 2000, **228**, 46
- ¹³⁹ I.P. Alimarin *et al.*, *Talanta*, 1987, **34**, 103
- ¹⁴⁰ A.R. Sarkar, P.K.Dutta and M. Sarkar, *Talanta*, 1996, **43**, 1857

-
- ¹⁴¹ V.I. Lygin, *Kinet. Catal.*, 1994, **35**, 480
- ¹⁴² J. Kramer in PhD thesis *Chelating Ion Exchangers for the Recovery of Rhodium*, 2002
- ¹⁴³ A. Warshawsky, Extraction with Solvent-Impregnated Resins. In *Ion Exchange and Solvent Extraction*, J.A. Marinsky Y. Marcus, Eds., Marcel Dekker: New York, 1981, **Vol. 8**, pp 229-331
- ¹⁴⁴ N.V. Deorkar and Tavlarides, *Ind. Eng. Chem. Res.*, 1997, **36**, 399
- ¹⁴⁵ D.E. Leyden and G.H. Luttrell, *Anal. Chem.*, 1975, **47**, 1612
- ¹⁴⁶ T. Seshadri and A. Kettrupt, *Fresenius Z. J. Anal. Chem.*, 1982, **310**, 1
- ¹⁴⁷ J. S. Bradshaw *et al.*, *J. Chem. Soc., Chem. Commun.*, 1988, **12**, 812
- ¹⁴⁸ D. Brunel *et al.*, *Stud. Surf. Sci. Catal.*, 1995, **97**, 173
- ¹⁴⁹ A. Cauvel *et al.*, in *Organic Coatings; Proceedings of 53rd International Meeting of Physical Chemistry; American institute of Physics*: New York, NY, 1996, Vol. 354, p. 477

Chapter 3

The Synthesis and Immobilisation of the Macrocyclic Ligands

3.1 Introduction

Various methods and techniques for the synthesis of medium sized macrocyclic ligands have been reported by Koyama and Yoshino¹ in 1972, Yang and Zompa² in 1976, Sabatini and Fabbrizzi³ in 1979 and Madeyski, Michael and Hancock² in 1984. Brucher and co-workers⁴ also described the synthesis of a number of triazamacrocycles with carboxylate pendant arms in an attempt to determine the effect of the macrocyclic cavity size and rigidity on the complexation of the ligand.

3.2 Methods and Pathways of Synthesis

3.2.1. Template synthesis

A major problem that occurred in the synthesis of macrocyclic molecules was how to control the two ends of the chains to finalize the cyclization step. In the template synthesis method (figure 3.1), it is essential to have a metal ion present to keep the cyclic precursors in position prior to the formation of the macrocycle.^{5,6,7} The metal ion will coordinate to the donor atoms and pre-organise the various intermediates. The pre-organised intermediates will now be in the desired conformation to form the required macrocycle. In figure 3.1, the circles represent the mutually reactive functional groups and the squares are the donor atoms. The binding of the donor atoms pre-organise the chain into the desired conformation for cyclization to occur.⁸ Not all donor atoms are shown.

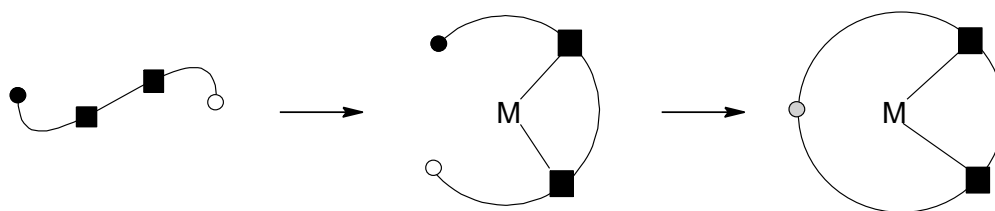


Figure 3.1 A schematic view of the cyclization step involved in a template macrocyclic synthesis.

The advantages of this method are good yields and obtaining a metal complex directly under very mild reaction conditions.⁸ Using the template synthesis, a metal complex is created and it would mean that the metal ion must first be removed before the ligand can be used for the desired extraction.

3.2.2. High dilution synthesis

Stetter and Roos reported a condensation reaction of terminal dihalides with bisulfonamide salts under high dilution conditions.⁹ The yields though were moderate to low. The macrocyclic ligands that were synthesised consisted of a ring system with two benzo rings connected with a carbon bridge to form the macrocycle (figure 3.2).

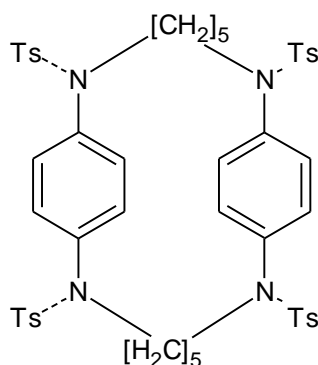


Figure 3.2 Bis-[N,N'-ditosyl-N,N'-pentamethylene-*p*-phenyldiamine] as synthesised by Stetter and Roos.⁹

Because the yield is not very high, it would not be the best method to use on an industrial scale.

3.2.3. Direct synthesis

By using the direct method of synthesis (figure 3.3), no metal ions are needed to keep the ends of the chains in the required positions prior to the formation of the macrocycle. This means that the donor atoms are free for coordination to the metal ions that are introduced to the solution. In figure 3.3, the circles represent the mutually reactive functional groups. In the first step, the appropriate conformation must be adopted so that the reactive functional groups are close to one another and in the correct orientation for reaction. Secondly, the new bond is formed and this will complete the macrocycle. The donor atoms have been excluded from the diagram.¹⁰

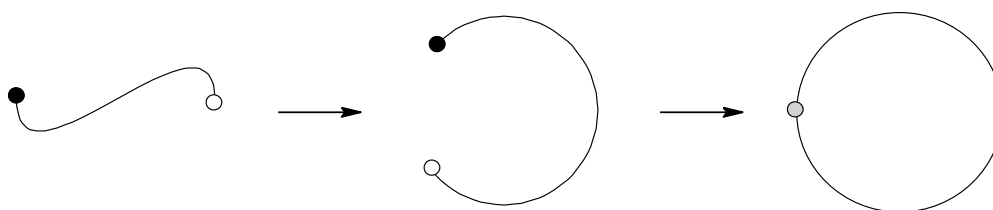


Figure 3.3 A schematic view of the cyclization step involved in a non-templated macrocycle synthesis.

Atkins, Richman and Oettle¹¹ thoroughly tested this method, and it was proven that the yields increased substantially and that it was possible to get rid of the high dilution method.¹² Searle and Geue¹³ proposed an improvement on the synthesis that was used by Richman and Atkins. Robb and Peacock¹⁴ also gave a full description of the method that they used in the synthesis of *N,N',N''*-tris[(*S*)-2-hydroxypropyl]-1,4,7-triazacyclononane. This method provided a way of creating macrocyclic ligands in high yields without forming metal complexes as with the template method, and thus the ligands can be used directly to complex with other metal ions that can be introduced to the solution.

3.2.4. Silica as an immobilization substrate

There are two different ways of immobilisation. The first method is the homogeneous method in which the silylant compound is first bound to the

inorganic carrier. The second route is the heterogeneous route and here the molecule is directly immobilised on the support through a silanizing agent.

All the supports that were used in this study, were analyzed and characterized by different techniques: BET surface area and low angle XRD analyses were conducted before immobilization of the ligands and after the immobilisation of the ligands, FTIR was done to determine whether the ligands were immobilized.

3.2.4.1. *Si gel (60 Å)*

Silica gel (60 Å) was bought from Sigma-Aldrich and has a particle size of 70 – 230 mesh and a pore diameter of 60 Å.

Silica gel is an inorganic, amorphous polymer of which the bulk consists of siloxane groups (Si-O-Si). The outside surface is made up of silanol groups (Si-OH). Commercial silica gel has very little silanol groups available for modification, therefore it is necessary to activate the silica gel prior to modification.

3.2.4.2. *MCM-41*

MCM-41 is a hexagonally ordered mesoporous molecular sieve, developed by a scientist from the Mobile Corporation in 1992.^{15,16,17} Depending on the alkyl chain length of the surfactant template and the synthesis conditions, the particle sizes may vary from 2 to 10 nm.¹⁵ Hexagonal mesoporous silicas, particularly MCM-41, have been investigated to explore potential applications,^{16,17,18} from catalysis,^{19,20} optically active materials,^{21,22} polymerisation sciences,^{23,24,25,26} separation technology^{17,27,28} and drug delivery.^{29,30,31,32,33} With the successful fabrication of hybrid mesoporous organosilicas, further applications seem very possible.^{34,35,36} The pore sizes of this class of materials has a relatively narrow distribution, ranging between 2 – 4 nm in diameter.³⁷

3.2.4.3. SBA-15

SBA-15 is a meso-porous molecular sieve with a large surface area and homogeneous pore diameters. It is nowadays commonly used as the basis for catalysts and adsorbants.¹⁵

Zhao and co-workers¹⁶ developed SBA-15, a material with a 2D hexagonal arrangement of pores, ranges from micro- to mesoporosity. SBA-15 can be prepared over a wide range of uniform pore sizes and wall thicknesses depending on the temperature at which it is prepared.¹⁶ The pores can be as wide as 30 nm.¹⁵ These properties give SBA-15 higher thermal and chemical stability.¹⁵ SBA-15 is a very attractive carrier because of its large surface area, well ordered meso-porous structure, tuneable pore sizes and volumes and well defined surface properties for modification.¹⁵

3.2.4.4. HMS

Of all the silica supports, HMS has the smallest surface area. It also has the smallest pore volume as well as the smallest pore diameters. Although HMS is smaller in all aspects, it can still be modified as a carrier for selective ligands. In certain aspects, it might even be a better support to use since the pores are very small and therefore will not allow too many molecules, solvent or metal, to enter into the pores, forcing them to complex to the ligands that are immobilised on the surface.

3.3 Experimental

3.3.1. Materials

All chemicals for the preparation of the ligands THTD and THTUD were bought from Sigma-Aldrich and used without further purification. The solvents that were used were dried and distilled to ensure ultra-purity. The (2-aminomethyl)-15-crown-5 (15-c-5) and (2-aminomethyl)-18-

crown-8 (18-c-6) were bought from Sigma-Aldrich and used without further purification.

Silica gel (60 Å) was bought from Sigma-Aldrich. The MCM-41, SBA-15 and HMS were prepared by Z. Gondongwana from the University of the Western Cape (UWC) and was analysed by BET to clarify its structure and surface areas. Activation of the different substrates was done by heating them to 50 °C under vacuum for 48 hours prior to use.

3.3.2. Instrumentation for analysis

3.3.2.1 FTIR

A Nexus FT-IR Thermo Nicolet instrument (ATR) was used to obtain the IR spectra of the immobilized ligands on the Si supports.

The FTIR was used since all the immobilized compounds that were synthesised are insoluble. There are very specific signals (NH, CN, CO) that are easily recognisable in the compounds that can confirm whether the desired product was formed or not.

3.3.2.2 NMR

Different instruments (below) were used to confirm that all intermediates and final products were indeed obtained and free from impurities.

All the intermediate products were soluble and the analysis was carried out (by a CAF technician) on the 600MHz: Varian Unity Inova 600.

The immobilized products are all insoluble and solid state NMR analysis was carried out on the 500MHz: Varian VMRS Wide Bore 500 Solids.



600MHz: Varian Unity Inova 600



500MHz: Varian VMRS Wide
Bore 500 Solids

Figure 3.4 The instruments that were used for the determination of the NMR spectra of the intermediate as well as the final products. The 600MHz was used for the soluble samples and the 500MHz was used for the solid samples.

Only the ^{13}C and ^{29}Si spectra were analysed to determine whether the ligands did attach to the silica and also the carbon will give the structure of the ligand.

3.3.2.3 X-ray diffraction

These studies were conducted to ensure that the products that were received from the co-workers are indeed the supports that were to be tested. The preparation and data collection was carried out by a CAF technician.

Instrument specifications: PANalytical X'Pert PRO MPD (Multi-Purpose Diffractometer) with X'Celerator detector and fixed divergence slits.

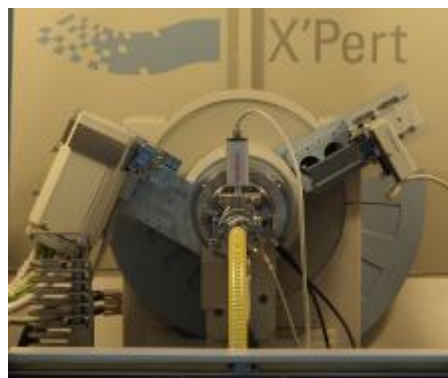
Source: Cu $K\alpha$ radiation

Optics: Fixed anti-scatter slits on incident and diffracted beams and Nickel filter and parallel plate collimator on diffracted beam optical attachments to allow parallel beam work.

Cryostat: Anton Paar TTK450 (with automated sample height adjustment) for non-ambient measurements from -193 °C to 450 °C in vacuum to -120 °C to 300 °C in inert gas



PANalytical X'Pert Pro MPD



Goniometer with variable temperature stage

Figure 3.5 The low angle powder XRD that was used for the determination of the diffraction patterns to confirm that the supports were indeed correct.

Low angle powder diffraction X-ray analyses were carried out to confirm the diffraction planes of the different Si supports.

3.3.2.4 BET

BET studies were conducted to determine the surface areas, pore sizes and pore volumes of the various silica supports. This will help in the determination of the amount of ligand that might be supported on the surface areas. The preparation and data collection was carried out by a technician.

3.3.2.5 TGA



TA Instruments Q500 thermogravimetric analyser

Figure 3.6 The thermogravimetric analyser that was used in the thermogravimetric analysis for the determination of the thermal stability of the immobilized products.

The TGA experiments were carried out on the immobilized ligands to determine the thermal stability of the ligands on the different supports. TGA is performed on samples to determine changes in weight in relation to change in temperature. Such analyses rely upon a high degree of precision in three measurements: weight, temperature, and temperature change. The samples were placed in the oven of the instrument and gradually heated from room temperature to 500°C over a time span of 60 minutes.

3.3.3. The direct immobilization of 15-c-5 and 18-c-6 to different silica substrates

The (2-aminomethyl) crown ethers (1.7×10^{-3} mol) were dissolved in approximately 10 mL of toluene and added to 0.45 g of the different silica substrates. The suspension was then stirred for 48 hours at room temperature. The product was then dried under vacuum till dry. The product was then washed with dry ethanol by means of a soxhlet apparatus for at least 6 hours. The product was then returned to the reaction vessel for drying under vacuum at room temperature.

The product was analysed by means of FTIR and the results were verified by solid state NMR (see section 2.5.1).

For the determination of the percentage yield of the crown ether on the support, the weight on weight percentage of nitrogen to silica was determined. Using elemental analysis, the calculated percentage nitrogen was determined and compared to the theoretical percentage. The determination of the actual yields are as follow:

E.g. Calculated weight percentage of nitrogen (15-c-5) immobilized on the substrate:

$$1.7 \times 10^{-3} \text{ mol} \times 1 = 1.7 \times 10^{-3} \text{ mol nitrogen}$$

$$1.7 \times 10^{-3} \text{ mol} \times 14 \frac{\text{g}}{\text{mol}} = 2.4 \times 10^{-2} \text{ g}$$

$$\frac{2.4 \times 10^{-2} \text{ g}}{0.45 \text{ g}} \times 100 = 5.3\% \text{ calculated}$$

Analytically determined using nitrogen:

$$\frac{1.24\%}{100} \times 0.45 = 5.58 \times 10^{-3} \text{ g}$$

$$\frac{5.58 \times 10^{-3}}{2.4 \times 10^{-2}} \times 100 = 23.3\%$$

The yields for 15-c-5 on the various substrates were as follow:

Si-gel (60Å)	23%
MCM-41	31%
SBA-15	26%

The yield for 18-c-6 on MCM is 37%

3.3.4. The immobilization of the glymo spacer to different silica substrates

0.4 g (1.7×10^{-3} mol) glymo was dissolved in approximately 10 mL of toluene. The solution was added to 0.45 g of the different substrates respectively and stirred for 48 hours at 80 °C. After completion, the product was dried under vacuum at room temperature. The product was then washed with dry ethanol by means of a soxhlet apparatus for at least 6 hours.

3.3.5. The immobilisation of 15-c-5 and 18-c-6 to different silica substrates by means of the glymo spacer

The product was returned to the original reaction vessel and approximately 5 mL toluene was added to suspend the glymo-silica substrate. The (2-aminomethyl) crown ethers (1.7×10^{-3} mol) were dissolved in approximately 5 mL of ethanol and added to the glymo-silica substrate. The reaction mixture was stirred for 48 hours at 80 °C. The product was then washed with dry ethanol by means of a soxhlet apparatus for at least 6 hours.

For the determination of the percentage yield of the crown ether, the weight on weight percentage of carbon to silica was determined. Using elemental analysis, the actual percentage carbon was determined and compared to the theoretical percentage. The determination of the actual yield is as follows:

The yield for 15-c-5 on MCM-41 is 31%

3.3.6. The synthesis of 223 and 332

The preparation of the azamacrocycles is similar to the condensation methods used for the crown ether ligands.³⁸ The method that was employed in the preparation of the medium sized cyclic tri-amines is described in detail by Koyama and Yoshino.¹ Figure 3.7 shows a schematic outline for the synthesis and immobilisation of the tri-azamacrocyclic ligands with the pendant arms.

3.3.7. Immobilisation of 223 and 332 to different silica substrates by means of the glymo spacer

The procedure that was used is fully described by J. Kramer.³⁹

Suspend the silica with the immobilised glymo spacer (section 2.4.3) in approximately 10 mL of toluene. Add 1.7×10^{-3} mol of the tri-

azamacrocyclic ligand to approximately 10 mL of ethanol and then add the mixture to the suspended silica solution. Reflux the mixture for 48 h at 80 °C. Dry the product under vacuum and wash the dried product with absolute ethanol for 6 hours, using a soxhlet apparatus. Dry the washed product at room temperature under normal conditions.

3.3.8. Addition of the pendant arms to the immobilised 223 and 332 to create THTD and THTUD

The methyl epoxide that was used for the addition of the pendant arms to the two azamacrocycles, was racemically pure as the (*S*)-enantiomer. This means that the same chiral centre was introduced to the ligands. So when each pendant arm incorporates the same chiral centre, one diastereomer of both the ligand and its metal complexes may be dominantly stable as been reported by R.S Dhillon and co-workers^{40, 41} and S.L. Whitbread and co-workers.⁴²

React 3.4×10^{-3} moles (0.078 g) of Na with 50 mL of ethanol. Add the freshly made EtO^-Na^+ to the immobilised tri-azamacrocyclic (section 3.3.8) and stir for 1 hour. Add 1.0956 g of the epoxide to the suspension and stir the reaction for a further 5 days at room temperature. The drying and washing of the product is the same as previously described in section 2.3.11.

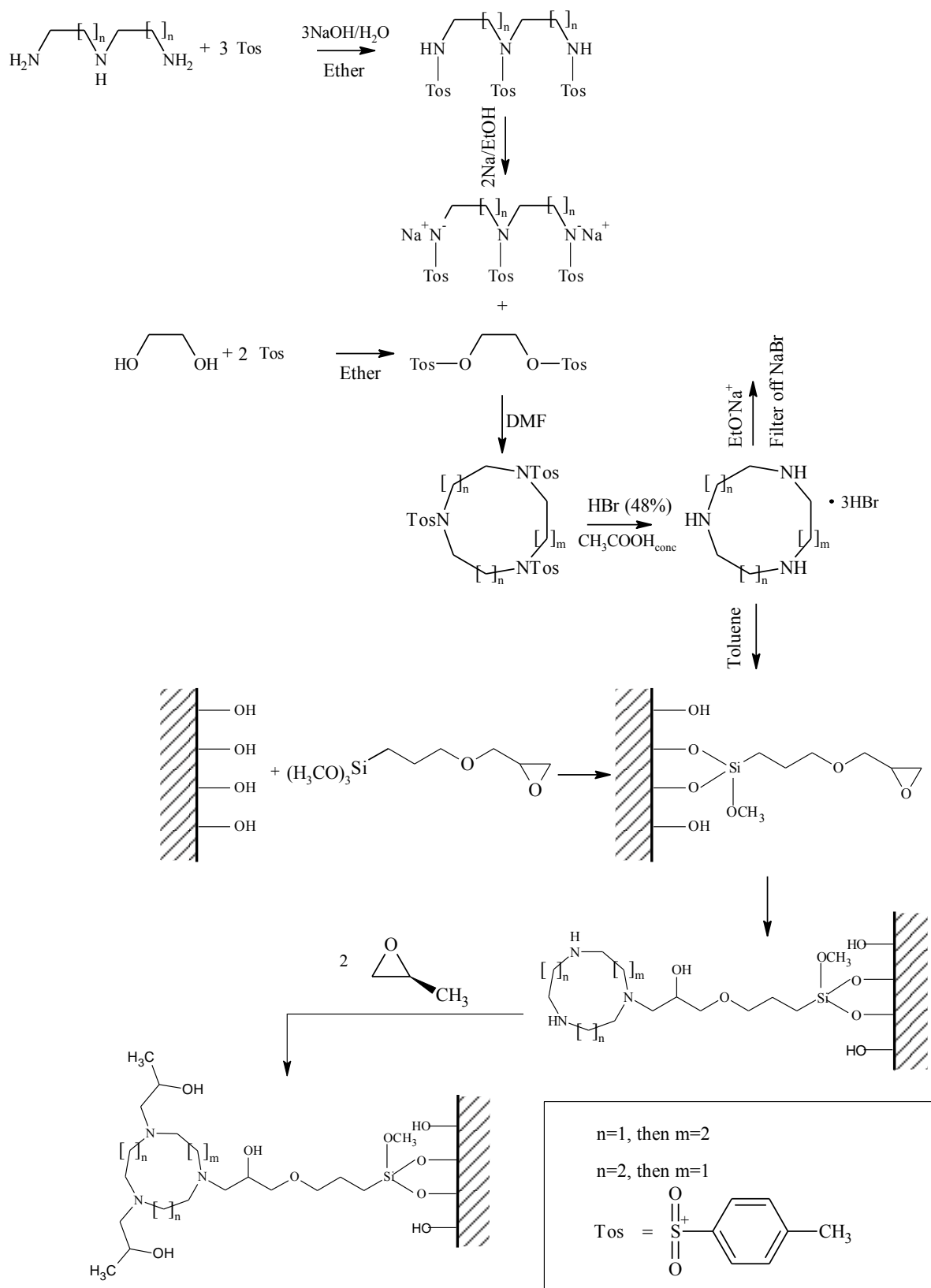


Figure 3.7 The synthesis and immobilisation of THTD and THTUD on the silica supports are shown. The legend indicates the different bridges between the donor atoms as well as the protection group that was used.

For the determination of the percentage yield of the THTD and THTUD, the weight on weight percentage of nitrogen to silica was determined. Using elemental analysis, the actual percentage nitrogen was determined and compared to the theoretical percentage. The determination of the actual yield is as follows:

The yield of the THTD on the various substrates is as follows:

Si-gel (60Å)	20%
SBA-15	12%
HMS	14%

The yield of the THTUD on the various substrates is as follows:

Si-gel (60Å)	13%
HMS	10%

The low average yields observed on the HMS can be ascribed to the fact that it has the smallest surface area, pore openings as well as pore volume as can be seen in the BET results (Figure 3.22, 3.25 and 3.28). These factors do therefore not allow the attachment of the ligands in high yields.

3.4 Results and Discussion

3.4.1. Powder X-ray diffraction of the various silica supports

All the silica supports were synthesised and prepared by Z. Gondongwana of the University of the Western Cape (UWC). The supports (as received) were all subjected to small angle powder x-ray diffraction and the spectra were compared to spectra in the literature.

3.4.1.1 MCM-41

MCM-41 was analysed by powder x-ray diffraction and the spectrum (figure 3.8) that was obtained compared very well to the spectra in the literature.⁴³

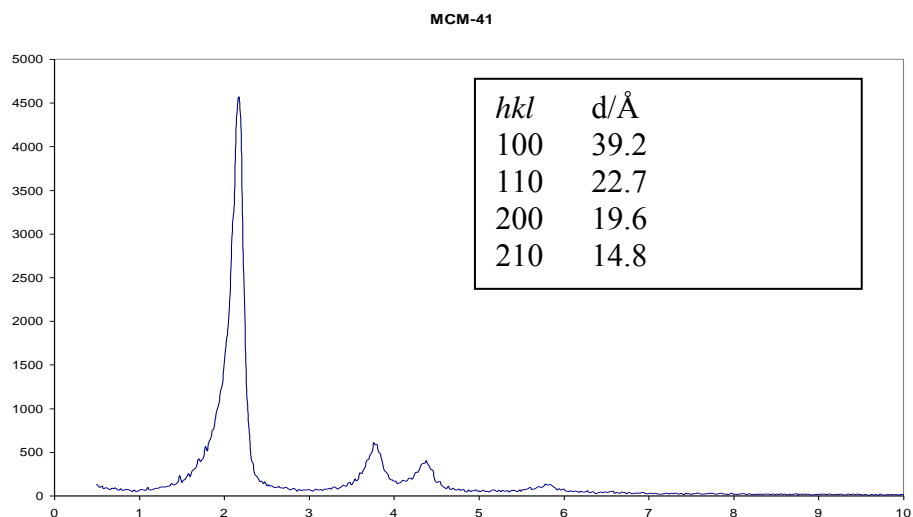


Figure 3.8 Powder X-ray diffraction pattern of MCM-41 (cubic). The hkl and $d/\text{\AA}$ values are shown and were compared to the literature.⁴³

3.4.1.2 HMS

HMS and MCM-41 have the same basic structure. The difference between the two substrates is that HMS has thicker walls. The spectrum (figure 3.9) is not as intense as MCM-41, but it compared well to the spectra found in the literature.⁴⁴

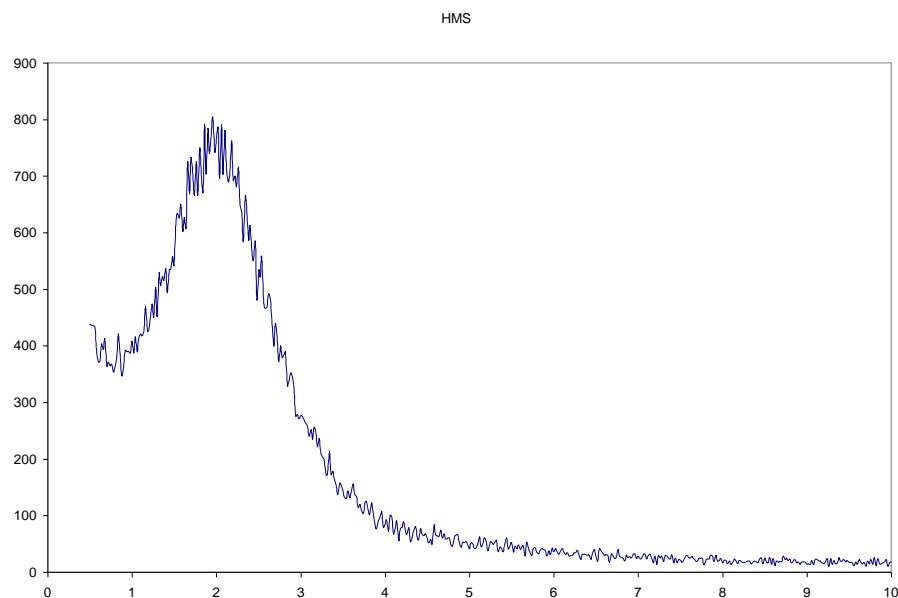


Figure 3.9 Powder X-ray diffraction pattern of HMS.

3.4.1.3 SBA-15

From the powder X-ray diffraction pattern (figure 3.10), it is clear that there are similarities between the SBA-15 and the HMS. There

is a characteristic strong signal (1 0 0) at about $2\theta = 1^\circ$. There are additional weak signals, although not clearly visible in this spectrum, at (1 1 0) and (2 0 0) in the small angle range that are typical for SBA-15.¹⁵ There is a characteristic strong signal (1 0 0) at about $2\theta = 1^\circ$. There are additional weak signals (1 1 0) and (2 0 0) in the small angle range that are typical for SBA-15.¹⁵

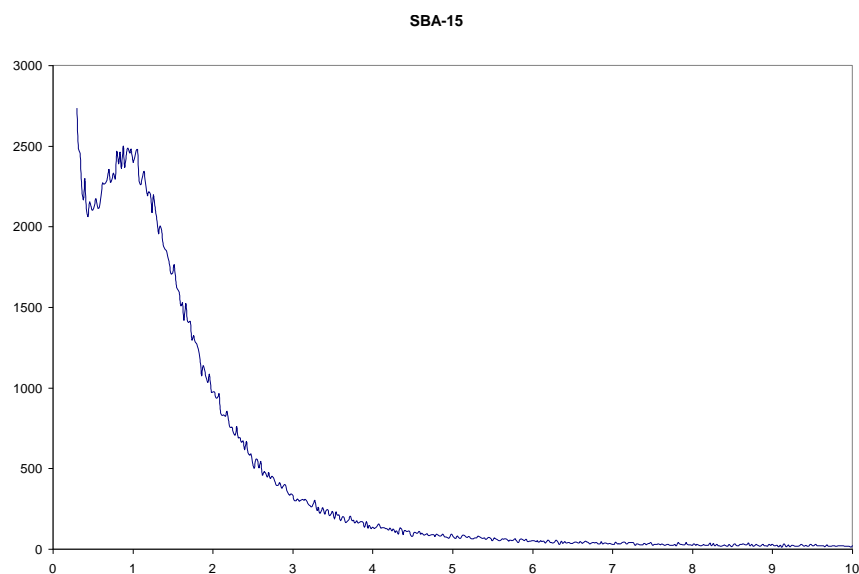


Figure 3.10 Powder X-ray diffraction pattern of SBA-15.

3.4.1.4 Si gel (60 Å)

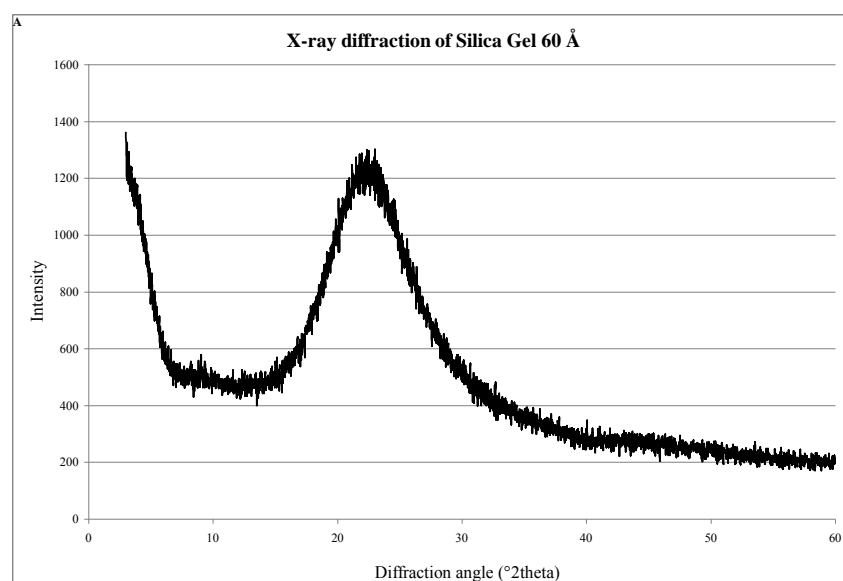


Figure 3.11 Powder X-ray diffraction pattern of Si gel (60 Å).

The Si was bought from Sigma_Aldrich and used without further purification. At $2\theta = 3^\circ$ and 22° there is a strong signal and a very weak signal is observed at 45° . These signals are characteristic of Si gel (60 Å) (figure 3.11).

3.4.2. FTIR spectra

3.4.2.1 Spectra of the direct immobilization of the crown ethers

Figure 3.12 shows the FTIR spectrum of 18-c-6 immobilised on silica gel (60 Å).

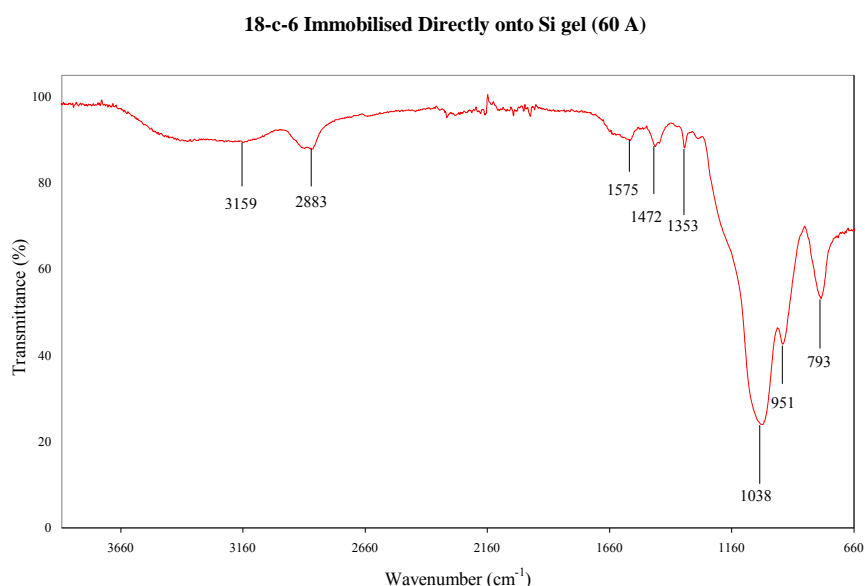


Figure 3.12 The FTIR spectrum of the direct immobilisation of 18-c-6 on silica gel. This spectrum is representative of 15-c-5 and 18-c-6 on all four supports.

According to Deorkar and Tavlarides, FTIR spectral studies show van der Waals type of interactions between the alkyl chain of the extractant and the functional groups bonded to the silica surfaces.¹⁶

It is proposed that there are a number of H-bonds that keep the crown ethers attached to the silica support. It seems like there is hydrogen bond interactions between the protons of the amine group and the oxygen atoms of the silanol groups. There are in all probability also hydrogen bond interactions between the lone pair of

electrons on the nitrogen of the amine group and the protons of the silanol groups of the silica supports.

The signals for the CH₂ stretch in the crown ethers can be seen in the 2883 cm⁻¹ region. The bend motion is visible at 1472 cm⁻¹. The NH stretch signal is obscured by the very broad signal at 3159 cm⁻¹, but the bend motion can clearly be seen at 1575 cm⁻¹. The CN single bond signal is observed at 1353 cm⁻¹.

The FTIR spectrum of 15-c-5 (on Si gel (60 Å)) is similar to that of 18-c-6 with the signals in the same regions.

The FTIR of SBA-15 was used to verify that the ligands did in fact attach to the substrate and was compared to that in the literature.¹⁵ The spectra for the immobilised crown ethers on HMS and MCM-41 are shown in the appendix. The interpretation of the signals corresponds to that of the immobilised 18-c-6 on Si 60 Å.

3.4.2.2 *Spectra of the immobilised crown ethers by means of the glymo spacer*

The FTIR spectrum of the glymo spacer with the immobilised 15-c-5 is shown in figure 3.13 and is representative of all the crown ethers that were immobilised with the glymo spacer. The other spectra can be seen in the appendix. The CH₂ stretch frequencies can be seen at 2866 cm⁻¹. The bend frequency is clearly visible at 1456 cm⁻¹. The NH stretch signal is obscured by the broad signal at 3373 cm⁻¹. The bend motion for NH is clear at 1586 cm⁻¹. The CN single bond stretch frequency can be seen at 1352 cm⁻¹. The crown ether signal is very clear in the 1033 cm⁻¹ region. The spectra for the glymo spacer on the silica support and the immobilised 18-c-6 is attached in the appendix.

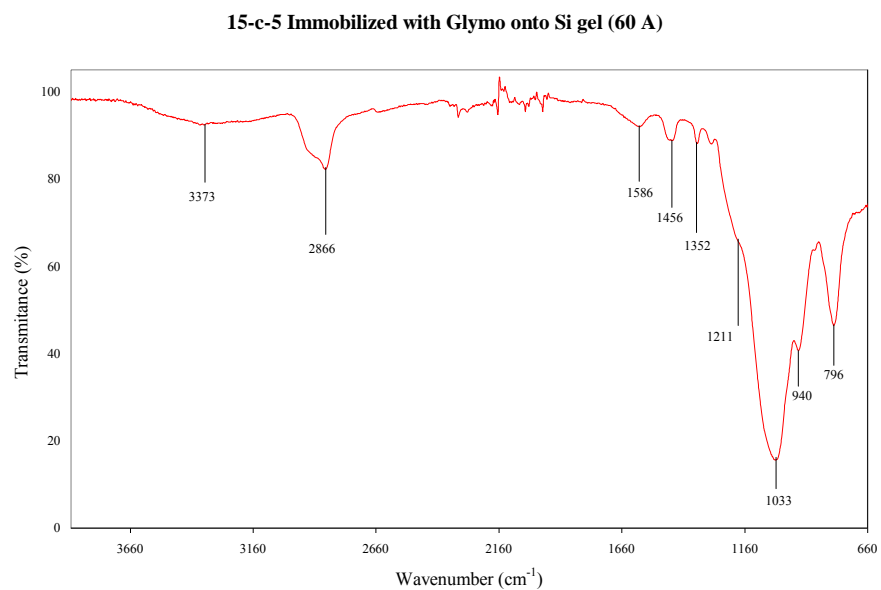


Figure 3.13 The FTIR spectrum of 15-c-5 on silica gel 60 Å by means of the glymo spacer. This spectrum is representative of 15-c-5 and 18-c-6 on all four supports.

3.4.2.3 Spectra of the immobilised azamacrocycles by means of the glymo spacer

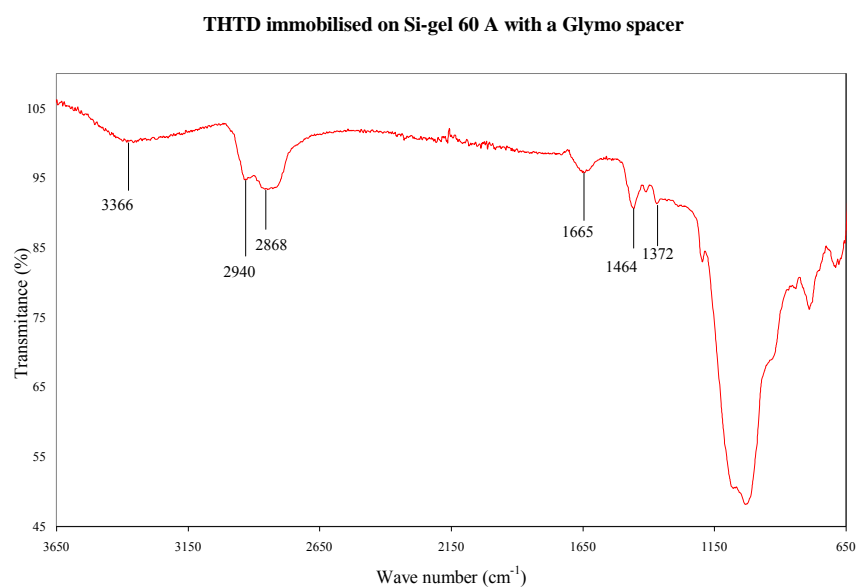


Figure 3.14 The FTIR spectrum of THTD immobilised by the glymo spacer on silica gel (60 Å). The spectrum is representative of THTUD as well. This spectrum is basically the same for the other supports that were also used.

The spectrum in figure 3.14 is representative of all the glymo immobilised THTD and THTUD ligands on all four different Si supports.

From the spectrum it is clear that the NH signals disappeared. Although the signals are weak, the CH₂ signals are visible in the expected regions. The OH signal is still present at 3366 cm⁻¹ while the CN single bond signal is visible at 1665 cm⁻¹. From the spectrum it was concluded that the attachment of the tri azamacrocycle did in fact take place. The result was verified by means of solid state NMR and will be discussed in the next section.

There are quite a number of synthetic routes for the chemical modification of polymer surfaces. Howarter and Youngblood⁴⁴ proposed a way of modifying the surfaces of polymers with 3-aminopropyltriethoxysilane (APTES). The reaction proceeds by initial APTES adsorption to the substrate, lateral bonding and multilayer formation which make this analogous to silane multilayer formation. The physisorption of APTES to the polymer surface is most likely through hydrogen-bonding.

It is thus clear that there is some dispute whether the modification is through hydrogen-bonding or whether it is Van der Waals interactions. The fact remains, it is possible to immobilize ligands on the silica surfaces because all the FTIR spectra indicated the immobilization of ligands and the NMR spectra confirmed this immobilization by showing a change in the backbone of ¹³C and ²⁹Si in the structure.

3.4.3. NMR

The NMR data of the intermediate products were compared to that of similar structures found in the literature. The data confirmed that the intermediate products of the ligands were indeed synthesized.⁴⁵

3.4.3.1 *The solid state NMR spectrum of the crown ethers directly immobilized on the silica supports*

As can be seen from figure 3.15, the CH₂ signal of the crown ether ring is very prominent at 71 ppm. The CH is a small signal at 79 ppm and the CH₂ of the attachment leg next to the amino group is at 41 ppm.

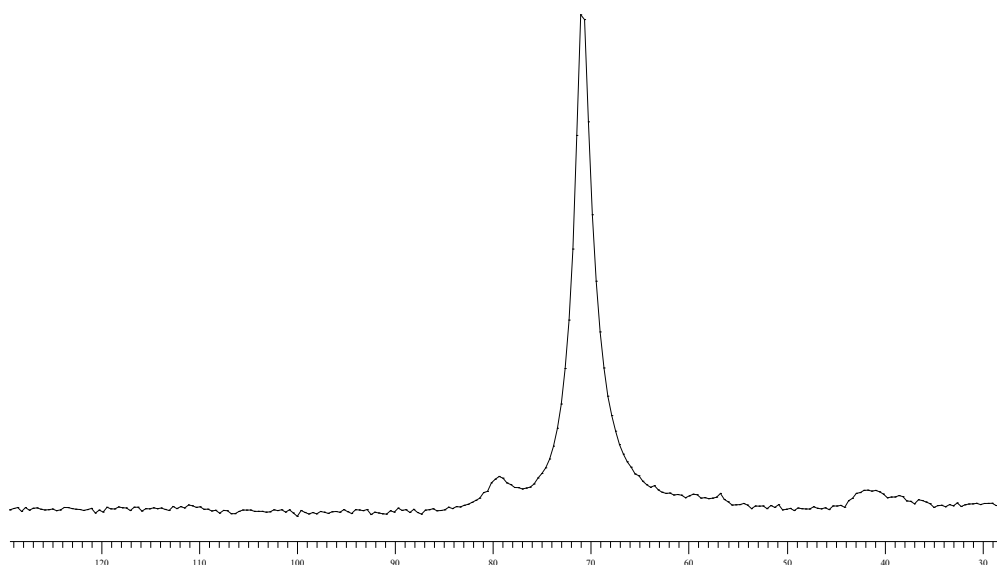


Figure 3.15 The solid state ¹³C NMR spectrum of 18-c-6 directly immobilised on a silica support. This spectrum is also representative of 15-c-5 immobilised directly onto the silica support.

From the spectrum it is clear that the crown ether must have attached itself to the support. The reference NMR of the silica supports showed that there is an overlap of two very broad signals. After immobilisation these overlapping peaks were still present, but a very distinct third peak appeared (figure 3.16), indicating that the amino group of the crown ether has attached itself to the silanol groups of the support. Hence, from the data obtained, it can be deduced that the immobilization did take place because of the change in the surface of the silica supports.

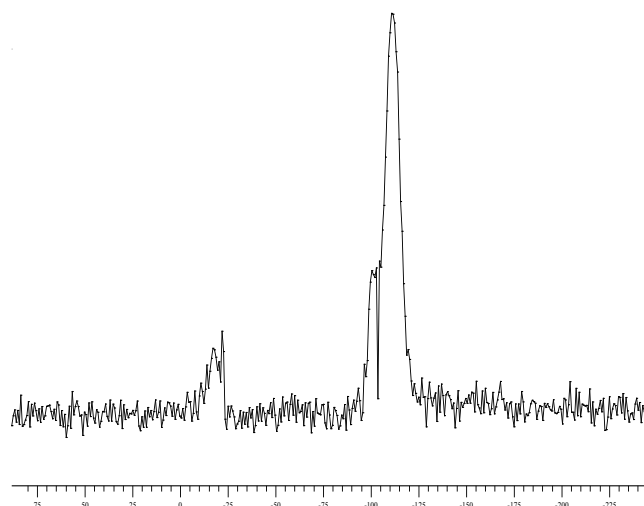


Figure 3.16 The solid state NMR spectrum shows the direct immobilisation of the crown ethers on the silica supports. This spectrum is representative of both crown ethers immobilized on all four supports.

3.4.3.2 The solid state NMR spectrum of the glymo spacer, immobilized on the silica supports

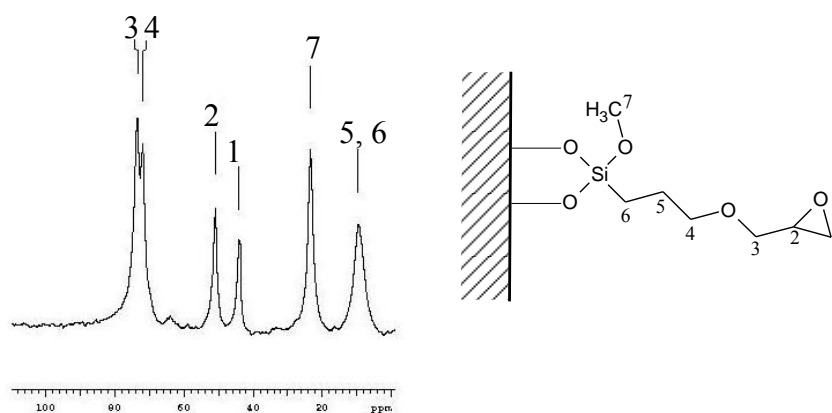


Figure 3.17 The spectrum is a representation of the immobilized glymo spacer on the silica supports.

The solid state ^{13}C NMR spectrum of the immobilized glymo spacer on silica gel is shown in figure 3.17. The split in the signal at 72 ppm are the carbon atoms of the $\text{CH}_2 - \text{O} - \text{CH}_2$ (no.3 & 4). The two singlets at 44 and 50 ppm are the carbon atoms of the epoxide (no.1 & 2). The three remaining signals are the CH_3 (no. 7) at 25 ppm and the two CH_2 's at 8 ppm (no. 5 & 6).

3.4.3.3 The solid state NMR spectra of the crown ethers immobilized on the silica supports with the glymo spacer

The solid state ^{13}C NMR spectrum of 15-c-5, immobilized with a glymo spacer on silica gel, is shown in figure 3.18. The signals of carbon atoms no.5 and 6 of the glymo spacer can still be seen at 8 ppm and the methyl signal of carbon no.7 can be observed at 25 ppm. There is a slight shoulder at 78 ppm on the main signal at 70 ppm, representing the carbon (no. 9) where the amino arm attaches to the crown ether. The other carbon atoms are all incorporated in the huge signal at 70 ppm.

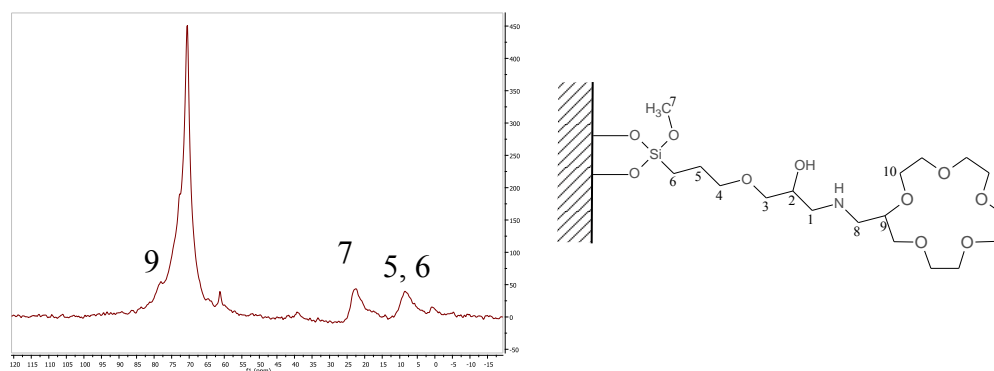


Figure 3.18 The solid state spectrum ^{13}C -NMR is representative of the immobilization of the crown ethers onto the silica supports by means of the glymo spacer.

3.4.3.4 The solid state NMR spectra of the aza crown ethers immobilized on the silica supports with the glymo spacer

The signals from the glymo (no's. 5, 6 & 7) can still be observed in both spectra (figure 3.19). The top spectrum shows the azamacrocycle, without the pendant arms, immobilized with the glymo spacer. The bottom spectrum shows the azamacrocycle, with the pendant arms attached, immobilized with the glymo spacer. The remainder of the top spectrum integrates to the amount of carbon atoms that are left in the rest of the glymo chain as well as the amount of the carbon atoms in the aza-crown macrocycle. In the bottom spectrum, the integration of signals between 45 and 80 ppm

increased to the amount of the carbon atoms that was added as the pendant arms.

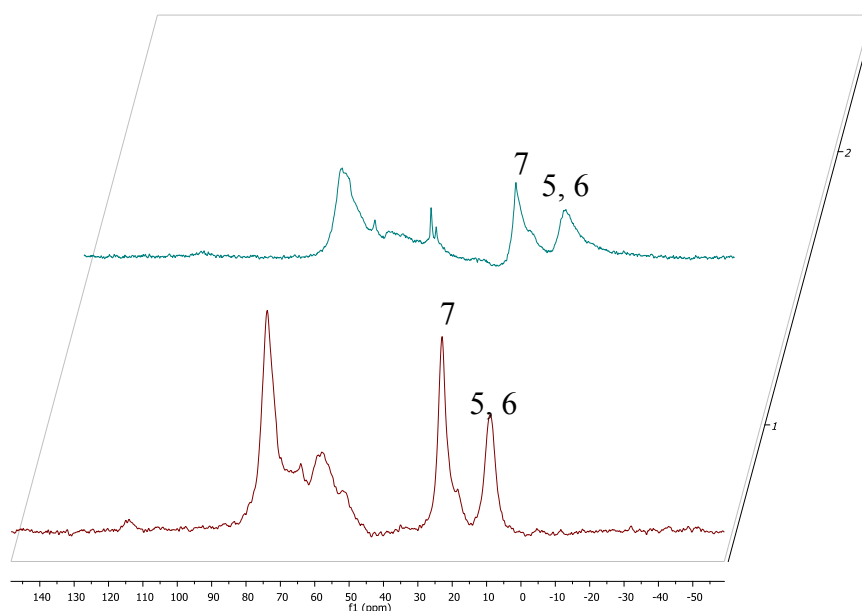


Figure 3.19 The solid state ^{13}C NMR spectrum is representative of the immobilization via the glymo spacer, of the aza-crown ethers onto the silica supports.

3.4.4. BET results of the silica supports

The supports were all subjected to BET experiments to determine the surface areas, pore volumes and pore diameters.

3.4.4.1. Surface area determination and comparison of the four silica supports

Table 3.1 The surface areas of Si-gel 60 Å and MCM-41 are shown according to the adsorption and desorption data as shown in the graphs in figure 3.20.

	Si-Gel (60Å)	MCM-41
Single Point Surface Area at P/Po 0.2039	451.0 m ² /g	981.8 m ² /g
BET Surface Area	469.0 m ² /g	1020.0 m ² /g
BJH Adsorption Cumulative Surface Area of pores between 17.0 and 3000.0 Å Diameter	517.1 m ² /g	1021.3 m ² /g
BJH Desorption Cumulative Surface Area of pores between 17.0 and 3000.0 Å Diameter	629.2 m ² /g	1343.5 m ² /g

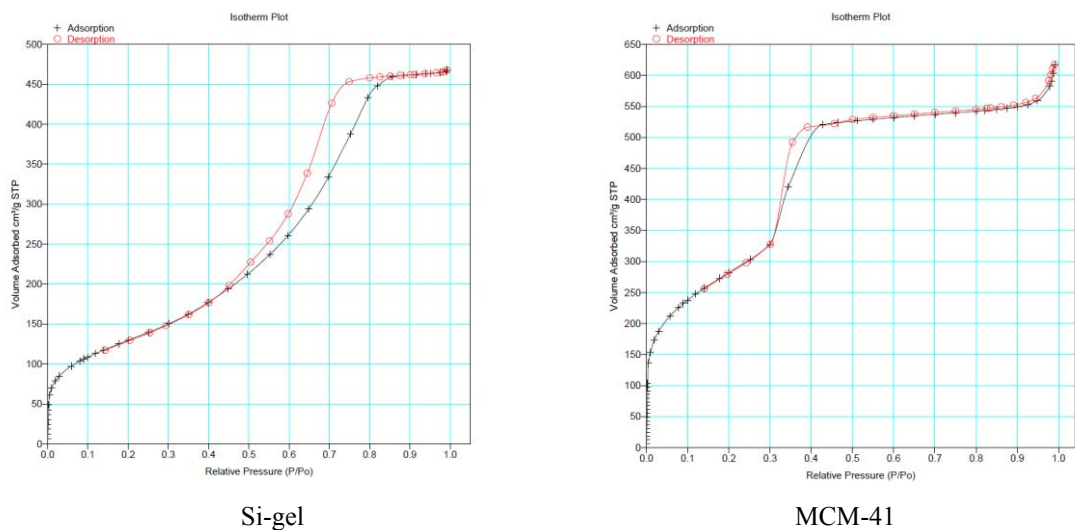


Figure 3.20 The isotherm plot of the adsorption and desorption data to determine the surface areas of Si-gel 60 Å and MCM-41.

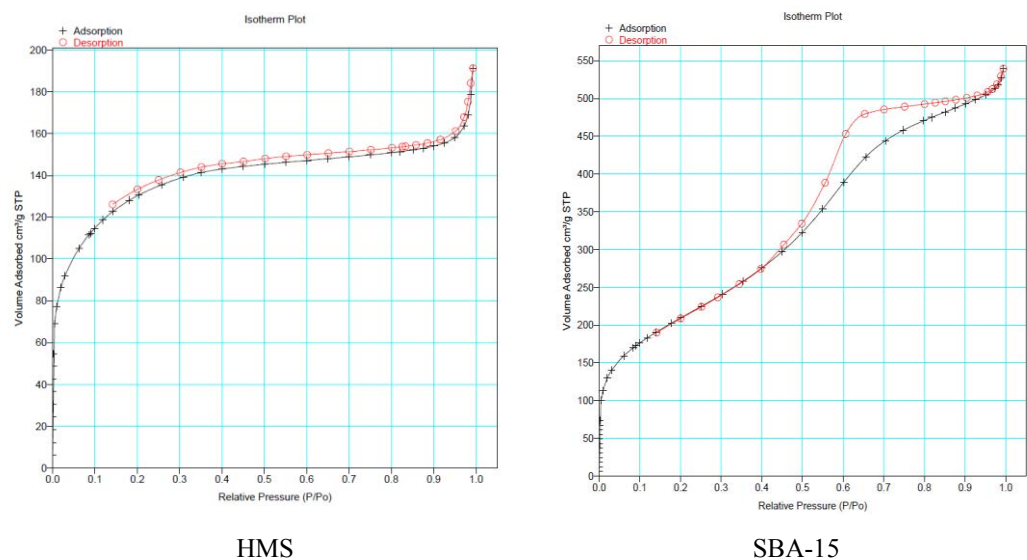


Figure 3.21 The isotherm plot of the adsorption and desorption data to determine the surface areas of HMS and SBA-15.

Table 3.2 The surface areas of SBA-15 and HMS are shown according to the adsorption and desorption data as shown in the graphs in figure 3.21.

	SBA-15	HMS
Single Point Surface Area at P/P ₀ 0.2039	729.3 m ² /g	453.0 m ² /g
BET Surface Area	758.0 m ² /g	466.0 m ² /g
BJH Adsorption Cumulative Surface Area of pores between 17.0 and 3000.0 Å Diameter	605.3 m ² /g	78.6 m ² /g
BJH Desorption Cumulative Surface Area of pores between 17.0 and 3000.0 Å Diameter	851.5 m ² /g	158.9 m ² /g

From the data (table 3.1 and 3.2) it can be seen that MCM-41 has the highest surface area (1020.0 m²/g), followed by SBA-15 (758.0 m²/g), Si-gel 60 Å (469.0 m²/g) and HMS (466.1 m²/g). Figure 3.22 gives a comparative summary of the surface areas of the silica supports as well as the methods that were employed in the determination thereof. It is likely to think that MCM-41 will be the best support, but other factors also need to be considered such as the active silanol sites for instance.

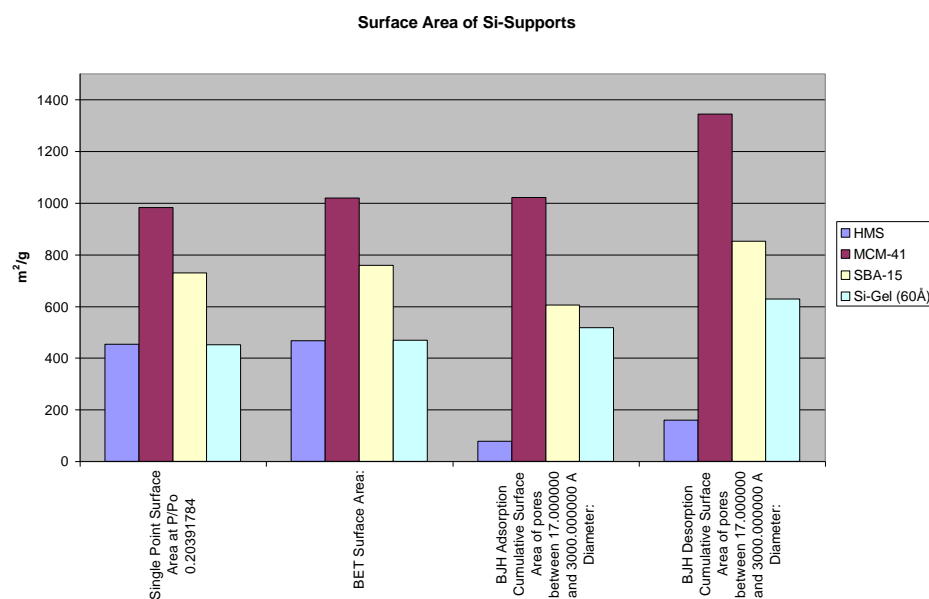


Figure 3.22 A comparison between surface areas of the four different silica supports.

3.4.4.2. Pore volume determination and the comparison between the four silica supports

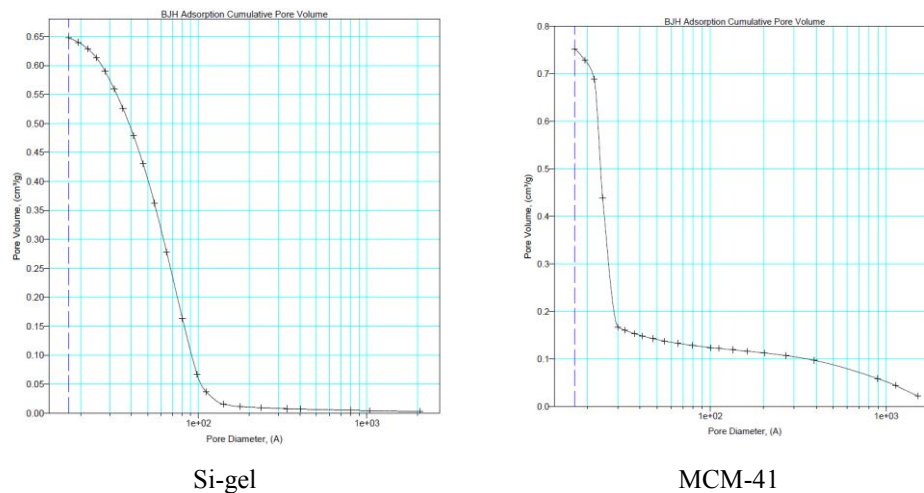


Figure 3.23 BJH Adsorption cumulative Pore Volume graph of Si gel (60 Å) and MCM-41 are shown. The pore volume ($\text{cm}^3 \cdot \text{g}^{-1}$) is plotted against the pore diameter (Å).

Table 3.3 The average size of the pore diameters and average pore volumes for MCM-41 and Si-gel (60 Å) are shown in the table below.

	MCM-41	Si-Gel (60Å)
Single Point Total Pore Volume of pores less than 1027.5 Å Diameter at P/Po 0.9808	0.9 cm^3/g	0.7 cm^3/g
BJH Adsorption Cumulative Pore Volume of pores between 17.0 and 3000.0 Å Diameter	0.8 cm^3/g	0.6 cm^3/g
BJH Desorption Cumulative Pore Volume of pores between 17.0 and 3000.0 Å Diameter	1.0 cm^3/g	0.7 cm^3/g

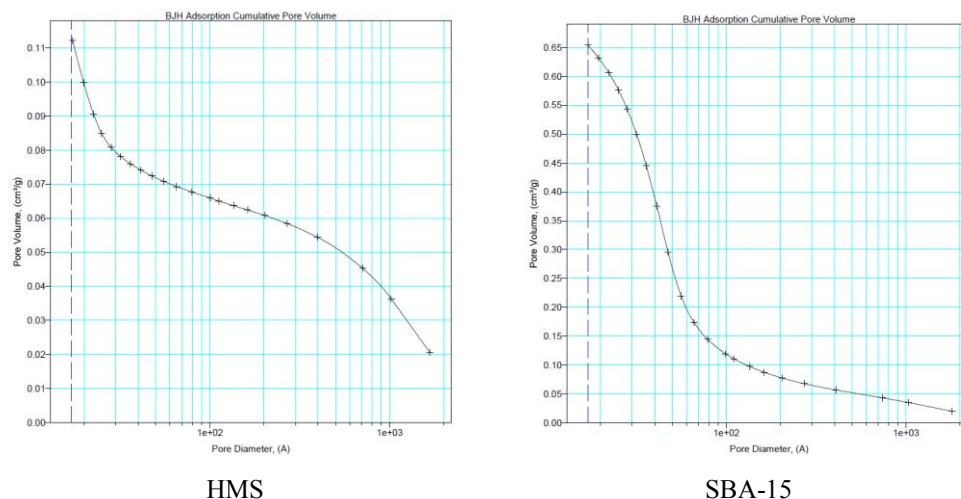


Figure 3.24 BJH adsorption cumulative pore volume graph of HMS Å and SBA-15 are shown. The pore volume (cm^3/g) is plotted against the pore diameter (Å).

The average pore volumes of MCM-41 are larger than those of Si gel 60 Å and SBA-15. HMS has by far the smallest pore volumes in comparison with the other three supports (tables 3.3 and 3.4). By looking at the single point determination in figure 3.25, it can be seen that the pores are about a third of that of Si gel (60 Å), which renders them in comparison almost insignificant.

Table 3.4 The average size of the pore diameters and average pore volumes for HMS and SBA-15 are shown in the table below.

	<u>HMS</u>	<u>SBA-15</u>
Single Point Total Pore Volume of pores less than 1027.5 Å Diameter at P/Po 0.9808	0.3 cm^3/g	0.8 cm^3/g
BJH Adsorption Cumulative Pore Volume of pores between 17.0 and 3000.0 Å Diameter	0.1 cm^3/g	0.7 cm^3/g
BJH Desorption Cumulative Pore Volume of pores between 17.0 and 3000.0 Å Diameter	0.2 cm^3/g	0.9 cm^3/g

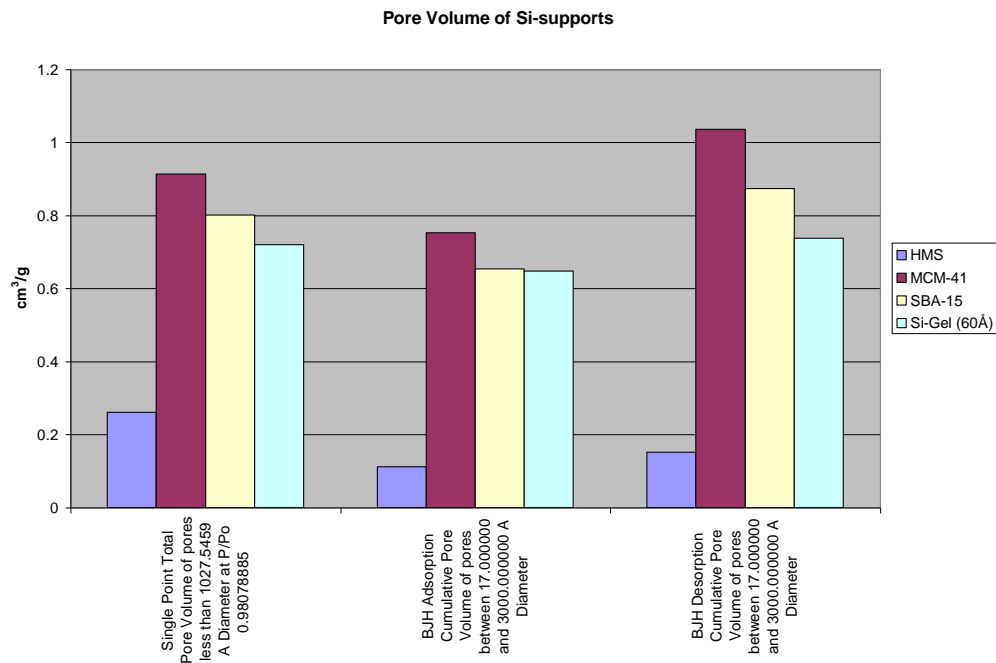


Figure 3.25 A comparison between average pore volumes of the different supports are shown.

3.4.4.3. Determination of the average pore volume of the different silica supports

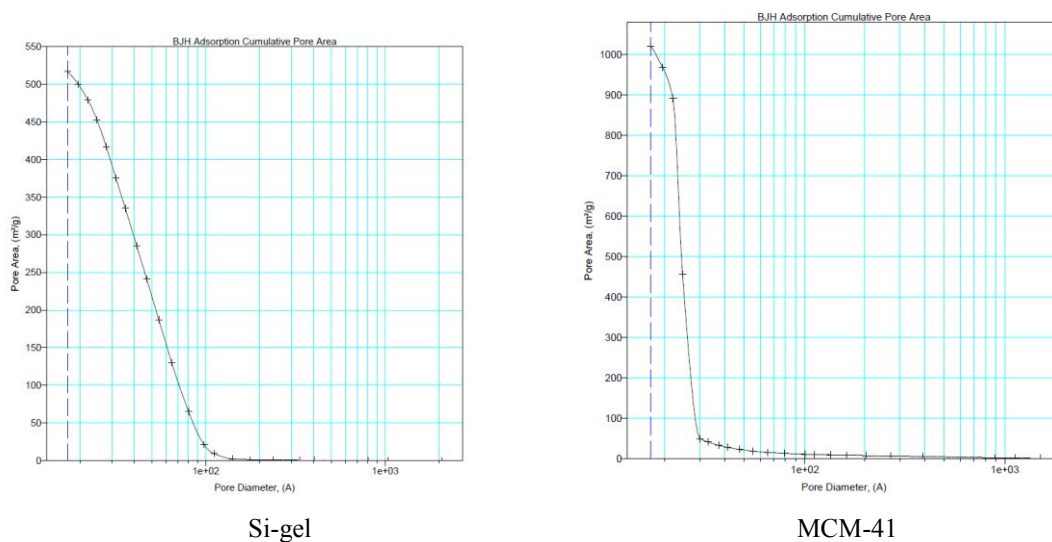


Figure 3.26 The graphs show the cumulative pore areas of Si-gel 60 Å and MCM-41. The pore area is plotted against the pore diameter.

The Si gel has on average the largest pore diameters. As expected, HMS with the smallest pore volumes has also the smallest pore diameter.

Table 3.5 The average pore diameter for Si-gel 60 Å and MCM-41 was determined by BET and is shown in the table below.

	Si-Gel (60Å)	MCM-41
Average Pore Diameter (4V/A by BET):	61.4 Å	35.8 Å
BJH Adsorption Average Pore Diameter (4V/A):	50.1 Å	29.5 Å
BJH Desorption Average Pore Diameter (4V/A):	46.9 Å	30.8 Å

On average, it appears that the Si gel is the obvious choice as a support considering the surface area, the average pore diameter and average pore volume. On the other hand, it is necessary to see whether the active sites (the areas where the spacers will attach) of the other supports will increase on activation and also whether the pore diameters and pore volumes will have an influence on the total available surface area for immobilization.

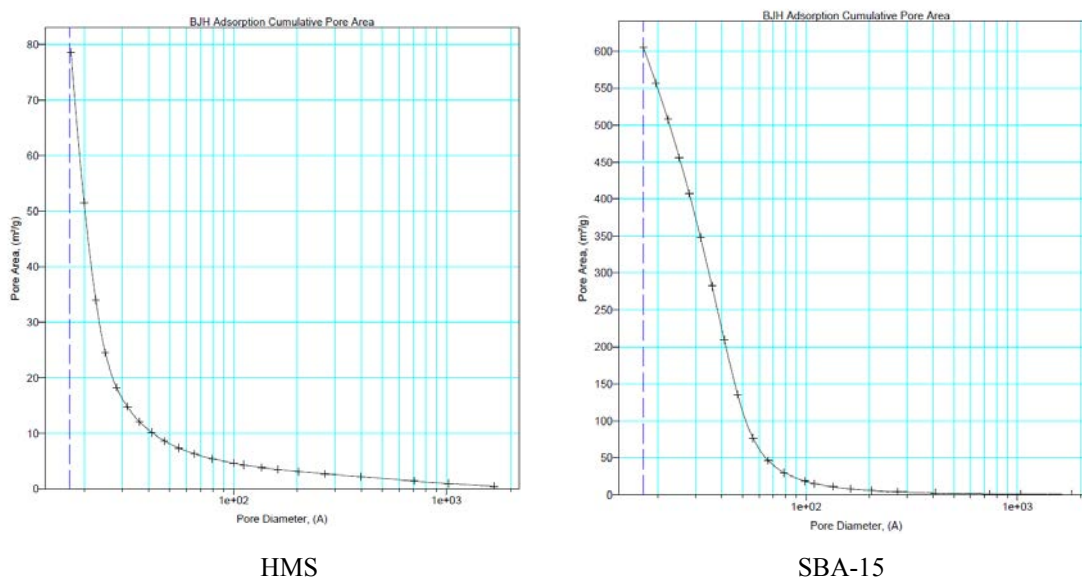


Figure 3.27 The graphs show the cumulative pore areas of HMS Å and SBA-15. The pore area is plotted against the pore diameter.

The average pore diameter for each of the silica supports are summarized in tables 3.5 and 3.6. The data were obtained from the graphs shown in figures 3.25 and 3.26. Figure 3.27 show the comparison between the different silica supports for the average pore diameters and the methods that were used to obtain the data.

Table 3.6 The average pore diameter for HMS and SBA-15 was determined by BET and is shown in the table below.

	HMS	SBA-15
Average Pore Diameter (4V/A by BET):	22.4 Å	42.3 Å
BJH Adsorption Average Pore Diameter (4V/A):	57.1 Å	43.2 Å
BJH Desorption Average Pore Diameter (4V/A):	38.2 Å	41.0 Å

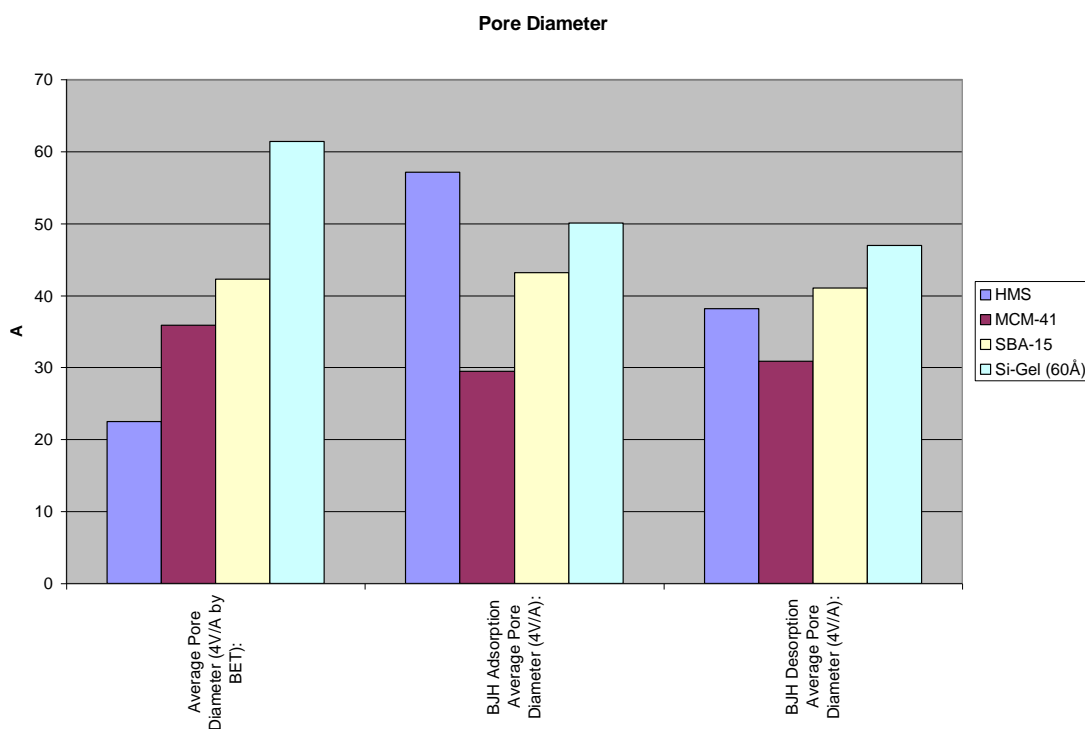


Figure 3.28 A comparison between average pore diameters of the different supports are shown.

3.4.5. TGA

3.4.5.1 TGA curve of the directly immobilized crown ethers.

From the TGA curve (figure 3.29), it can be seen that water is the first to be released from the immobilized 18-c-6 on SBA-15. From about 200 °C, the ligand starts to break away from the support. From 400 °C, the support disintegrates. The same pattern was observed for 15-c-5. This was the pattern for both ligands on all four supports.

In general it is then concluded that the directly immobilized ligands are stable on the supports up to about 250 °C.¹⁵ After 250 °C, the immobilization becomes unstable and the molecule starts to disintegrate.

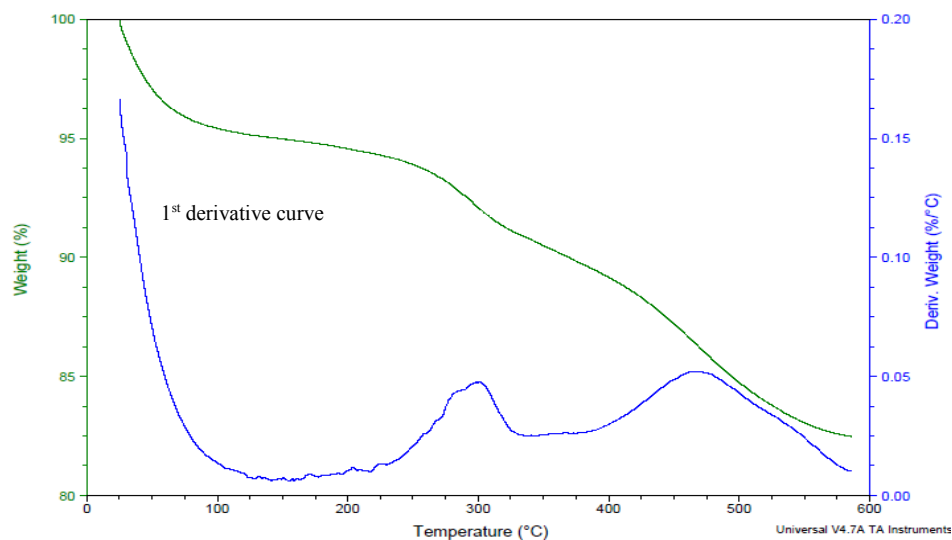


Figure 3.29 The curve is representative of the thermal degradation of the directly immobilized crown ethers on the silica surfaces.

3.4.5.2 *The TGA curve of the immobilized crown ethers by means of a spacer.*

From the curve (figure 3.30) it can be seen that there is a loss of water (5%) over the first 100 °C. The immobilized ligand and the support remains stable to about 150 °C where after the degradation starts. It appears that the ligand comes apart from the spacer because there is a 15% weight loss. At 325 to 475 °C, the spacer gets detached from the support. Thereafter the support starts to disintegrate. The degradation of the support is consistent with the literature which states that these supports are stable up to about 600 °C.

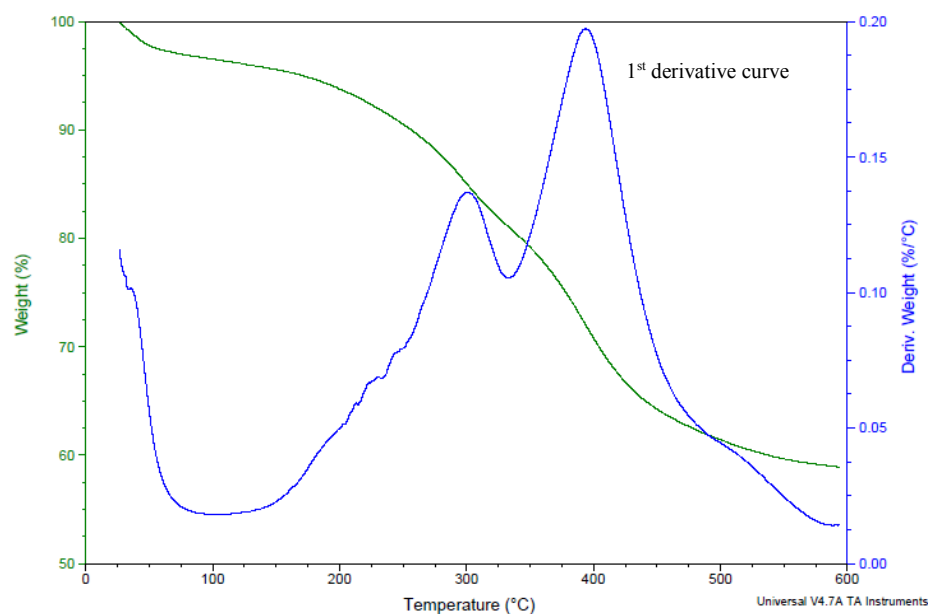


Figure 3.30 The curve is representative of the thermal degradation of the immobilized crown ethers with the glymo spacer on the silica surfaces.

3.4.5.3 *The TGA curve of the immobilized aza crown ethers by means of a spacer.*

Figure 3.31 shows the TGA curve of the stepwise degradation of the immobilized tri-azamacrocyclic ligands. It is clear that the immobilized ligands are hygroscopic since there is a loss of water (8%) over the first 100 °C. The molecule then remains stable until it reaches 275 °C. The tri-azamacrocycle, the pendant arms and the glymo spacer then degrades at separate stages as can be seen from the TGA curve. The support reaches 600 °C where after it is clear that the immobilized ligand is completely destroyed.

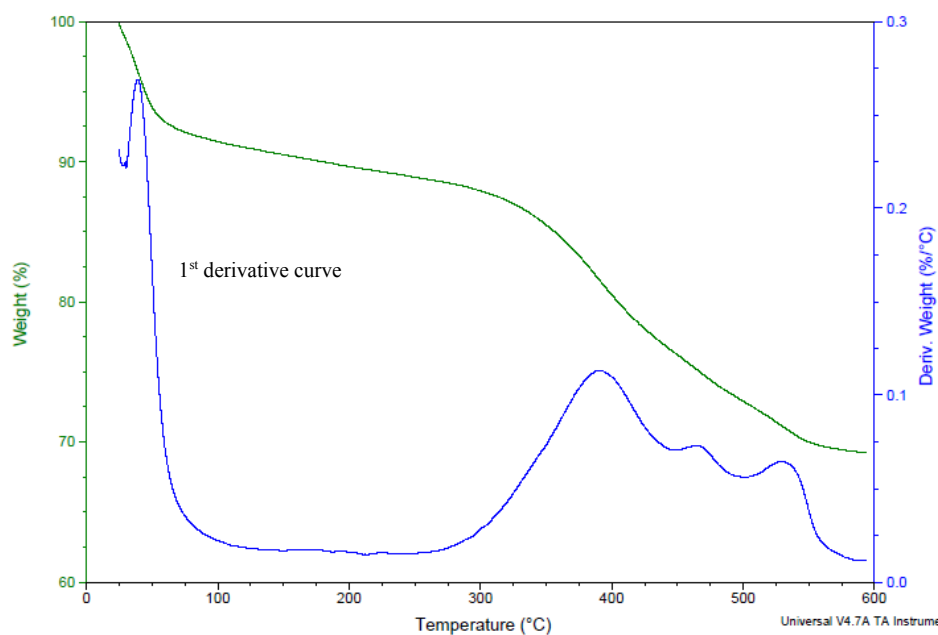


Figure 3.31 The curve is representative of the thermal degradation of the immobilized crown ethers with the glymo spacer on the silica surfaces.

3.4.6. Elemental analysis

The elemental analyses (C, H, O and N) were carried out on the various immobilized ligands.⁴⁶

E.g. Calculated weight percentage of nitrogen (15-c-5) immobilized on the substrate:

$$1.7 \times 10^{-3} \text{ mol} \times 1 = 1.7 \times 10^{-3} \text{ mol nitrogen}$$

$$1.7 \times 10^{-3} \text{ mol} \times 14 \frac{\text{g}}{\text{mol}} = 2.4 \times 10^{-2} \text{ g}$$

$$\frac{2.4 \times 10^{-2} \text{ g}}{0.45 \text{ g}} \times 100 = 5.3\% \text{ calculated}$$

Analytically determined using nitrogen:

$$\frac{1.24\%}{100} \times 0.45 = 5.58 \times 10^{-3} \text{ g}$$

$$\frac{5.58 \times 10^{-3}}{2.4 \times 10^{-2}} \times 100 = 23.3\%$$

3.4.6.1. The elemental analysis of the directly immobilized 15-crown-5 (%)

Table 3.7 The calculated and the analytically found analysis (in %) of the directly immobilized 15-crown-5 on various substrates.

	C	H	N	O
Calculated (Ligand on its own)	52.99	9.30	5.62	32.09
	Analytically found			
On Si gel (60 Å):	17.19	4.02	1.24	
On MCM-41	18.36	4.80	1.67	
On SBA-15	15.01	4.10	1.39	

3.4.6.2. The elemental analysis of the directly immobilized 18-crown-6 (%)

Table 3.8 The calculated and the analytically found analysis (in %) of the directly immobilized 18-crown-6 on various substrates.

	C	H	N	O
Calculated (Ligand on its own)	53.23	9.28	4.77	32.72
	Analytically found			
On MCM-41	24.09	6.97	1.96	

3.4.6.3. The elemental analysis of the immobilized 15-crown-5 by means of the glymo spacer

Table 3.9 The calculated and the analytically found analysis (in %) of the immobilized 15-crown-5 by means of the glymo spacer on various substrates.

	C	H	N	O
Calculated (Ligand on its own)	49.46	8.92	2.88	32.94
	Analytically found			
On MCM-41	29.16	7.15	1.65	

3.4.6.4. The elemental analysis of the immobilized THTD by means of the glymo spacer

Table 3.10 The calculated and the analytically found analysis (in %) of the immobilized THTD on various substrates by means of the glymo spacer.

	C	H	N	O
Calculated (Ligand on its own)	60.53	11.11	13.24	15.12
	Analytically found			
On Si gel (60 Å):	21.46	5.77	3.08	
On SBA-15	14.55	4.10	1.73	
On HMS	15.89	5.07	2.11	

3.4.6.5. The elemental analysis of the immobilized THTUD by means of the glymo spacer

Table 3.11 The calculated and the analytically found analysis (in %) of the immobilized THTUD on various substrates by means of the glymo spacer.

	C	H	N	O
Calculated (Ligand on its own)	61.59	11.25	12.68	14.48
	Analytically found			
On Si gel (60 Å):	23.62	6.14	1.92	
On HMS	14.09	4.62	1.35	

The experimental results obtained are lower than the yields published in the literature. J. Kramer found yields between 28 and 37%.⁴⁷ Due to availability constraints, only selected analysis was possible.

3.5 Conclusion

The BET and X-ray studies indicated that the supports that were received from our collaborators were indeed correct. The surface areas, pore volumes and pore sizes which were determined by BET results gave an indication of the areas that were available for modification. Unfortunately, no further BET results could be obtained after immobilization of the ligands since the products were not stable enough to determine how much of the various surface areas were used.

The FTIR and solid state NMR spectra confirmed that the crown ethers are indeed immobilised directly onto the different supports. The TGA spectra showed that these immobilized ligands are fairly hygroscopic and also that they are stable to a temperature of 200 °C. These immobilized ligands can therefore be used at relatively high temperatures.

The successful immobilization of the crown ethers by means of the glymo spacer was confirmed by FTIR and solid state NMR.

The successful synthesis of the parent macrocyclic ligands, 1,4,7-tri-azacyclodecane and 1,4,8-tri-azacycloundecane, made it possible for immobilization onto the various silica supports. With the addition of pendant arms after immobilization, the parent ligands could be modified to create the hexadentate ligands.

By using the various analytical techniques, it was concluded that THTD and THTUD were successfully immobilized on the different supports by means of the glymo spacer.

References

- ¹ H. Koyama and T. Yoshino, *Bull. Chem. Soc. Jpn.*, 1972, **45**, 481
- ² R. Yang and L.J. Zompa, *Inorg. Chem.*, 1976, **15**, 1499
- ³ L. Sabatini and L. Fabbrizzi, *Inorg. Chem.*, 1979, **18**, 438
- ⁴ E. Brucher *et al.*, *Inorg. Chem.*, 1991, **30**, 2092
- ⁵ L.F. Lindoy, *Chem. Soc. Rev.*, 1975, **4**, 421
- ⁶ P.Comba *et al.*, *Inorg. Chem.*, 1986, **25**, 4260
- ⁷ A.M. Sargeson, *Pure Appl. Chem.*, 1984, **56**, 1603
- ⁸ E.C. Constable in *Coordination Chemistry of Macrocyclic Compounds*, Oxford University Press, 1999, pp. 42 – 46
- ⁹ H. Stetter and E-E. Roos, *Chem. Ber.*, 1954, **87**, 566
- ¹⁰ E.C. Constable in *Coordination Chemistry of Macrocyclic Compounds*, Oxford University Press, 1999, p. 33
- ¹¹ T.J. Atkins, J.E. Richman and W.F. Oettle, *Org. Synth.*, 1978, **58**, 86
- ¹² J.E. Richman and T.J. Atkins, *J. Am. Chem. Soc.*, 1974, **96**, 2268
- ¹³ G.H. Searle and R.J. Geue, *Aust. J. Chem.*, 1984, **37**, 959
- ¹⁴ J. Robb and R.D. Peacock, *Inorg. Chim. Acta*, 1986, **121**, L15
- ¹⁵ J.S. Beck *et al.*, *J. Am. Chem. Soc.*, 1992, **114**, 10834
- ¹⁶ T. Jansen, *Acta Crystallogr. A*, 1986, **42**, 261
- ¹⁷ A. Yamamoto, *Acta Crystallogr. A*, 1996, **52**, 509
- ¹⁸ T. Socolar *et al.*, *Phys. Rev. B*, 1986, **34**, 3345
- ¹⁹ M.V. Jaric and D.R. Nelson, *Phys. Rev. B*, 1988, **37**, 4458
- ²⁰ Y. Ishii, *Phys. Rev. B*, 1992, **45**, 5228
- ²¹ C.L. Henley in *Quasicrystals: The state of the Art* (eds D. DiVincenzo and P.J. Steinhardt), (World Scientific Singapore), 1991, pp. 429 – 524
- ²² H.C. Yeong and P.J. Steinhardt, *Phys. Rev. B*, 1993, **48**, 9394
- ²³ P.A. Bancel in *Quasicrystals: The state of the Art* (eds D. DiVincenzo and P.J. Steinhardt), (World Scientific Singapore), 1991, pp. 17 – 55
- ²⁴ R. Colella *et al.*, *Phys. Rev. B*, 2000, **63**, 014202
- ²⁵ J. Dolinsek *et al.*, *Phys. Rev. Lett.*, 1999, **82**, 572
- ²⁶ G. Coddens and W. Steurer, *Phys. Rev. B*, 1999, **60**, 270
- ²⁷ K. Edagawa, K. Suzuki and S. Takeuchi, *Phys. Rev. Lett.*, 2000, **85**, 1674
- ²⁸ M. de Boissieu *et al.*, *Phys. Rev. Lett.*, 1995, **75**, 89
- ²⁹ G. Zeger *et al.*, *Phys. Rev. Lett.*, 1995, **82**, 5273
- ³⁰ S.J. Pennycook and D.E. Jesson, *Ultramicroscopy*, 1991, **37**, 14
- ³¹ S.J. Pennycook and D.E. Jesson, *Acta Metall. Mater.*, 1992, **40**, S149
- ³² D.A. Muller *et al.*, *Ultramicroscopy*, 2001, **86**, 371
- ³³ S. Ritch *et al.*, *Phil. Mag. Lett.*, 1996, **74**, 99
- ³⁴ K. Saito *et al.*, *Jpn. J. Appl. Phys.*, 1997, **36**, L1400
- ³⁵ Y. Yan, S.J. Pennycook and A.P. Tsai, *Phys. Rev. Lett.*, 1998, **81**, 5145

-
- ³⁶ P.J. Steinhardt *et al.*, *Nature*, 1999, **399**, 84
- ³⁷ N.K. Mal, M. Fujiwara and Y. Tanaka, *Nature*, 2003, **421**, 350
- ³⁸ C.J. Pederson and H.K. Frensdorff, *Angew. Chem. Internat. Edit.*, 1972, **11**, 16
- ³⁹ J. Kramer in *Chelating Ion Exchangers for the Recovery of Rhodium, PhD Thesis*, University Leiden, 2002, p.53
- ⁴⁰ R.S. Dhillon *et al.*, *J. Am. Chem. Soc.*, 1997, **119**, 6126
- ⁴¹ R.S. Dhillon *et al.*, *J. Am. Chem. Soc.*, 1998, **120**, 11212
- ⁴² S.L. Whitbread *et al.*, *J. Am. Chem. Soc.*, 1998, **120**, 2862
- ⁴³ A. Corma, *Chem. Rev.*, 1997, **97**, 2373
- ⁴⁴ J.A. Howarter and J.P. Youngblood, *Macromolecules*, 2007, **40**, 1128
- ⁴⁵ J. Huskens and A.D. Sherry, *J. Chem. Soc., Chem. Commun.*, 1997, 845
- ⁴⁶ J. Kramer, N.E. Dhladhla and K.R. Koch, *Separation and Purification Technology*, 2006, **49**, 181
- ⁴⁷ J. Kramer in *Chelating Ion Exchangers for the Recovery of Rhodium, PhD Thesis*, University Leiden, 2002, p.127

Chapter 4

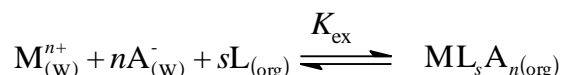
The Extraction of Toxic Metal Ions from Water

4.1. Introduction

It is known that some water has a pH of 2 or even lower. The immobilized ligands are very unstable at a pH of approximately 2 and it disintegrates at a pH of 1.9. It is therefore necessary to buffer the system to prevent the disintegration of the ligands. This procedure is explained in section 4.2.

The hydrophobicity of heavy metals, as well as the supports for the ligands, is an important issue; this was not brought into consideration. The main focus of this project was the structure of the ligand and the interaction thereof with the metal ion.

In the liquid-liquid extraction studies by Gloe *et al.*,¹ the ligands that were studied are neutral and the extraction equilibria are described by:



The corresponding extraction constant, K_{ex} , is a function of the complex stability of the complex formed, and of the distribution of the ligands between the two phases.²

For separation experiments, it can be seen from table 4.1 that there is a greater selectivity for Hg(II) over Cd(II) with the use of THEC and TMC.³ These stability constants were determined for the free ligands and although these ligands were not part of the study, it is important to compare the stabilities to other macrocyclic ligands to determine whether better extractions are possible or not.

Table 4.1 Formation constants of complexes of some tetraaza macrocycles.

	THEC	TMC	CTA	Cyclam ⁴
Metal ion	logK(ML)	logK(ML)	logK(ML)	logK(ML)
Cd(II)	9.38	9.0	15.5	11.2
Hg(II)	17.94	20.3	N.D.*	23.0

The selectivity for one metal ion over another can be measured as the difference in log K_1 (formation constant) between the different metal ions with a specific ligand.⁵



$$K = \frac{[ML^{x+}]}{[M^{x+}][L]} \quad 4.2$$

Since there are two different phases in the extraction, the following equation is used to determine the distribution coefficient K_d . K_d is a mass-weighted partition coefficient (mL.g⁻¹) between the solid phase and the liquid supernatant phase:

$$K_d = \frac{C_o \times C_f}{C_f} \times \frac{V}{M} \quad 4.3$$

where: C_o = initial concentration

C_f = final concentration

V = solution volume in mL

M = mass in gram

The rate at which the complexation reaction occurs is very important in the industry. One reason for the slowness of the metalation reactions of the N-donor macrocycles, is due to the slow rates of reaction of the metal ion with the protonated forms of the ligands.^{6,7} There are different ways of overcoming this problem. The first method is to attach a donor atom outside of the macrocyclic ring.¹ Another and more efficient way is just to use neutral ligands.

4.2 Extraction of the Toxic Elements

Metal ion solutions were prepared from the various metal ion salts. The aqueous source phase consisted first, of single metal ion solutions (table 4.2 – solutions 1 – 6). Next, an equi-molar mixture of four different metal ion solutions (table 4.2 – solutions 1 – 4) were made up as one solution, as well as a solution containing the other two metal ions (table 4.2 – solutions 5, 6) to determine the selectivity of the ligands on the different supports. The two mixed metal ion solutions were split due to their very different acidic properties. Hg^{2+} and U^{6+} must first be dissolved in glacial acetic acid after which it had to be adjusted to the desired pH. The other metal salts were dissolved directly in the buffer solution.

Table 4.2 The metal salts that were used for the preparation of the different solutions.

	1	2	3	4	5	6
Metal salt	CrO_3	As_2O_5	$\text{Sr}(\text{NO}_3)_2$	$\text{Cd}(\text{NO}_3)_2$	$\text{Hg}(\text{NO}_3)_2$	$\text{UO}_2(\text{CH}_3\text{COO})_2$
Metal ions	Cr^{6+}	As^{5+}	Sr^{2+}	Cd^{2+}	Hg^{2+}	UO_2^{2+}

All the solutions for the first series of extraction experiments were buffered with an acetic acid/sodium acetate buffer solution at pH 4.5 (Perrin and Dempsey).⁸ The solutions for the second series of extraction experiments were buffered at pH of 5.9. Again the buffer solutions consisted of an acetic acid/sodium acetate buffer. This method was also described and used by Black and co-workers.⁹ It must be stressed that pH 5.9 is right on the border for an acetic acid/acetate buffer as was determined by Perrin and Dempsey.⁸

All solutions were made up to as close to $1.000 \times 10^{-3} \text{ mol.L}^{-1}$ as possible with their exact concentrations recorded. Equal weights of ligand per substrate were weighed off and 10 mL of each metal ion solution were added for the extraction.

The extractions were carried out over a period of 24 hours at a constant temperature of 25 °C.¹⁰ After this period of time, equilibrium must have been established. The solutions were shaken on an automatic shaker at a tempo of 220 rev.min⁻¹. Thereafter, the solutions were filtered using normal filter paper. The solutions were then analysed before and after extraction, using ICP to determine the quantities of metal ions

remaining in aqueous phase, hence the effectiveness of the extraction capabilities of the different ligands.

4.3 Results and Discussion

To explain the very low extraction yields, it is also important to have a look at the speciation of the different metal ions in aqueous solution. Since only a small percentage of the ligands were immobilised, the effectiveness of the ligands are actually much higher.

It must be mentioned that all extraction values below 2.5%, falls within instrumental error that was reported by the instrument operator, and can be considered to be zero.

4.3.1. Extraction of As(V) with various ligands immobilized on four different silica supports

Arsenic is present in aqueous solutions as two species: as HAsO_4^{2-} or H_2AsO_4^- .

The average extraction of $\text{H}_n\text{AsO}^{-x}$ at a pH of 4.5 with the various ligands immobilized on any of the four supports were less than 2.5% and are therefore considered to be zero.

Even with the pH raised to 5.9, the average extraction with the ligands immobilized on the various supports remained less than 2.5 %.

It is therefore clear that no extraction was obtained with any of the ligands immobilized on the various supports with the pH level at 4.5.

The results indicate that no extraction took place. This is due to the fact that there are lone pairs of electrons on the donor atoms that are trying to coordinate to the already negatively charged arsenic ions resulting in no extraction.

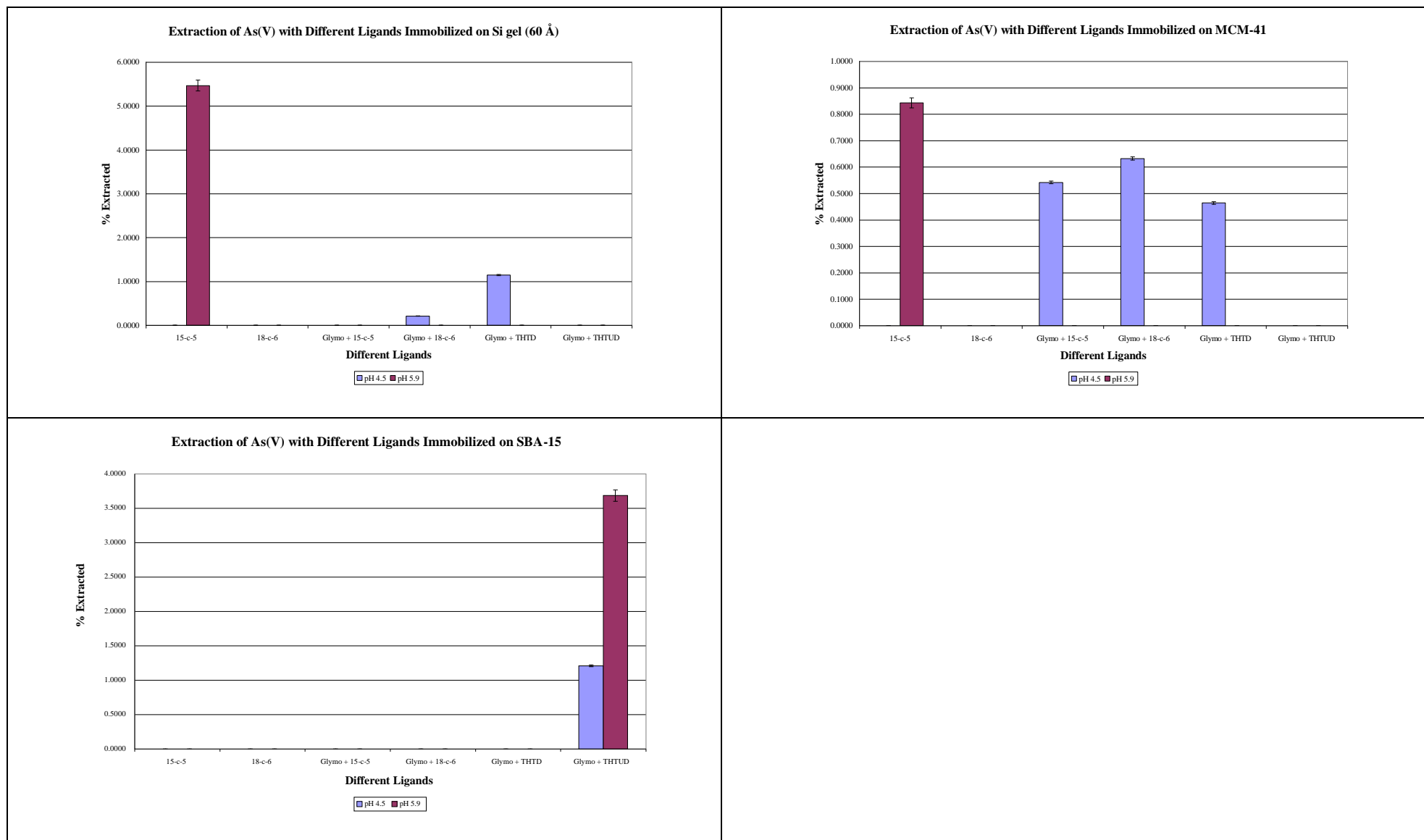


Figure 4.1 The extraction of As(V) with various ligands immobilized on four different silica supports

4.3.2. Extraction of Cd(II) with various ligands immobilized on four different silica supports

Kumbasar studied the extraction of Cd in detail. The extraction depended on surfactant concentration, acid concentration, solute concentration and time. At optimum conditions, Kumbasar achieved 96% extraction using selective membranes. Cadmium iodide anions were targeted by using an Amberlite LA-2 exchanger.^{11,12} Mahmoud and Al-bishri worked at a pH of 1 using Emim⁺Tf₂N⁻ and Omim⁺Tf₂N⁻ on nano-silica. The adsorption capacities obtained ranged between 1.2 and 1.3 mmol g⁻¹ (97.25 -99.30%).¹³

The decision for immobilizing THTD and THTUD as ligands on the silica supports, were based on their unusually high formation constants with Cd²⁺, as can be seen in table 4.3.

Table 4.3 The comparison between the stability constants (log*K*) of THTD, THTUD, [10]-ane-N₃, THETAC and TETA are shown.¹⁴

	THTD	THTUD	[10]-ane-N ₃	THETAC	TETA
Cd(II)	19.38	18.05	9.1	10.6	18.25

THTD has the highest formation constant – 19.38 while THTUD¹⁴ and TETA have almost the same value. Since THTD and THTUD have the same design and basic structure, it was decided to use these two similar ligands to immobilize on the silica substrates.

Table 4.4 The p*K*_a values of the two free azamacrocyclic ligands are shown.¹⁴

	p <i>K</i> ₁	p <i>K</i> ₂
THTD	9.18	4.26
THTUD	11.32	5.87

The p*K*_a values in table 4.4 indicate that the free ligands are deprotonated at the pH values that are being used for the extractions. It is anticipated though that the electronic structure and behaviour of the ligands will change slightly once they are immobilized on the silica substrates due to the influence of the supports as well as the influence of the spacer. These changes should not be so drastic that it would change the behaviour of the ligands after immobilization.

The average extraction of Cd^{2+} at a pH of 4.5 with the various ligands immobilized on Si gel (60 Å), was less than 2.5%. Although THPTD showed some extraction with Cd^{2+} , it was still less than 2.5% and is therefore considered to have zero extraction with Cd^{2+} . The other ligands did not extract any Cd^{2+} at all (figure 4.2). All the values fall within the experimental error.

With the pH raised to 5.9, the average extraction with the immobilized ligands on Si gel (60 Å) increased to 15.2% (ligands are 45% effective). With the exception of 18-c-6 and 15-c-5 with glymo, the other ligands all participated in the extraction (figure 4.2). The only support that failed to extract any of the Cd^{2+} was HMS. The ligands on this support show no extraction at all.

The average extraction increased significantly with the various supports with the exception of HMS at the higher pH of 5.9.

At the lower pH, no extraction with any of the ligands immobilized on any of the supports was possible. It appears that THPTD, although slightly lower than the crown ether, is more selective towards the Cd^{2+} at the two pH values since it shows extraction with all the supports except with HMS, while the crown ethers only extracted with Si gel (60 Å) and SBA-15.

Cd^{2+} is considered to be a fairly soft metal ion and it has a radius of 0.95 Å.^{4,15} The Cd^{2+} metal ions should therefore not favour the oxygen donors of the crown ethers, but rather that of the softer nitrogen donors. The cavity sizes of the azamacrocycles are smaller than that of the crown ethers and this should then lead to the azamacrocycles being more selective towards the Cd^{2+} metal ions. It is interesting to note that 18-c-6 on SBA-15 (35.9%) and the glymo 18-c-6 (37.7%) on Si gel (60 Å) show almost the same extraction for Cd^{2+} . It might be because the crown ether can fold itself around the smaller Cd^{2+} , much the way it does with K^+ , since Cd^{2+} is smaller than K^+ . Also, because of the presence of the N atoms which are used as an anchor point to the glymo spacer, Cd^{2+} can perhaps be incorporated between the N atom of the “anchor”, the O atom of the hydroxyl group and an O atom of the crown ether.

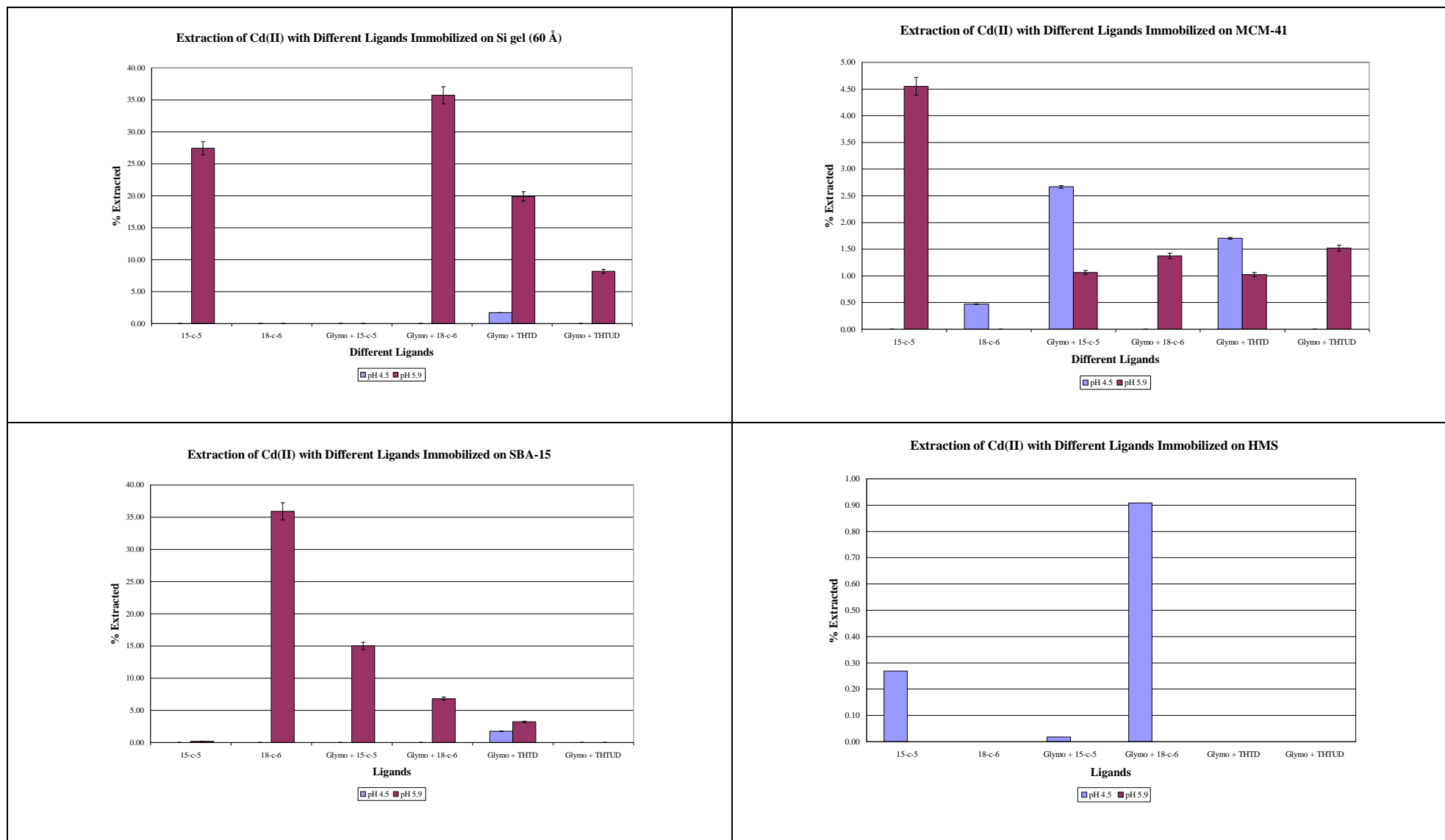


Figure 4.2 The extraction of Cd(II) with various ligands immobilized on four different Si supports

For comparison purposes we have looked at other work involving Cd^{2+} extraction. Equilibrium constants ($\log K$) have been determined by Wassink and co-workers² for the extraction of Cd^{2+} chloride complexes with Aliquat 336 in benzene from LiCl solutions and were found to be 8.17. In chloroform, the extraction from HCl was lower with a value of 5.66. This means that Cd^{2+} is strongly extracted from chloride solutions by Aliquat 336.²

4.3.3. Extraction of Cr(VI) with various ligands immobilized on four different silica supports

A number of experiments were conducted by various groups to find the best and most efficient way for the removal of chromium from waste solutions. Agrawal, Pal and Sahu used cyanex 923 and obtained very high yield of up to 99% under optimum conditions which included an initial feed of 1 g/L. The only metal to interfere with their results was Zn.¹⁶ Hossain used non-traditional solvents such as sunflower oil and lubricant oil in conjunction with Aliquat 336 to remove hexavalent chromium from ground water and industrial water. Extraction of 50 – 96% was achieved at a pH of between 6 and 8.¹⁷

Chromium is normally found as one of the following species: $\text{Cr}_2\text{O}_7^{2-}$, CrO_4^{2-} or HCrO_4^- .¹⁸ It appears that the ligands have the right configuration to accommodate the metal ions. The extraction was carried out in an acidic medium, which means that the ligands were partially protonated. The ligands could be positively charged. The ligands could thus coordinate the negatively charged chromium species.

With the solution buffered at 4.5, the average extraction for the different ligands, immobilized on Si gel (60 Å) were 11.7% (ligands are 34% effective), of which THTD (21.4% - 64% effective) and THTUD (23.9% - 90% effective) were the best performing ligands (figure 4.3).

With the pH raised to 5.9, the average extraction increased dramatically, as expected, to 25.8%. The THTD (33.8% - 90% effective) and THTUD (33.7% - 95% effective) were again the most effective ligands to use (figure 4.3).

With the pH at 4.5, MCM-41 was the least effective support to use. SBA-15 and HMS were almost the same with an average extraction of $\pm 10\%$ (ligands are 40% effective). THTD was the best ligand to use.

With the pH at 5.9, even the other supports showed a dramatic increase in the extraction capabilities with the various ligands. THTD again proved the most selective ligand of the “six” to use when extracting $H_xCr_yO_z^{-n}$.

With the Si gel (60 Å), it is interesting to note that the extraction increased as the length of the spacer increased. With the MCM-41 and SBA-15, the extraction stayed almost constant, but there was a slight decline when HMS was used as a support. 15-c-5 was the worst ligand with an average extraction of 18.7% (52% effective). THTD performed the best on all supports and it had an average extraction capability of 33.1% (90% effective). 18-c-6 immobilized with glymo and THTUD were very close to each other with an average extraction of $\pm 25\%$.

The increase in the extraction when a spacer is used with the ligand on the Si gel (60 Å), is most probably because there is more freedom for the ligands to move about in the solution. When a shorter spacer is used, the ligand is very close to the support and the metal ions may find it harder to get close to the ligand.

$H_xCr_yO_z^{-n}$ is known as a hard acid, and the ligands that were used contain hard oxygen and borderline/hard nitrogen donors. Therefore it is quite a reasonable assumption that the hard donors and the hard acid will complex very well in the case of $H_xCr_yO_z^{-n}$.

It does not look like the different surface areas of the silica supports had any influence on the working of the ligands because with the higher pH, the extraction was also high. The only factor that had a profound influence on the degree of extraction was the difference in the pH. With all the different ligands attached to the different supports, it is clear that there is a dramatic increase in the extraction as the pH increased from 4.5 to 5.9.

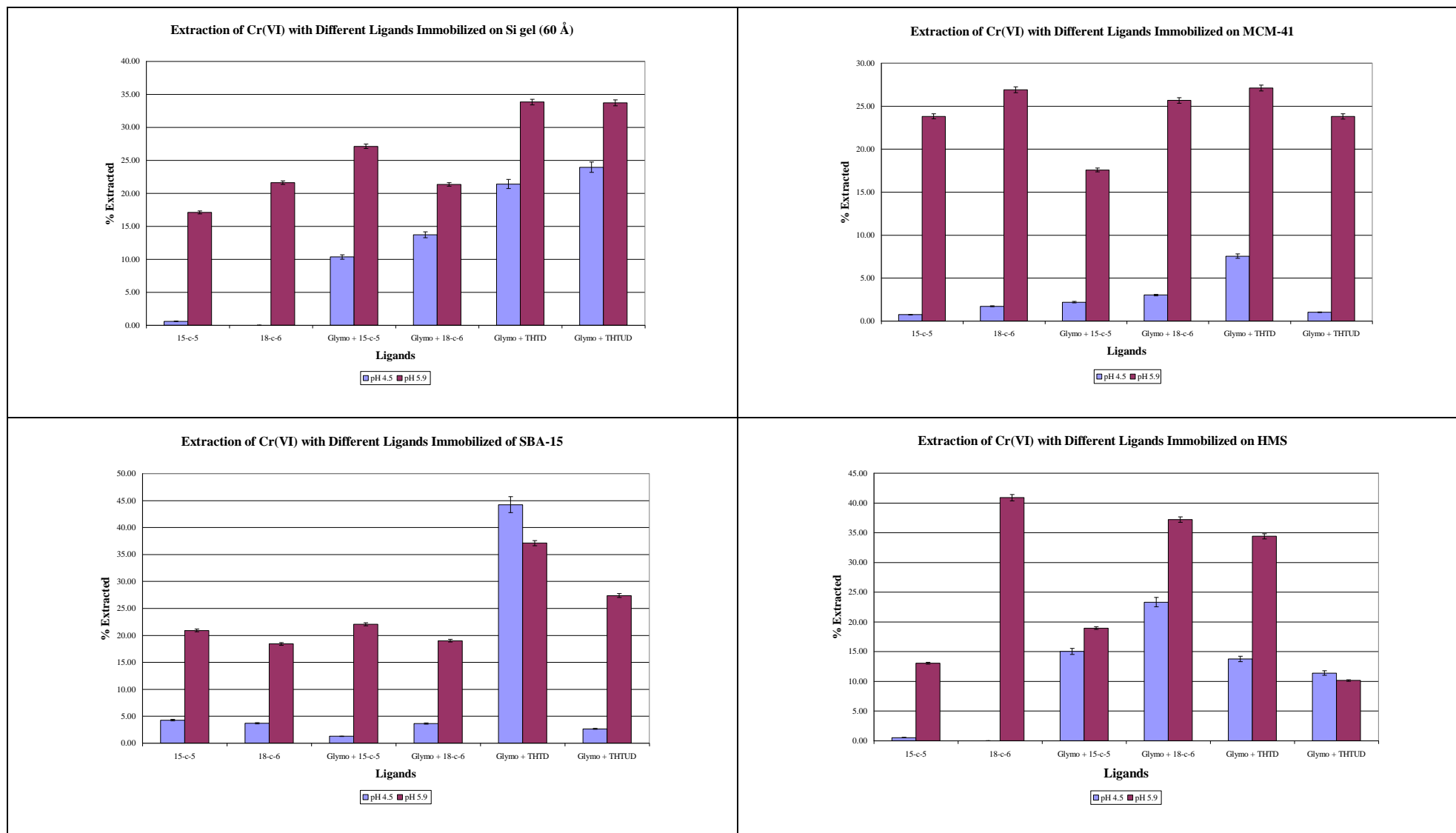


Figure 4.3 The extraction of Cr(VI) with various ligands immobilized on four different Si supports

The average extraction for Si gel (60 Å) with each of the different ligands immobilized increase from approximately 11.46% to 25.79%.

For MCM-41 there was an increase from 2.70% to 24.14%. There was an increase from 9.40% to 24.13% for SBA-15 and finally for HMS the increase was from 10.62% to 25.76%. It appears that Si gel (60 Å) is the best support for immobilization of each of the ligands when used for the extraction of $H_xCr_yO_z^{-n}$. A reason for this observation is that the Si gel (60 Å) has a much more evenly distribution of the immobilized ligands on the surface. This even distribution will give a larger contact surface for the $H_xCr_yO_z^{-n}$ ions to coordinate to the ligands.

4.3.4. Extraction of Sr(II) with various ligands immobilized on four different silica supports

Wood *et al.* used DtBuCH18C6 for the removal of ^{90}Sr and Pb (>99%) in batch solvent extraction experiments. It was found that this method was more selective towards Pb. The extraction was very much dependent on the nitric acid concentration of the solutions.¹⁹

Wai *et al.* reported that Sr^{2+} is selectively extracted from aqueous solutions into supercritical fluid CO_2 by DC18C6. They also reported that any of the 18-membered crown ethers with a radius in the range of 1.3 – 1.4 Å are most suitable as hosts for Sr^{2+} which has a radius of 1.13 Å.²⁰ Izatt *et al.* determined the $\log K$ value for Sr^{2+} with the free ligand 18-c-6, to be 2.72.²¹ Hancock *et al.*^{4,22} reported the radius of Sr^{2+} as 1.18 Å. 18-c-6 has an estimated radius of 1.38 Å. This means that Sr^{2+} should fit very well into the cavity of this crown ether. It may therefore appear that size match selectivity plays a role in the extraction process. Sr^{2+} is considered to be a hard acid. The crown ethers contain hard oxygen donors that prefer to coordinate with hard acids. This may be another reason why there is better selectivity when the crown ethers are used. The azamacrocycles have two slight drawbacks. Firstly, the radii are much smaller than that of the crown ethers and secondly, the nitrogen donor atoms are not as hard as the oxygen donors. The nitrogen donors are considered to be borderline/hard in their soft/hard properties. With regards to

the better extraction when a spacer is introduced, it could well mean that there is better interaction between the metal ions and the ligands. The influence of the supports are minimised, and the longer spacer gives more freedom to the ligands to move around in solution as constrained by the spacer.

With the pH at 4.5, it was found that no Sr^{2+} was extracted with any of the ligands immobilized on any of the supports. There was a remarkable improvement in the extraction when the pH was increased to 5.9. The average extraction with all the ligands immobilized on Si gel (60 Å) was 10.0% (ligands are 30% effective) and with MCM-41 as a support the average extraction was 9.0% (ligands are 27% effective). The extraction with SBA-15 as support was less than 1% (figure 4.4).

As expected, the best extraction was obtained using the crown ethers. The 15-c-5 immobilized with the glymo spacer on Si gel (60 Å) gave an extraction of 25.4% (ligand is 75% effective) while 18-c-6 immobilized with the glymo spacer on MCM-41 yielded 24.5%. With the exception of 18-c-6 immobilized directly on HMS (30.2%), it is clear that the better extraction was obtained as the spacer was introduced. THTD and THTUD did not perform well with the extraction of the Sr^{2+} , as was expected. There is an unusual occurrence with the THTD and THTUD immobilized on MCM-41. The nitrogen donating ligands performed better than the crown ethers with the exception of 18-c-6 immobilized with the glymo to the support. It is also interesting to note that 15-c-5 immobilized with a spacer on Si gel (60 Å) performed the same as the 18-c-6 immobilized with the spacer on MCM-41. Both 15-c-5 and 18-c-6 immobilized with spacers on SBA-15 extracted Sr^{2+} equally well. It was found that the best average extraction was obtained by using the 18-c-6 ligand (11.0%) and the best support is the Si gel (60 Å). The 15-c-5 and 18-c-6 ligands that were immobilized with the glymo spacer yielded an *average* extraction of 9.3% and 9.3% respectively (figure 4.4).

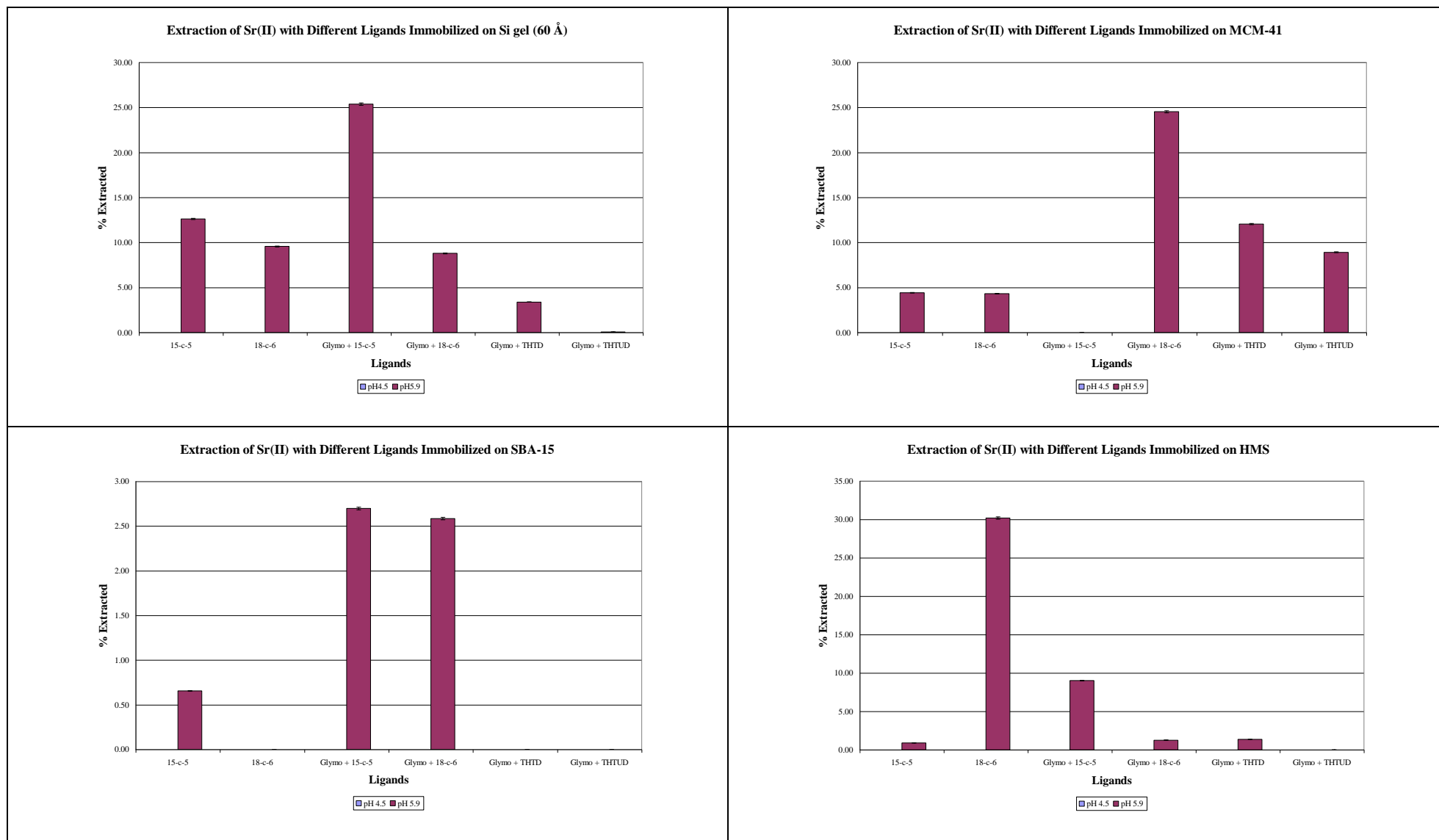


Figure 4.4 The extraction of Sr(II) with various ligands immobilized on four different Si supports

4.3.5. Extraction of Hg(II) with various ligands immobilized on four different silica supports

No extraction occurred at a pH of 5.9 when using any of the ligands in any combination with the supports. Since no extraction was possible at the higher pH, it was decided not to do the extraction at pH 4.5.

Hg^{2+} is considered to be a soft acid. The ligands that were used for the extraction are all hard or borderline. Although Hg^{2+} has a radius of 1.1 Å, and can fit into the cavities of the crown ethers, the size match selectivity cannot overcome the hardness of the ligands and thus no extraction was possible.

Since Hg^{2+} is very acidic, this means that other species may be present to prevent complexation with the crown ethers. With the free ligands, the $\log K$ value for Hg^{2+} with 18-C-6 is 2.42 and for 15-C-5 it is 1.68 according to Izatt *et al.*²¹ The $\log K$ values are very low, so complexation with the crown ethers are not all that favourable

4.3.6. Extraction of U(VI) with various ligands immobilized on four different silica supports

Sadeghi and Sheikhzadeh adjusted their pH to 5.5. It was proven that hydrolysis of the APMS system was resistant to a pH range between 3 and 8. It was also shown that a lowering of the pH decreased the uptake capacity of the sorbent. A maximum extraction of 1.13 mmol g⁻¹ was achieved.²³ Yuan *et al.* showed that the maximum sorption of U(VI) with DIMS (dihydroimidazole functionalised SBA-15) was 268 mg g⁻¹ at pH 5.0.²⁴ The extraction of UO_2^{2+} was therefore done only at pH 5.9. Because UO_2^{2+} is so acidic, it was decided that the extraction at pH 4.5 would not provide better results since all other extraction showed that a higher extraction is obtained at the higher pH (figure 4.5). Grüner and co-workers also reported that only very weak complexation with UO_2^{2+} occurs at pH 4.5 – 5.^{25, 26}

The average extraction for the different ligands on the various supports was between 13% and 16.5%. HMS was the best support (16.5%) and MCM-41

was the worst (13%). Yuan *et al.* compared various supports and found that the results between SBA-15 and MCM-41 were similar.²⁴

All the ligands showed extraction with the uranyl. The best ligand for the extraction is 15-c-5 (17.5% -ligand is 50% effective) which was directly immobilized on the supports. The second best was the 18-c-6 (15.0%), also directly immobilized on the supports. When the spacer was introduced, the extraction of the uranyl decreased. This trend was observed for the crown ethers on all the supports. This confirmed the findings of Szigethy and Raymond.²⁷ The chelator orientation about the uranyl strongly depends on the length of the spacer and it was found that ligands that were immobilized with short flexible spacers coordinate better to the uranyl than the same ligand with a longer spacer. The best extraction was achieved with 15-c-5 (25.7% ligand is 70% effective), immobilized directly on HMS (Figure 4.5).

THTD (14.7%) and THTUD(13.6%) performed better than the crown ethers that was immobilized with the spacers.

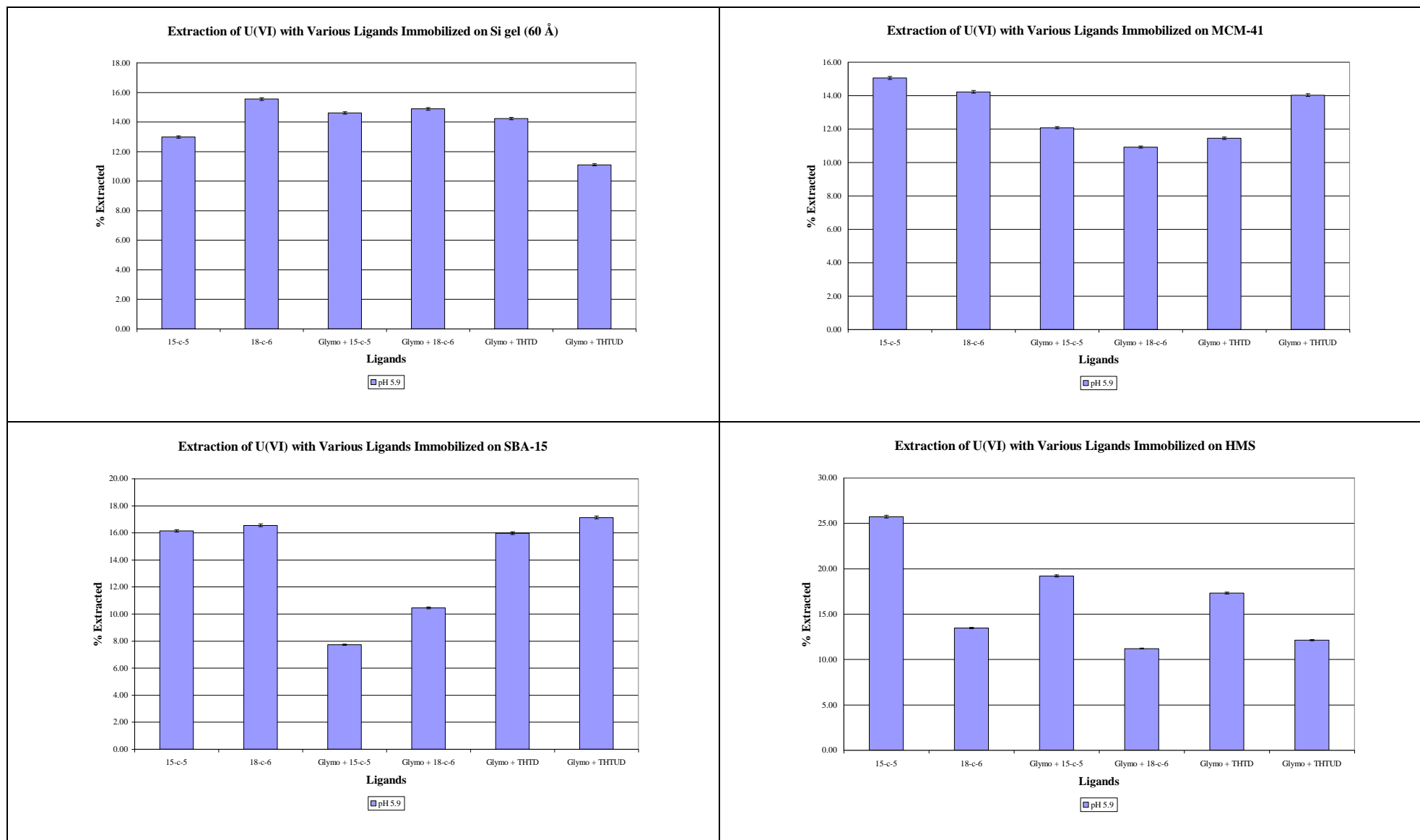


Figure 4.5 The extraction of UO_2^{2+} with various ligands immobilized on four different Si supports

The uranyl ion is considered to be a hard Lewis acid. This means that the uranyl ion will have a greater affinity for hard donors. Szigethy and Raymond²⁷ found that there was a profound affinity between uranyl and the crown ethers. Since the crown ethers contain only hard oxygen donors, it is understandable that the crown ether should have a great affinity for the uranyl ion according to the Irving-Williams classification system. The tri-azamacrocycles are borderline/hard donors and it is thus not strange that there would be some affinity for the uranyl. The nitrogen may not be as hard as the oxygen donors in the ring, but there are oxygen donors on the pendant arms that will show affinity towards the uranyl ion.

Uranyl is a big molecule and cannot fit into the cavities of the crown ethers and definitely not in the azamacrocycles. It is therefore clear that the uranyl must be situated on the outside of the cavities of the macrocycles. It was found by Szigethy and Raymond that the uranyl ion definitely coordinates to form the preferred pentagon. Even when there was considerable strain when the ideal angle changed from 72° to 65.2°, the preferred structure was still the pentagon.²⁷

4.3.7. The extraction of two metal ions with various ligands immobilized on four different silica supports

The competition extraction of Hg^{2+} and UO_2^{2+} was executed at pH 5.9 since the extraction at pH 4.5 is very weak. There was high selectivity in the extraction between Hg^{2+} and UO_2^{2+} since no Hg^{2+} was extracted. Only UO_2^{2+} was extracted.

Again it was clear that the crown ethers that was immobilized directly onto the support, extracted the UO_2^{2+} better than the crown ethers that was immobilized with the glymo spacer. On average, the ligands that are supported on the Si gel (60 Å) produced the best results (9.2% - ligands are 27% effective)). 18-c-6 (13.6%) and THTUD (14.4% ligand is 56% effective) were the best ligands for the extraction (figure 4.6).

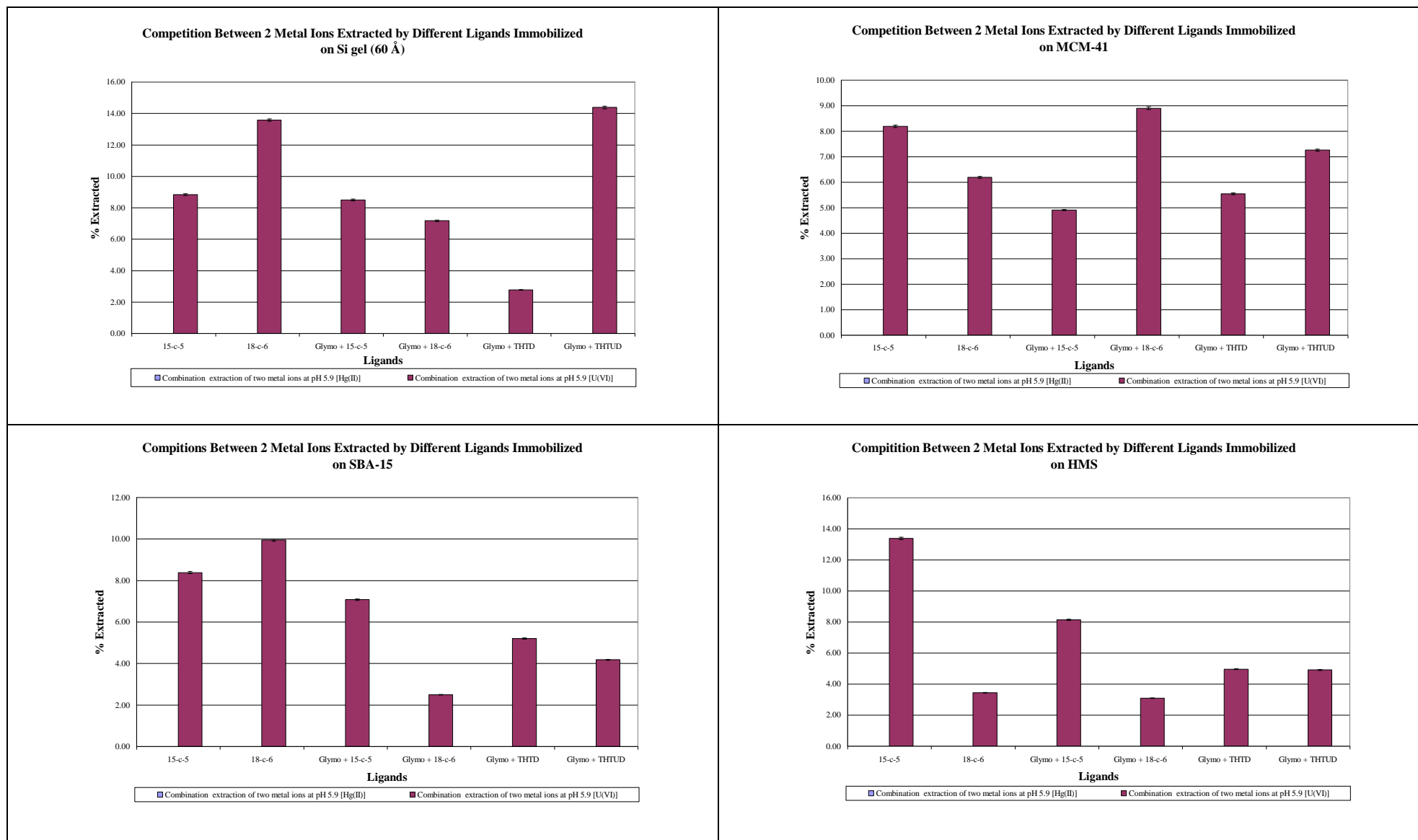


Figure 4.6 The extraction of 2 metal ions with various ligands immobilized on four different Si supports

The average extraction for 15-c-5, directly immobilized on the supports is 9.7% (ligand is 30% effective). Of the crown ethers, the highest extraction was achieved with 18-c-6 (13.6%), directly immobilized on Si gel (60 Å). The best extraction though was achieved with THTUD (14.4% - ligand is 56% effective) immobilized on Si gel (60 Å).

There is a slight decline in the extraction capacity when two metal ions are in competition with each other. Both uranyl and the mercury ions are very big ions and one reason could thus be that there is a lot of shielding by the Hg^{2+} which means that the UO_2^{2+} cannot get close to the ligands for extraction in the time that was allowed. It appears therefore that the immobilized ligands are just so overwhelmed by the sheer amount of metal ions, that the time allowed for extraction was just not enough. Since there is less contact between the UO_2^{2+} and the ligands in the extraction time period, the extraction will not be as efficient as was the case when only UO_2^{2+} was extracted. The extraction trend with the single metal ion and that of the combination with two metal ions are similar in almost all respects, except for the extraction percentage that was achieved.

4.3.8. The extraction of four different metal ions with various ligands immobilized on four different silica supports.

With the pH at 4.5, it can be seen that the only extraction occurred with $\text{H}_x\text{Cr}_y\text{O}_z^{-n}$. The overall extraction of the $\text{H}_x\text{Cr}_y\text{O}_z^{-n}$ is 7.0%. The other metal ions had an extraction of less than 2.3%. With the pH increased to 5.9, the overall percentage of the extraction of metal ions decreased. The interesting fact is actually that more metal ions now get extracted and the extraction is not limited to the $\text{H}_x\text{Cr}_y\text{O}_z^{-n}$ alone. Although more metal ions get extracted, it can be seen that the $\text{H}_x\text{Cr}_y\text{O}_z^{-n}$ is preferred in the competition extraction (figure 4.7).

The ligand that is more selective towards $\text{H}_x\text{Cr}_y\text{O}_z^{-n}$ with this combination of metal ions, is the THTD. It appears that the hardness of the ligand and that of

the metal ion is the major driving force for the extraction. Size match selectivity is therefore a secondary contributing factor.

The two supports that yielded the best results with the immobilized ligands in the competition extraction with 4 metal ions, were Si gel (60 Å) and HMS. It will appear that the surface area, pore volume and pore diameters distribute the immobilized ligands more evenly. This gives the ligands, attached to their supports, the freedom to move about in the solution. The metal ions in the solution on the other hand also move about the solution easier and can get close to the ligands. The other supports have smaller surface areas, pore diameter and pore volumes. This influences the total surface areas of the supports that can be used for immobilization. Because of the “smaller” surface area that is available for immobilization, the ligands are forced closer to each other. This hampers the free movement of the ligands on their supports. The metal ions can also not get into close proximity of the ligands and thus less metal ions can be extracted.

The slight decline in the extraction capacities can be contributed to the amount of metal ions that were introduced to the solution. In this instance, it could be a matter of “first come first served”. Once a metal ion is complexed to the ligand, there is little chance that another metal will replace it. There is also the H_nAsO^{-x} that might act in a kind of shielding manner, preventing other metal ions from coming into contact with the ligands in the time that was allowed.

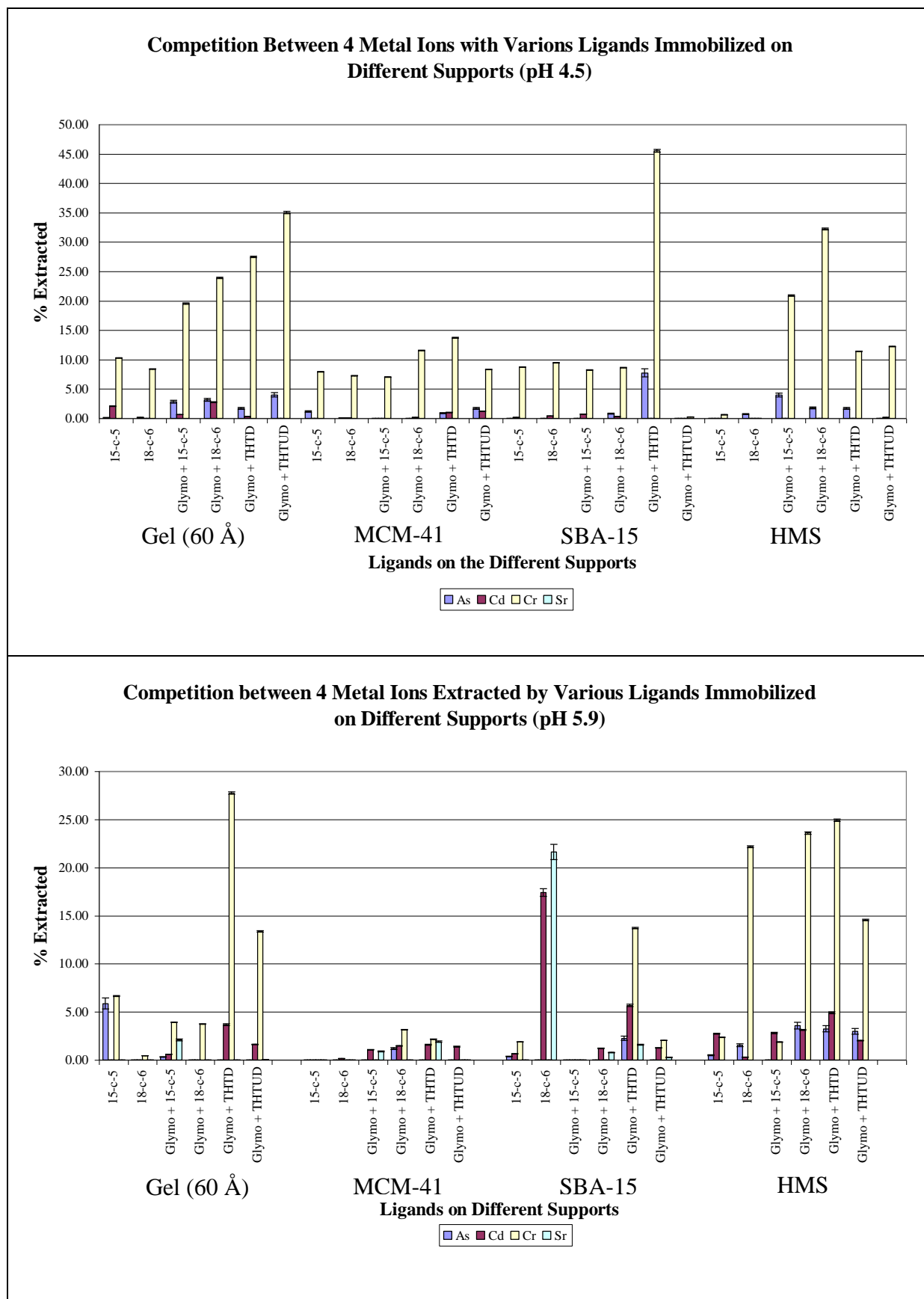


Figure 4.7 The extraction of four different metal ions with various ligands immobilized on four different Si supports.

4.3.9. The extraction of various metal ions with 15-c-5 directly immobilized on different silica supports.

At a pH of 4.5 there is very little extraction of any metal ions with the exception of a small amount of $\text{H}_x\text{Cr}_y\text{O}_z^{-n}$. With the pH at 5.9, the extraction of $\text{H}_x\text{Cr}_y\text{O}_z^{-n}$ increased to more than 20%. It was also found that UO_2^{2+} was extracted in significant amount. With the ligand supported on HMS, the extraction of uranyl increased to 25.7% (Figure 4.8 –ligand is 75% effective).

From figure 4.8, it is clear that the best support though, is Si gel (60 Å). More metal ions are extracted with 15-c-5 immobilized on this particular support than with any of the other ligands and supports. It is proposed that the overall surface area is more accessible than the other supports due to the fact that the pore diameter and pore volume is also available while with the other supports, the pore opening is so small, the ligands cannot enter the cavity, leaving just the outside surface to be used for immobilization. It is proposed that there is crowding of the ligands on the surface of the support, and the metal ions cannot get in between the ligands to be extracted.

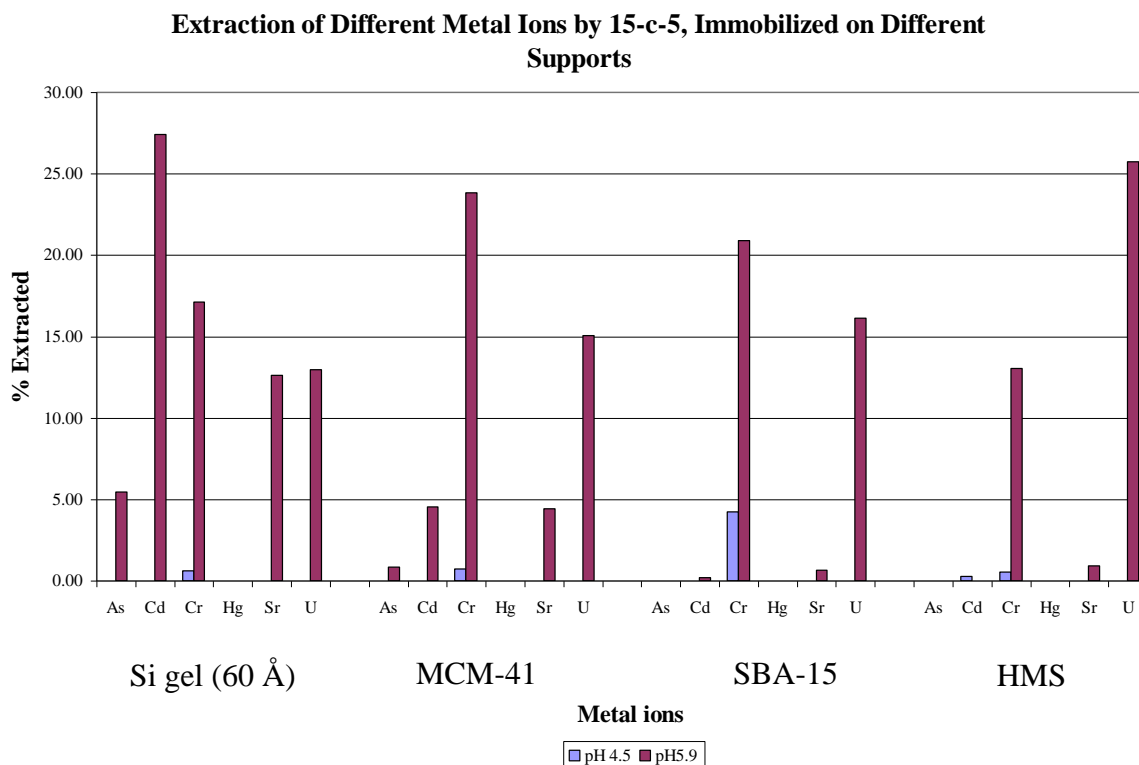


Figure 4.8 The extraction of various metal ions with 15-c-5, directly immobilized on different silica supports.

4.3.10. The extraction of various metal ions with 18-c-6 directly immobilized on different silica supports.

With the pH at 4.5, there is no extraction of any of the metal ions with the exception of a small amount of $\text{H}_x\text{Cr}_y\text{O}_z^{-n}$ in conjunction with the supports MCM-41 and SBA-15. With the pH raised to 5.9, the extraction of $\text{H}_x\text{Cr}_y\text{O}_z^{-n}$ increased remarkably, especially with HMS as support (40.9%). It can also be seen that the extraction of Cr^{6+} increased as the length of the spacer increased. As expected, the extraction of UO_2^{2+} also increased with all 18-c-6 immobilized on the different supports. The extraction of Sr^{2+} shows a significant increase with HMS as the support. Only with SBA-15 no extraction of Sr^{2+} was achieved (Figure 4.9).

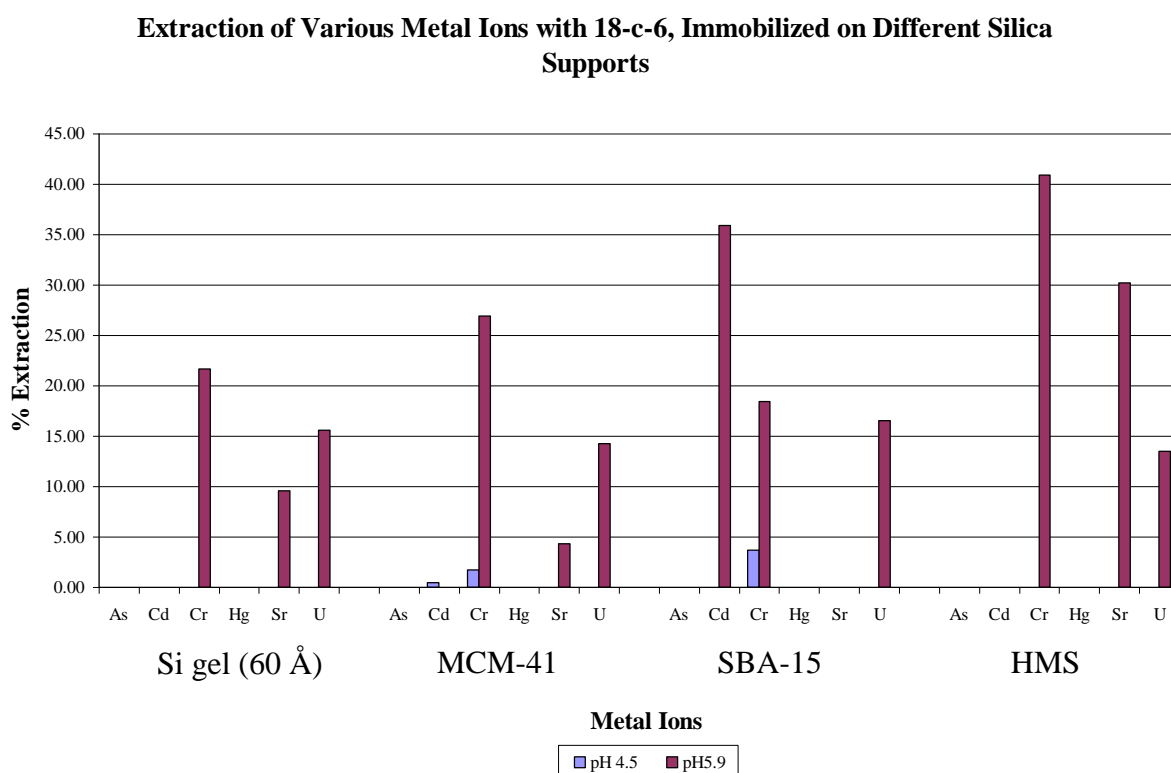


Figure 4.9 The extraction of various metal ions with 18-c-6, directly immobilized on different silica supports.

The fact that Cd^{2+} is extracted by 18-c-6 on SBA-15 is perhaps due to synergism. It is quite strange that no other support showed the same enhanced cooperation.

4.3.11. The extraction of various metal ions with 15-c-5 immobilized with a glymo spacer on different silica supports.

$H_xCr_yO_z^{-n}$ showed a fairly low extraction with the two supports, Si gel (60 Å) and HMS with the pH at 4.5.

When the pH was increased to 5.9, the extraction of $H_xCr_yO_z^{-n}$, Sr^{2+} and UO_2^{2+} increased significantly (Figure 4.10). With Si gel (60 Å) as support, the percentage extraction was considerably higher. The extraction decreased with the use of MCM-41 and was even lower with SBA-15, and the worst support was HMS (Figure 4.10).

From the data (Figure 4.10) it can be seen that 15-c-5, immobilized with a glymo spacer is more selective towards $H_xCr_yO_z^{-n}$, Sr^{2+} and UO_2^{2+} , irrespective of the silica support that was used.

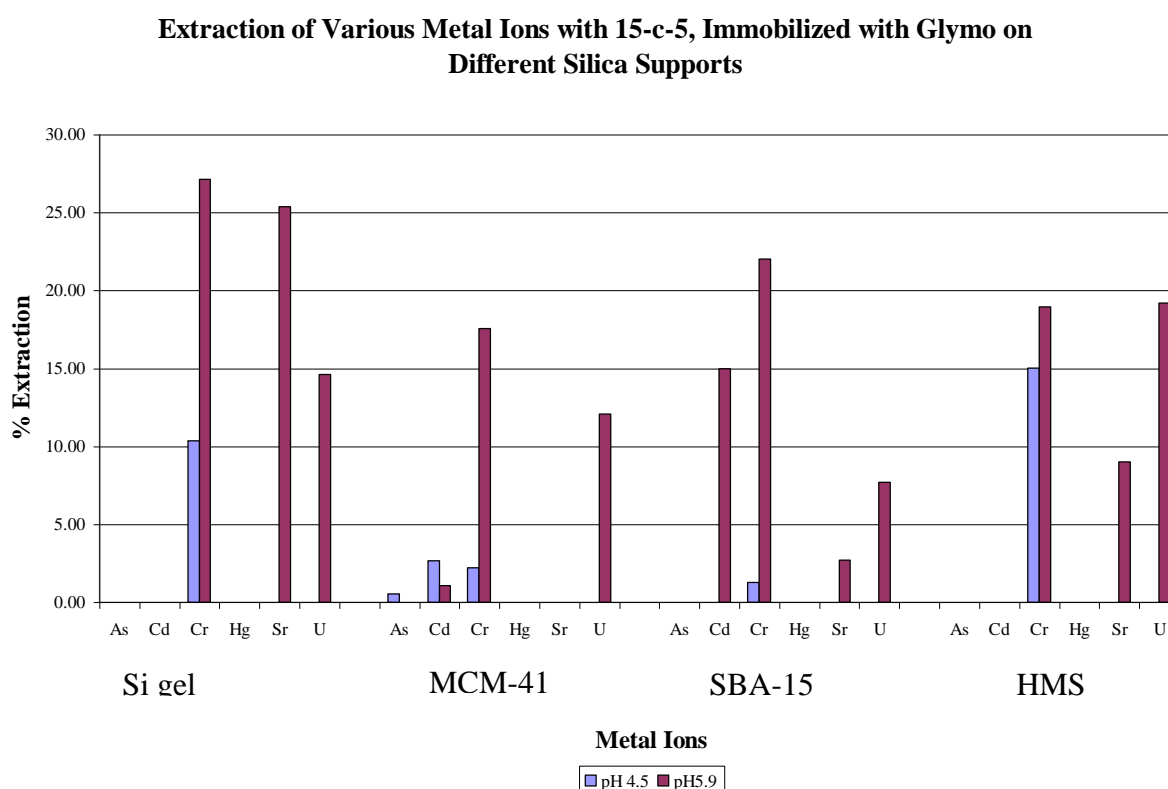


Figure 4.10 The extraction of various metal ions with 15-c-5, immobilized with a glymo spacer on different silica supports.

4.3.12. The extraction of various metal ions with 18-c-6, immobilized with a glymo spacer on different silica supports.

Only $H_xCr_yO_z^{-n}$ shows any extraction at all with the pH at 4.5 (Figure 4.11). At pH 5.9 there is quite a substantial increase in the extraction of all the metal ions, especially Sr^{2+} with the MCM-41 as support. Cd^{2+} shows good extraction (36%) with the ligand supported on Si gel (60 Å). This is extraordinary considering that no Cd^{2+} is extracted with the ligands supported directly onto the support. It appears that the ligand has more flexibility to move about in the solution to coordinate to the metal ion. Sr^{2+} and UO_2^{2+} are being extracted in more significant quantities as is expected. Si gel (60 Å) again is the best support to use, since it can be seen that the extractions of all the metal ions, with the exception of the extraction of Cr^{6+} (HMS), is much higher than that of any of the other supports (Figure 4.11).

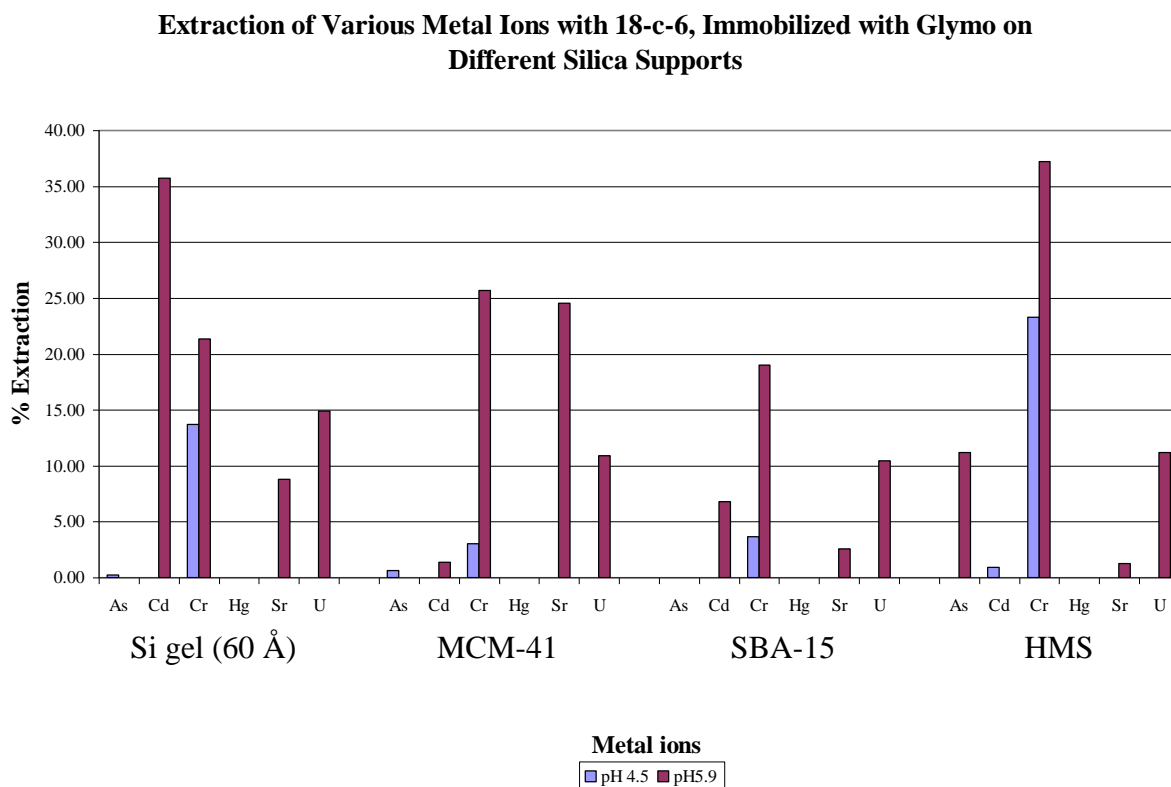


Figure 4.11 The extraction of various metal ions with 18-c-6, immobilized with a glymo spacer on different supports.

4.3.13. The extraction of various metal ions with THTD, immobilized with a glymo spacer on different silica supports.

At the lower pH of 4.5, there is a small extraction of Cd^{2+} and $\text{H}_x\text{Cr}_y\text{O}_z^{-n}$ (Figure 4.12).

The extraction of $\text{H}_x\text{Cr}_y\text{O}_z^{-n}$ at the pH value of 4.5 is quite prominent, especially when Si gel (60 Å) and SBA-15 were used as supports. There is the unusual result of the extraction being better at pH 4.5 rather than 5.9. As expected, with the increase in the pH to 5.9, the average extraction also increased. Cd^{2+} shows an improvement in extraction with Si gel (60 Å) as a support. The % extraction of $\text{H}_x\text{Cr}_y\text{O}_z^{-n}$ also increased significantly. Previously, no Sr^{2+} was extracted, but with the higher pH, all the supports except SBA-15 show a slight extraction. THTD extracted significant amounts of uranyl on all the supports. Si gel (60 Å) is again better to use as a support with this ligand (figure 4.12).

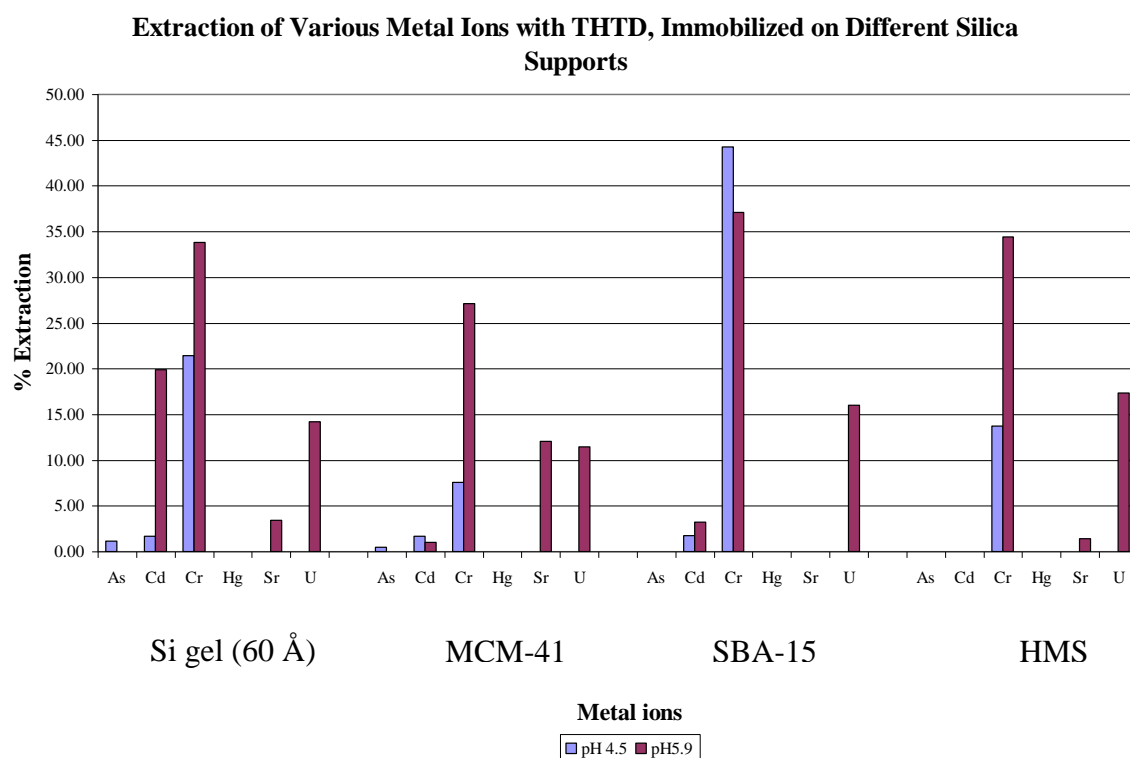


Figure 4.12 The extraction of various metal ions with THTD, immobilized with a glymo spacer on different silica supports.

4.3.14. The extraction of various metal ions with THTUD, immobilized with a glymo spacer on different silica supports.

The only notable extraction at pH 4.5 is that of $\text{H}_x\text{Cr}_y\text{O}_z^{-n}$ with the Si gel (60 Å) as support (Figure 4.13).

As expected, the extraction increased with the pH at 5.9 (Figure 4.13). Cd^{2+} shows extraction when Si gel (60 Å) is used as a support and to a much lesser extent, with the MCM-41 as well. The $\text{H}_x\text{Cr}_y\text{O}_z^{-n}$ is extracted in the range of 10 – 34% with this ligand anchored on any of the 4 supports. THTUD extracted the UO_2^{2+} in quite significant amounts (11 – 17.5%) with any of the supports that were used (Figure 4.13).

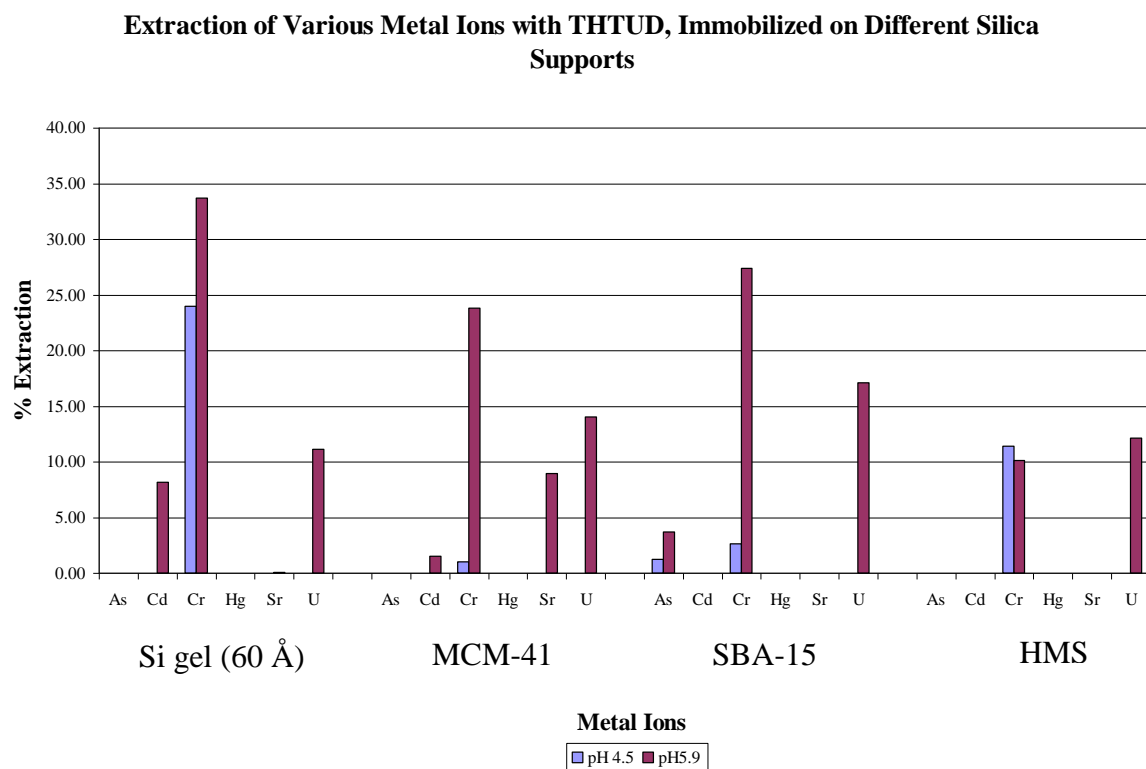


Figure 4.13 The extraction of various metal ions with THTUD, immobilized with a glymo spacer on different silica supports.

Si gel (60 Å) is best support to use, while the other supports show a definite decline in the extraction of the various metal ions.

The higher extraction percentage of $H_xCr_yO_z^{-n}$ at a pH value of 4.5 when HMS was used, is a negligible difference on HMS which is the lowest in terms of surface area, pore size and pore volume of the four supports. Throughout the extraction experiments, it performed the least effective.

4.4 Discussion of the Protonation Constants: Influence of the pH on the Extraction

There is competition between the protons and the metal ion for the ligand. For coordination of the ligand to the metal ion to take place, the ligand and/or the metal ion must be deprotonated. As the solution becomes more basic, the metal ions can form hydroxide complexes because of the excess OH^- . Other species may also be found when the species distribution is investigated.

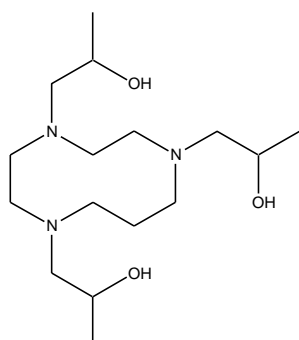
For the tri-azamacrocycles, it is possible to determine protonation constants, for this will give an indication of the competition that can arise during the complexation with metal ions when extraction experiments are conducted at various pH levels. These protonation constants for the free ligands, THTD and THTUD (Figure 4.14), are shown in table 4.5 along with the parent and other similar ligands. These protonation constants are determined for the free ligands, however, when the ligands are attached (via spacers) to the supports, the protonation constants could be different, because electronically, the immobilized ligands are now different from the free ligands.

At the lower pH of 4.5 THTD will be protonated. THTUD has 2 protons on the nitrogen atoms. One of these protons is held in position in the cavity by the two nitrogen donor atoms. The occupation of the macrocyclic cavity, and the fact that the donor atoms are already attached to the protons, will prevent the complexation with the metal ions. In order to achieve complexation, it is necessary to work at a higher pH to prevent the ligands from being protonated.

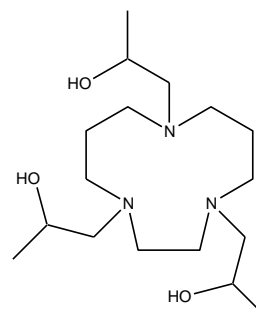
There are no protonation constants for the crown ethers.

Table 4.5 The log(*K*) values of ligands with similar structures as THTD and THTUD.

No.		Log(<i>K</i> ₁)	Log(<i>K</i> ₂)	Log(<i>K</i> ₃)
1	1,4,7-tris[2-(<i>S</i>)-hydroxypropyl]-1,4,7-triazacyclodecane (THTD)¹⁴	9,18	4,20	
2	1,4,8-tris[2-(<i>S</i>)-hydroxypropyl]-1,4,8-triazacycloundecane (THTUD)¹⁴	11,32	5,87	
3	1,4,7-tris(2-hydroxyethyl)-1,4,7-triazacyclononane ^{28, 29} (THETAC)	11.50	3.42	
4	1,4,7-triazacyclononane (9-ane-N ₃) ³⁰	10.44	6.81	
5	1,4,7-triazacyclodecane (10-ane-N ₃) ²⁹	12.00	6.61	
6	1,4,8-triazacycloundecane (11-ane-N ₃) ²⁹	12.00	7.61	
7	1,4,7-triazacyclononane-N,N',N''-triacetic acid (NOTA)	11.60	5.70	3.17
8	1,4,7-triazacyclodecane-N,N',N''-triacetic acid (DETA)	N/A	6.12	3.69
9	1,4,8-triazacyclodecane-N,N',N''-triacetic acid	N/A	7.20	3.40



THTD



THTUD

Figure 4.14 Structures of the neutral, free ligands , THTD and THTUD.

4.5 Conclusion

Extraction experiments with just the supports were also conducted. The amount of metal ions extracted was below 2.5 % and can be considered to be zero.

It is evident that a better extraction is achieved at a higher pH, in this particular study, a pH-value of 5.9, compared to 4.5. The reason may well be because the ligands are less protonated at the higher pH. This leaves the cavity, as well as the donating atoms exposed and complexation can take place.

It was found that Si gel (60 Å) is the most effective support to use. It does not always have the highest yields, but in all the extraction experiments, some extraction was obtained when Si gel (60 Å) was used as the support. A reason for this result may be because of the more favourable BET results concerning the surface area of Si gel (60 Å). The area of the Si gel (60 Å) is more accessible and can be modified more easily. MCM-41 is also a very good and easy support to use, but it is very expensive, even more than Si gel (60 Å) and the pore openings are very small which might prevent the ligands and metal ions to enter. This leads to crowding of the ligands on the surface of MCM-41 which in turn leads to less contact area for the metal ions. SBA-15 and HMS showed the least effective results as supports with all of the ligands. Their BET results showed that the usable surface areas were cramped and much smaller than that of Si gel (60 Å) or that of MCM-41.

There was no affinity for As^{5+} or Hg^{2+} at either of the two pH levels. There is slight selectivity for Cd^{2+} extraction by 18-c-6, THTD and THTUD. Cr^{6+} is selectively extracted by all the ligands, independent of the support that was used. Sr^{2+} is selectively extracted by 15-c-5 and to a lesser extent by 18-c-6. Uranyl showed the same preferential affinity towards 18-c-6 and 15-c-5.

It was shown that the extraction increased for the same ligands as soon as a spacer was introduced except for the extraction of the uranyl. As the length of the spacer increased, the extraction of the immobilized ligands increased as well except for the uranyl extraction. The reason is that the metal ions can come into better contact with the ligands because the ligands have more flexibility to move about in the solution, and that there is less interference from the Si supports.

References

- ¹ K. Gloe *et al.*, *Coord. Chem. Rev.*, 2001, **222**, 103
- ² B. Wassink, D. Dreisinger and J. Howard, *Hydrometallurgy*, 2000, **57**, 235
- ³ C.M. Madeyski, J.P. Michael and R.D. Hancock, *Inorg. Chem.*, 1984, **23**, 1487
- ⁴ R.C. Luckay and R.D. Hancock, *J. Chem. Soc., Dalton Trans.*, 1991, 1491
- ⁵ J.E. Huheey, E.A. Keiter and R.L. Keiter in *Inorganic Chemistry, Principles of Structure and Reactivity*, HarperCollins College Publishers, New York, 1993, 344-346
- ⁶ D.K. Cabbiness and D.W. Margerum, *J. Am. Chem. Soc.*, 1970, **92**, 2151
- ⁷ A.P. Leugger, L. Hertli and T.A. Kaden, *Helv. Acta*, 1978, **61**, 2296
- ⁸ D.D. Perrin and B. Dempsey in *Buffers for pH and Metal Ion Control*, Chapman and Hall, 1974
- ⁹ D. Black *et al.*, *Chem. Commun.*, 2002, 340
- ¹⁰ J. Kramer, N.E. Dhladhla and K.R. Koch, *Separation and Purification Technology*, 2006, **49**, 181
- ¹¹ R.A. Kumbasar, *J. Ind. Eng. Chem.*, 2010, **16**, 207
- ¹² R.A. Kumbasar, *Separation Sciences and tech.*, 2013, **48**, 1841
- ¹³ M.E. Mahmoud and H.M. Al-bishri, *J. Environ. Eng.*, 2012, 1138
- ¹⁴ B.F. Barnard (MSc Thesis), 2008
- ¹⁵ R. Luckay *et al.*, *Inorg. Chim. Acta.*, 1996, **246**, 159
- ¹⁶ A. Agrawal, C. Pal and K.K. Sahu, *J. Hazard. Mater.*, 2008, **159**, 458
- ¹⁷ M. Hossain, *Desalination and Water Treatment*, 2014, **52**, 3147
- ¹⁸ V. Lugo-Lugo *et al.*, *J. Haz. Mat.*, 2010, **176**, 418
- ¹⁹ Wood *et al.*, *Solvent Extr., And Ion Exch.*, 1997, **15(1)**, 65
- ²⁰ C.M. Wai *et al.*, *Chem. Commun.*, 1999, 2533
- ²¹ R.M. Izatt *et al.*, *J. Am. Chem. Soc.*, 1976, **98**, 7620
- ²² R.D. Hancock *et al.*, *Coord. Chem. Rev.*, 2007, **251**, 1678
- ²³ S. Sadeghi and E. Sheikhzadeh, *J. Hazard. Mater.*, 2009, **163**, 861
- ²⁴ L-Y. Yuan *et al.*, *J. Mater. Chem.*, 2012, **22**, 17019
- ²⁵ B. Grüner *et al.*, *New J. Chem.*, 2002, **26**, 867
- ²⁶ A. Avdeef *et al.*, *J. Am. Chem. Soc.*, 1978, **100**, 5362
- ²⁷ G. Szigethy and K.N. Raymond, *Inorg. Chem.*, 1999, **38**, 308
- ²⁸ R.M. Smith, A.E. Martell and R.J. Motekaites, *NIST Standard Reference Database 46 (Critically Selected Stability Constants of Metal Complexes), Version 8.0*, 2004
- ²⁹ B.A. Sayer, J.P. Michael and R.D. Hancock, *Inorg. Chim. Acta*, 1983, **77**, L63
- ³⁰ A.E. Martell and R.J. Motekaites in *Determination and use of Stability Constants*, VCH Publishers, New York, 1988, pp. 1-31

Chapter 5

Conclusions and Future Work

5.1 Conclusions

Two tri-azamacrocyclic ligands (THTD and THTUD) were successfully synthesised and all intermediates and final products were fully characterised using various analytical methods.

15-c-5 and 18-c-6 were successfully immobilized directly on the four different silica supports. These ligands were also immobilized on the various silica supports by means of a glymo spacer.

The THTD and THTUD were immobilized successfully on the silica supports by using a glymo spacer. The immobilization was confirmed by means of FTIR and solid state NMR. The TGA data showed that the immobilized crown ether ligands are thermally stable to ± 150 °C. The immobilized THTD and THTUD are stable to ± 250 °C.

Extraction experiments for the removal of selected metal ions were conducted at 2 different pH values. It was shown that better extraction can be achieved at a higher pH. It was also shown that when a spacer was introduced for the immobilization of the ligands, the extraction of the ligands improved significantly in all cases except for the uranyl ion. To a certain extent, selectivity was achieved by the ligands towards certain metal ions. It was shown that $H_xCr_yO_z^{-n}$ is greatly preferred by all the ligands that were used. There is a slight selectivity of THTD and THTUD towards the extraction of Cd^{2+} . Previous publications mentioned selectivity of the free ligands 15-c-5 and 18-c-6 towards UO_2^{2+} and Sr^{2+} . It was confirmed that the immobilized ligands, 15-c-5 and 18-c-6, showed slight selectivity towards UO_2^{2+} and to a lesser extent for Sr^{2+} . The selectivity decreased when these ligands were immobilized on the Si supports. When a spacer was introduced for the immobilization of the crown ethers, the extraction decreased. It was shown that better extraction is achieved with the crown ethers when the spacer is kept to a minimum length for the extraction of uranyl. It was shown that Si gel (60 Å) is the best support to use. Although the extractions were not always the

highest, Si gel (60 Å) was the most consistent support throughout. HMS and SBA-15 performed the least favourable of the four supports used when the extractions were carried out.

5.2 Future work

It was shown that the crown ether can be immobilized directly on the silica supports. Future work will include the determination of the optimal length of the “amino-anchor” that must be used for direct immobilization of the crown ethers. New pendant arms can be considered to enhance the selectivity of the THTD and THTUD. The optimum amount of ligand per mass of silica support must be determined. The optimum temperature and time for extractions must be determined. It is known that the immobilized ligands disintegrate at a pH lower than 1.9 and it is known the higher pH of 5.9 provides the better extraction. The next step is to determine which pH produces the optimum extraction.

Another aspect that should be investigated in the future is the recovery of the metal ions and the regeneration of the ligand – immobilised systems.

It was shown that it is possible to make specialized ligands for the selective extraction of toxic metal ions from water. This may be an expensive process, but this is a small price to pay when considering the scarcity of water in a country that does not have much room to gamble with its water resources. Rather spend money and develop these types of ligands for cleaning up the water now. In 10 years time it might be too late.

ADENDUMS

ADDENDUM A

FTIR Spectra

1. Si gel (60 Å)

a. 15-c-5 immobilized on Si gel (60 Å)	IV
b. 18-c-6 immobilized on Si gel (60 Å)	V
c. Glymo immobilized on Si gel (60 Å)	VI
d. 15-c-5 immobilized with glymo on Si gel (60 Å)	VII
e. 18-c-6 immobilized with glymo on Si gel (60 Å)	VIII
f. THTD immobilized on Si gel (60 Å)	IX
g. THTUD immobilized on Si gel (60 Å)	X

2. MCM-41

a. 15-c-5 immobilized on MCM-41	XI
b. 18-c-6 immobilized on MCM-41	XII
c. Glymo immobilized on MCM-41	XIII
d. 15-c-5 immobilized with glymo on MCM-41	XIV
e. 18-c-6 immobilized with glymo on MCM-41	XV
f. THTD immobilized on MCM-41	XVI
g. THTUD immobilized on MCM-41	XVII

3. SBA-15

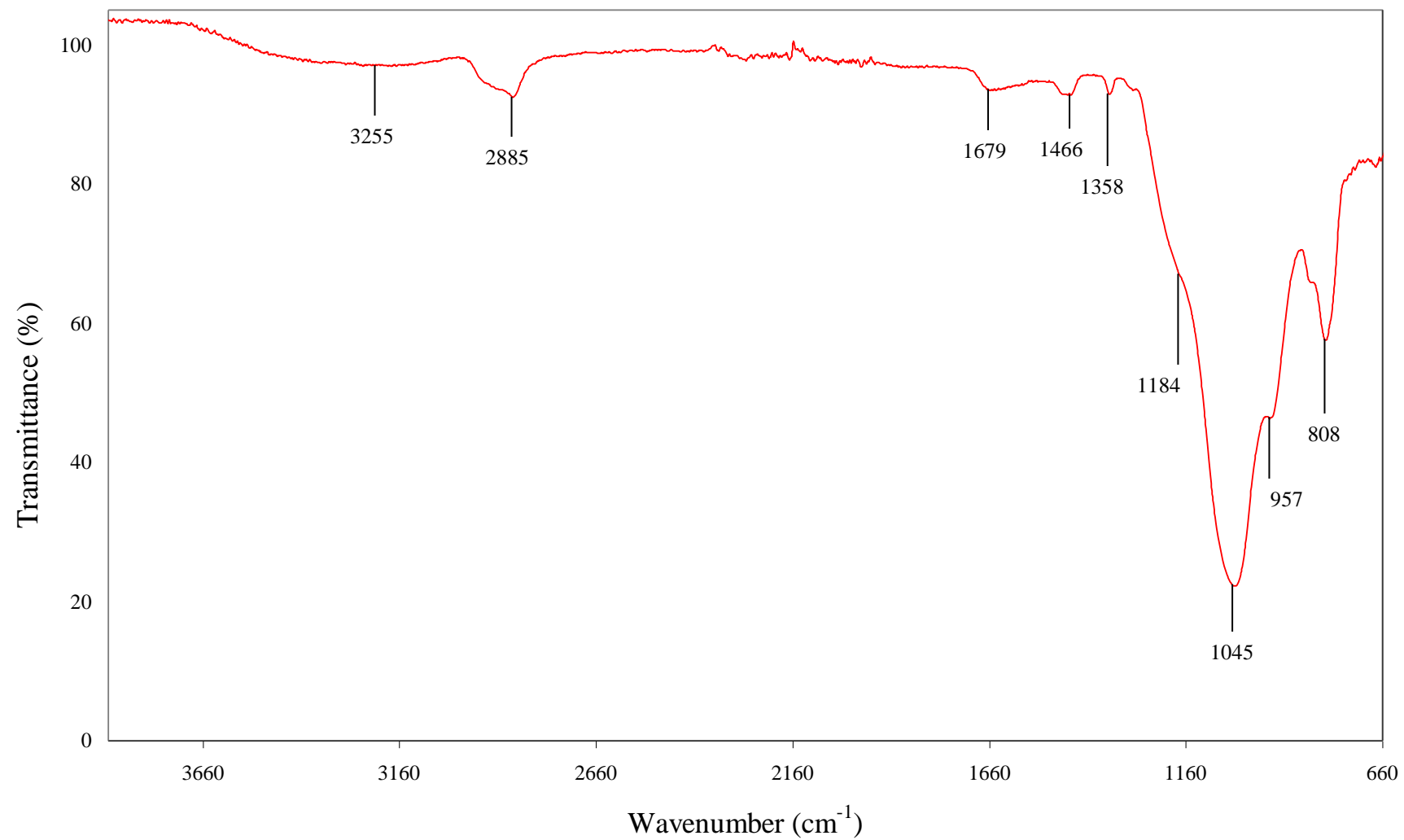
a. 15-c-5 immobilized on SBA-15	XVIII
b. 18-c-6 immobilized on SBA-15	XIX
c. 15-c-5 immobilized with glymo on SBA-15	XX

d. 18-c-6 immobilized with glymo on SBA-15	XXI
e. THTD immobilized on SBA-15	XXII
f. THTUD immobilized on SBA-15	XXIII

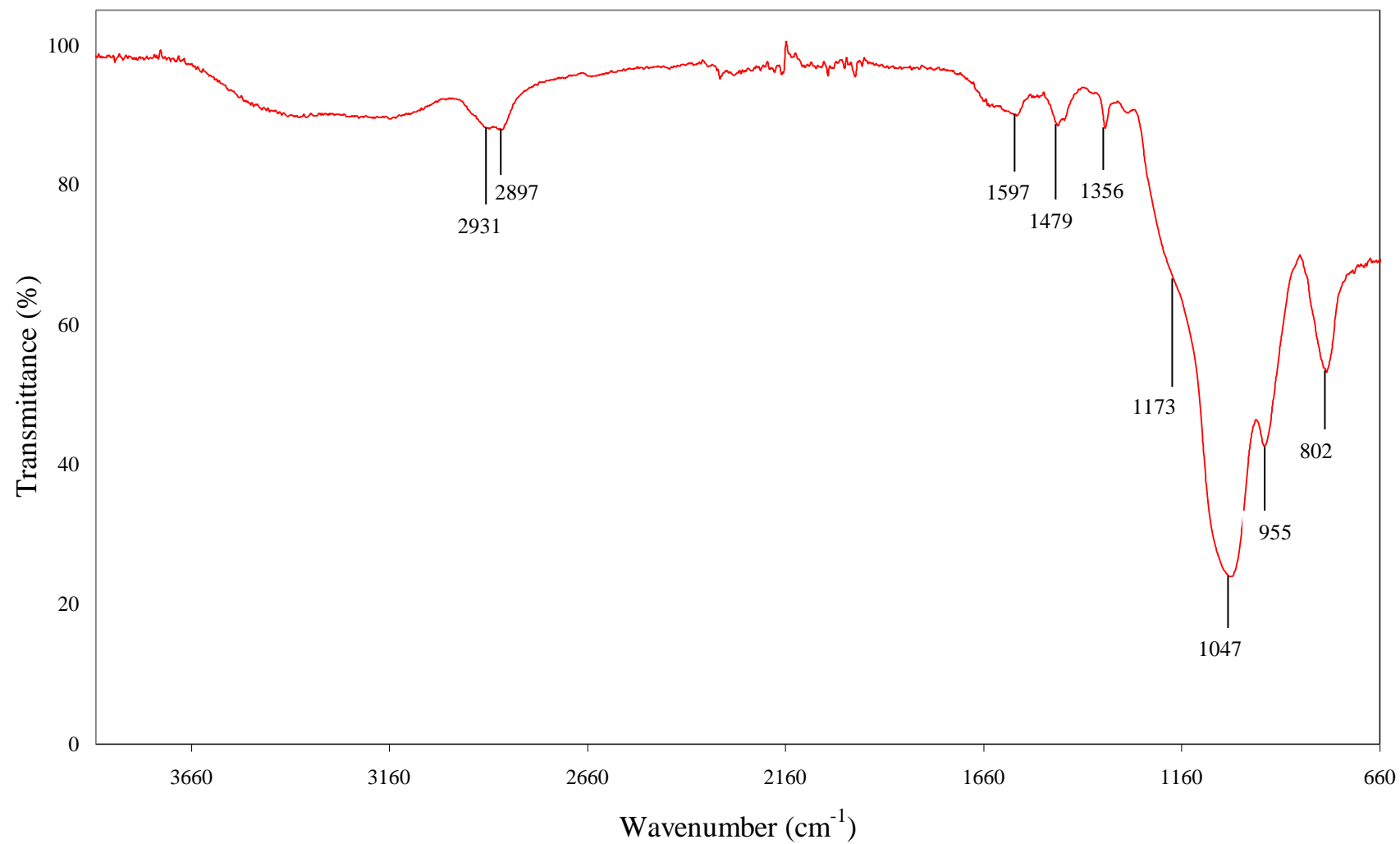
4. HMS

a. 15-c-5 immobilized on HMS.....	XXIV
b. 18-c-6 immobilized on HMS.....	XXV
c. 15-c-5 immobilized with glymo on HMS	XXVI
d. 18-c-6 immobilized with glymo on HMS	XXVII
e. THTD immobilized on HMS	XXVIII
f. THTUD immobilized on HMS	XXIX

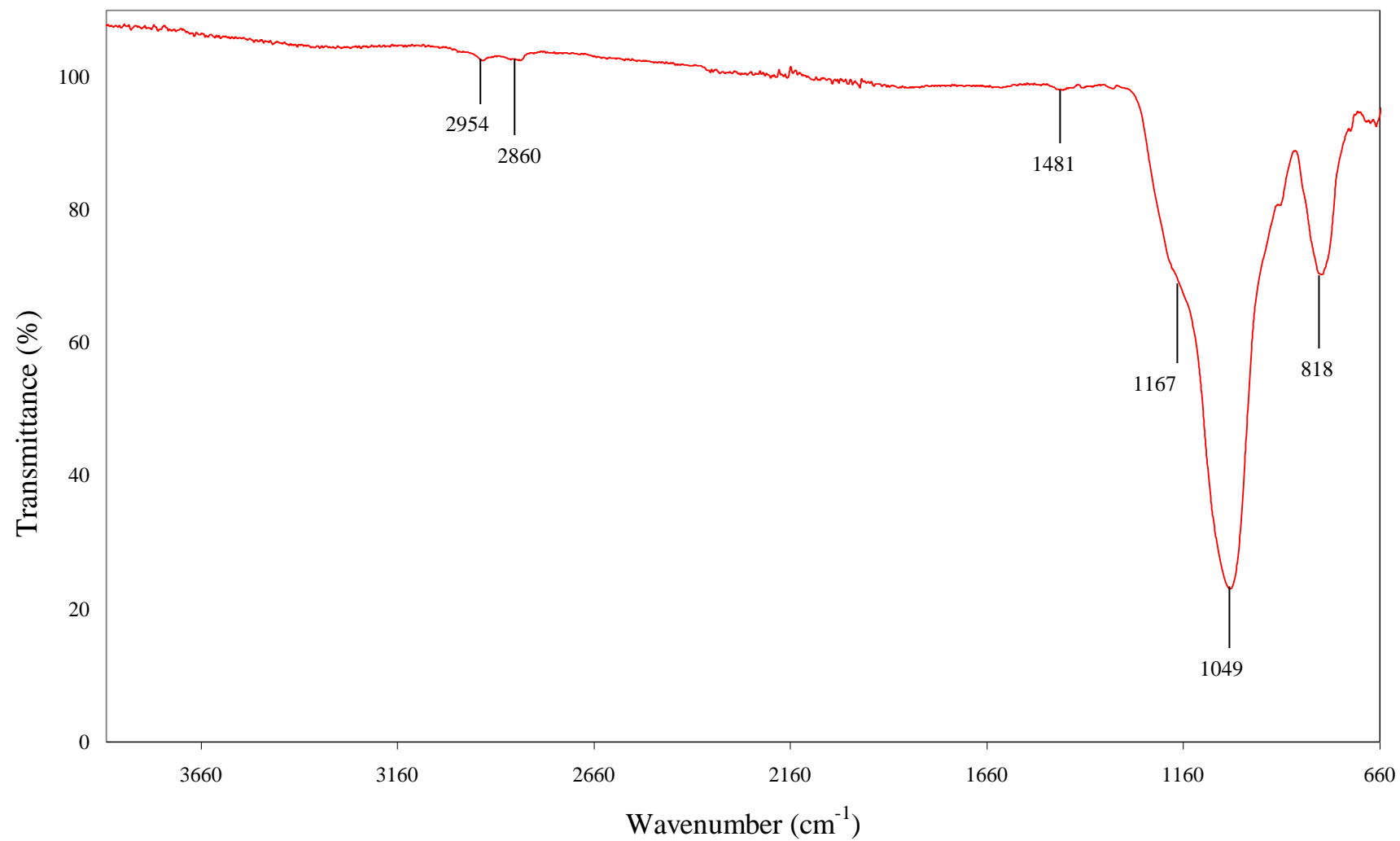
15-c-5 Immobilized Directly onto Si gel gel (60Å)



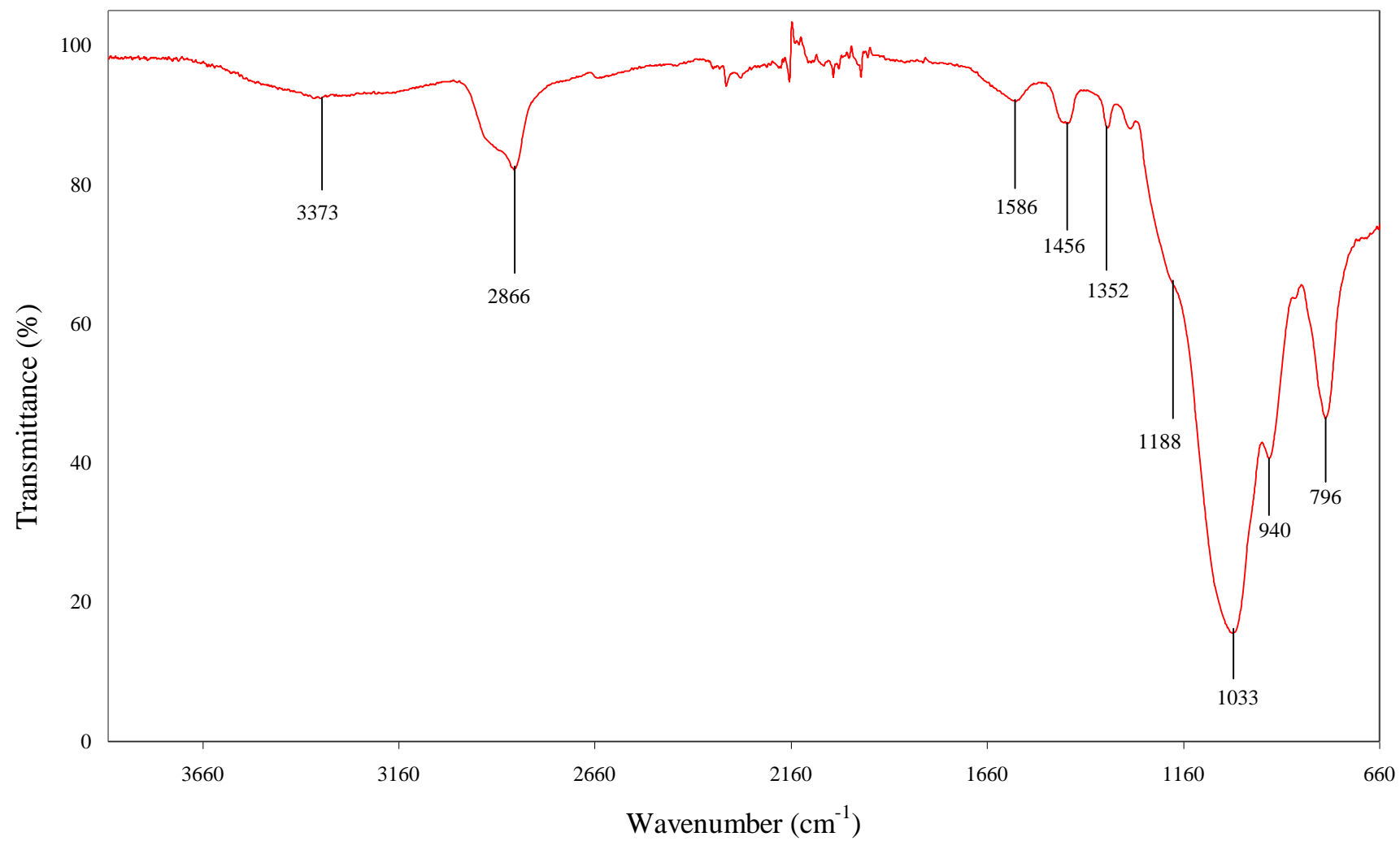
18-c-6 Immobilised Directly onto Si gel (60 Å)



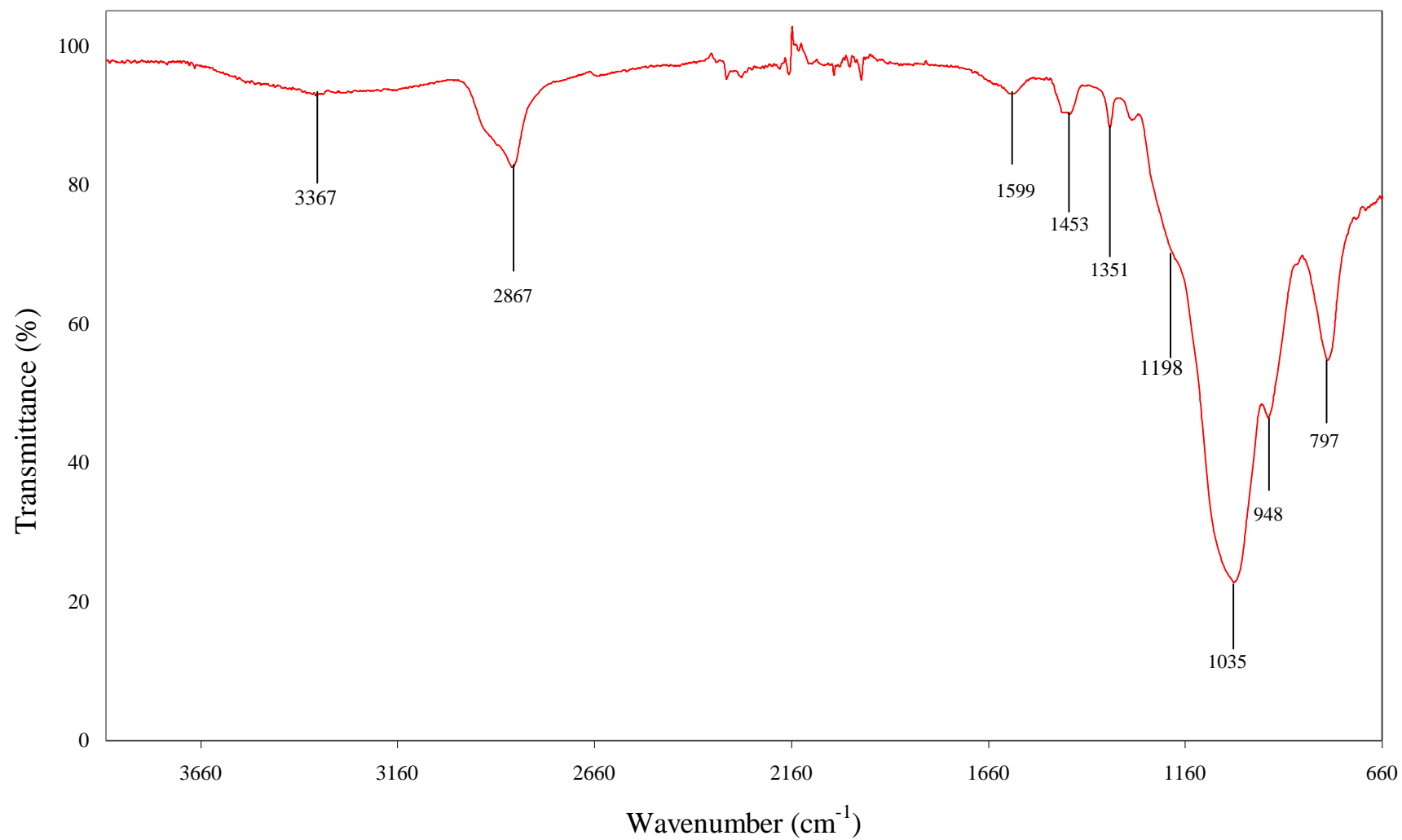
Glymo Immobilized onto Si gel (60 Å)



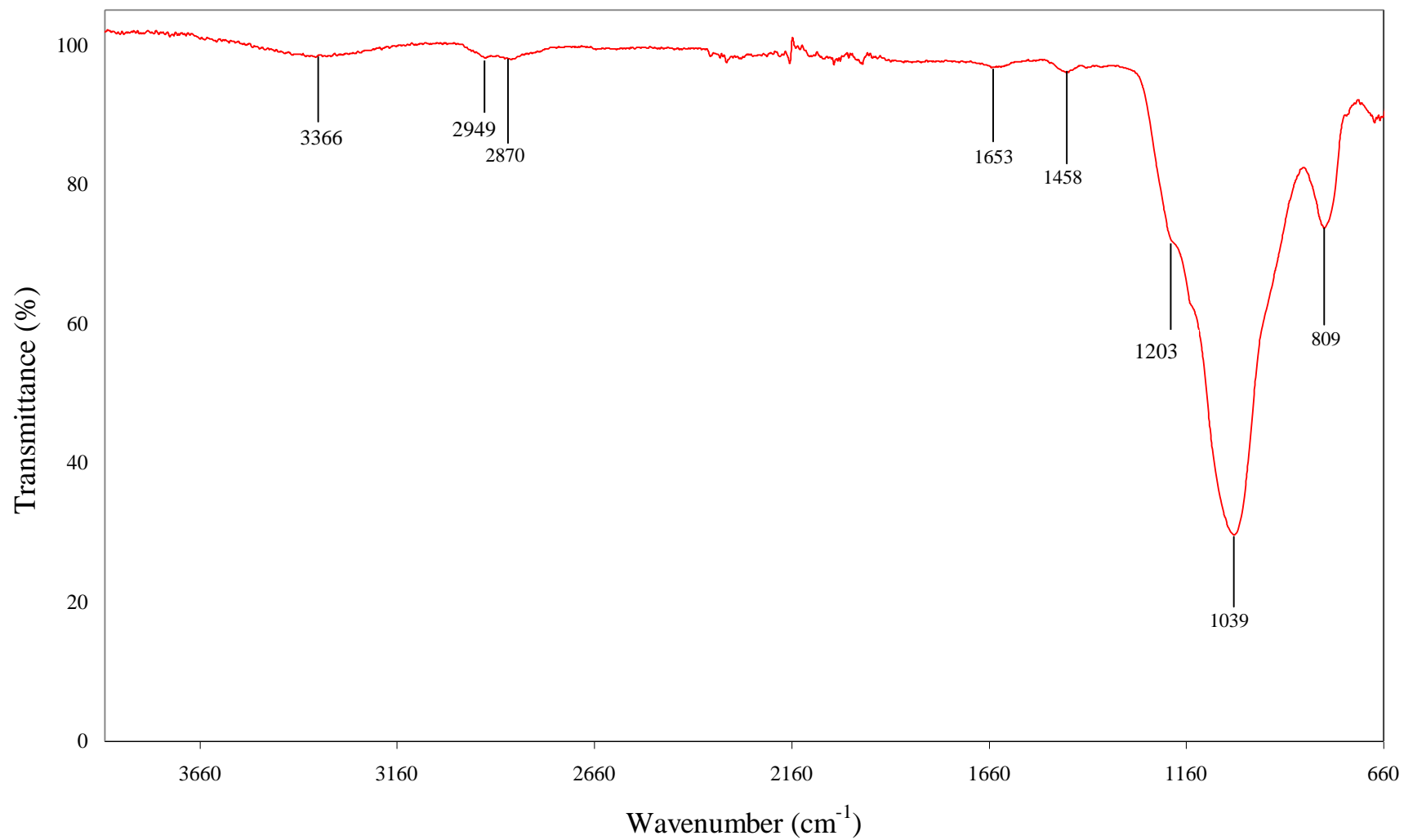
15-c-5 Immobilized with Glymo onto Si gel (60 Å)



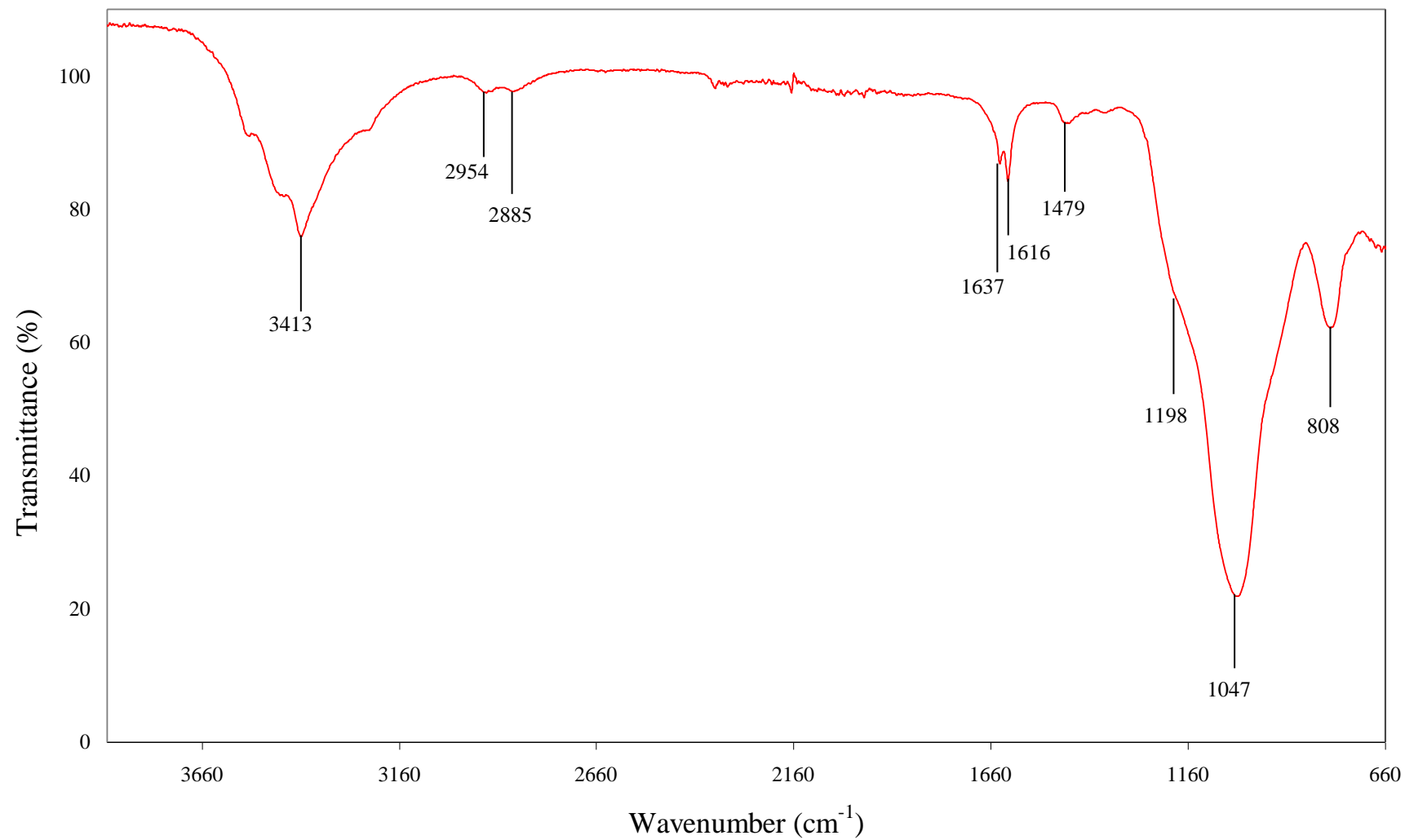
18-c-6 Immobilized with Glymo onto Si gel (60 Å)



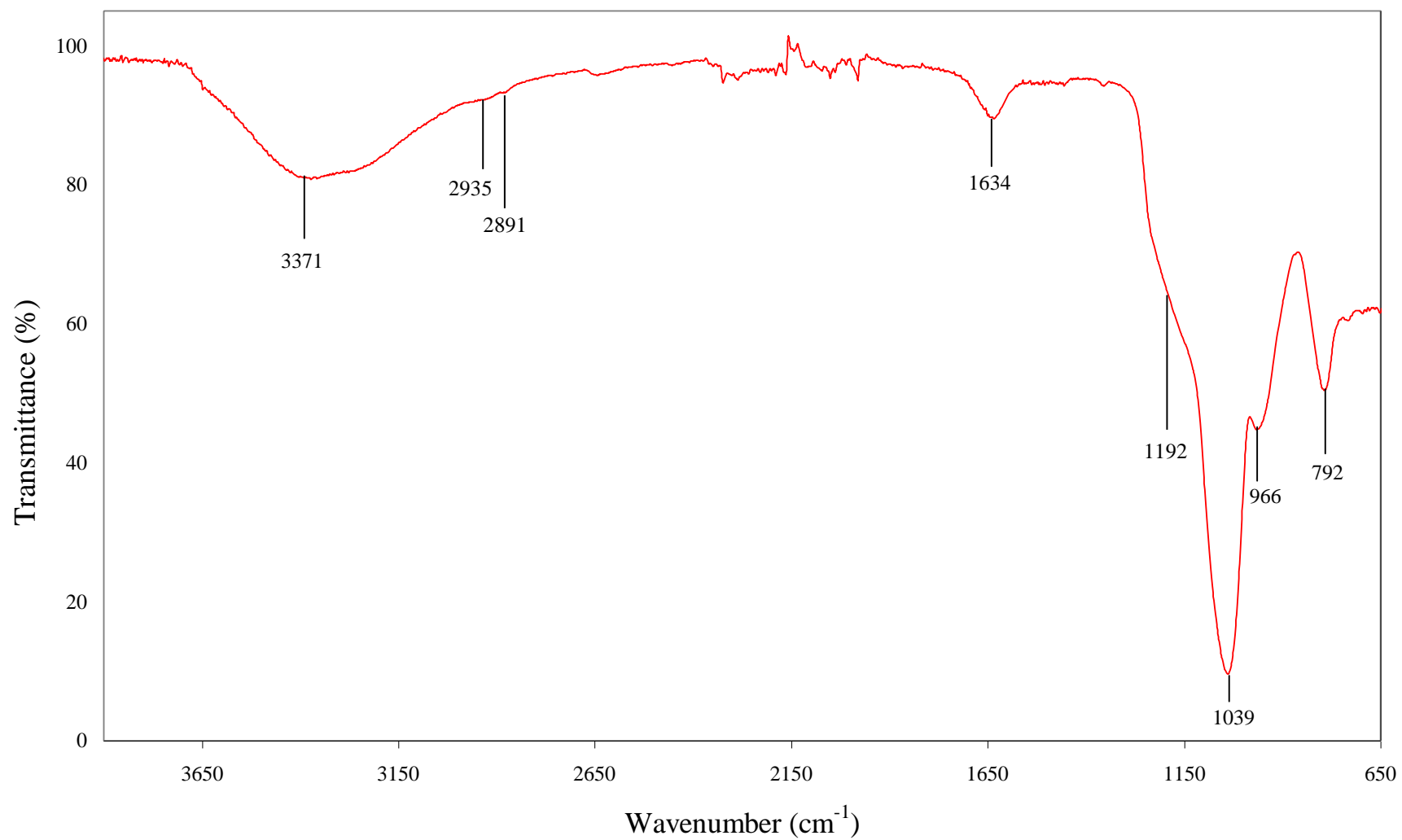
THTD Immobilized onto Si gel (60 Å)



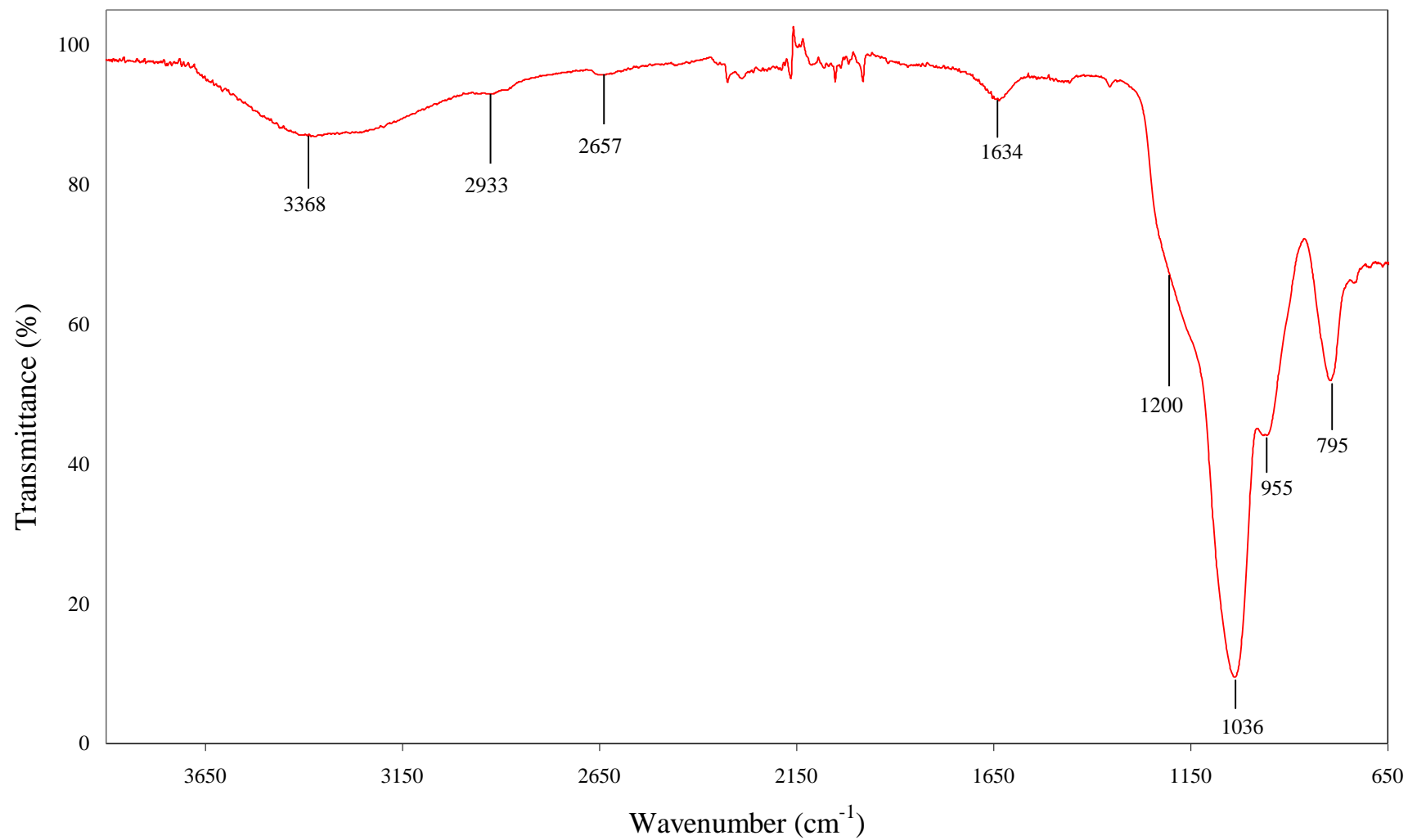
THTUD Immobilized onto Si gel (60 Å)



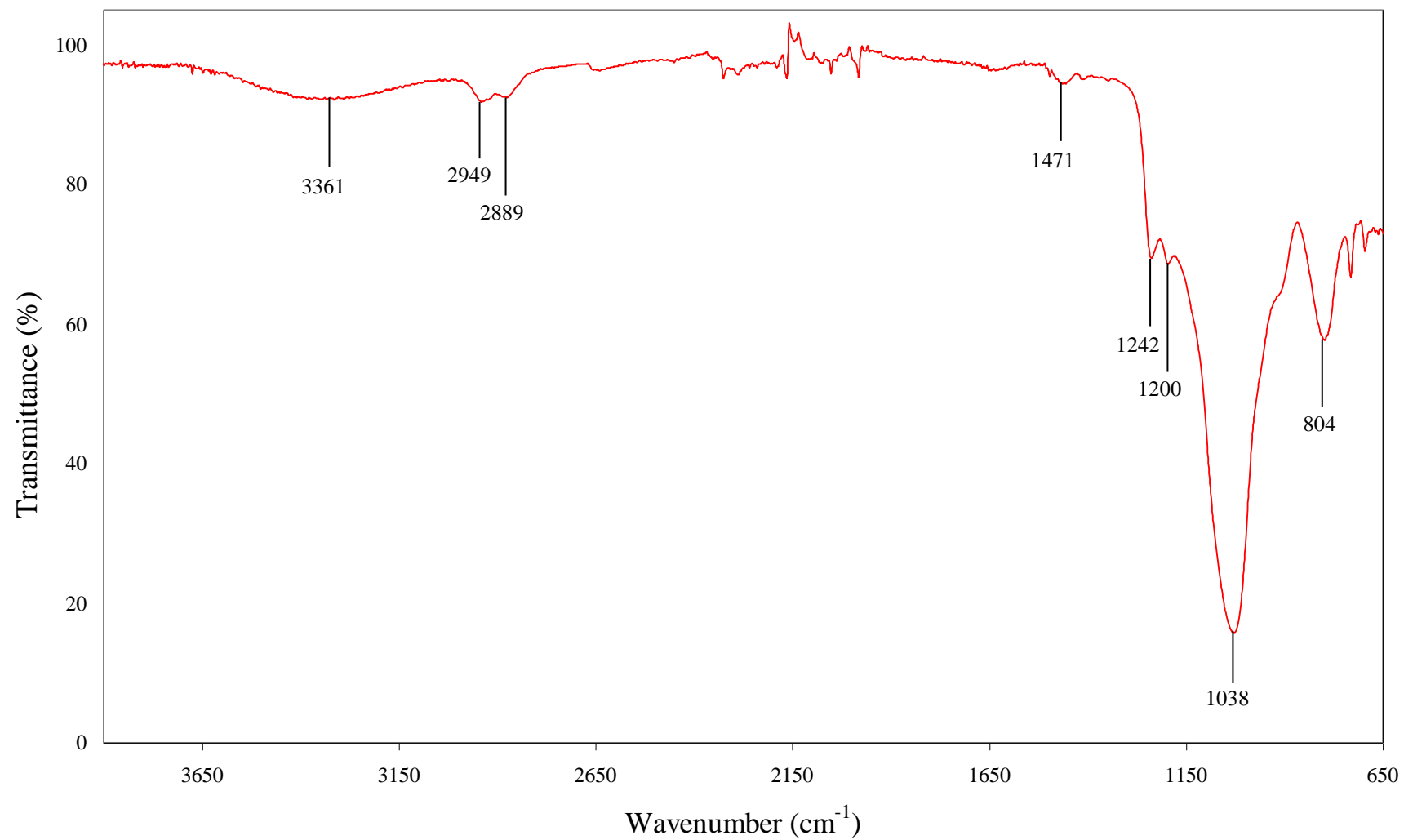
15-c-5 Immobilized Directly onto MCM-41



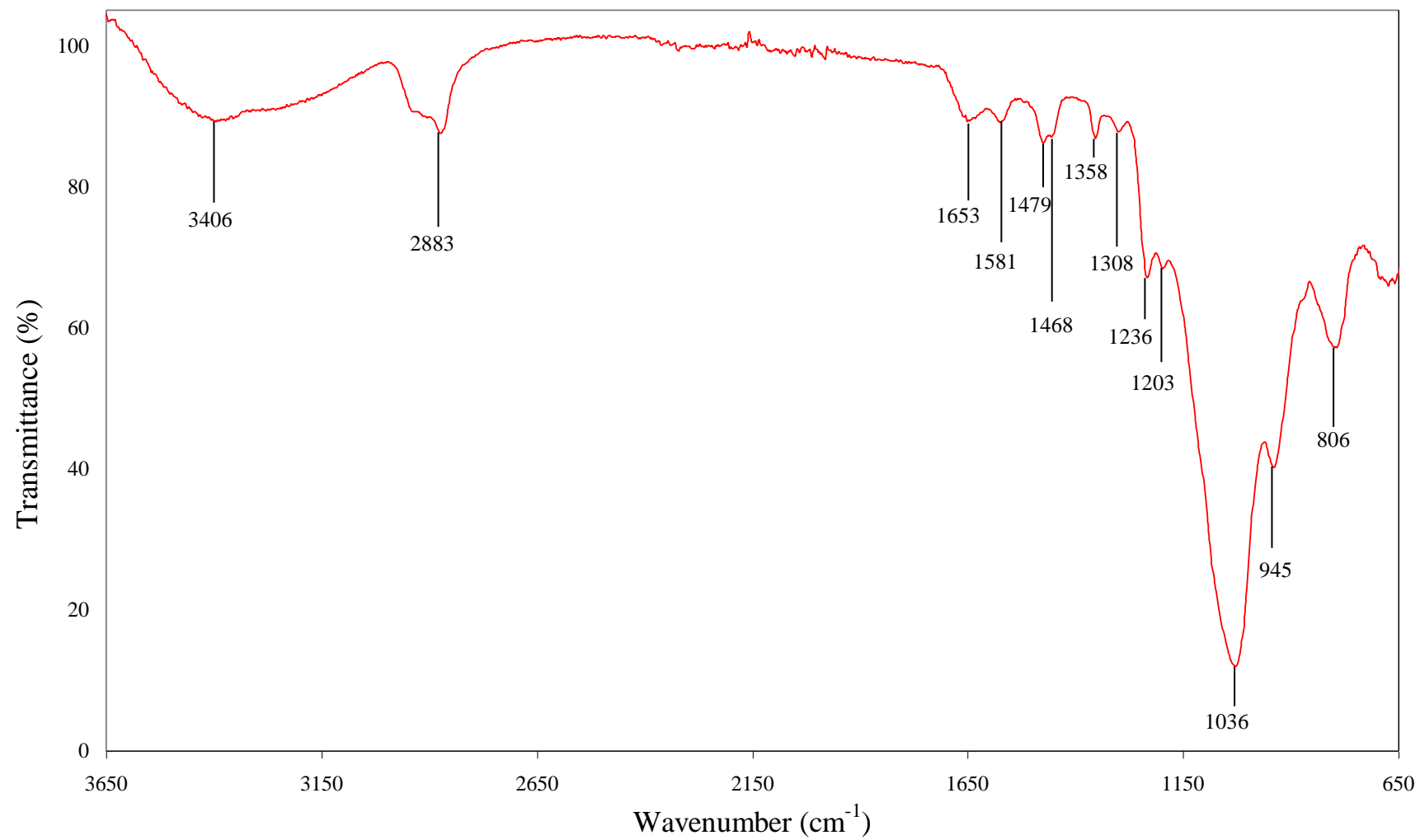
18-c-6 Immobilized Directly onto MCM-41



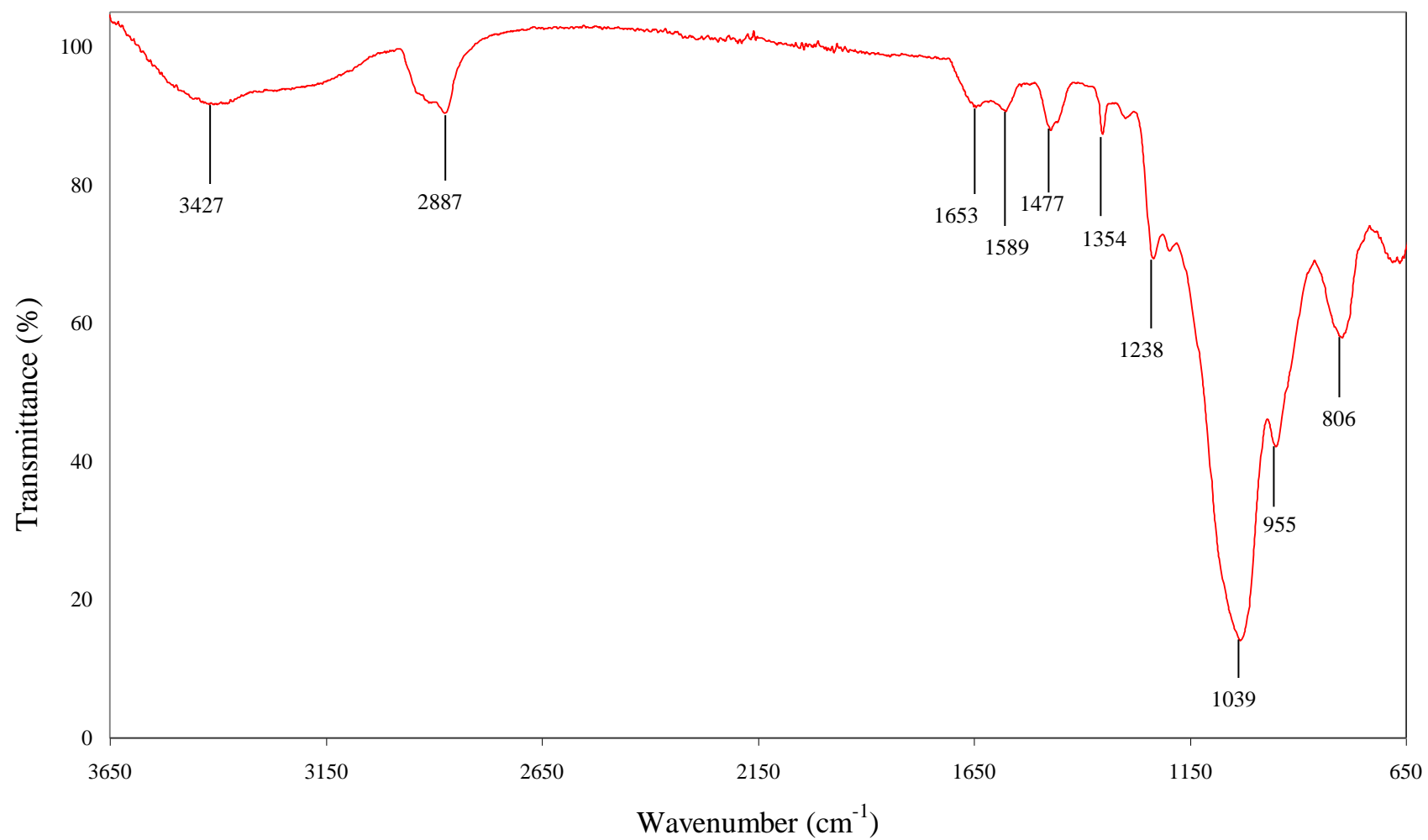
Glymo Immobilized onto MCM-41



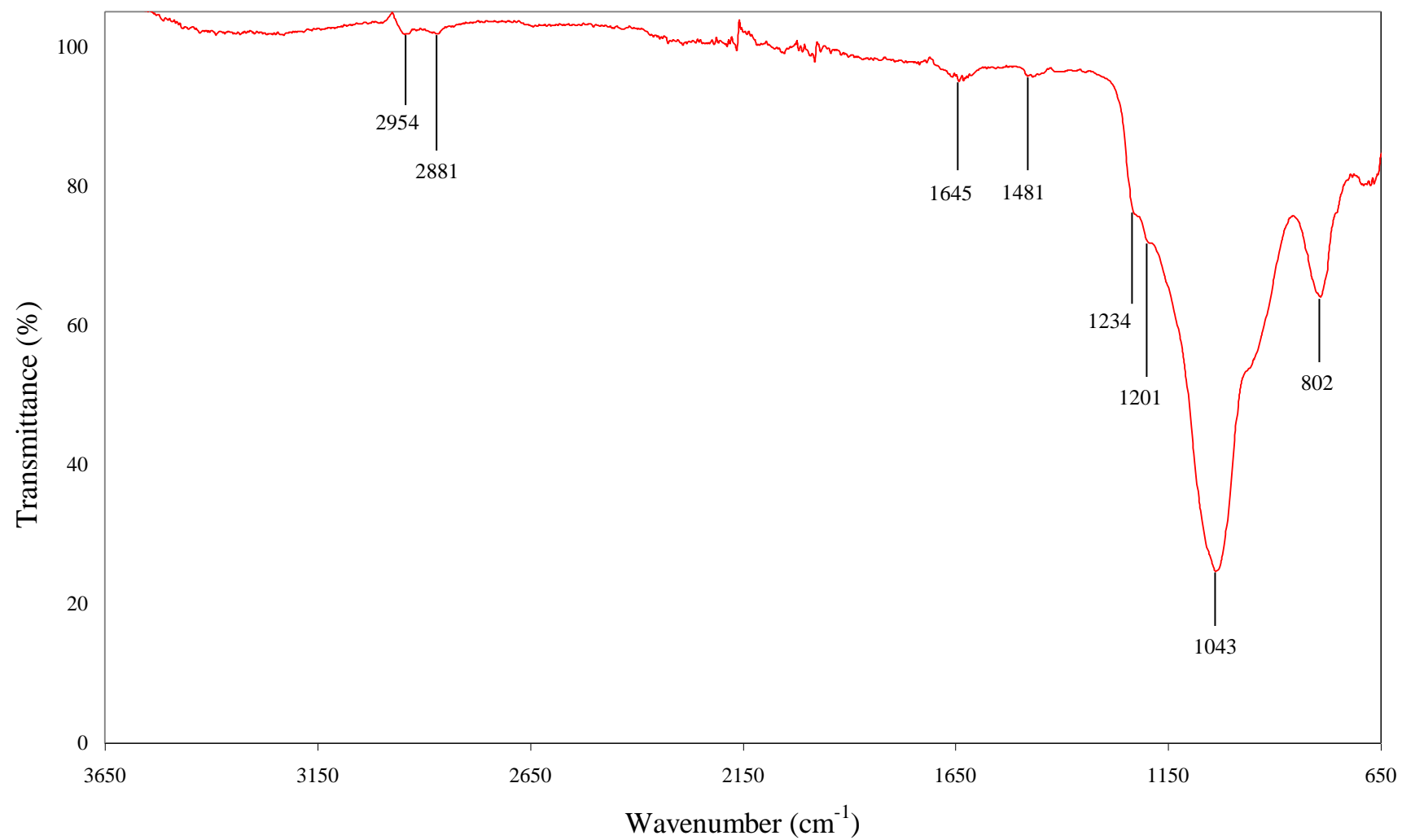
15-c-5 Immobilized with Glymo onto MCM-41



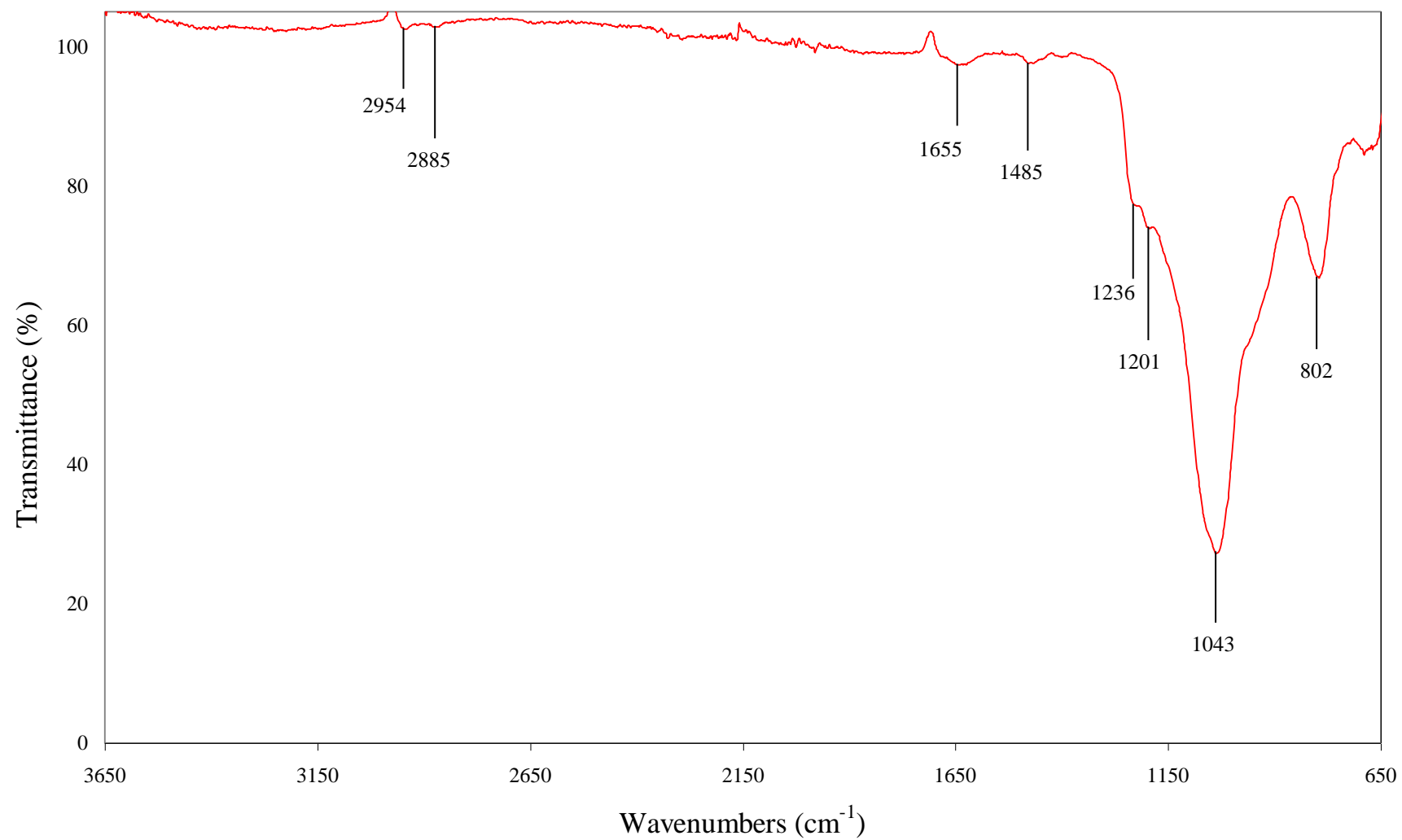
18-c-6 Immobilized with Glymo onto MCM-41



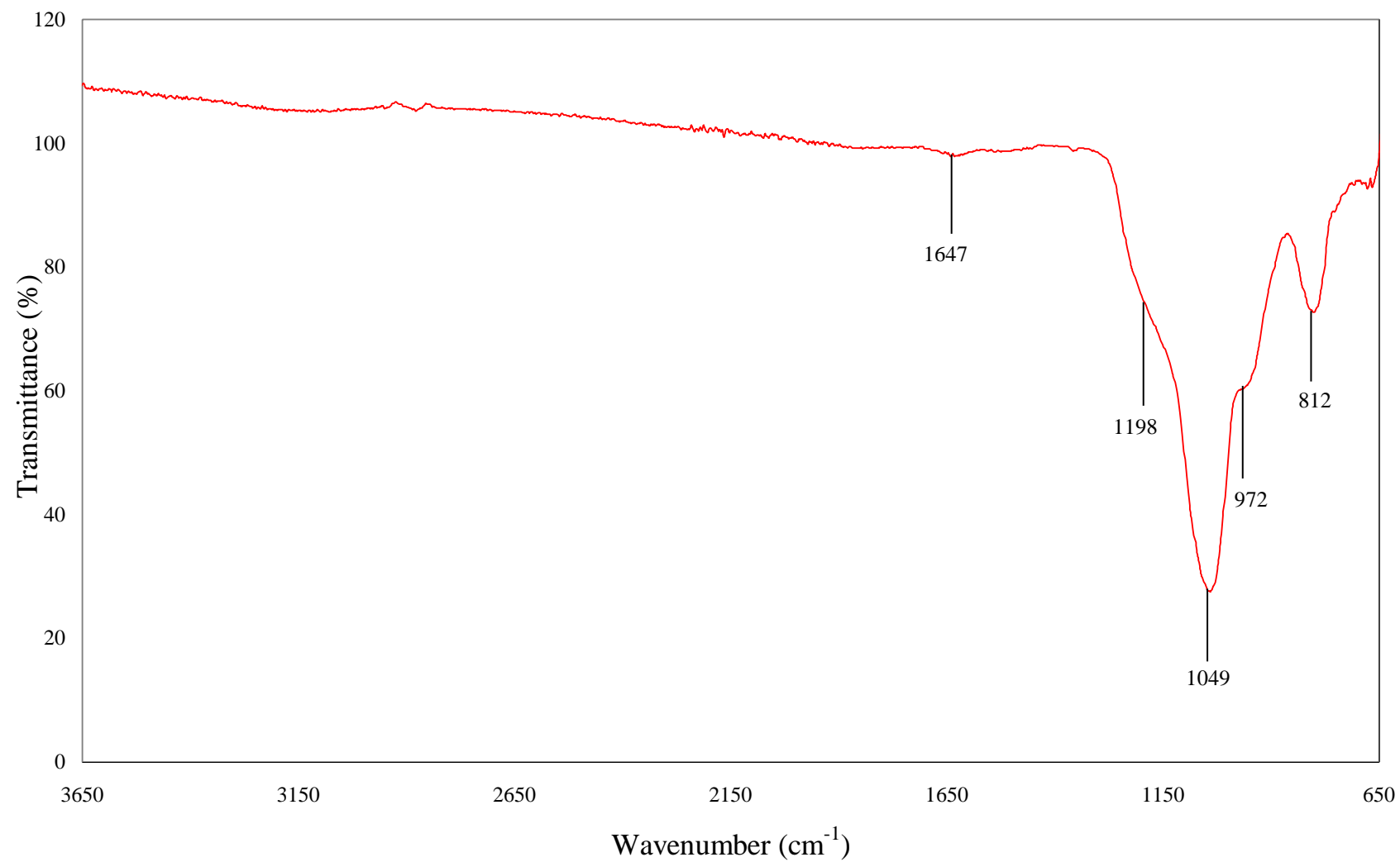
THTD Immobilized onto MCM-41



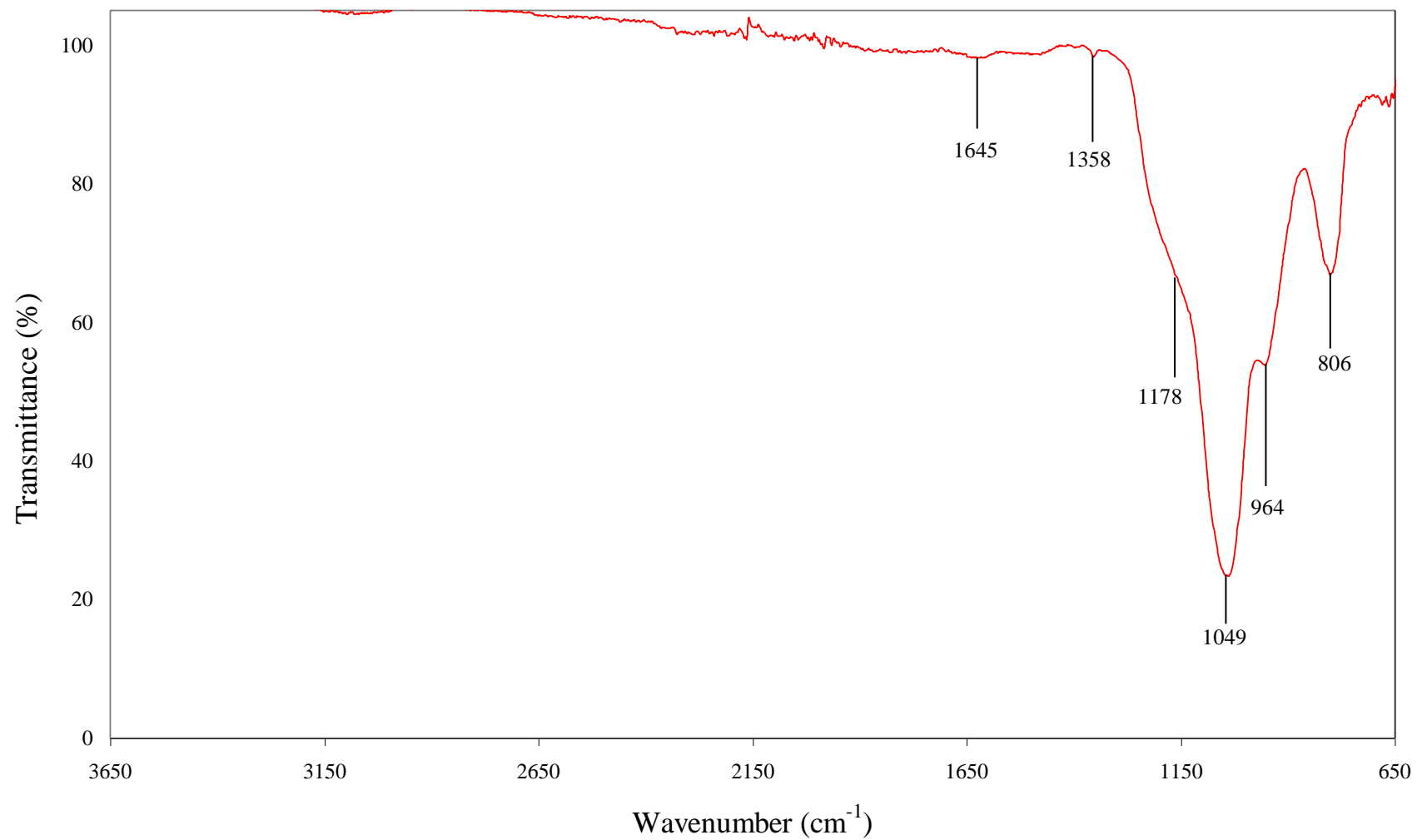
THTUD Immobilized onto MCM-41



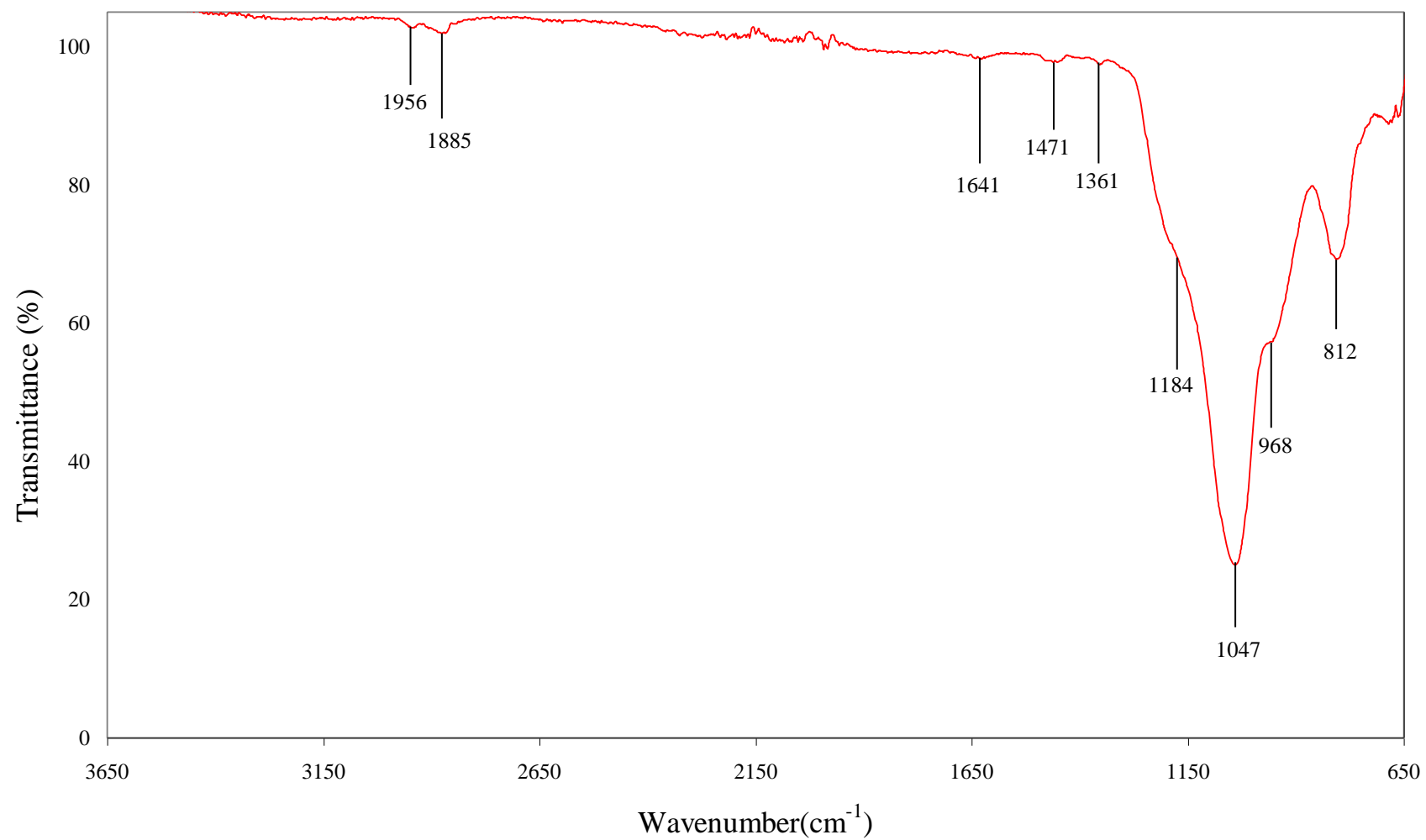
15-c-5 Immobilised Directly onto SBA-15



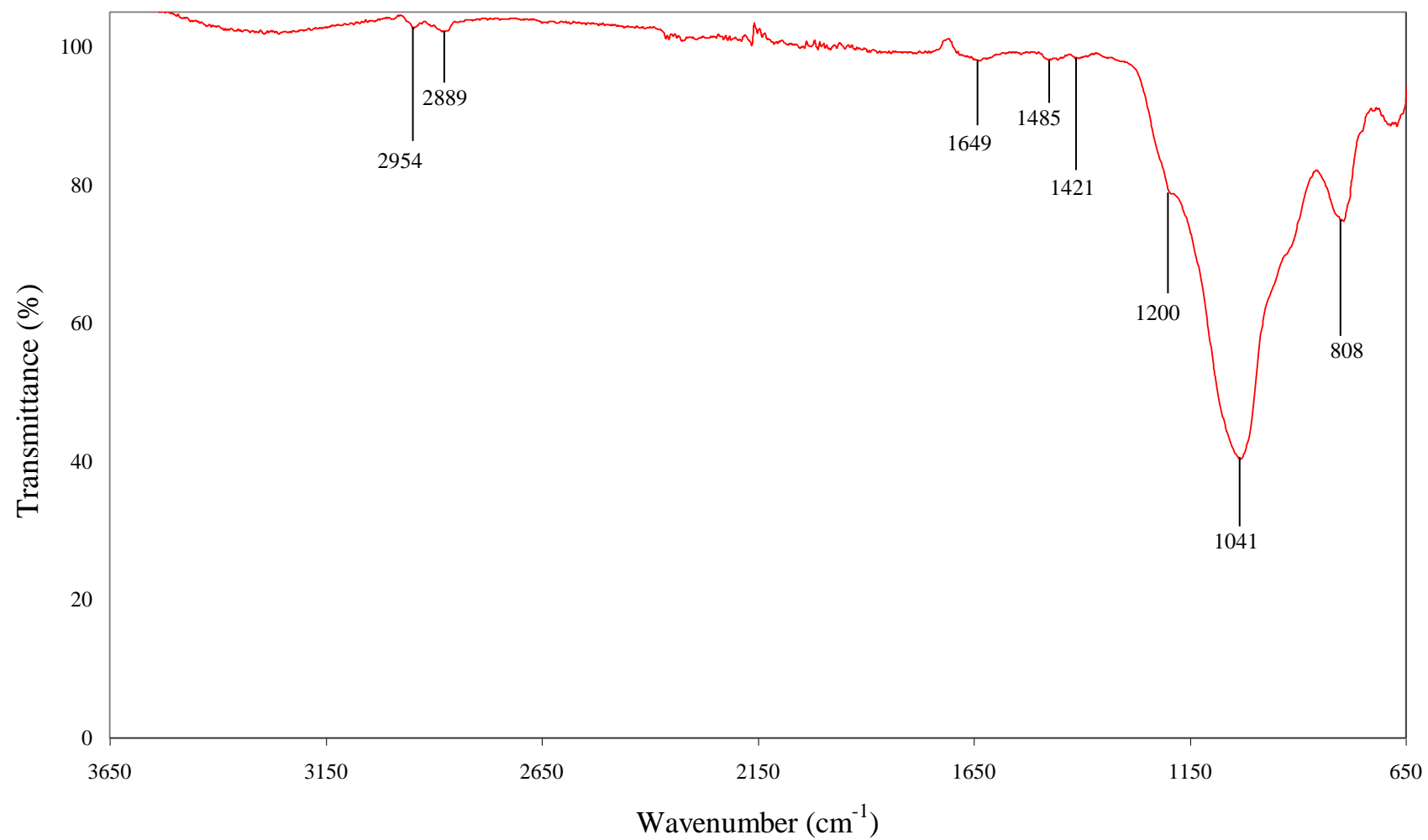
18-c-6 Immobilized Directly onto SBA-15



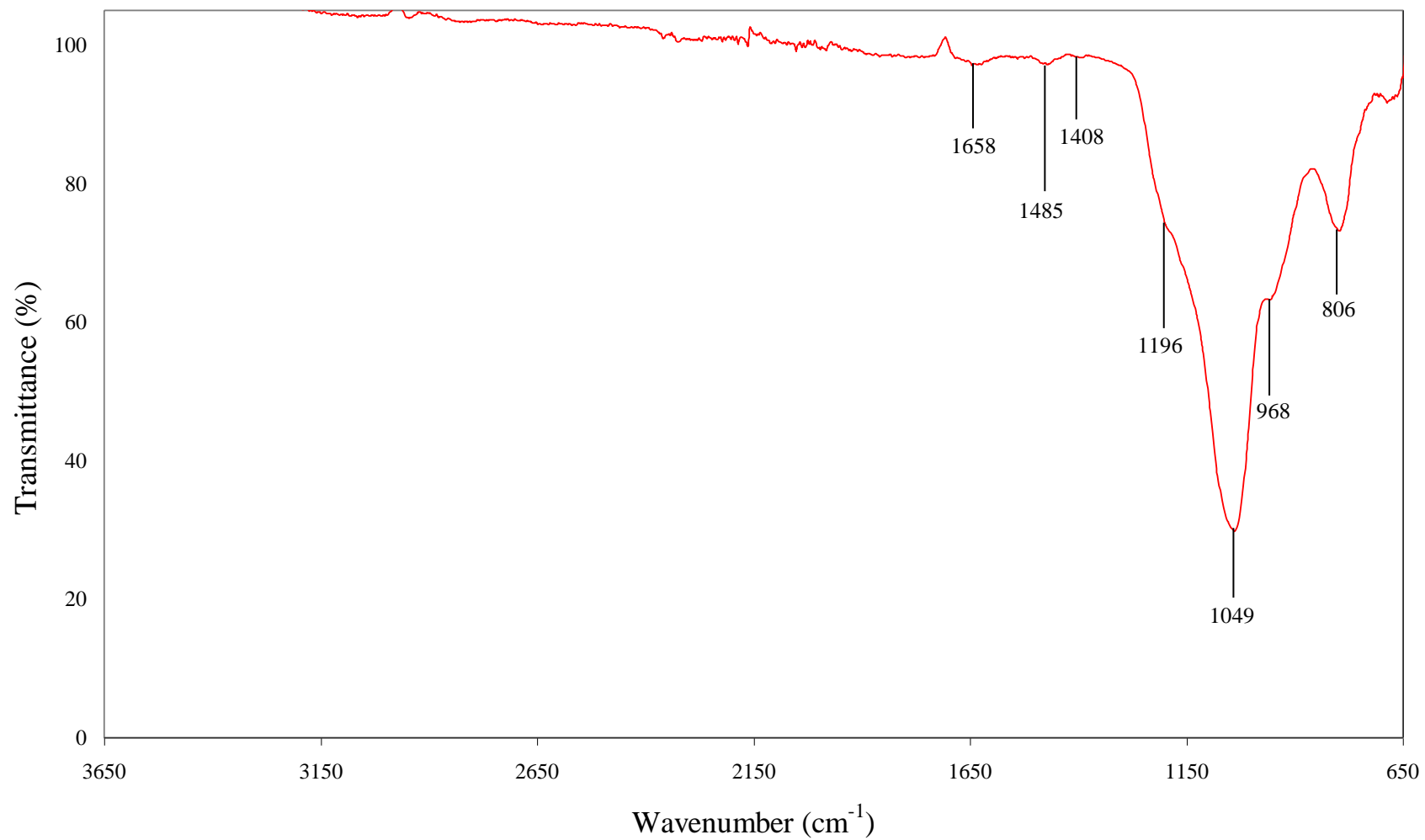
15-c-5 Immobilized with Glymo onto SBA-15



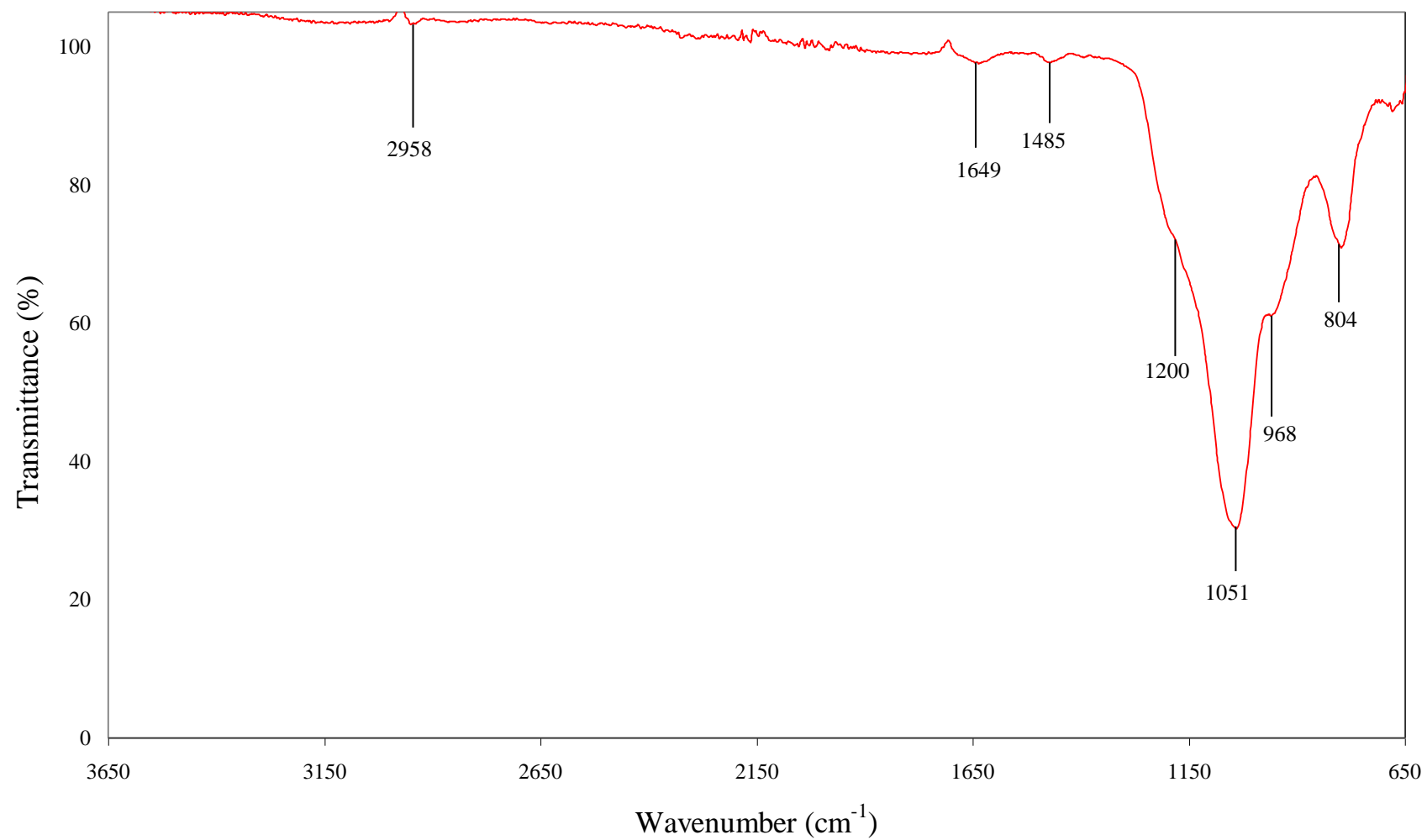
18-c-6 Immobilized with Glymo onto SBA-15



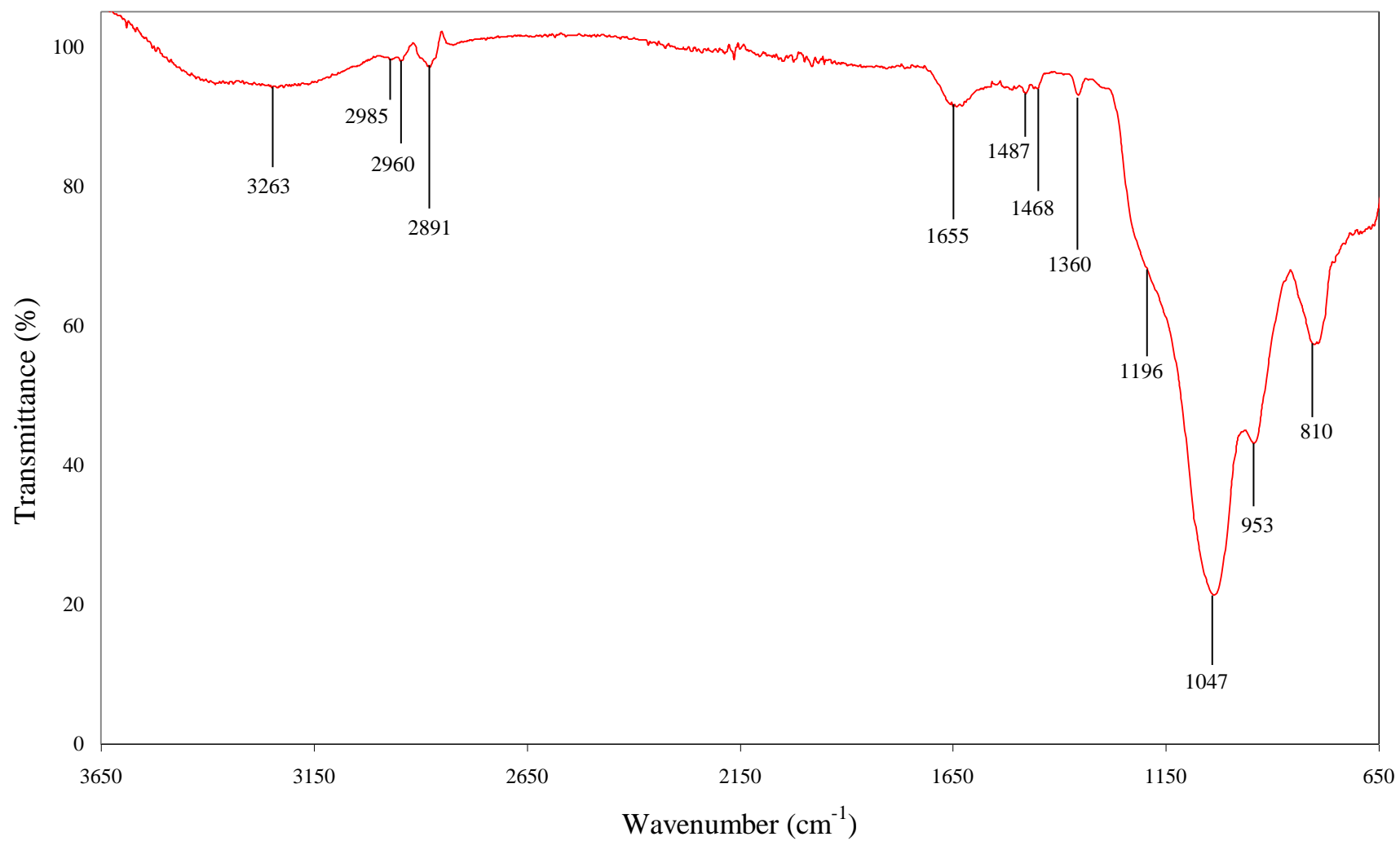
THTD Immobilized onto SBA-15



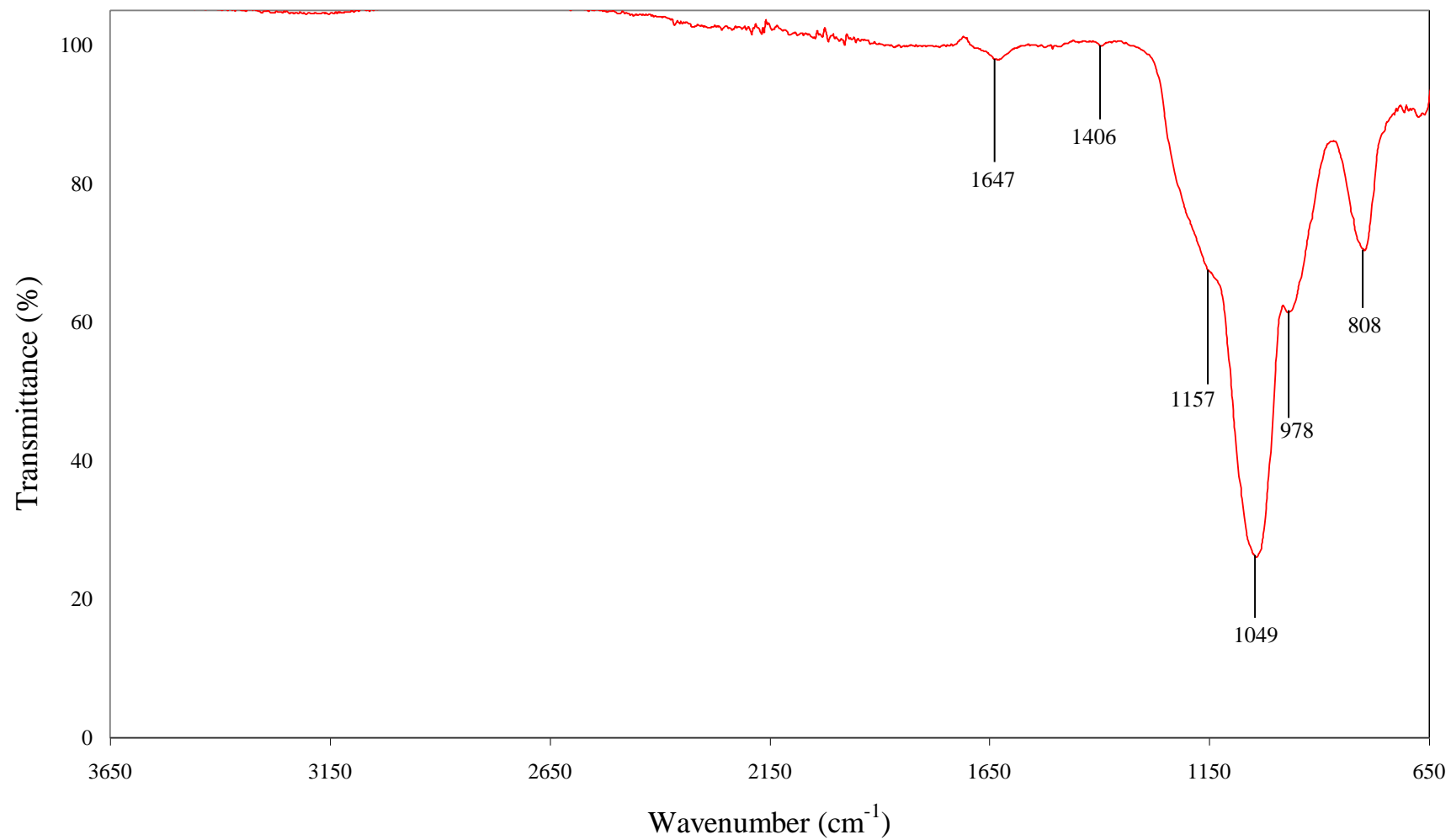
THTUD Immobilized onto SBA-15



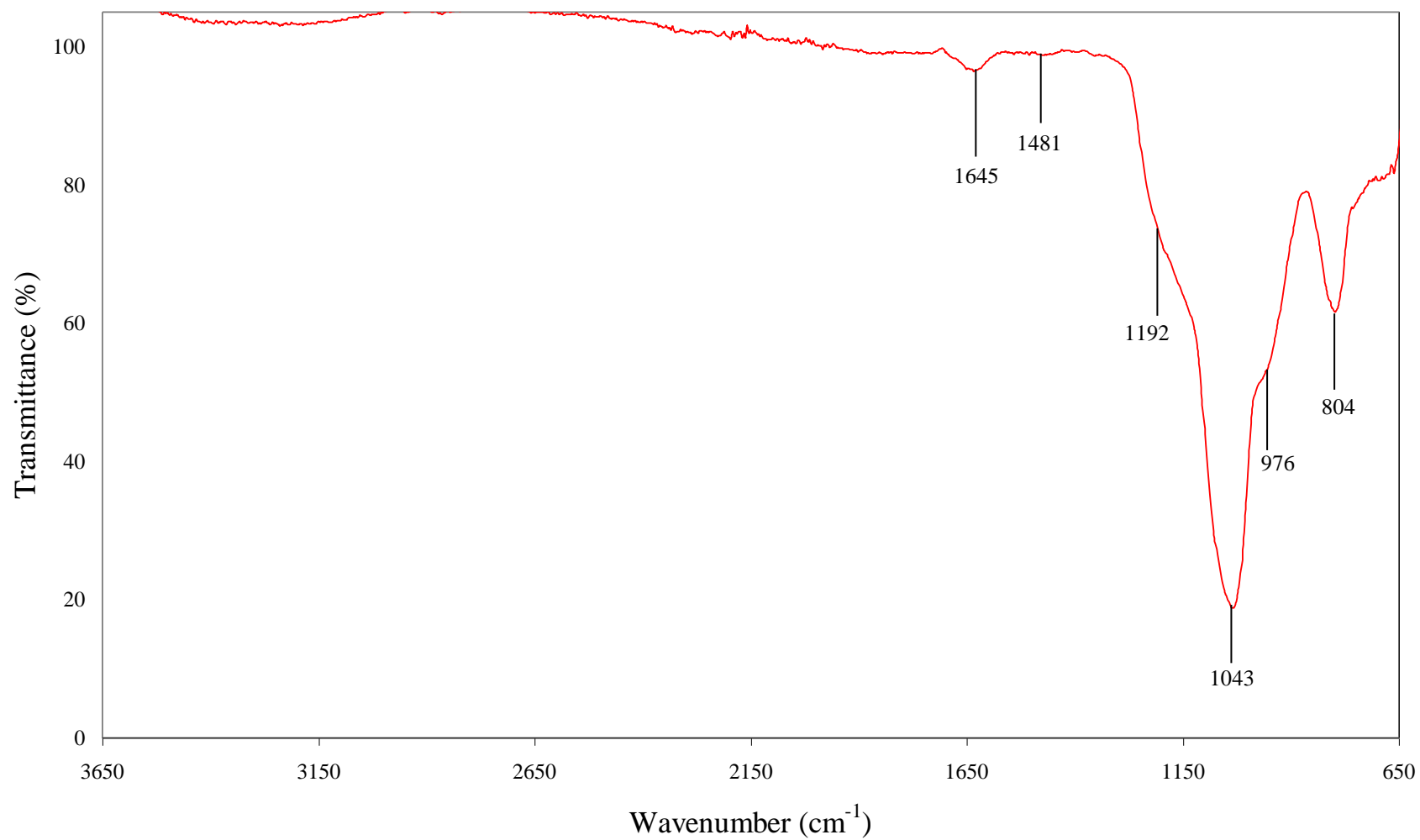
15-c-5 Immobilized Directly onto HMS



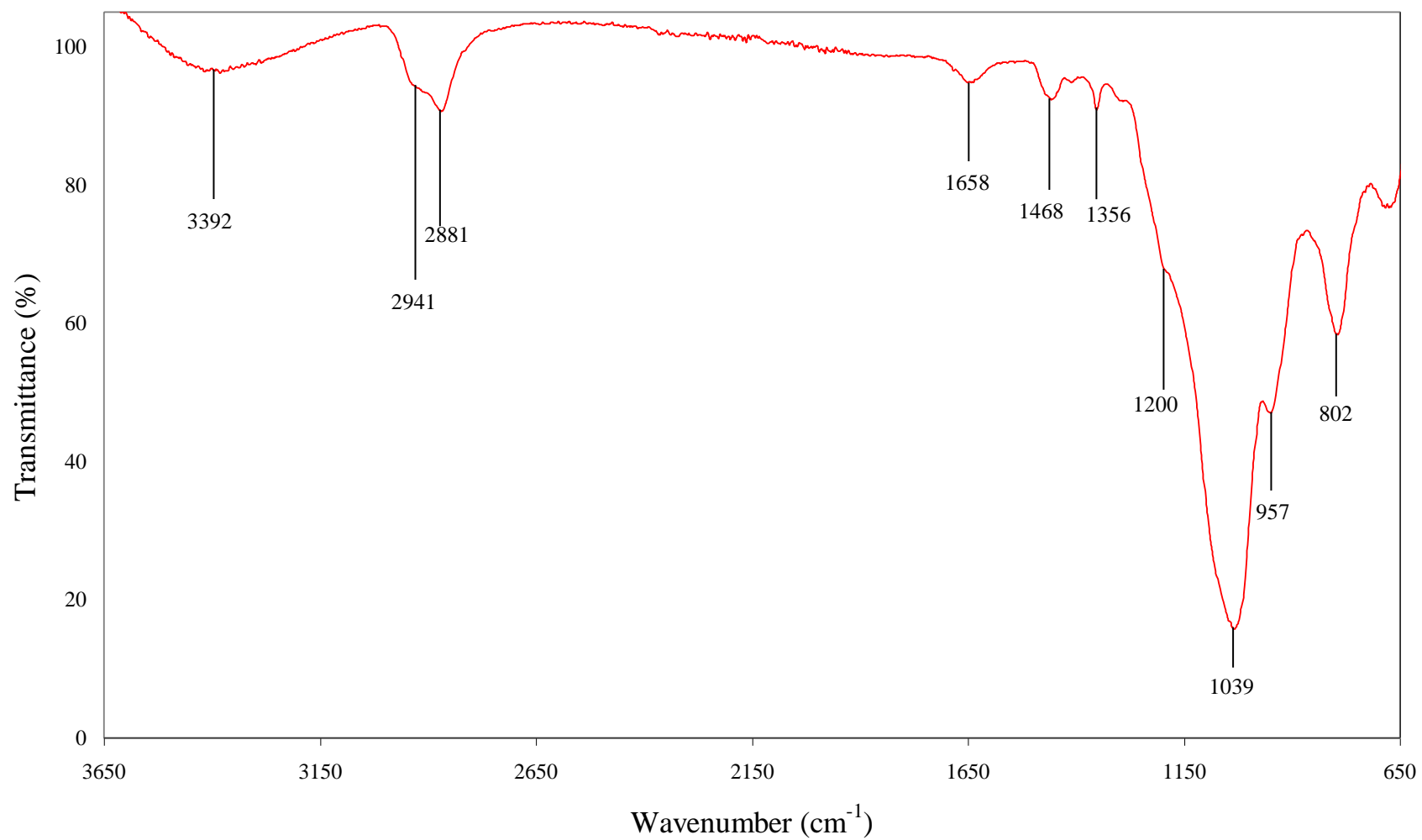
18-c-6 Immobilized Directly onto HMS



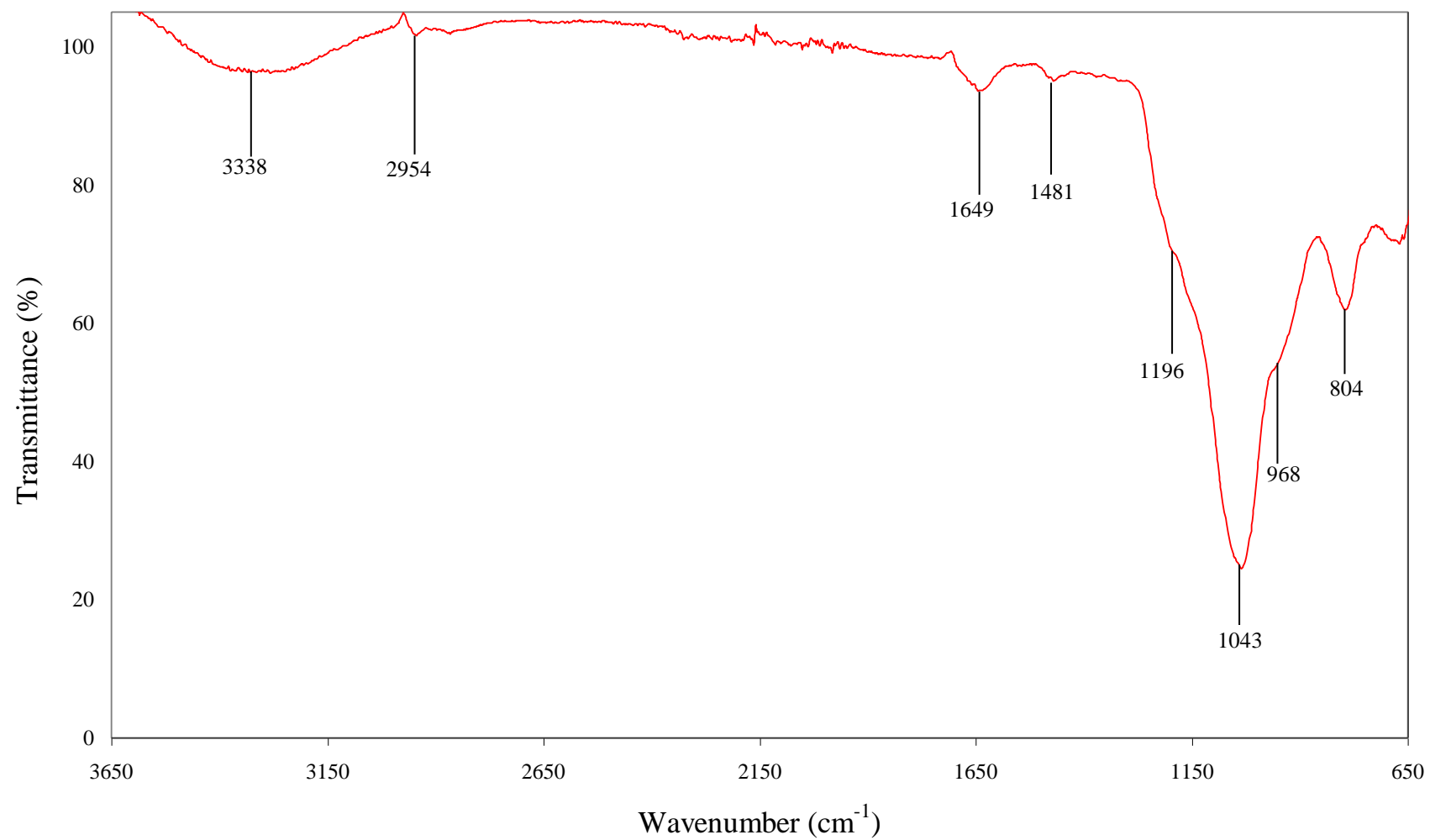
15-c-5 Immobilized with Glymo onto HMS



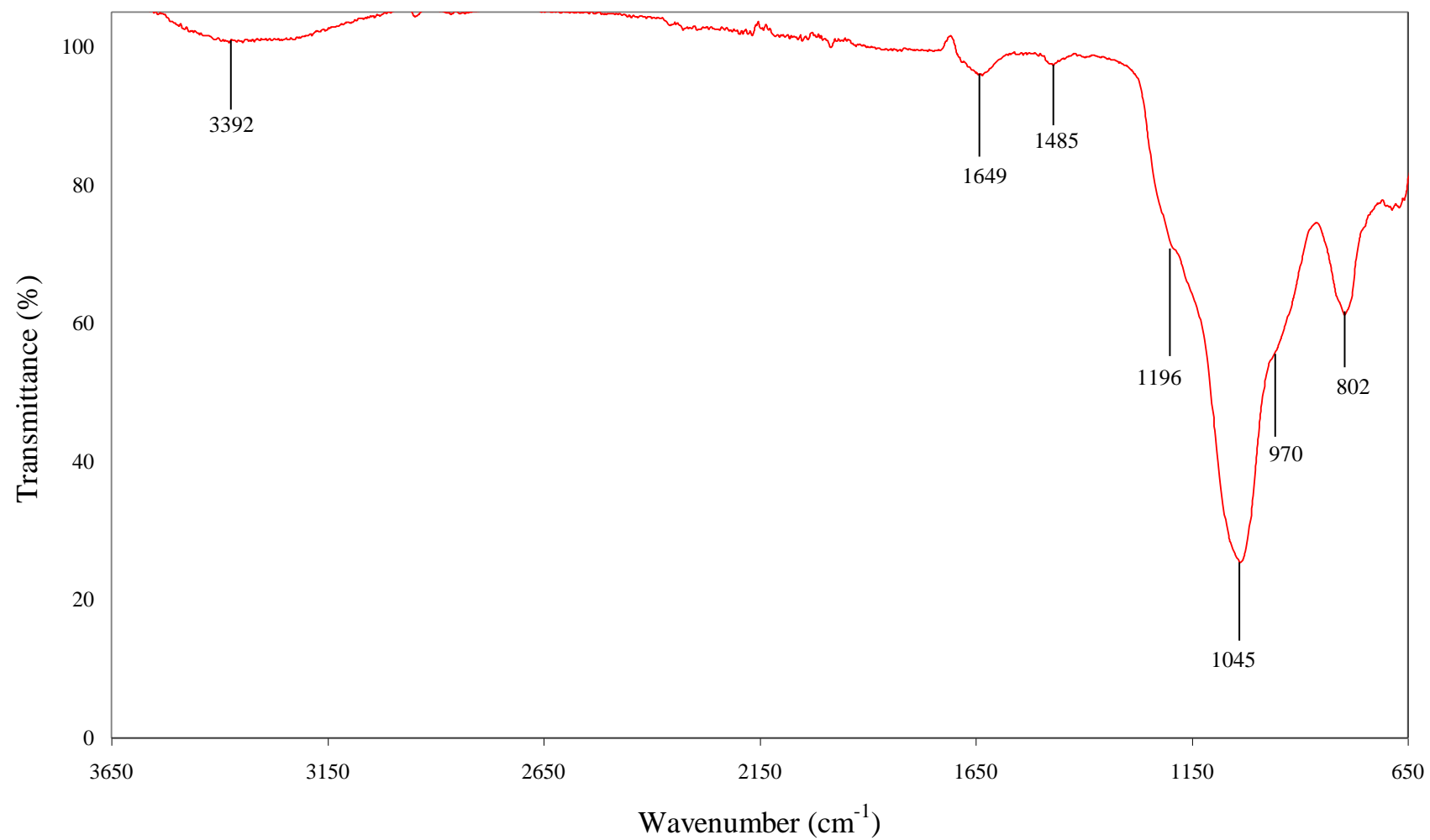
18-c-6 Immobilized with Glymo onto HMS



THTD Immobilized onto HMS



THTUD Immobilized onto HMS



ADDENDUM B

Solid State NMR Spectra

1. *Si gel (60 Å)*

a. 15-c-5 immobilized on Si gel (60 Å)	XXXII
b. 18-c-6 immobilized on Si gel (60 Å)	XXXII
c. Glymo immobilized on Si gel (60 Å)	XXXIII
d. 15-c-5 immobilized with glymo on Si gel (60 Å)	XXXIII
e. 18-c-6 immobilized with glymo on Si gel (60 Å)	XXXIV
f. THTD immobilized on Si gel (60 Å)	XXXIV
g. THTUD immobilized on Si gel (60 Å)	XXXV

2. *MCM-41*

a. 15-c-5 immobilized on MCM-41	XXXV
b. 18-c-6 immobilized on MCM-41	XXXVI
c. 15-c-5 immobilized with glymo on MCM-41	XXXVI
d. 18-c-6 immobilized with glymo on MCM-41	XXXVII
e. THTD immobilized on MCM-41	XXXVII
f. THTUD immobilized on MCM-41	XXXVIII

3. *SBA-15*

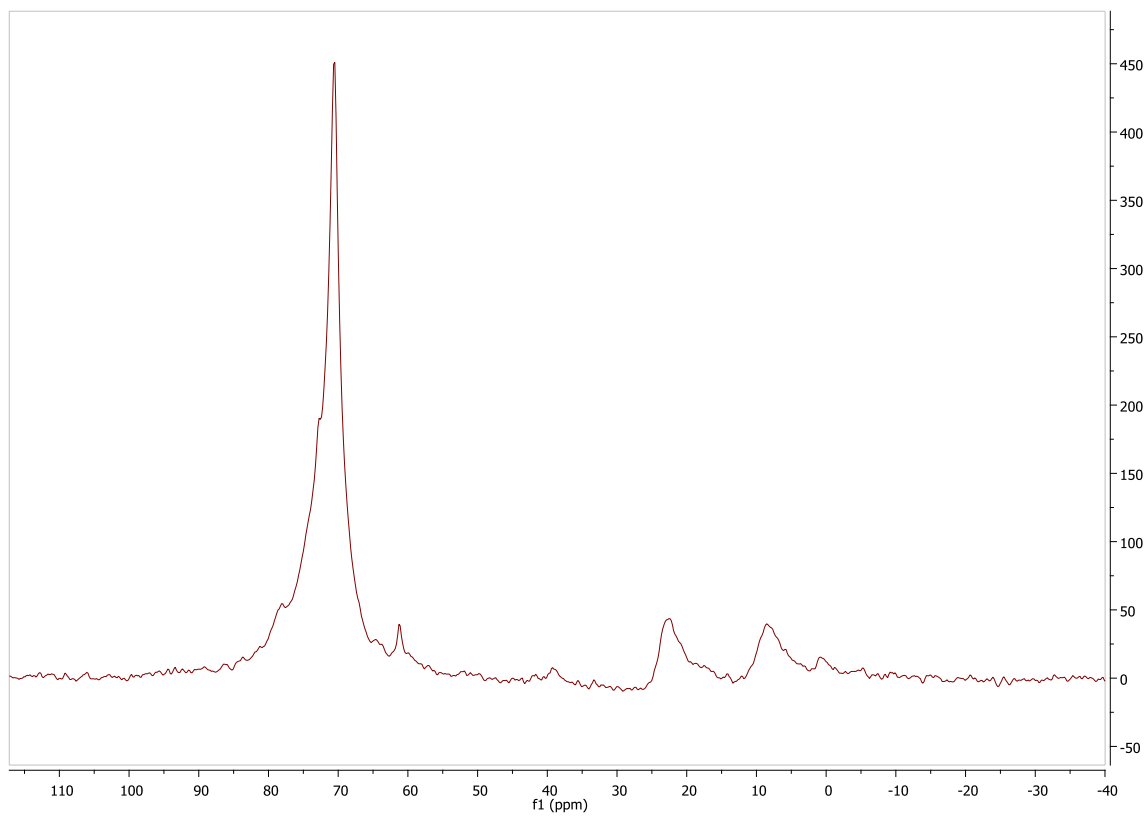
a. 15-c-5 immobilized on SBA-15	XXXVIII
b. 18-c-6 immobilized on SBA-15	XXXIX
c. 15-c-5 immobilized with glymo on SBA-15	XXXIX
d. 18-c-6 immobilized with glymo on SBA-15	XL

- e. THTD immobilized on SBA-15 XL
- f. THTUD immobilized on SBA-15 XLI

4. HMS

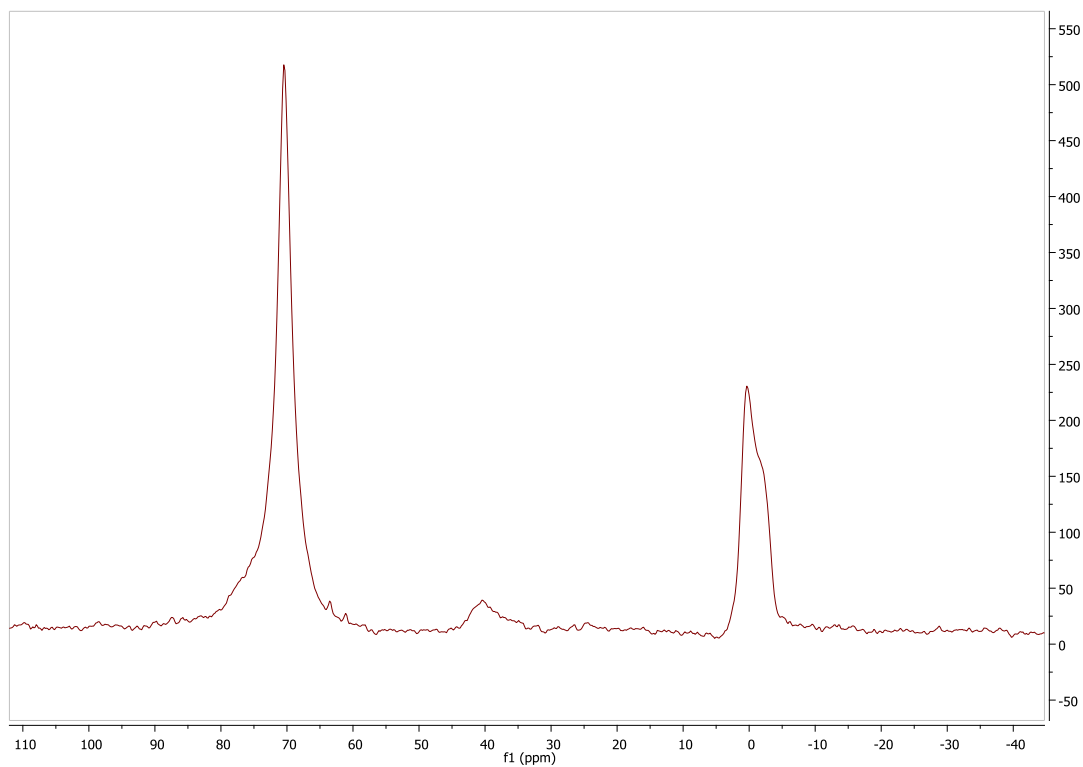
- a. 15-c-5 immobilized on HMS.....XLI
- b. 18-c-6 immobilized on HMS..... XLII
- c. 15-c-5 immobilized with glymo on HMS XLII
- d. 18-c-6 immobilized with glymo on HMS XLIII
- e. THTD immobilized on HMS XLIII
- f. THTUD immobilized on HMS XLIV

^{13}C Si 15-c-5



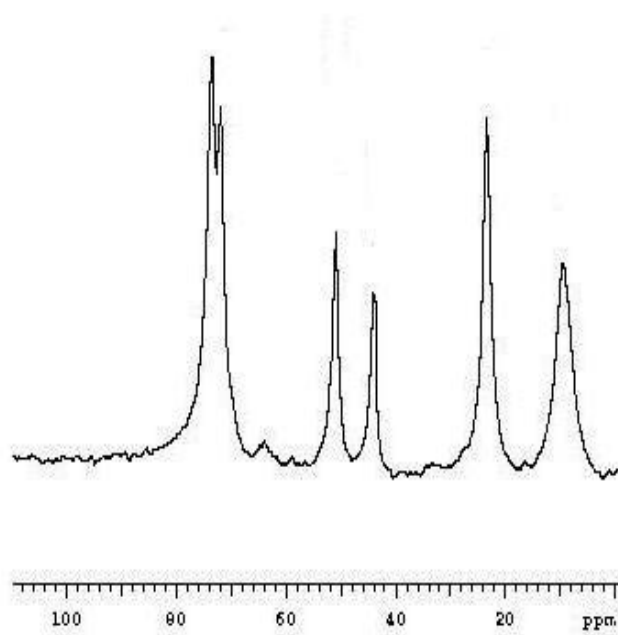
15-c-5 immobilized on Si gel (60 Å)

^{13}C Si 18-c-6



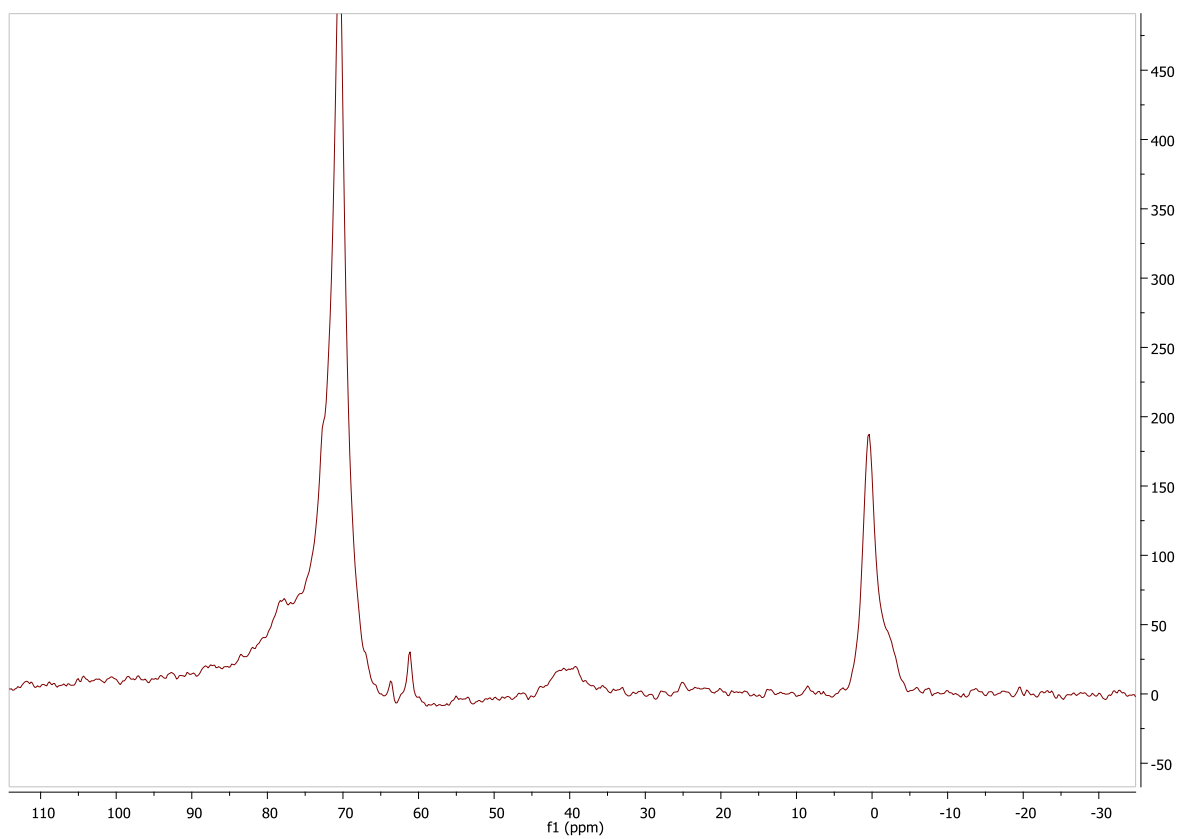
18-c-6 immobilized on Si gel (60 Å)

^{13}C Si Glymo



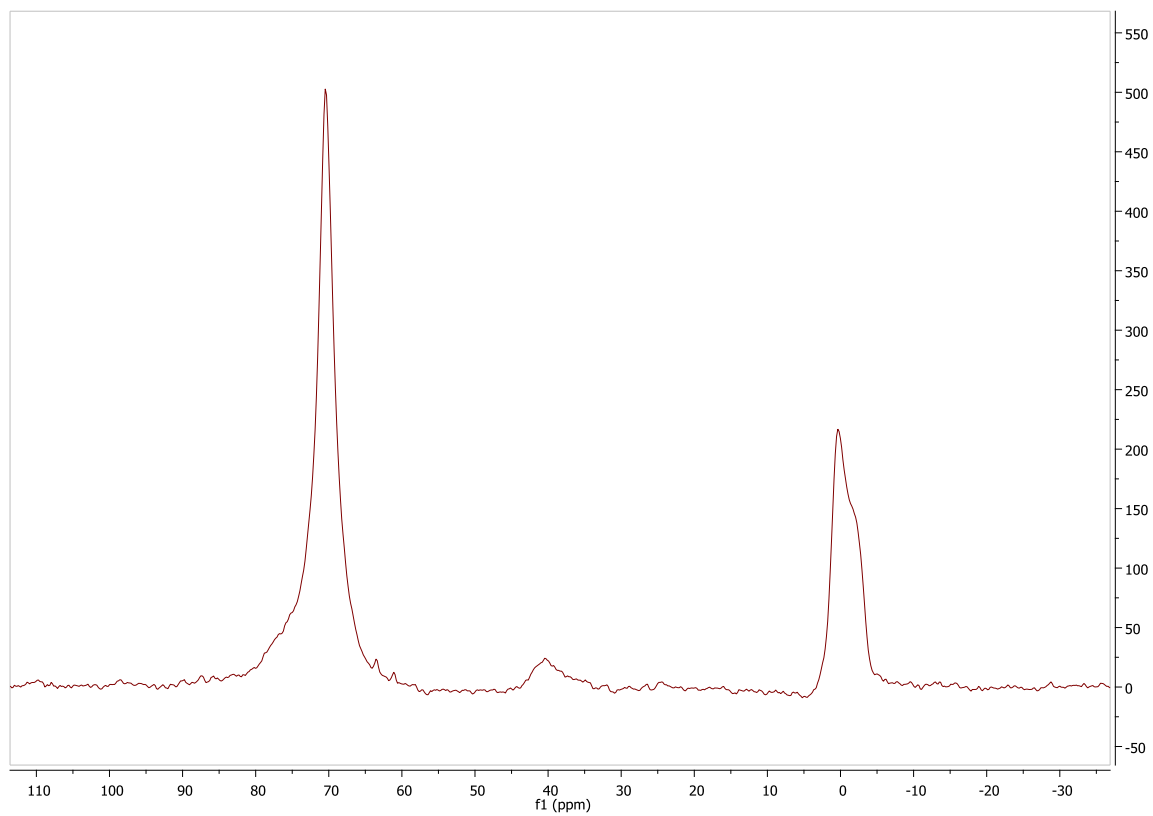
Glymo immobilized on Si gel (60 Å)

^{13}C Si G15-c-5



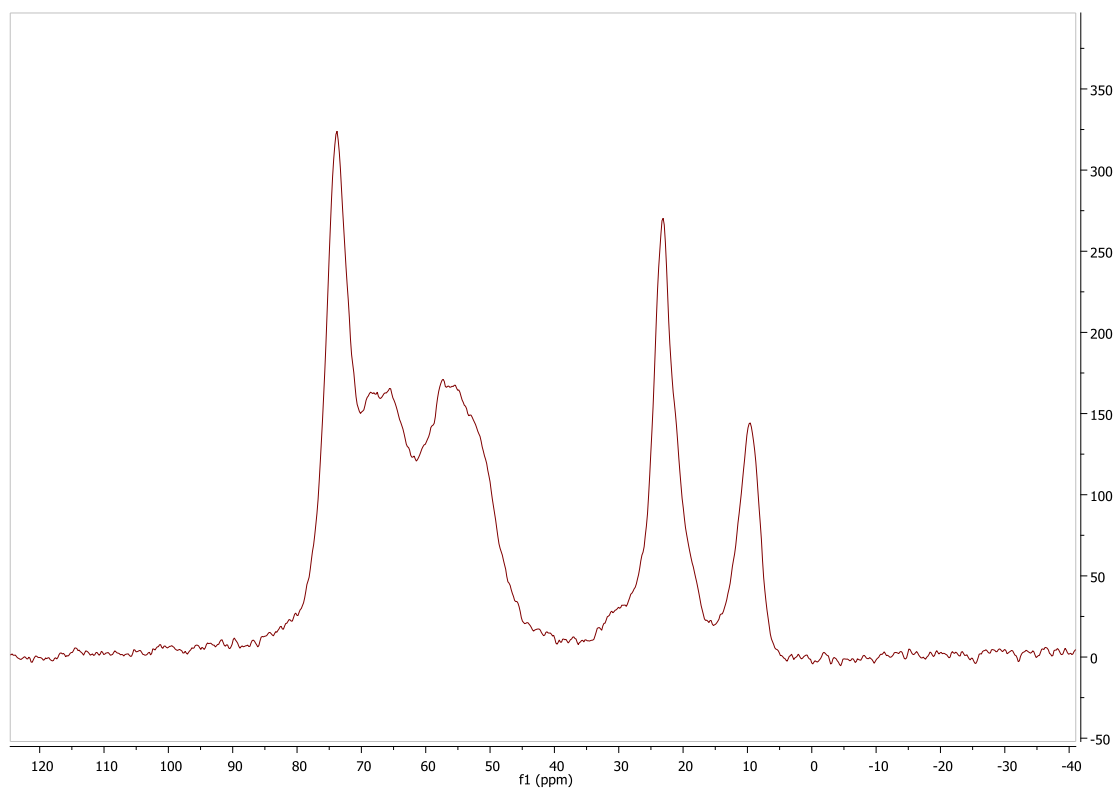
15-c-5 immobilized with glymo on Si gel (60 Å)

^{13}C Si G18-c-6



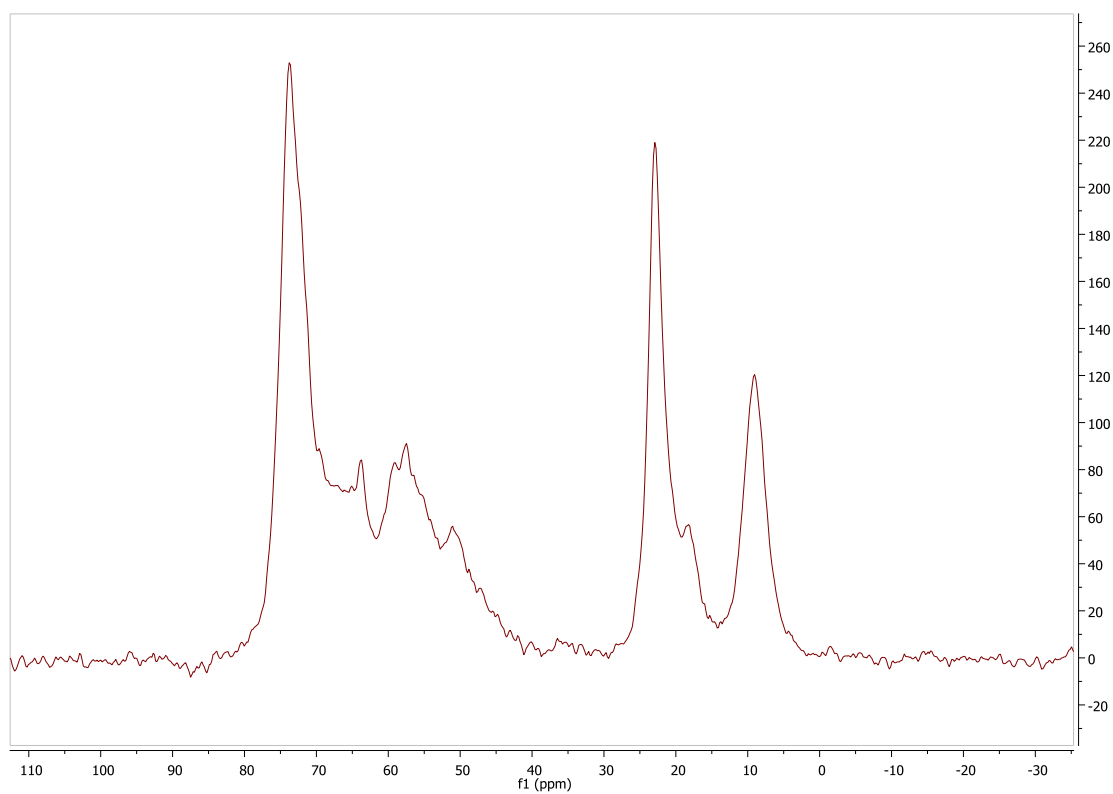
18-c-6 immobilized with glymo on Si gel (60 Å)

^{13}C Si THTD



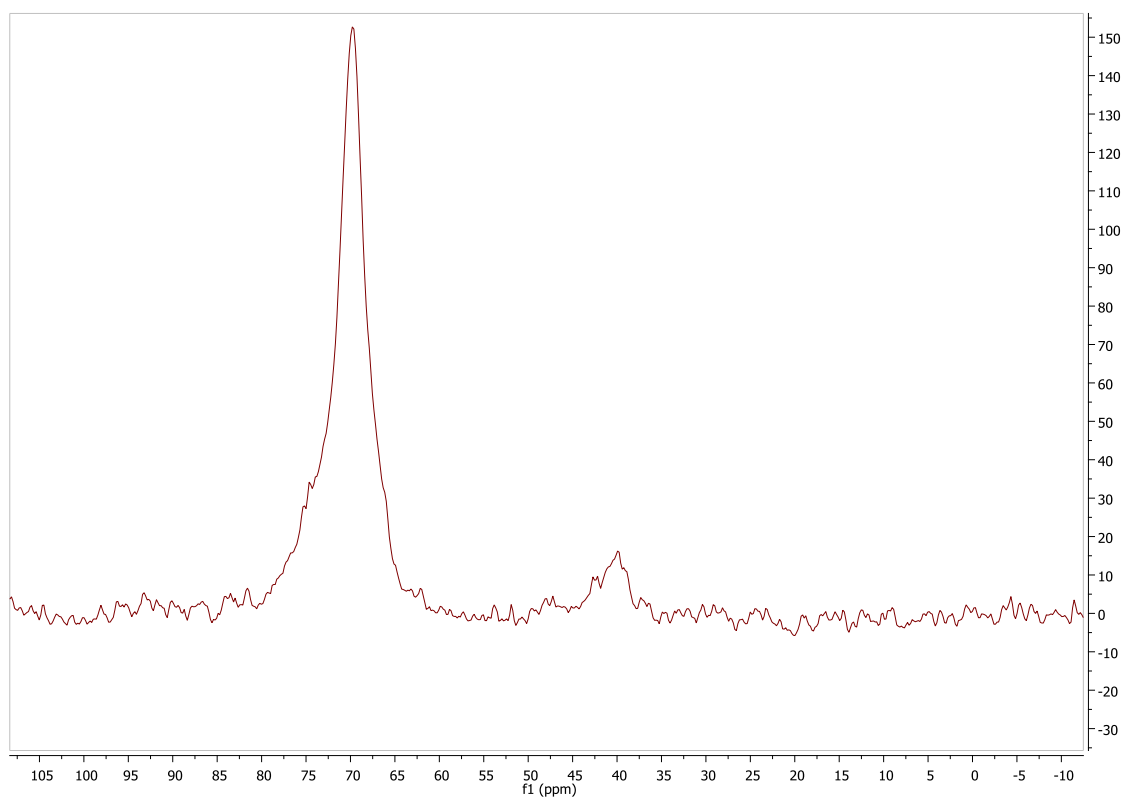
THTD immobilized on Si gel (60 Å)

^{13}C Si THTUD



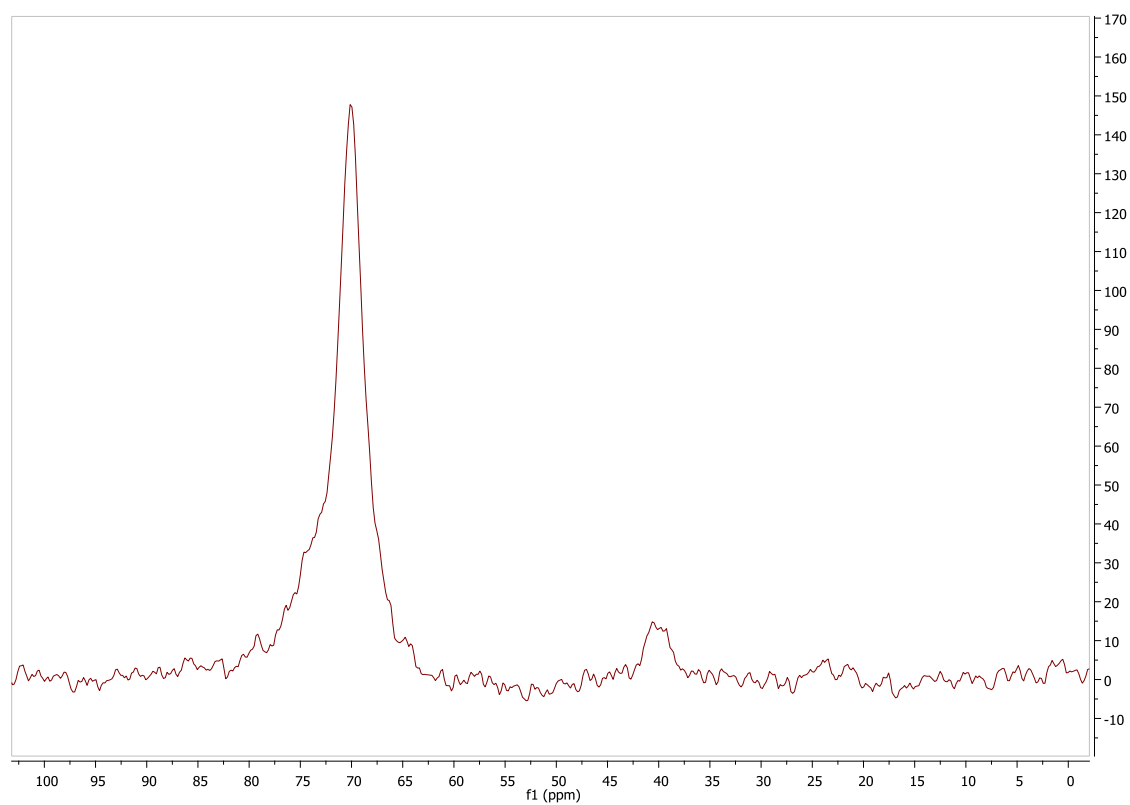
THTUD immobilized on Si gel (60 Å)

^{13}C MCM 15-c-5



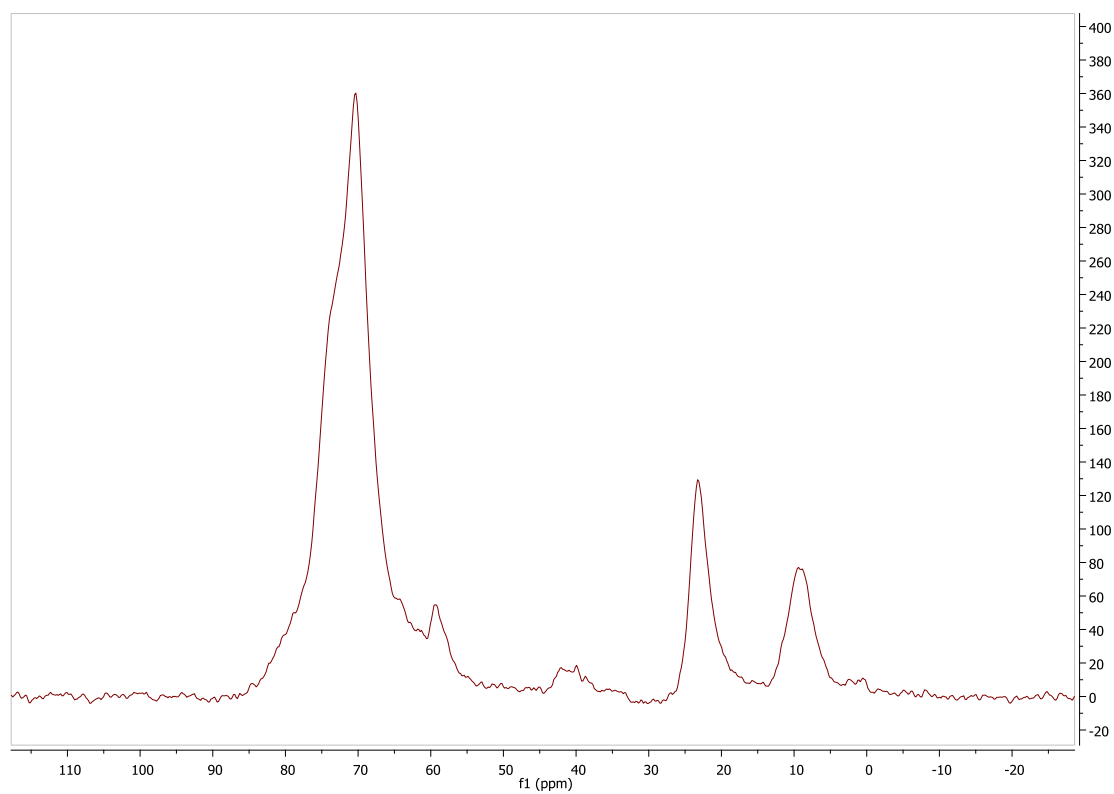
15-c-5 immobilized on MCM-41

^{13}C MCM 18-c-6



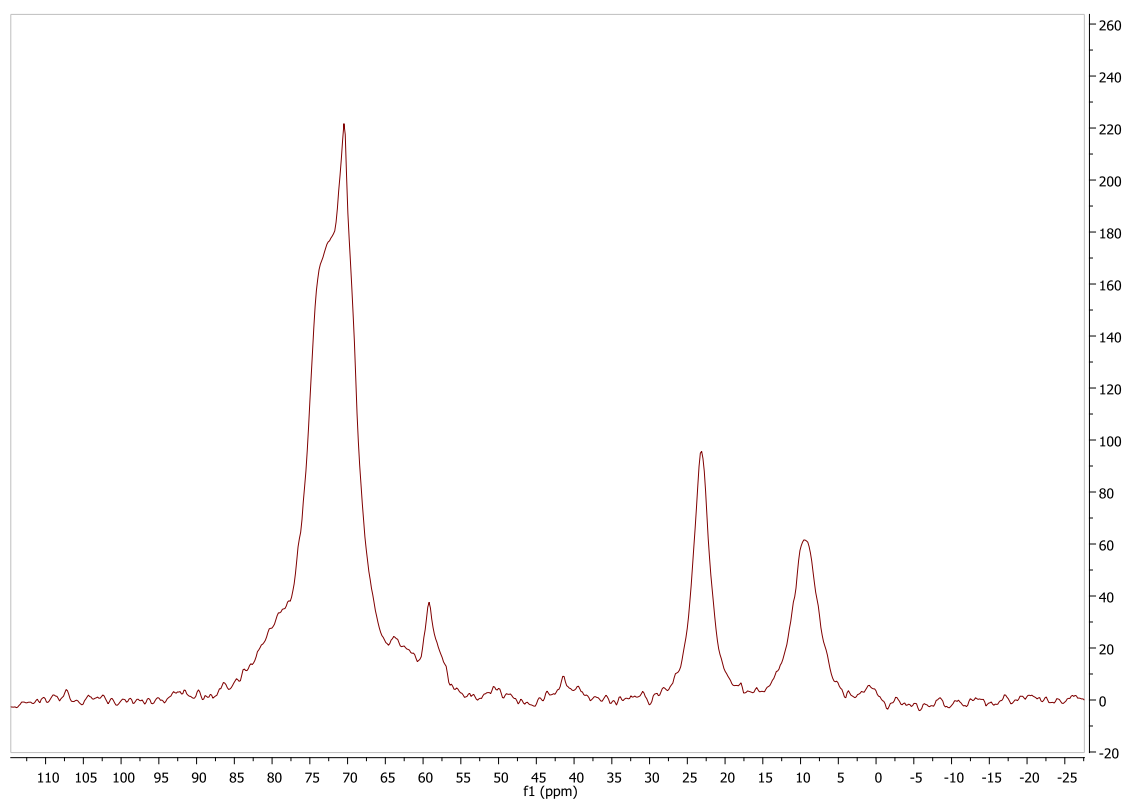
18-c-6 immobilized on MCM-41

^{13}C MCM G15-c-5



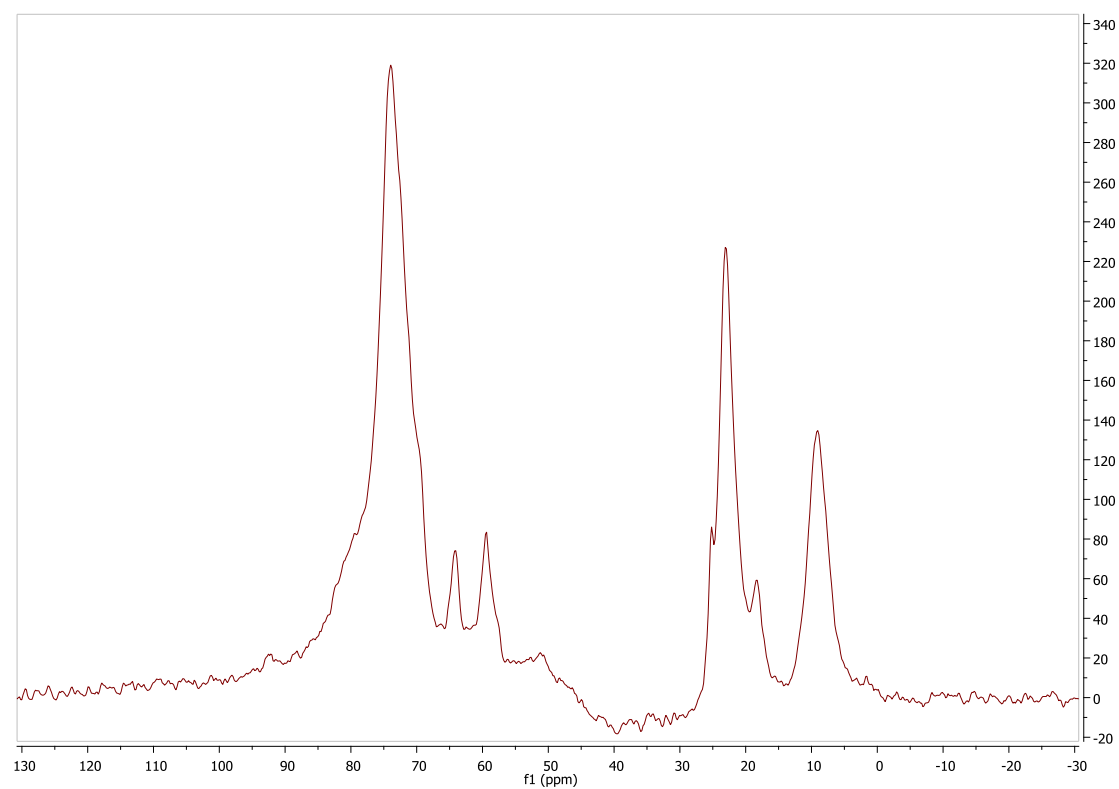
15-c-5 immobilized with glymo on MCM-41

^{13}C MCM G18-c-6



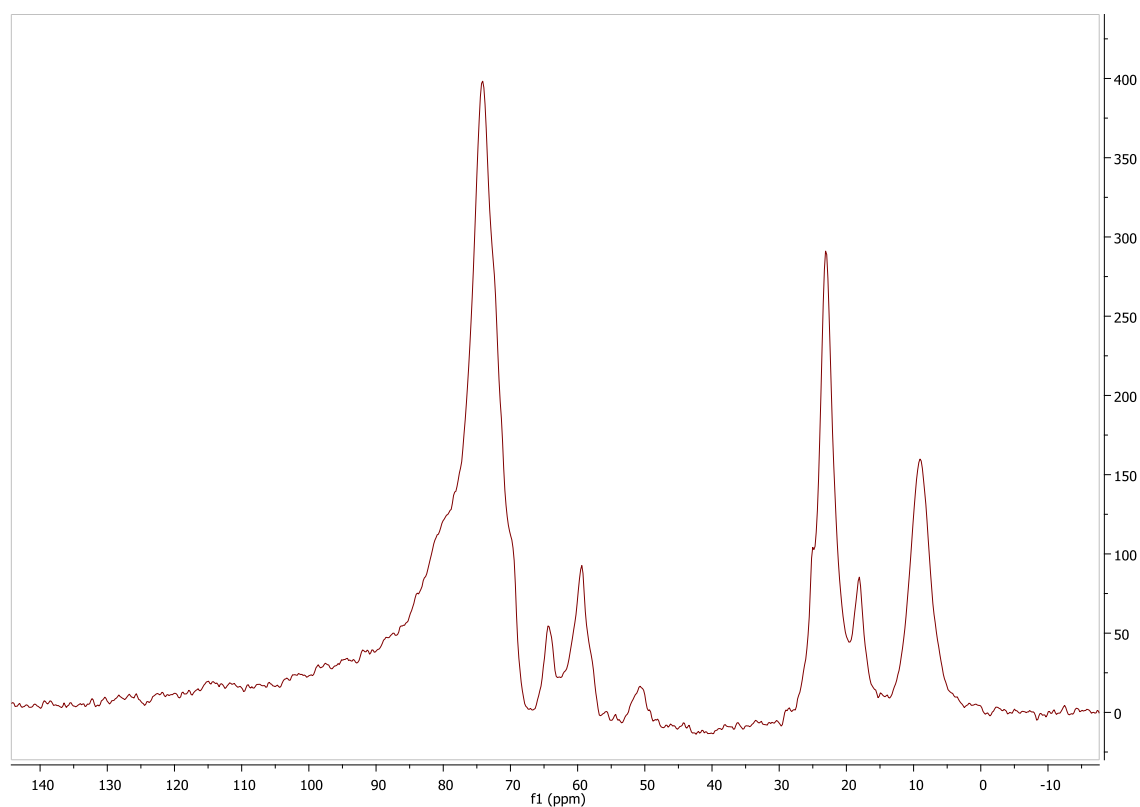
18-c-6 immobilized with glymo on MCM-41

^{13}C MCM THTD



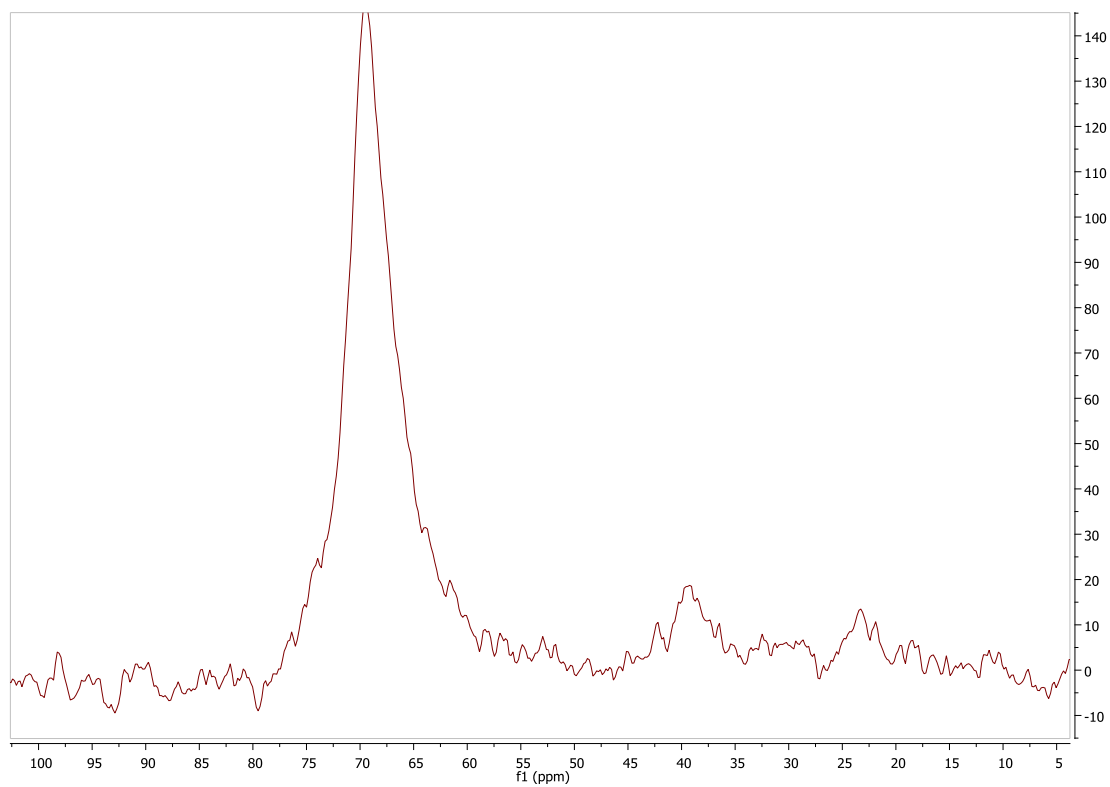
THTD immobilized on MCM-41

¹³C MCM THTUD



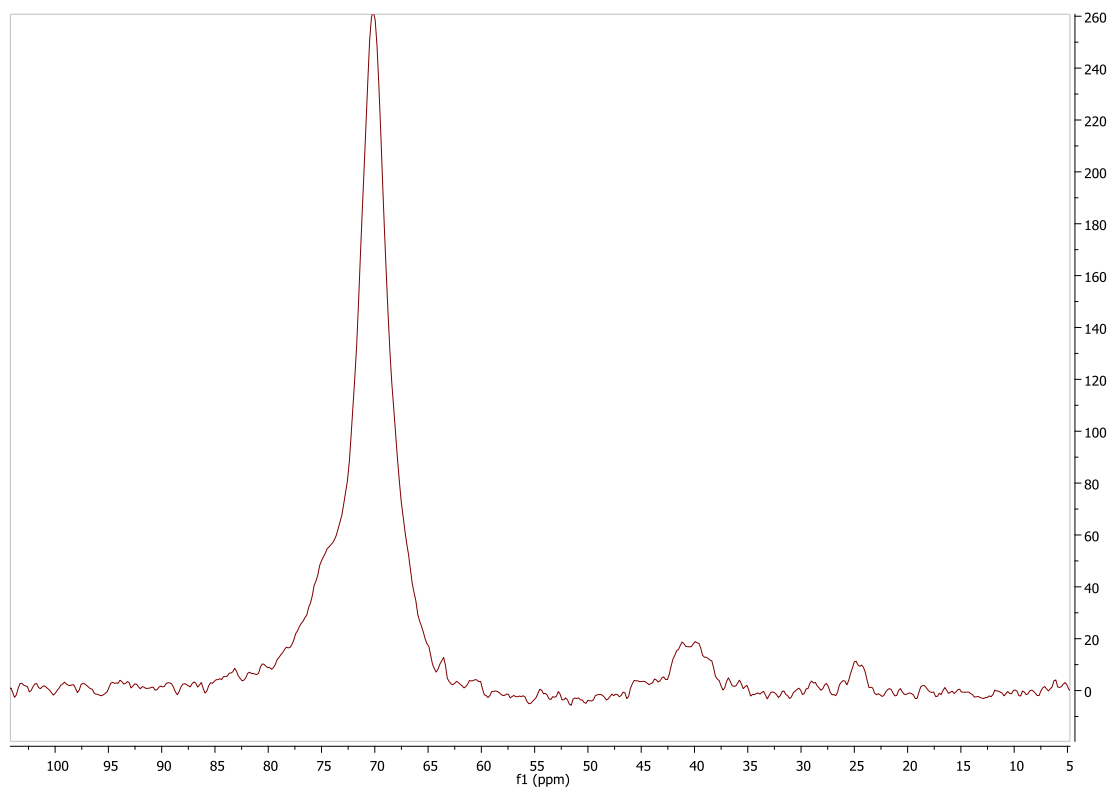
THTUD immobilized on MCM-41

¹³C SBA 15-c-5



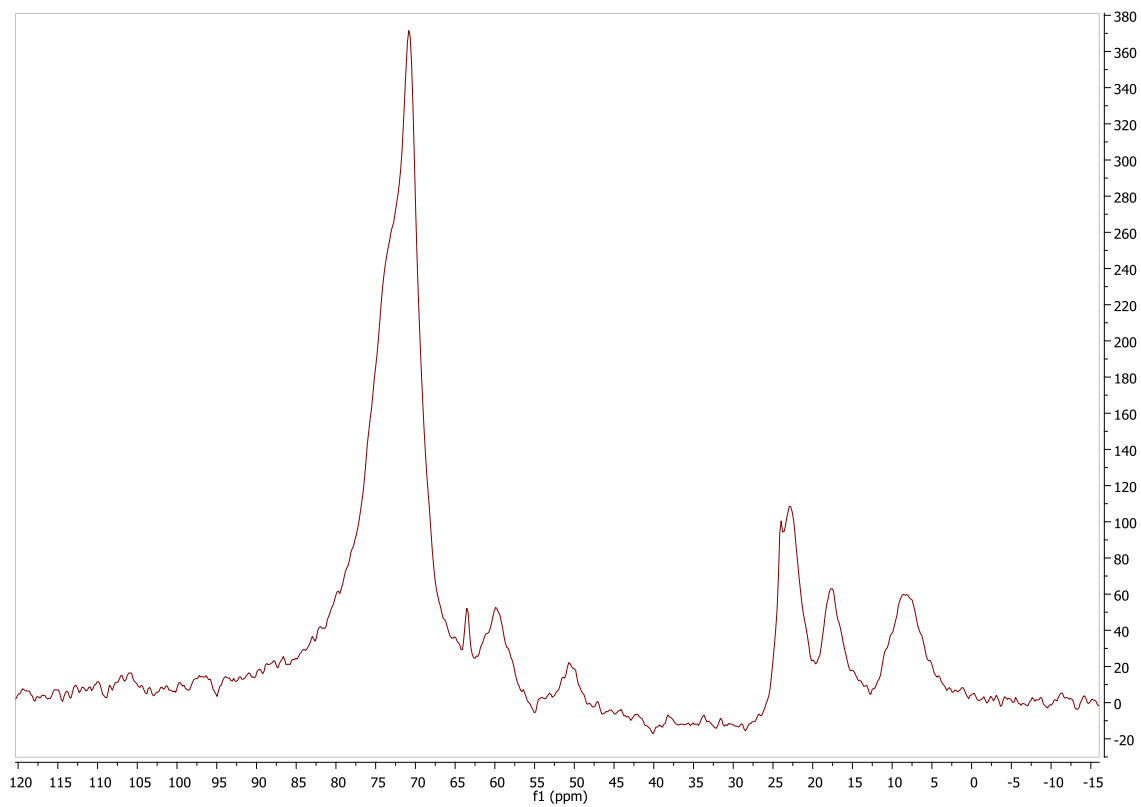
15-c-5 immobilized on SBA-15

^{13}C SBA 18-c-6



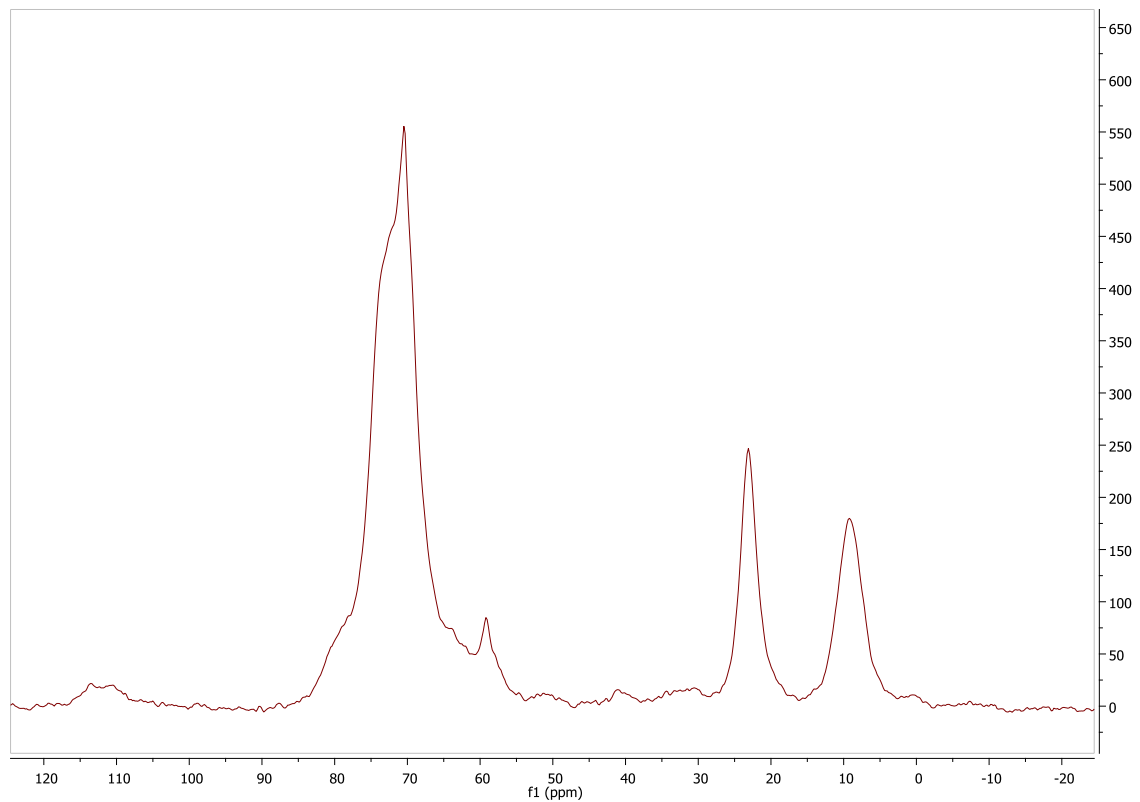
18-c-6 immobilized on SBA-15 17

^{13}C CSBA G15-c-5



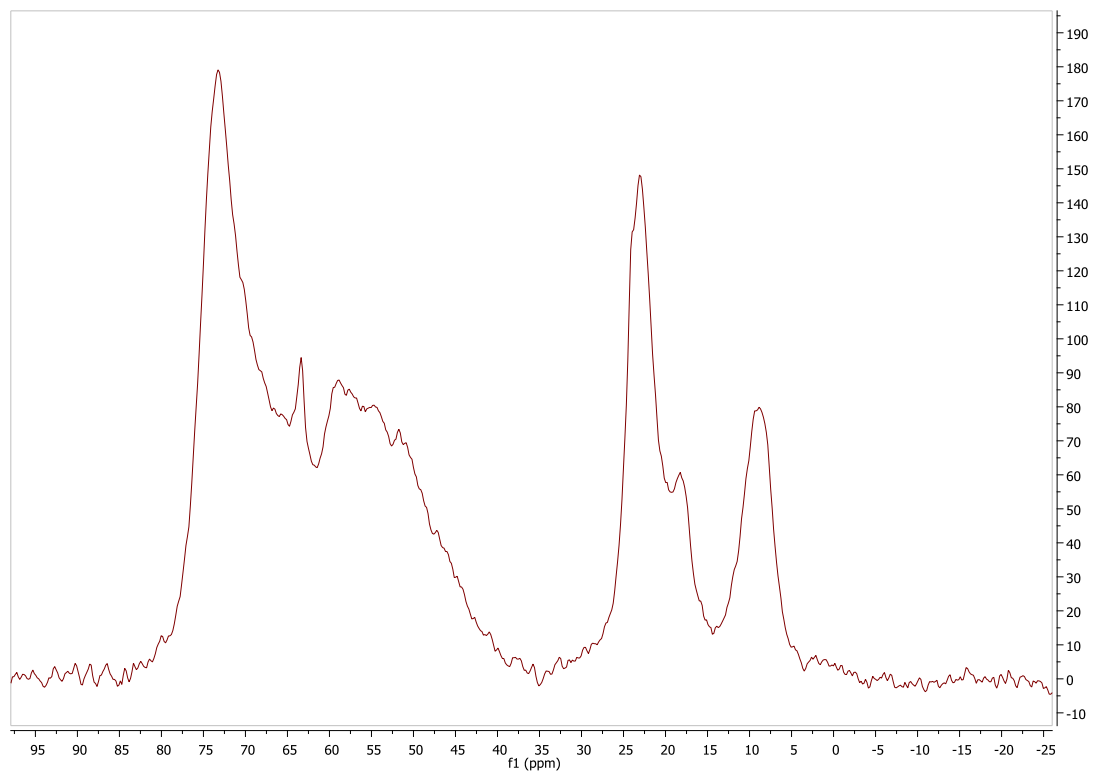
15-c-5 immobilized with glymo on SBA-15

^{13}C SBA G18-c-6



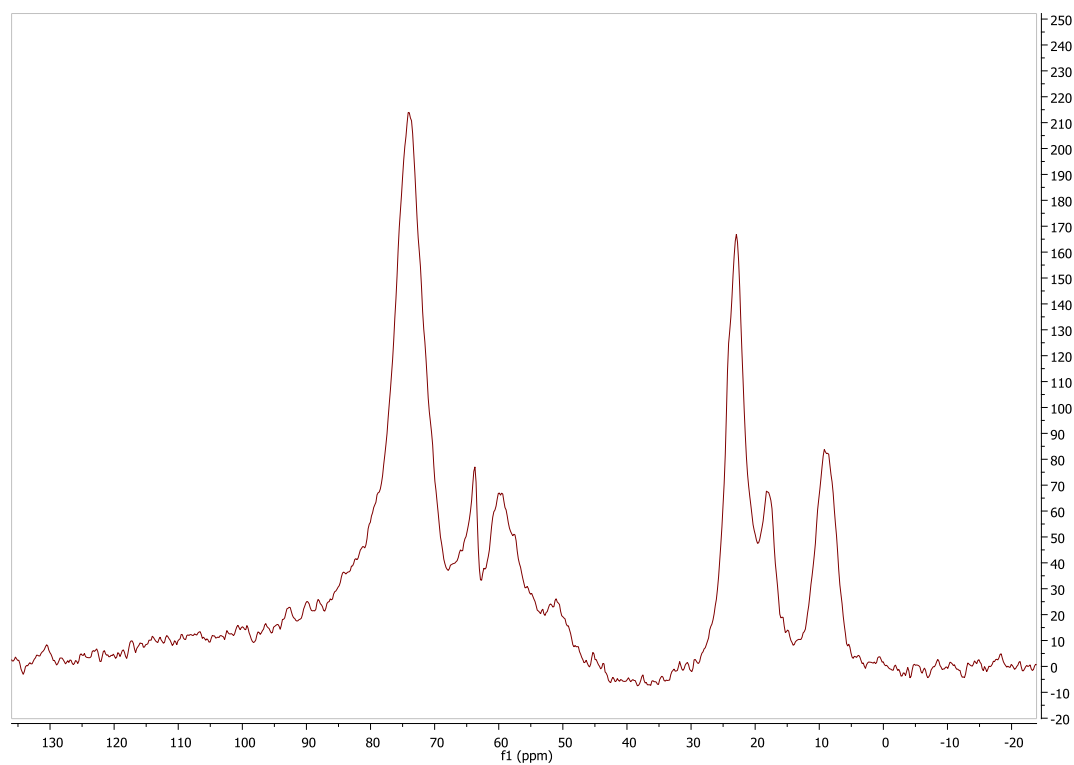
18-c-6 immobilized with glymo on SBA-15

^{13}C SBA THTD



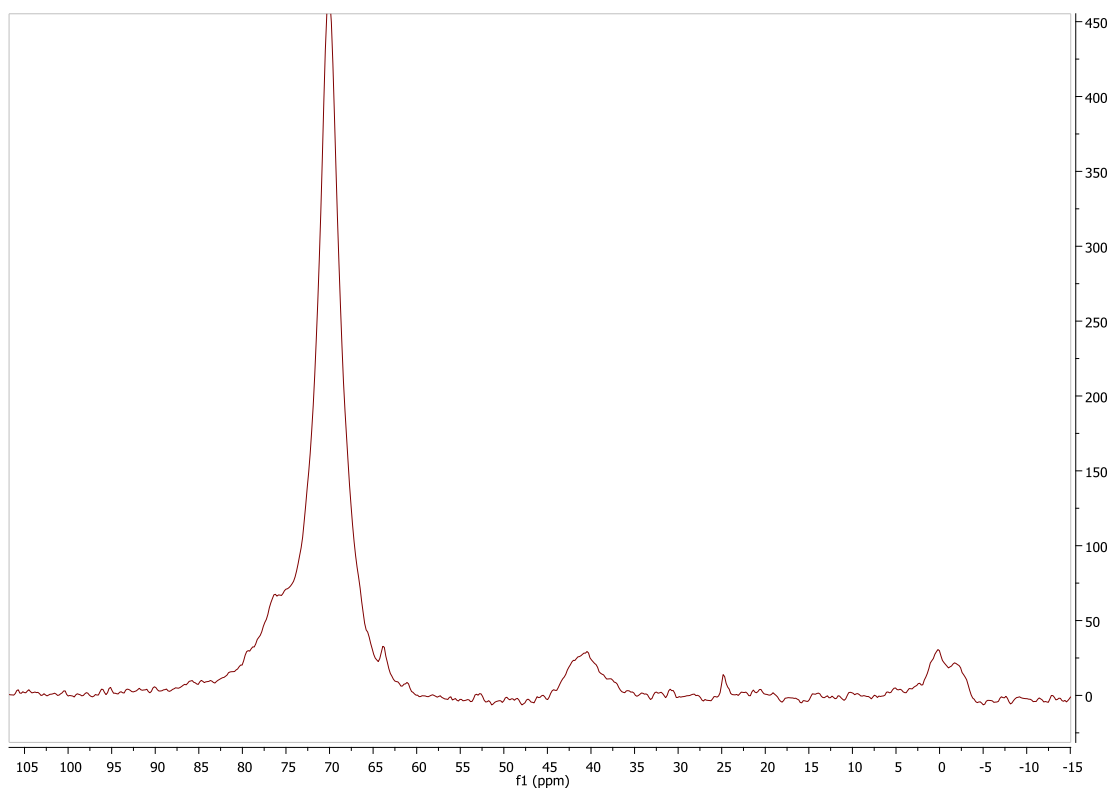
THTD immobilized on SBA-15

^{13}C SBA THTUD



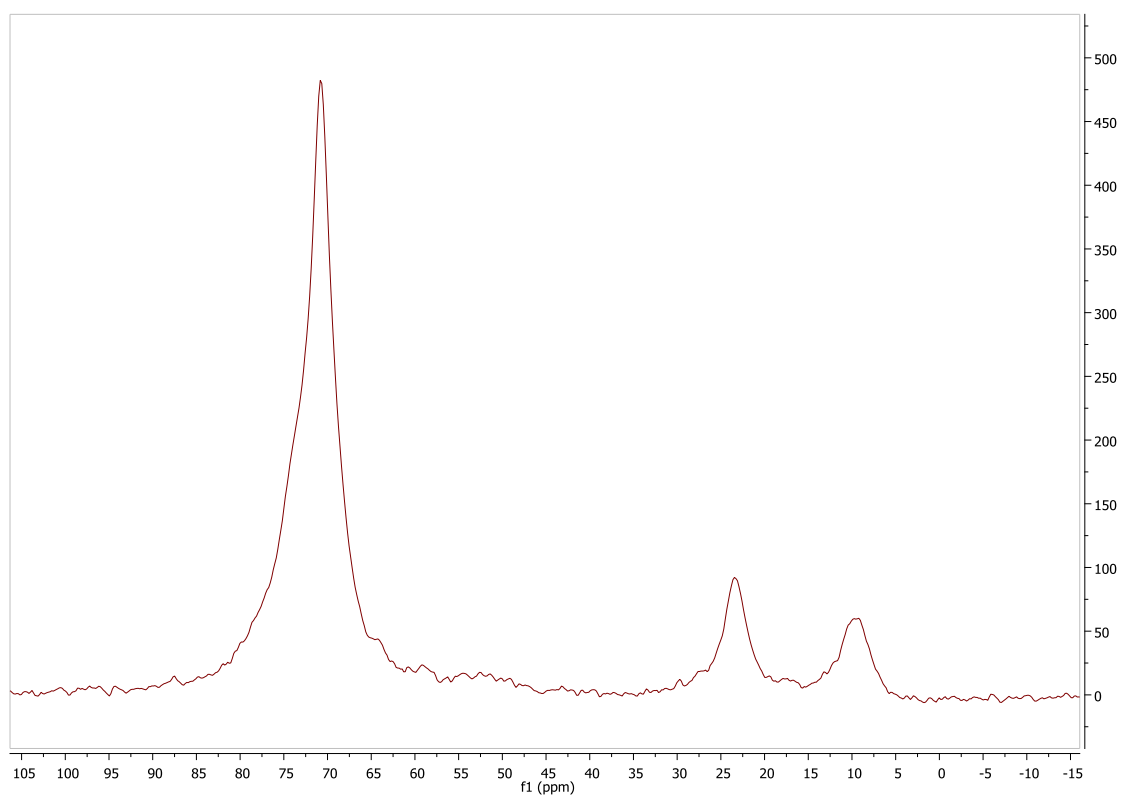
THTUD immobilized on SBA-15

^{13}C HMS 15-c-5



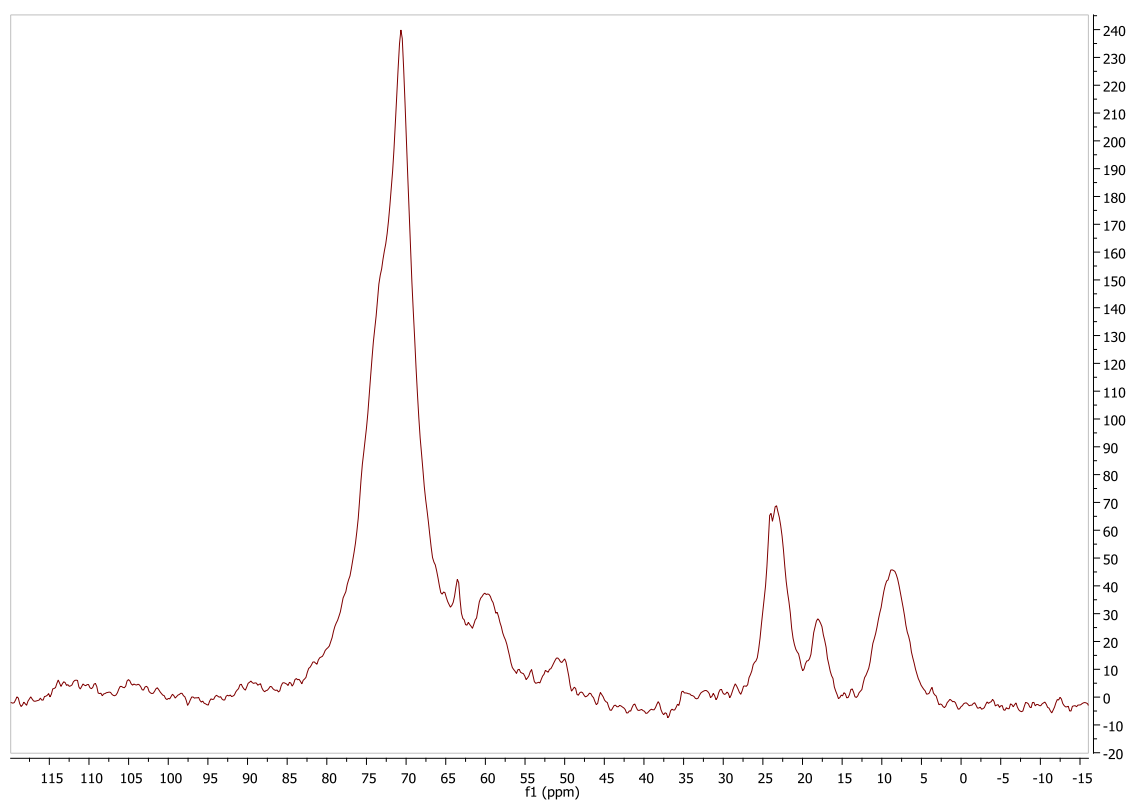
15-c-5 immobilized on HMS

^{13}C HMS 18-c-6



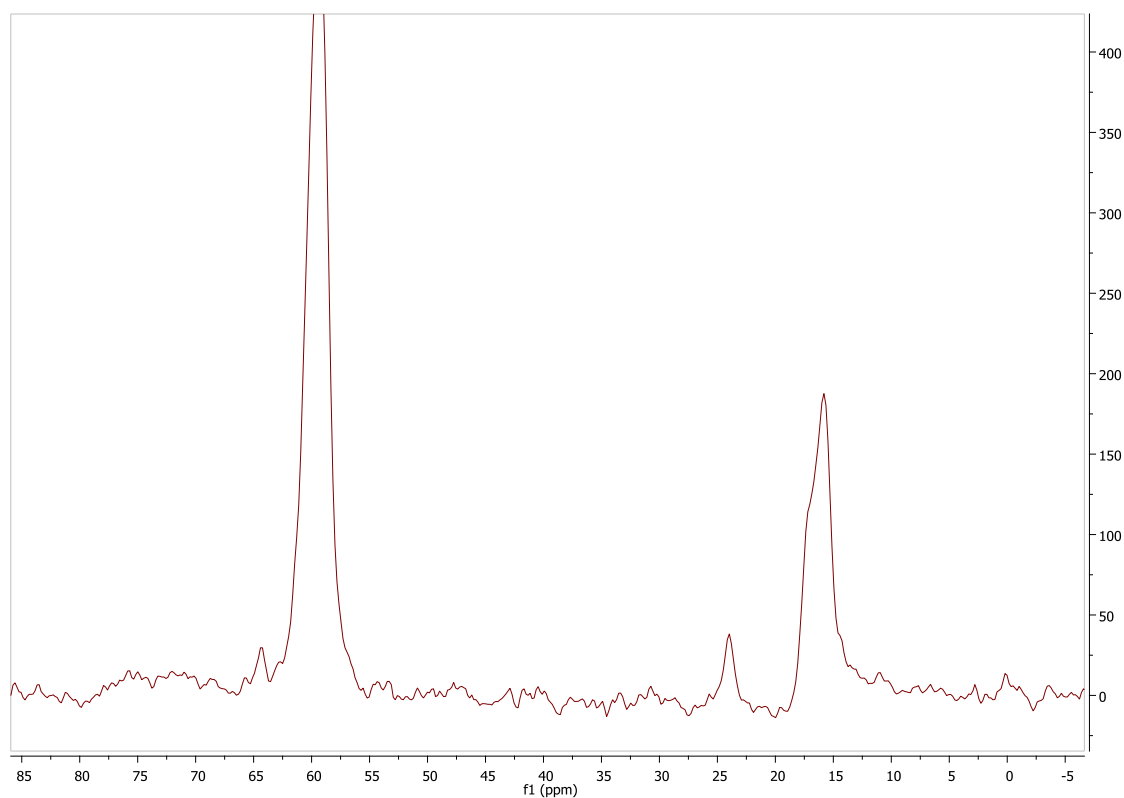
18-c-6 immobilized on HMS

^{13}C HMS G15-c-5



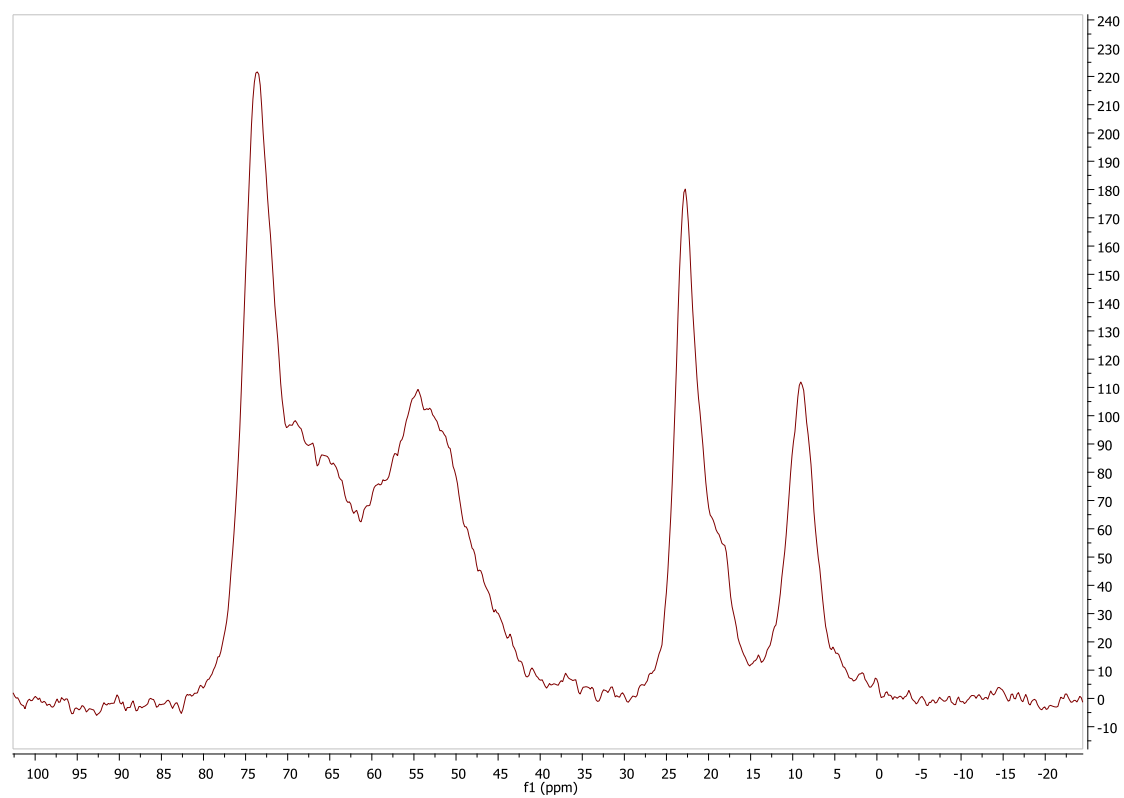
15-c-5 immobilized with glymo on HMS

^{13}C HMS G18-c-6



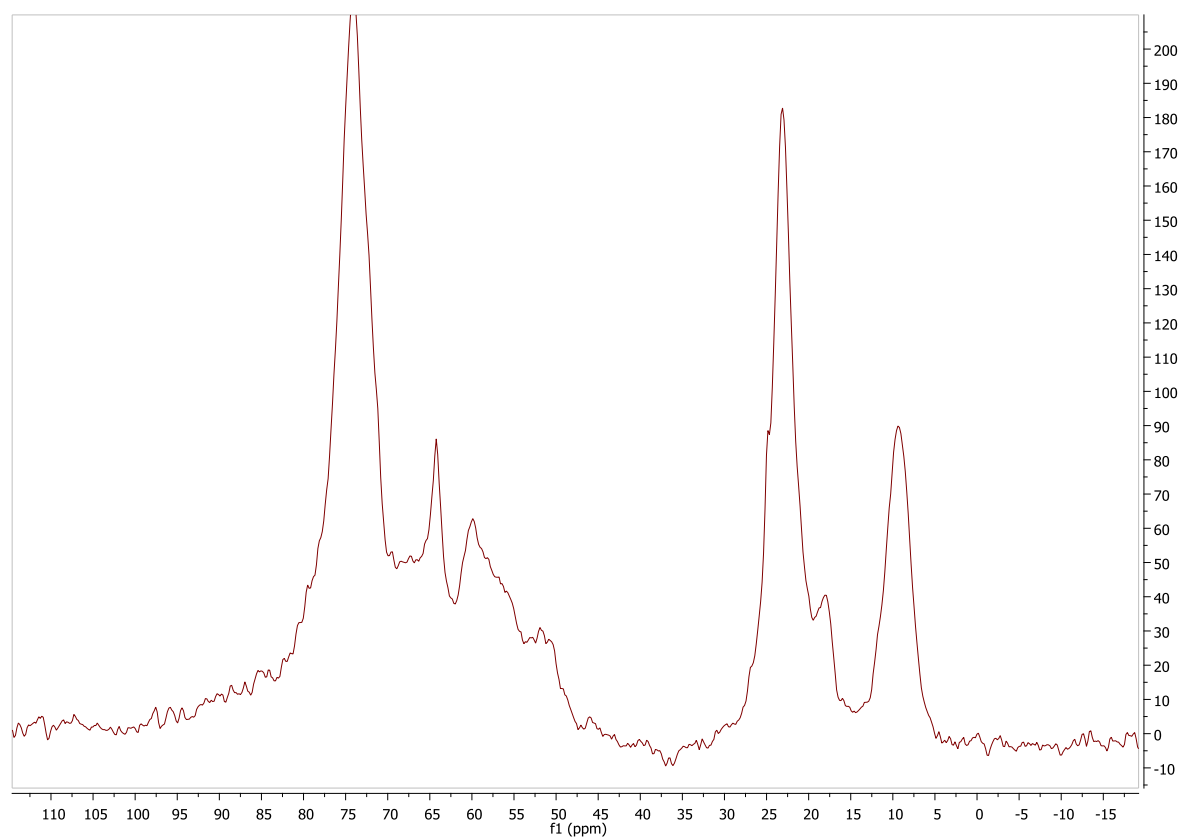
18-c-6 immobilized with glymo on HMS

^{13}C HMS THTD



THTD immobilized on HMS

¹³C HMS THTUD



THTUD immobilized on HMS

ADDENDUM C

Extraction data

1. Extraction of Cr^{6+}	XLVI
2. Extraction of As^{5+}	LV
3. Extraction of Sr^{2+}	LXIV
4. Extraction of Cd^{2+}	LXXIII
5. Extraction of Hg^{2+}	LXXXII
6. Extraction of UO_2^{2+}	LXXXIII
7. Competition extraction of 2 metal ions	LXXXIX
8. Competition extraction of 4 metal ions	XCIX

Cr(VI) extraction at pH 4.5

Accuracy	Certified std value	11.60
	Analysed %	11.98
	Deviation	3.31

Standard Solution (ppm)	Support	Ligand	Extracted ppm	% Extracted
52.20	Si-gel (60Å)	15-k-5	51.88	0.31
		18-k-6	52.83	0.00
		Glymo + 15-k-5	46.80	5.39
		Glymo + 18-k-6	45.05	7.15
		Glymo + THTD	41.03	11.17
		Glymo + THTUD	39.70	12.50
		Average %		11.66
	MCM-41	15-k-5	51.81	0.39
		18-k-6	51.30	0.89
		Glymo + 15-k-5	51.05	1.15
		Glymo + 18-k-6	50.62	1.58
		Glymo + THTD	48.26	3.94
		Glymo + THTUD	51.67	0.53
		Average %		2.70
	SBA-15	15-k-5	49.98	2.22
		18-k-6	50.28	1.91
		Glymo + 15-k-5	51.54	0.66
		Glymo + 18-k-6	50.30	1.90
		Glymo + THTD	29.12	23.08
		Glymo + THTUD	50.82	1.38
		Average %		9.94
	HMS	15-k-5	51.92	0.28
		18-k-6	52.34	0.00
		Glymo + 15-k-5	44.35	7.85
		Glymo + 18-k-6	40.03	12.16
		Glymo + THTD	45.02	7.18
		Glymo + THTUD	46.26	5.94
		Average %		10.67

Cr(VI) extraction at pH 4.5

Accuracy	Certified std value	11.60
	Analysed	11.98
	% Deviation	3.31

Support	Ligand		% Extracted
Si-gel (60Å)	15-k-5		0.60
MCM-41	15-k-5		0.74
SBA-15	15-k-5		4.25
HMS	15-k-5		0.53
		Average %	1.53
Si-gel (60Å)	18-k-6		0.00
MCM-41	18-k-6		1.71
SBA-15	18-k-6		3.67
HMS	18-k-6		0.00
		Average %	1.35
Si-gel (60Å)	Glymo + 15-k-5		10.34
MCM-41	Glymo + 15-k-5		2.20
SBA-15	Glymo + 15-k-5		1.26
HMS	Glymo + 15-k-5		15.03
		Average %	7.21
Si-gel (60Å)	Glymo + 18-k-6		13.70
MCM-41	Glymo + 18-k-6		3.02
SBA-15	Glymo + 18-k-6		3.63
HMS	Glymo + 18-k-6		23.31
		Average %	10.91
Si-gel (60Å)	Glymo + THTD		21.40
MCM-41	Glymo + THTD		7.54
SBA-15	Glymo + THTD		44.22
HMS	Glymo + THTD		13.75
		Average %	21.73
Si-gel (60Å)	Glymo + THTUD		23.94
MCM-41	Glymo + THTUD	1.01	
SBA-15	Glymo + THTUD		2.64
HMS	Glymo + THTUD		11.38
		Average %	9.74

Cr(VI) extraction at pH 5.9

Accuracy	Certified std value	24.68
	Analysed	24.99
	% Deviation	1.27

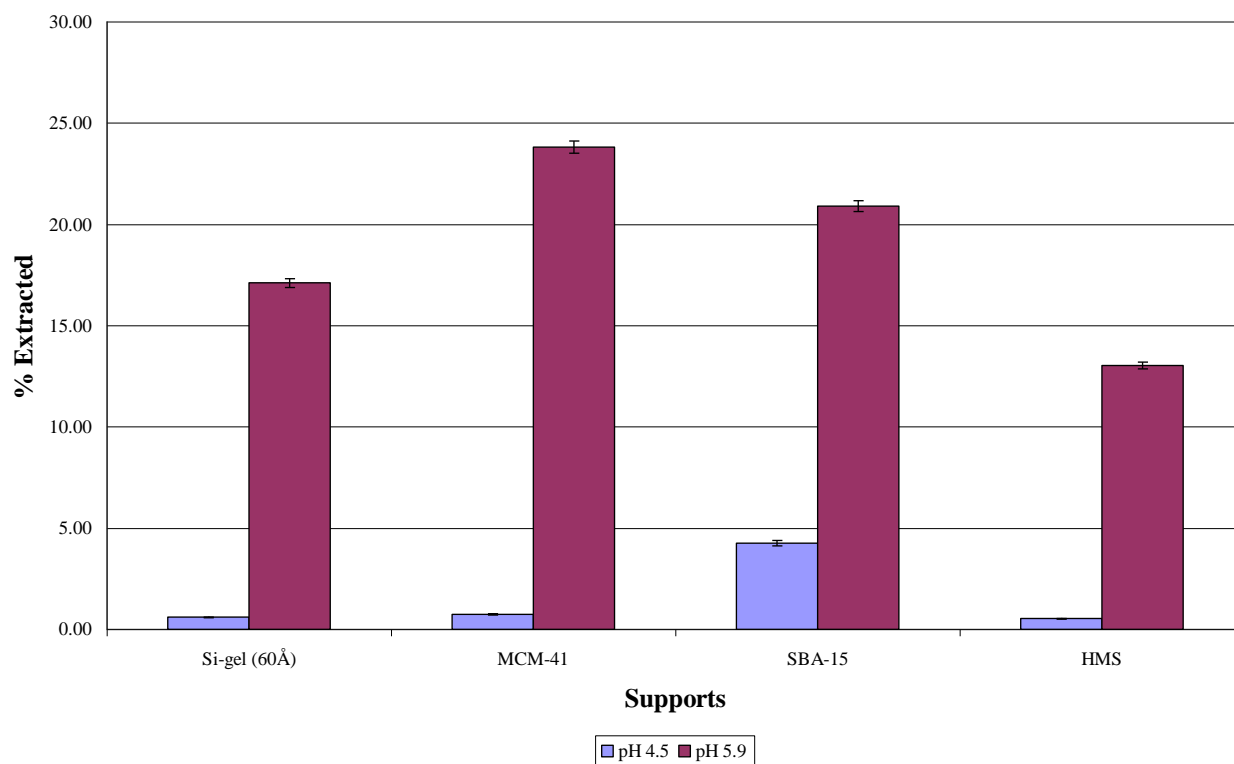
Standard Solution (ppm)	Support	Ligand		Extracted ppb	% Extracted
589.11	Si-gel (60Å)	15-k-5	488.36	100.75	17.10
		18-k-6	461.74	127.38	21.62
		Glymo + 15-k-5	429.35	159.76	27.12
		Glymo + 18-k-6	463.40	125.71	21.34
		Glymo + THTD	389.82	199.30	33.83
		Glymo + THTUD	390.57	198.54	33.70
				Average %	25.79
	MCM-41	15-k-5	448.84	140.27	23.81
		18-k-6	430.64	158.47	26.90
		Glymo + 15-k-5	485.64	103.47	17.56
		Glymo + 18-k-6	437.94	151.17	25.66
		Glymo + THTD	429.47	159.65	27.10
		Glymo + THTUD	448.94	140.18	23.79
				Average %	24.14
	SBA-15	15-k-5	466.02	123.10	20.90
		18-k-6	480.79	108.32	18.39
		Glymo + 15-k-5	459.31	129.81	22.03
		Glymo + 18-k-6	477.27	111.84	18.98
		Glymo + THTD	370.59	218.52	37.09
		Glymo + THTUD	427.88	161.23	27.37
				Average %	24.13
	HMS	15-k-5	512.32	76.79	13.03
		18-k-6	348.34	240.77	40.87
		Glymo + 15-k-5	477.51	111.61	18.94
		Glymo + 18-k-6	370.01	219.10	37.19
		Glymo + THTD	386.62	202.49	34.37
		Glymo + THTUD	529.41	59.70	10.13
				Average %	25.76

Cr(VI) extraction at pH 5.9

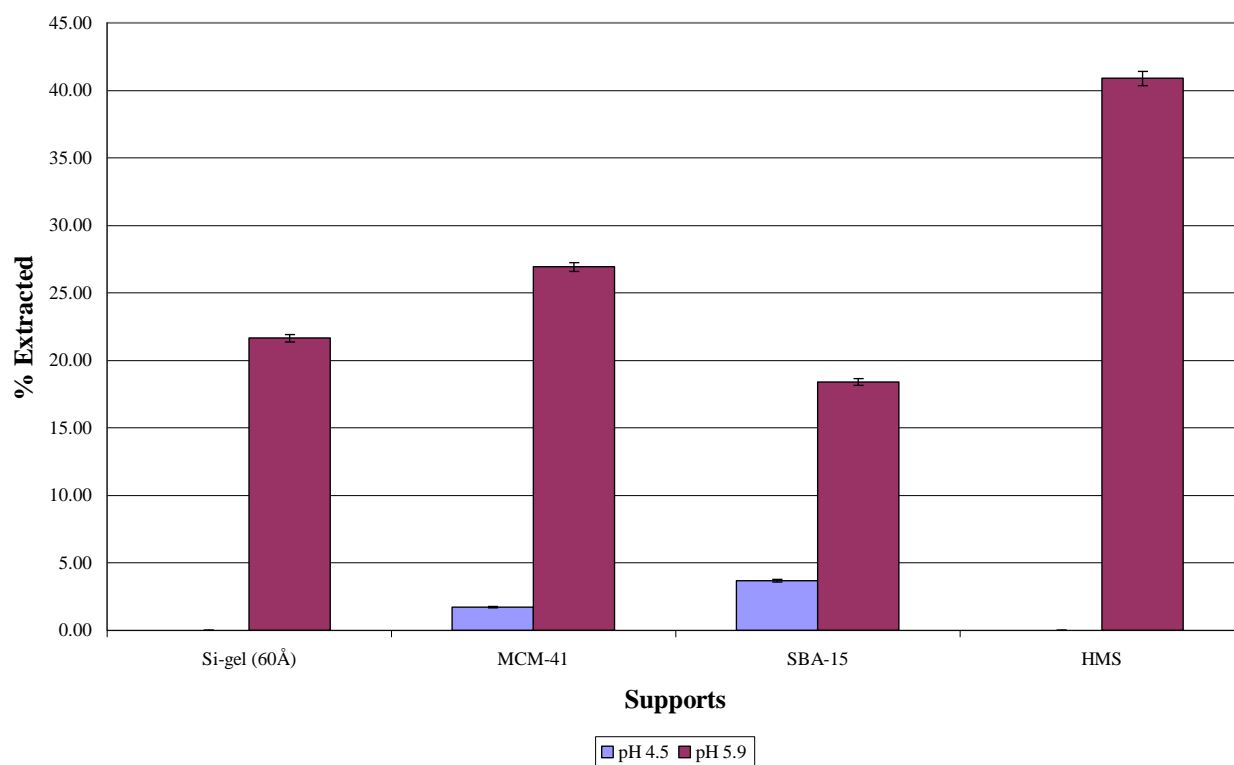
Accuracy	Certified std value	24.68
	Analysed	24.99
	% Deviation	1.27

Support	Ligand	% Extracted
Si-gel (60Å)	15-k-5	17.10
MCM-41	15-k-5	23.81
SBA-15	15-k-5	20.90
HMS	15-k-5	13.03
	Average %	18.71
Si-gel (60Å)	18-k-6	21.62
MCM-41	18-k-6	26.90
SBA-15	18-k-6	18.39
HMS	18-k-6	40.87
	Average %	26.95
Si-gel (60Å)	Glymo + 15-k-5	27.12
MCM-41	Glymo + 15-k-5	17.56
SBA-15	Glymo + 15-k-5	22.03
HMS	Glymo + 15-k-5	18.94
	Average %	21.42
Si-gel (60Å)	Glymo + 18-k-6	21.34
MCM-41	Glymo + 18-k-6	25.66
SBA-15	Glymo + 18-k-6	18.98
HMS	Glymo + 18-k-6	37.19
	Average %	25.79
Si-gel (60Å)	Glymo + THTD	33.83
MCM-41	Glymo + THTD	27.10
SBA-15	Glymo + THTD	37.09
HMS	Glymo + THTD	34.37
	Average %	33.10
Si-gel (60Å)	Glymo + THTUD	33.70
MCM-41	Glymo + THTUD	23.79
SBA-15	Glymo + THTUD	27.37
HMS	Glymo + THTUD	10.13
	Average %	23.75

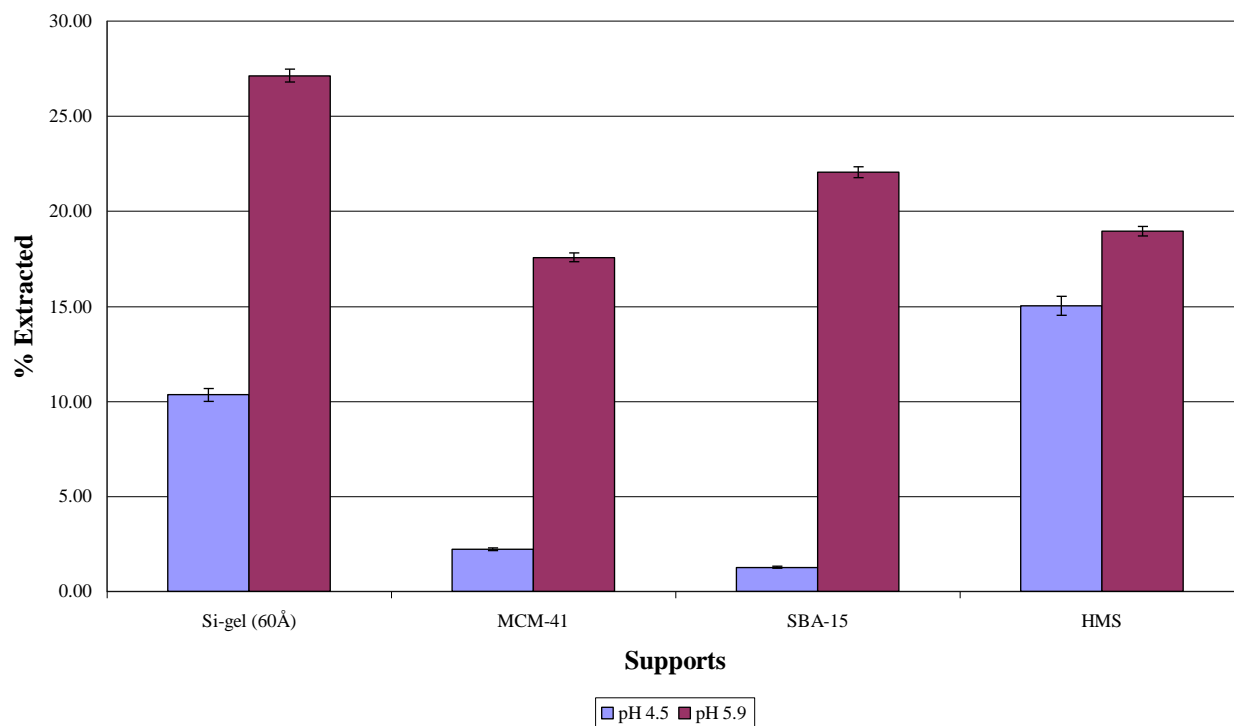
Extraction of Cr(VI) with 15-c-5 Immobilized Directly on Different Supports



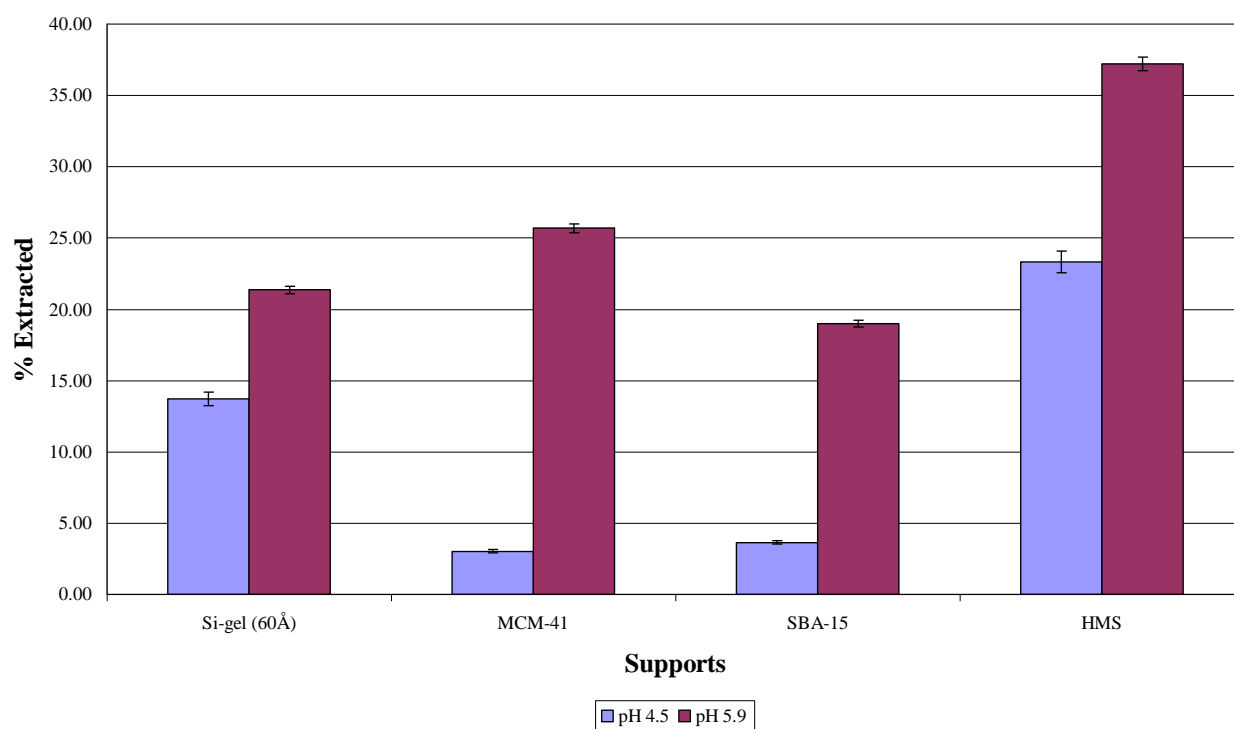
Extraction of Cr(VI) with 18-c-6 Immobilized Directly on Different Supports



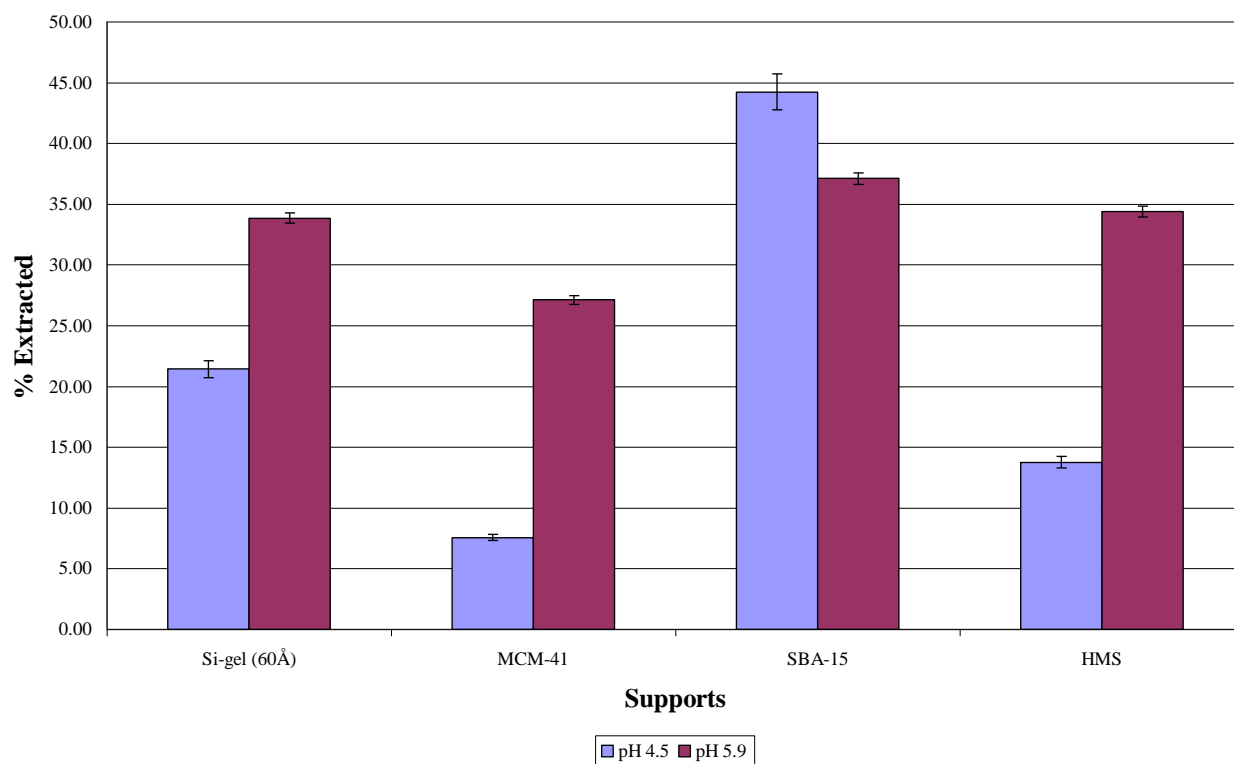
Extraction of Cr(VI) with 15-c-5 Immobilized with Glymo on Different Supports



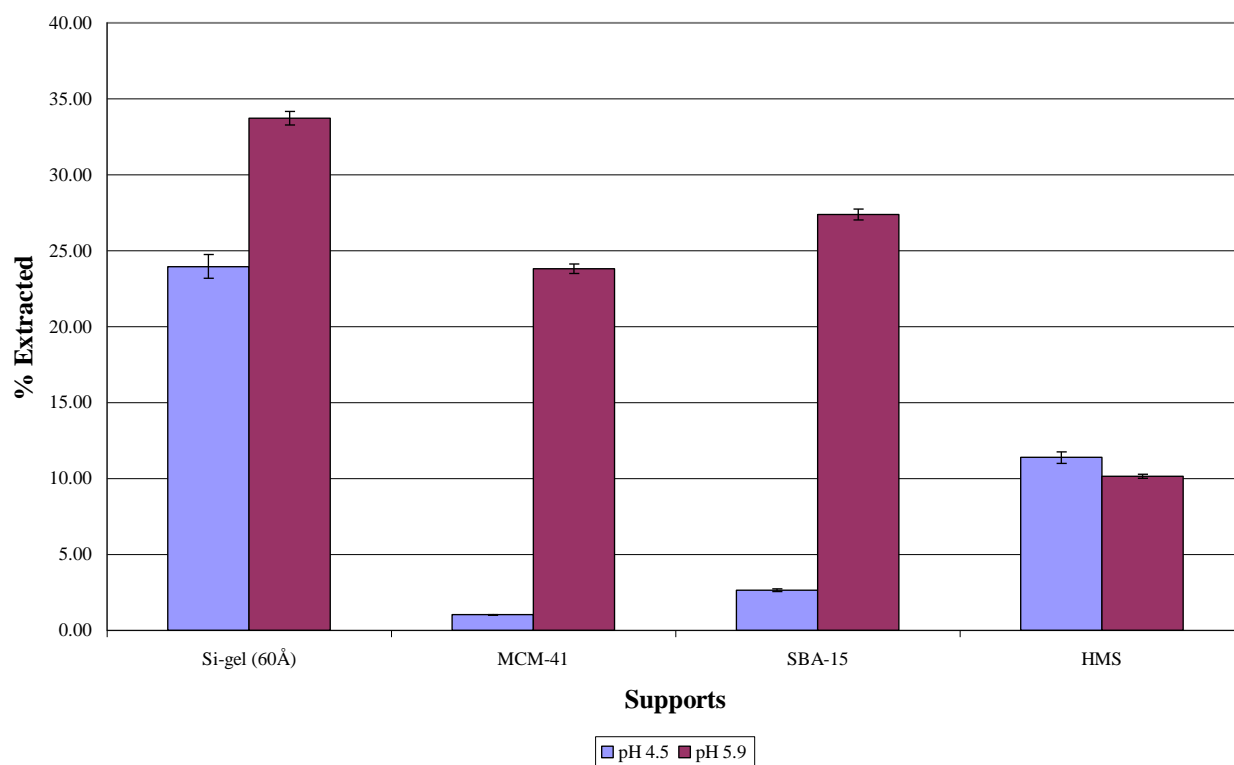
Extraction of Cr(VI) with 18-c-6 Immobilized with Glymo on Different Supports



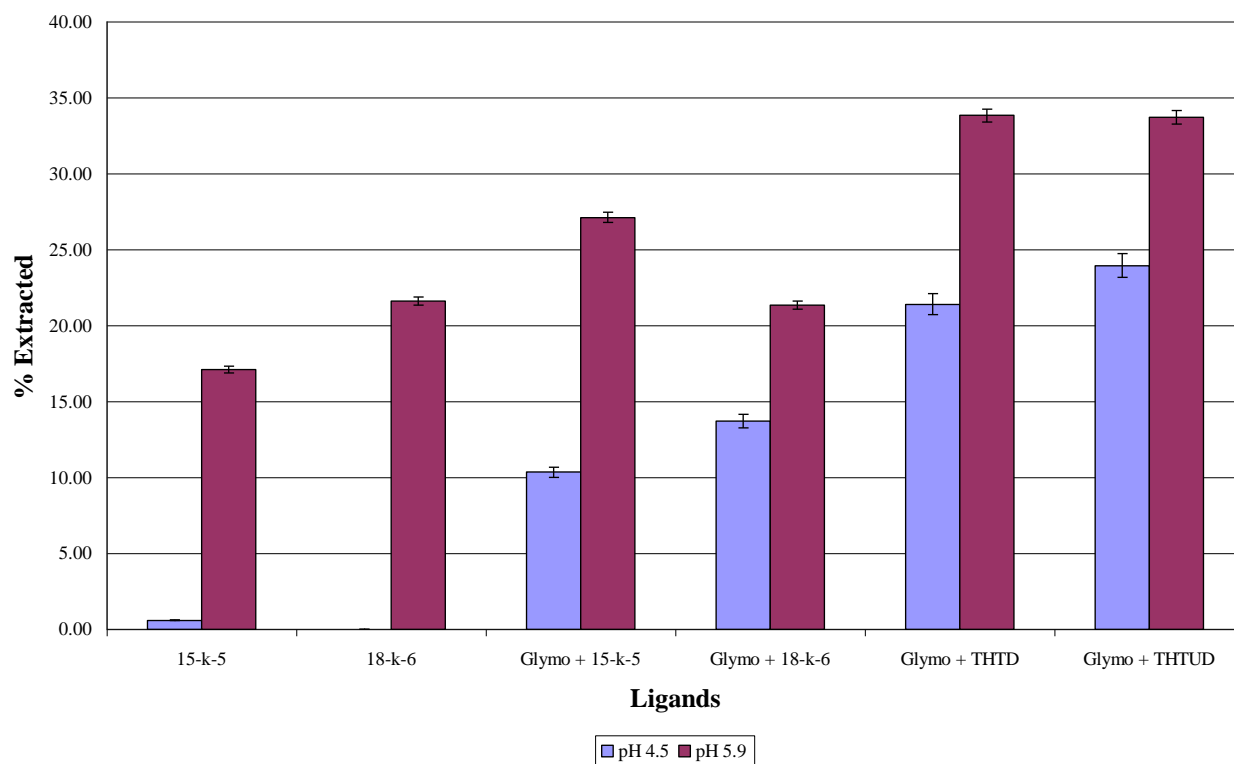
Extraction of Cr(VI) with THTD Immobilized on Different Supports



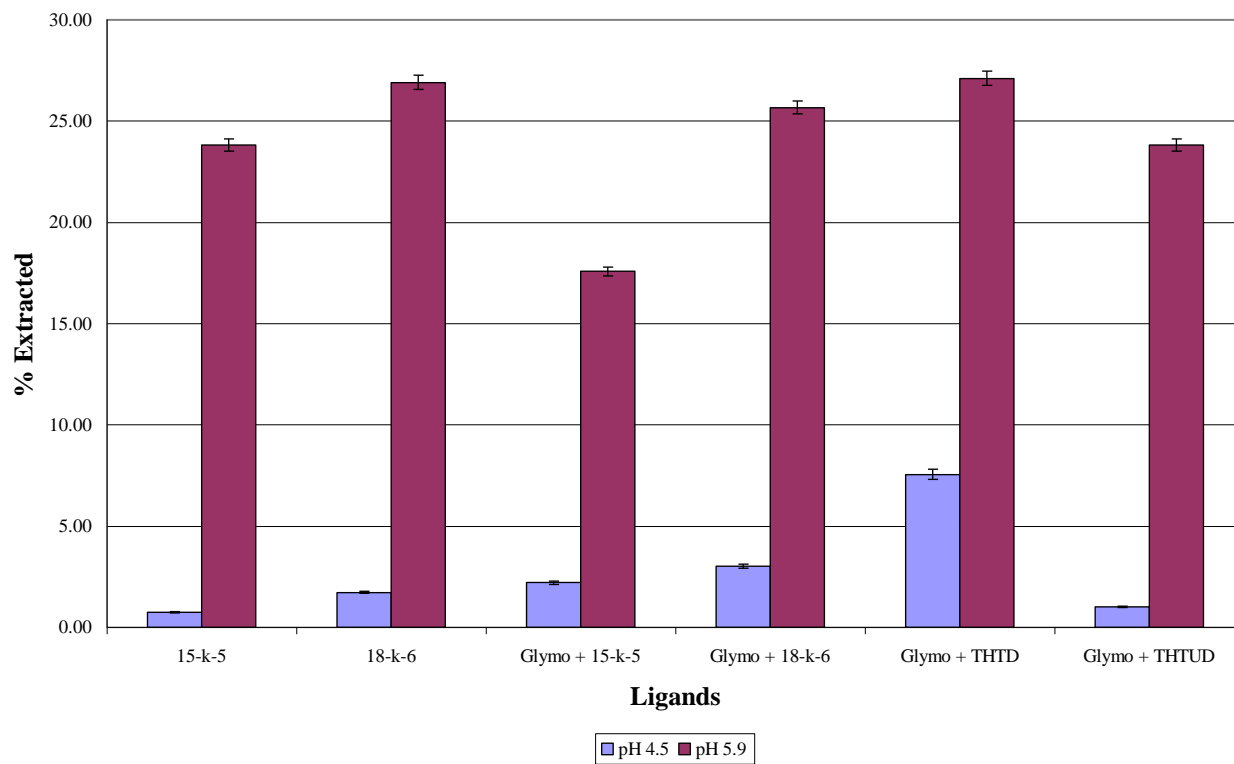
Extraction of Cr(VI) with THTUD Immobilized on Different Supports



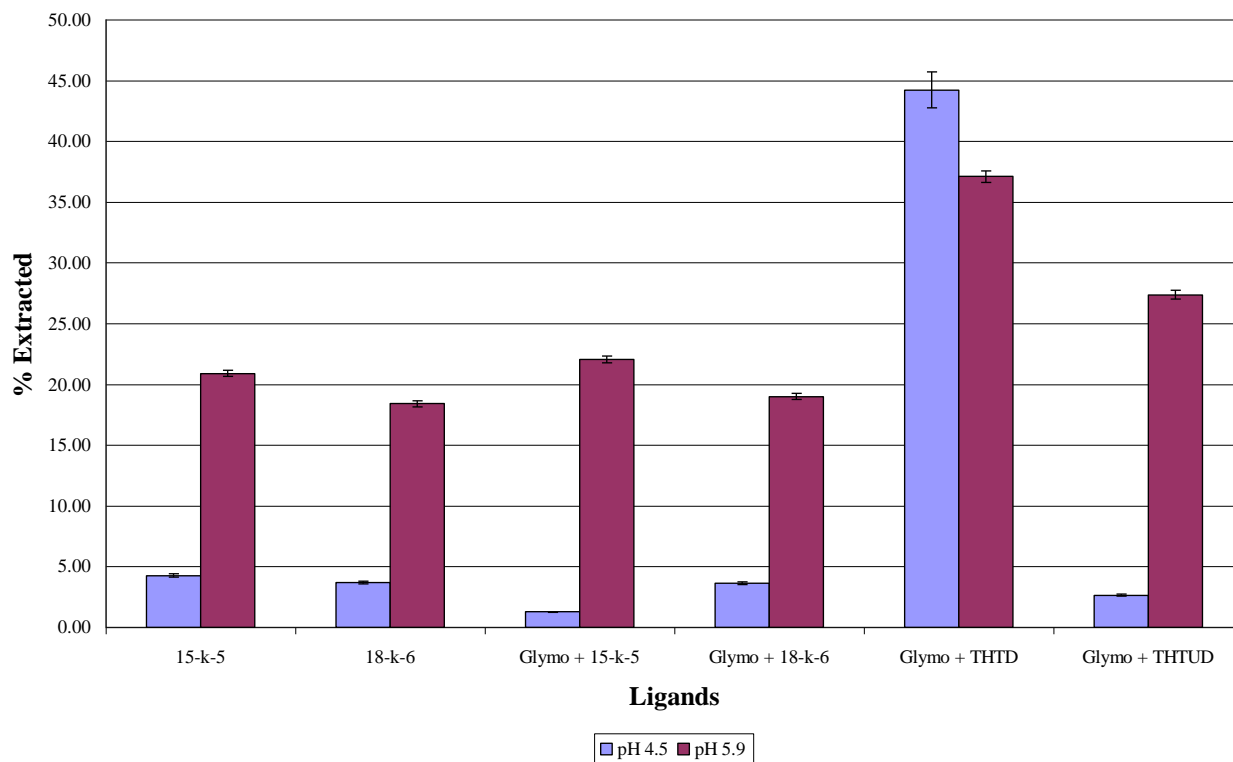
Extraction of Cr(VI) with Different Ligands Immobilized on Si gel (60 Å)



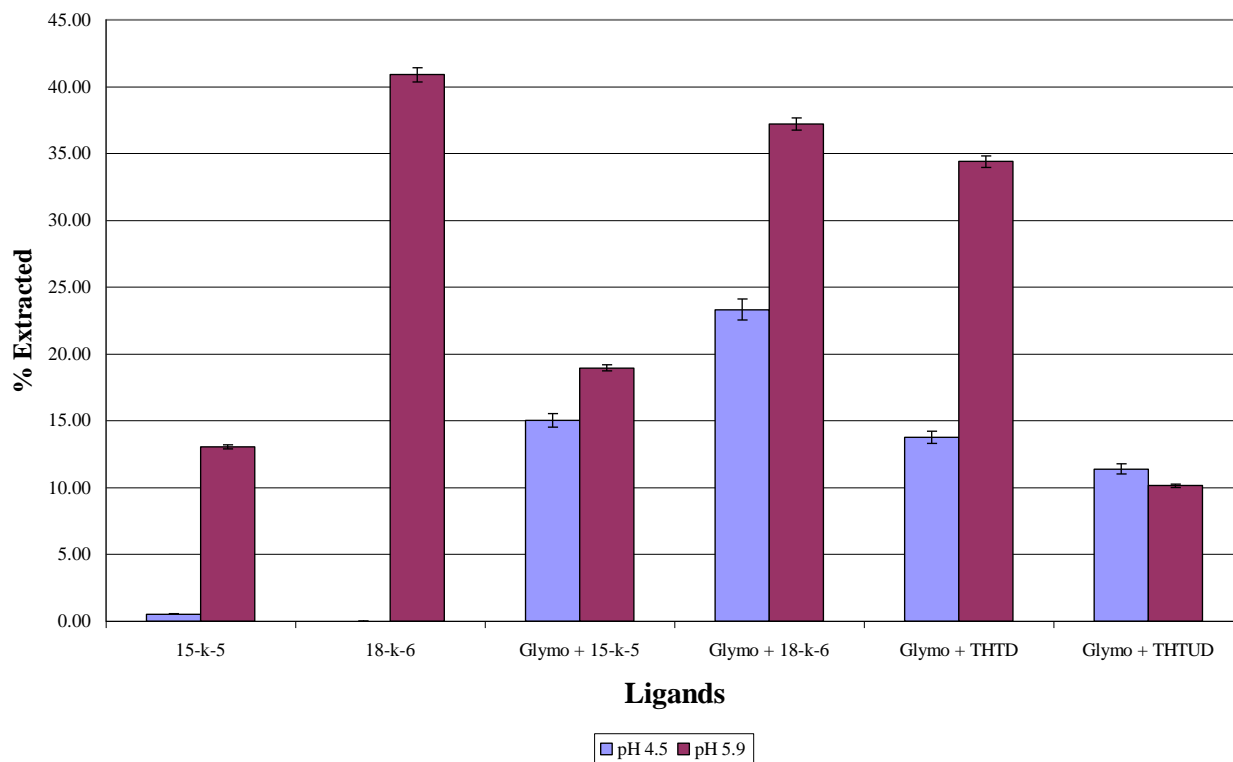
Extraction of Cr(VI) with Different Ligands Immobilized on MCM-41



Extraction of Cr(VI) with Different Ligands Immobilized of SBA-15



Extraction of Cr(VI) with Different Ligands Immobilized on HMS



As(V) extraction at pH 4.5

Accuracy	Certified std value	11.6000
	Analysed	11.7146
	% Deviation	0.9879

Standard Solution (ppm)	Support	Ligand	Extracted ppm	% Extracted
67.2753	Si-gel (60Å)	15-c-5	67.7320	0.0000
		18-c-6	68.4788	0.0000
		Glymo + 15-c-5	70.2818	0.0000
		Glymo + 18-c-6	67.1335	0.1418
		Glymo + THTD	66.5050	0.7703
		Glymo + THTUD	67.8612	0.0000
				Average %
				0.2260
	MCM-41	15-c-5	68.6062	0.0000
		18-c-6	68.1304	0.0000
		Glymo + 15-c-5	66.9108	0.3645
		Glymo + 18-c-6	66.8502	0.4251
		Glymo + THTD	66.9633	0.3120
		Glymo + THTUD	69.8054	0.0000
				Average %
				0.2729
	SBA-15	15-c-5	67.4648	0.0000
		18-c-6	71.4294	0.0000
		Glymo + 15-c-5	69.5973	0.0000
		Glymo + 18-c-6	69.3893	0.0000
		Glymo + THTD	67.9361	0.0000
		Glymo + THTUD	66.4615	0.8138
				Average %
				0.2016
	HMS	15-c-5	70.9248	0.0000
		18-c-6	70.1604	0.0000
		Glymo + 15-c-5	67.3812	0.0000
		Glymo + 18-c-6	68.2340	0.0000
		Glymo + THTD	67.7392	0.0000
		Glymo + THTUD	68.6534	0.0000
				Average %
				0.0000

As(V) extraction at pH 4.5

Accuracy	Certified std value	11.6000
	Analysed	11.7146
	% Deviation	0.9879

Support	Ligand	% Extracted
Si-gel (60Å)	15-c-5	0.0000
MCM-41	15-c-5	0.0000
SBA-15	15-c-5	0.0000
HMS	15-c-5	0.0000
	Average %	0.0000
Si-gel (60Å)	18-c-6	0.0000
MCM-41	18-c-6	0.0000
SBA-15	18-c-6	0.0000
HMS	18-c-6	0.0000
	Average %	0.0000
Si-gel (60Å)	Glymo + 15-c-5	0.0000
MCM-41	Glymo + 15-c-5	0.5418
SBA-15	Glymo + 15-c-5	0.0000
HMS	Glymo + 15-c-5	0.0000
	Average %	0.1355
Si-gel (60Å)	Glymo + 18-c-6	0.2108
MCM-41	Glymo + 18-c-6	0.6319
SBA-15	Glymo + 18-c-6	0.0000
HMS	Glymo + 18-c-6	0.0000
	Average %	0.2107
Si-gel (60Å)	Glymo + THTD	1.1450
MCM-41	Glymo + THTD	0.4638
SBA-15	Glymo + THTD	0.0000
HMS	Glymo + THTD	0.0000
	Average %	0.4022
Si-gel (60Å)	Glymo + THTUD	0.0000
MCM-41	Glymo + THTUD	0.0000
SBA-15	Glymo + THTUD	1.2097
HMS	Glymo + THTUD	0.0000
	Average %	0.3024

As(V) extraction at pH 5.9

Accuracy	Certified std value	24.68
	Analysed	25.23
	% Deviation	2.23

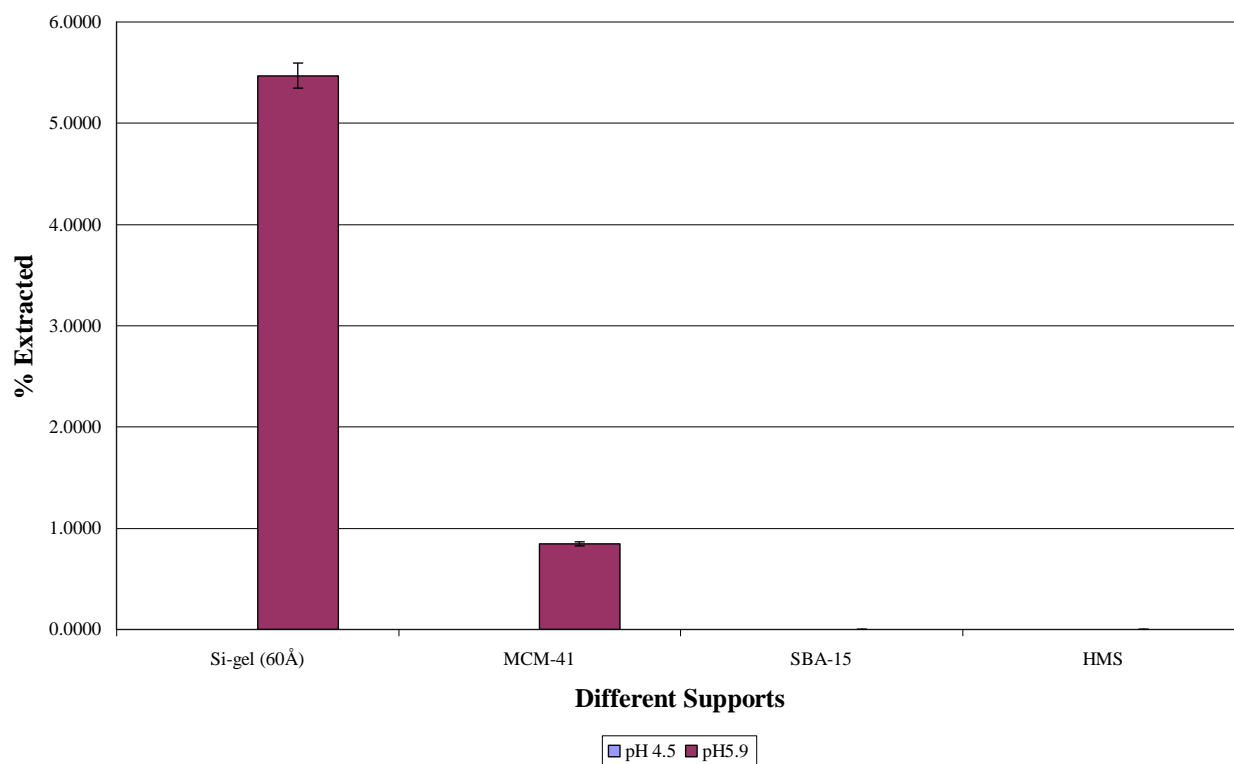
Standard Solution (ppb)				Extracted ppb	% Extracted
660.77	Si-gel (60Å)	15-k-5	624.65	36.13	5.47
		18-k-6	828.52	0.00	0.00
		Glymo + 15-k-5	853.63	0.00	0.00
		Glymo + 18-k-6	670.44	0.00	0.00
		Glymo + THTD	687.64	0.00	0.00
		Glymo + THTUD	665.98	0.00	0.00
				Average %	0.91
	MCM-41	15-k-5	655.21	5.57	0.84
		18-k-6	705.22	0.00	0.00
		Glymo + 15-k-5	692.30	0.00	0.00
		Glymo + 18-k-6	670.46	0.00	0.00
		Glymo + THTD	718.29	0.00	0.00
		Glymo + THTUD	691.32	0.00	0.00
				Average %	0.14
	SBA-15	15-k-5	715.57	0.00	0.00
		18-k-6	714.25	0.00	0.00
		Glymo + 15-k-5	878.02	0.00	0.00
		Glymo + 18-k-6	668.75	0.00	0.00
		Glymo + THTD	937.97	0.00	0.00
		Glymo + THTUD	636.41	24.36	3.69
				Average %	0.61
	HMS	15-k-5	737.25	0.00	0.00
		18-k-6	718.36	0.00	0.00
		Glymo + 15-k-5	693.78	0.00	0.00
		Glymo + 18-k-6	512.95	73.92	11.19
		Glymo + THTD	695.62	0.00	0.00
		Glymo + THTUD	665.19	0.00	0.00
				Average %	1.86

As(V) extraction at pH 4.5

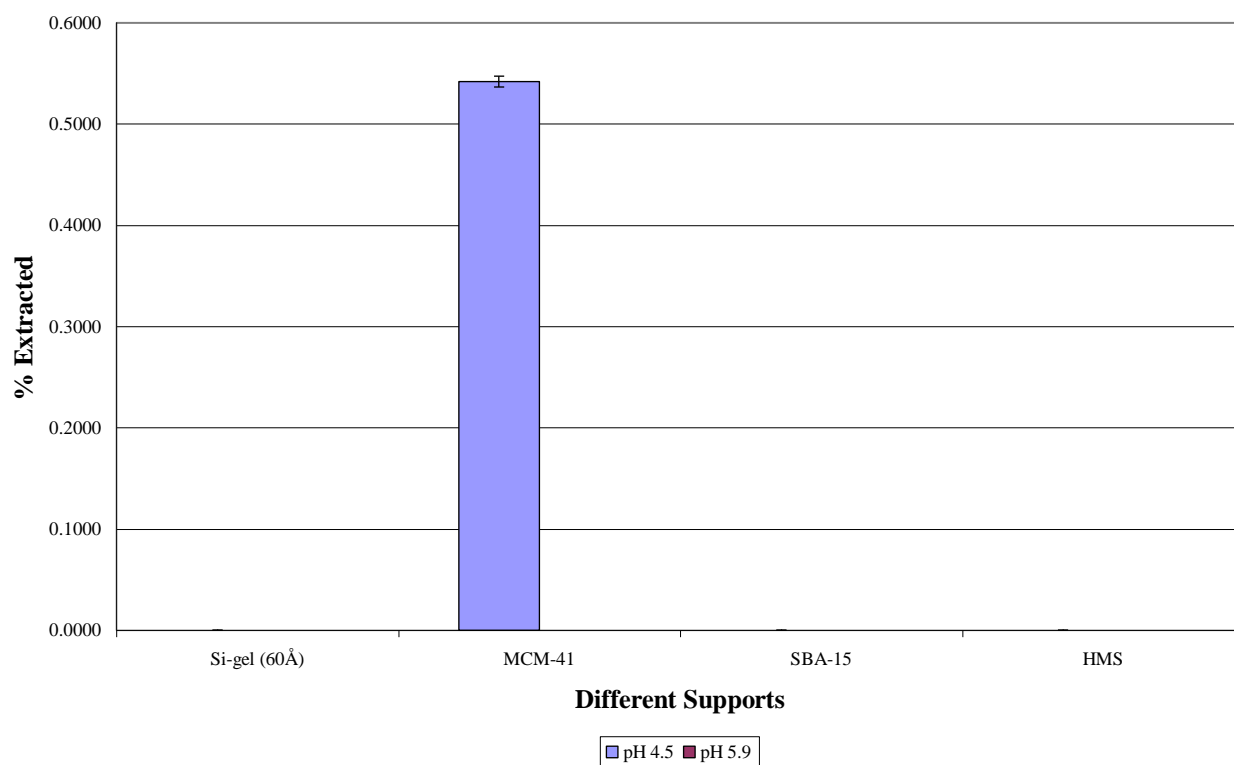
Accuracy	Certified std value	11.6000
	Analysed	11.7146
	% Deviation	0.9879

Support	Ligand	% Extracted
Si-gel (60Å)	15-c-5	5.47
MCM-41	15-c-5	0.84
SBA-15	15-c-5	0.00
HMS	15-c-5	0.00
	Average %	1.58
Si-gel (60Å)	18-c-6	0.00
MCM-41	18-c-6	0.00
SBA-15	18-c-6	0.00
HMS	18-c-6	0.00
	Average %	0.00
Si-gel (60Å)	Glymo + 15-c-5	0.00
MCM-41	Glymo + 15-c-5	0.00
SBA-15	Glymo + 15-c-5	0.00
HMS	Glymo + 15-c-5	0.00
	Average %	0.00
Si-gel (60Å)	Glymo + 18-c-6	0.00
MCM-41	Glymo + 18-c-6	0.00
SBA-15	Glymo + 18-c-6	0.00
HMS	Glymo + 18-c-6	11.19
	Average %	2.80
Si-gel (60Å)	Glymo + THTD	0.00
MCM-41	Glymo + THTD	0.00
SBA-15	Glymo + THTD	0.00
HMS	Glymo + THTD	0.00
	Average %	0.00
Si-gel (60Å)	Glymo + THTUD	0.00
MCM-41	Glymo + THTUD	0.00
SBA-15	Glymo + THTUD	3.69
HMS	Glymo + THTUD	0.00
	Average %	0.92

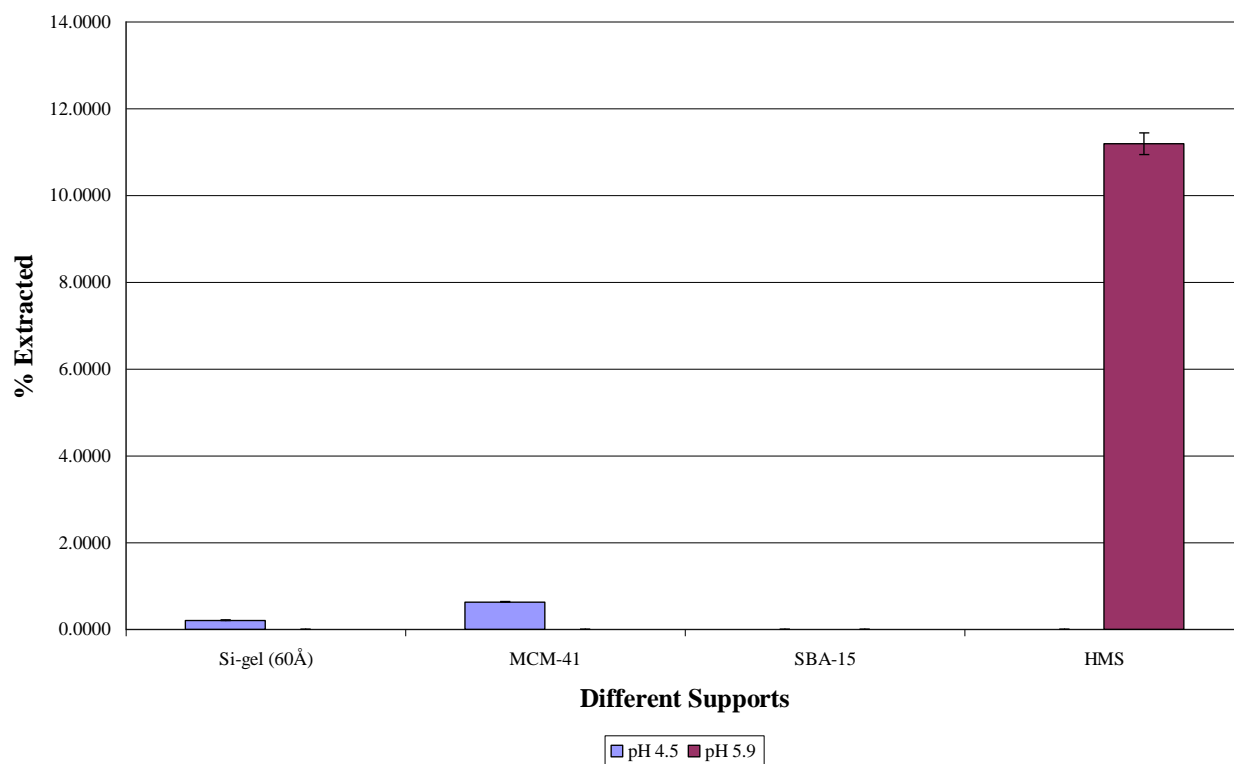
Extraction of As(V) with 15-c-5 Immobilized Directly on the Different Supports



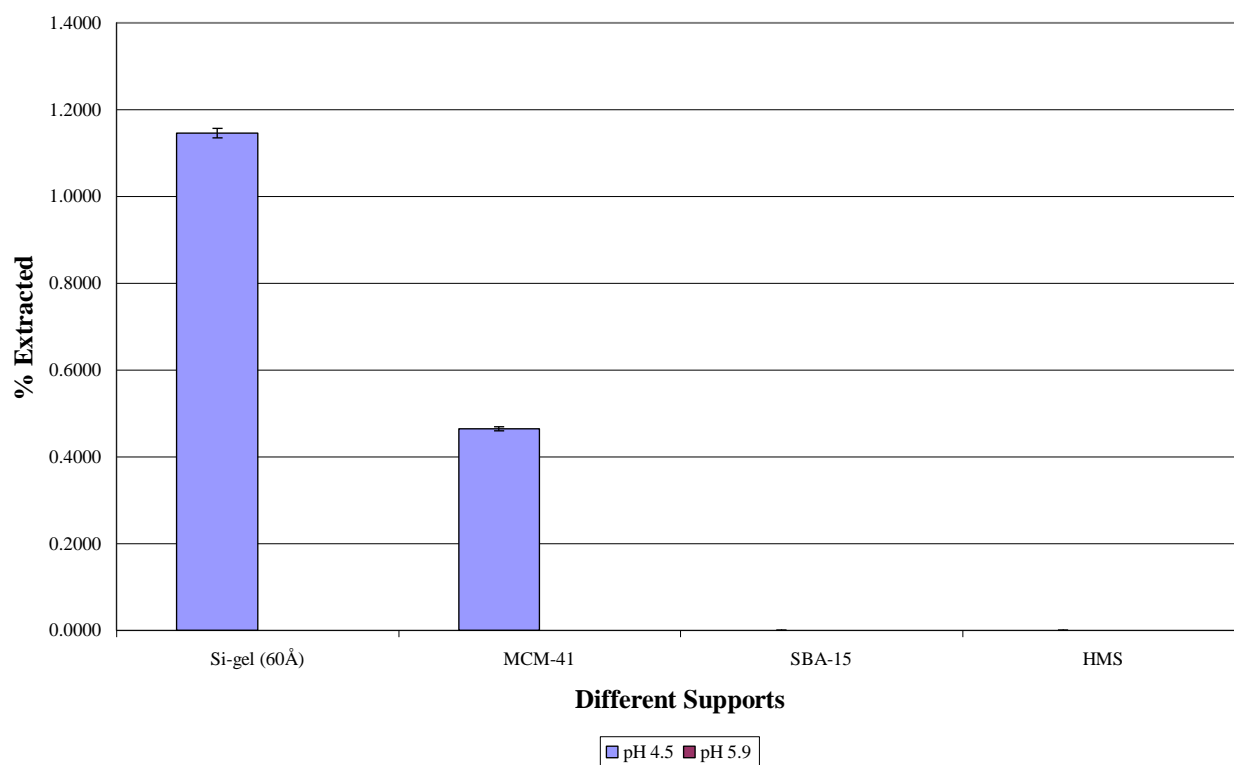
Extraction of As(V) with 15-c-5 Immobilized with Glymo on Different Supports



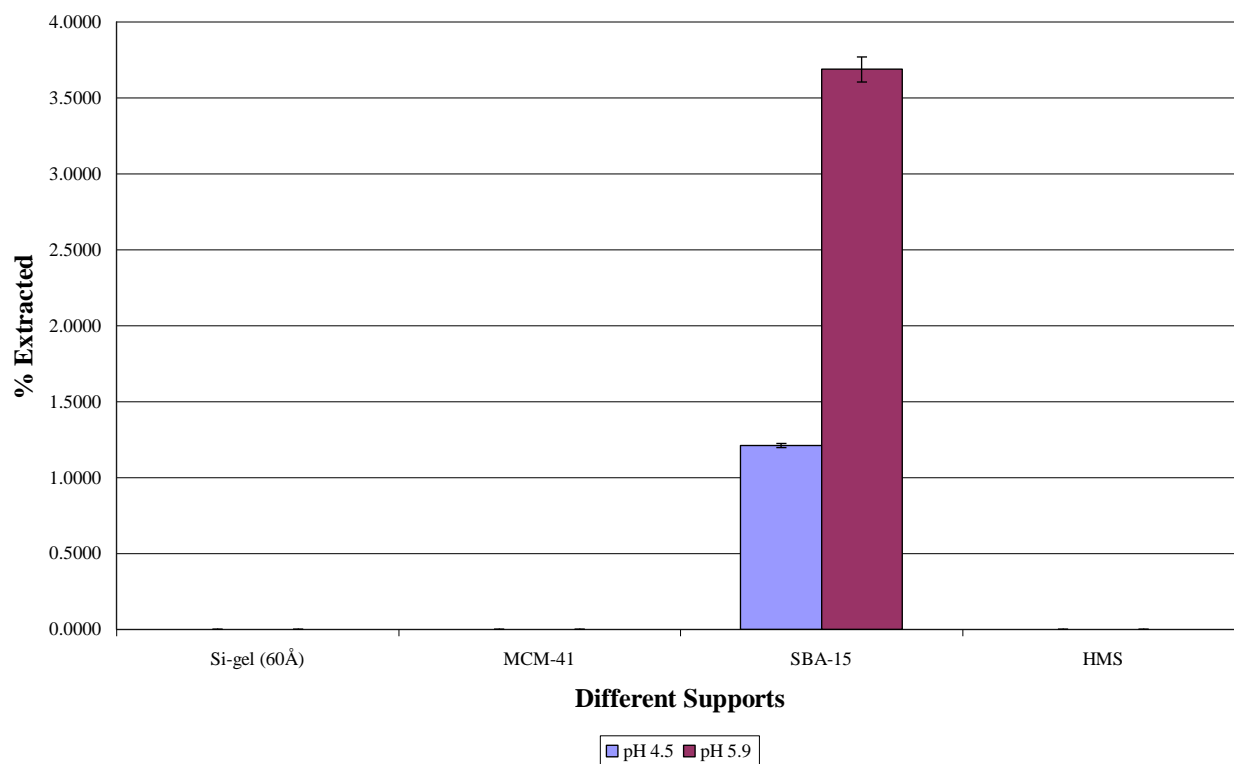
Extraction of As(V) with 18-c-6 Immobilized with Glymo on Different Supports



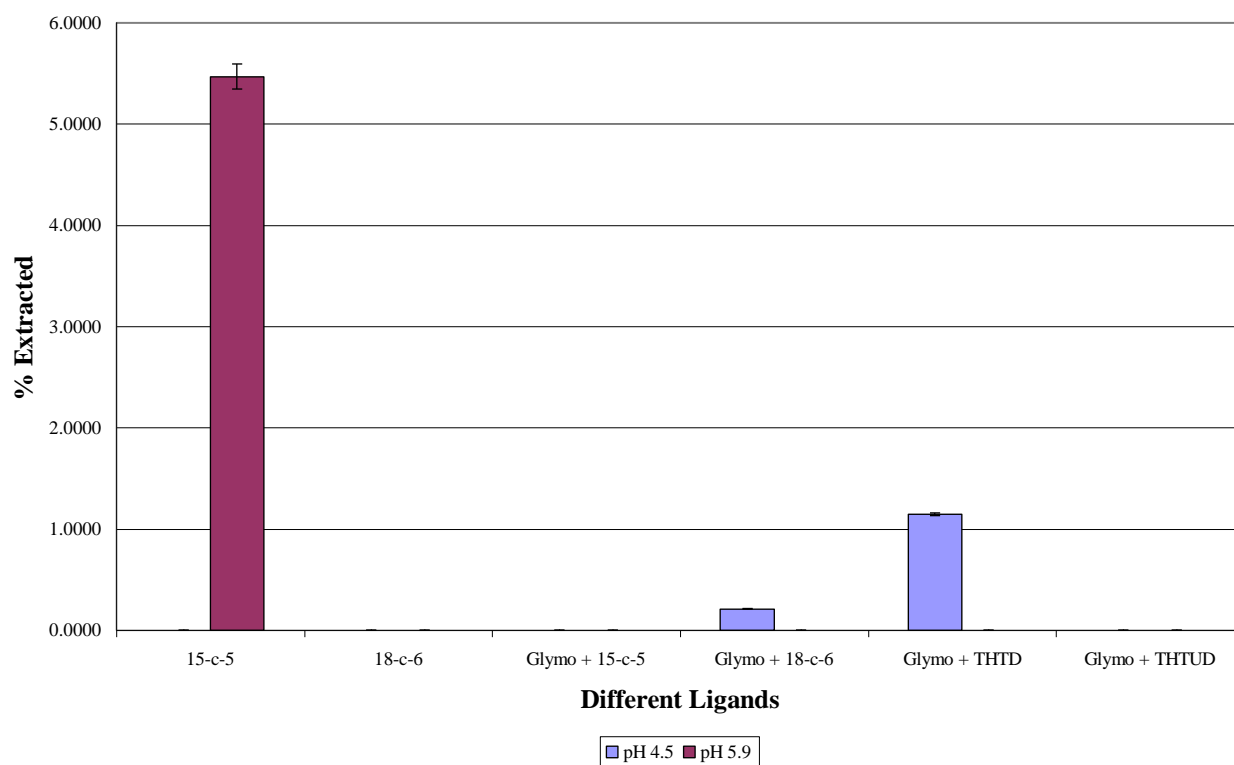
Extraction of As(V) with THTD Immobilized on Different Supports



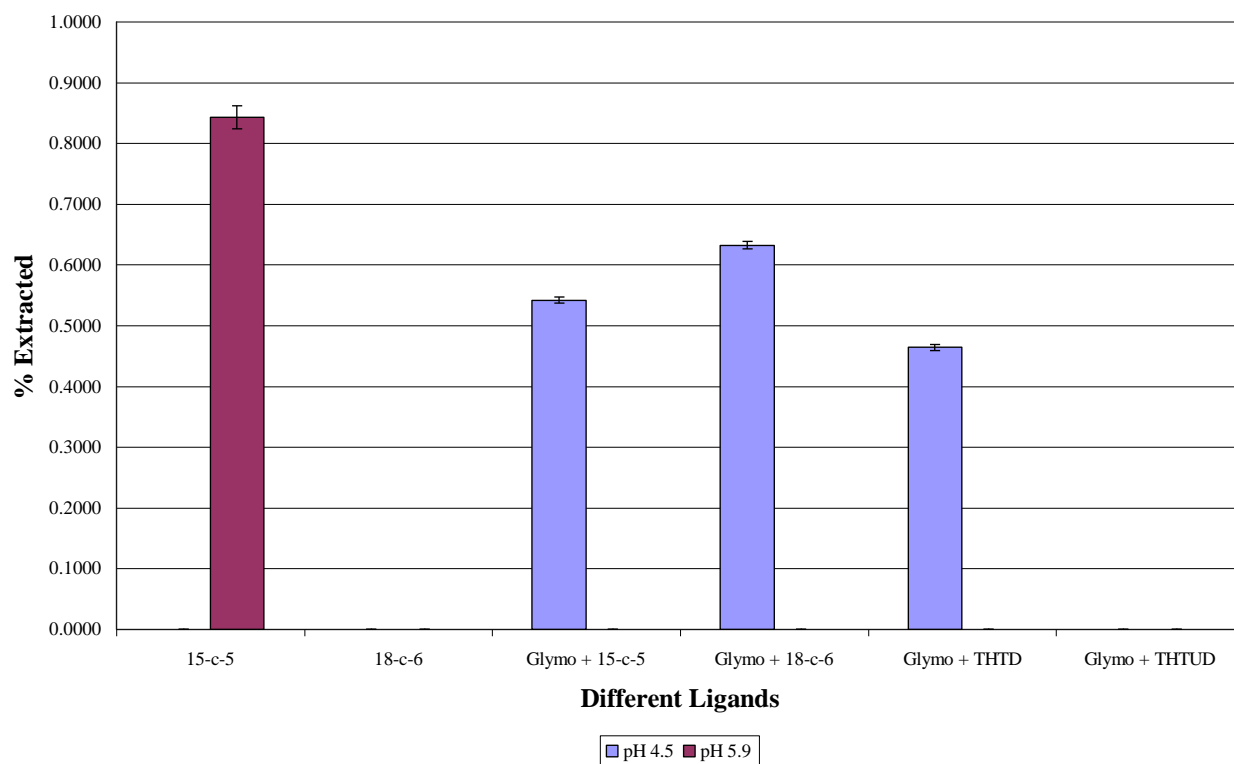
Extraction of As(V) with THTUD Immobilized on Different Supports



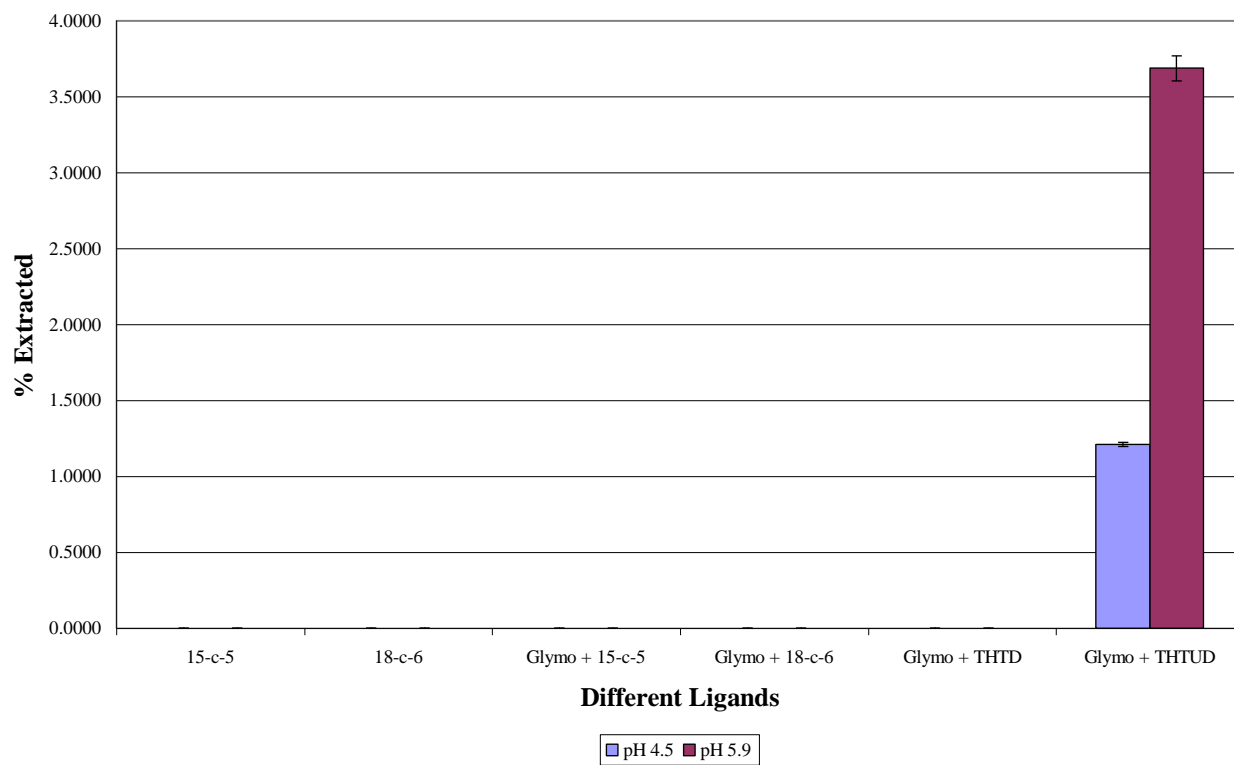
Extraction of As(V) with Different Ligands Immobilized on Si gel (60 Å)



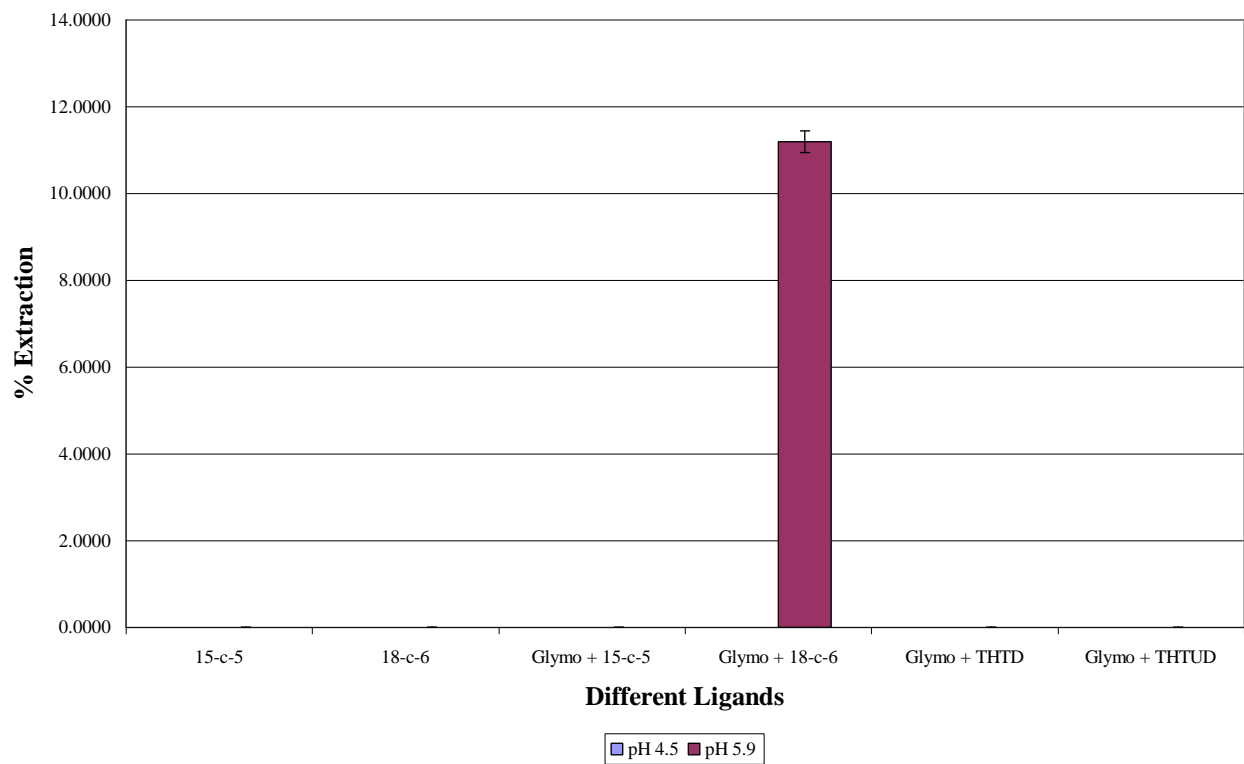
Extraction of As(V) with Different Ligands Immobilized on MCM-41



Extraction of As(V) with Different Ligands Immobilized on SBA-15



Extraction of As(V) with Different Ligands Immobilized of HMS



Sr(II) extraction at pH 4.5

Accuracy	Certified std value	0.97
	Analysed	0.98
	% Deviation	1.46

Standard Solution (ppm)				Extracted ppm	% Extracted
80.0035	Si-gel (60Å)	15-k-5	82.83	0.00	0.00
		18-k-6	81.27	0.00	0.00
		Glymo + 15-k-5	86.83	0.00	0.00
		Glymo + 18-k-6	81.02	0.00	0.00
		Glymo + THTD	80.48	0.00	0.00
		Glymo + THTUD	80.15	0.00	0.00
				Average %	0.00
	MCM-41	15-k-5	84.02	0.00	0.00
		18-k-6	82.82	0.00	0.00
		Glymo + 15-k-5	80.43	0.00	0.00
		Glymo + 18-k-6	80.86	0.00	0.00
		Glymo + THTD	83.72	0.00	0.00
		Glymo + THTUD	85.60	0.00	0.00
				Average %	0.00
	SBA-15	15-k-5	85.76	0.00	0.00
		18-k-6	85.07	0.00	0.00
		Glymo + 15-k-5	84.68	0.00	0.00
		Glymo + 18-k-6	82.93	0.00	0.00
		Glymo + THTD	85.47	0.00	0.00
		Glymo + THTUD	84.27	0.00	0.00
				Average %	0.00
	HMS	15-k-5	82.16	0.00	0.00
		18-k-6	82.67	0.00	0.00
		Glymo + 15-k-5	81.47	0.00	0.00
		Glymo + 18-k-6	82.00	0.00	0.00
		Glymo + THTD	82.06	0.00	0.00
		Glymo + THTUD	82.13	0.00	0.00
				Average %	0.00

Sr(II) extraction at pH 4.5

Accuracy	Certified std value	0.97
	Analysed	0.98
	% Deviation	1.46
Support	Ligand	% Extracted
Si-gel (60Å)	15-k-5	0.00
MCM-41	15-k-5	0.00
SBA-15	15-k-5	0.00
HMS	15-k-5	0.00
	Average %	0.00
Si-gel (60Å)	18-k-6	0.00
MCM-41	18-k-6	0.00
SBA-15	18-k-6	0.00
HMS	18-k-6	0.00
	Average %	0.00
Si-gel (60Å)	Glymo + 15-k-5	0.00
MCM-41	Glymo + 15-k-5	0.00
SBA-15	Glymo + 15-k-5	0.00
HMS	Glymo + 15-k-5	0.00
	Average %	0.00
Si-gel (60Å)	Glymo + 18-k-6	0.00
MCM-41	Glymo + 18-k-6	0.00
SBA-15	Glymo + 18-k-6	0.00
HMS	Glymo + 18-k-6	0.00
	Average %	0.00
Si-gel (60Å)	Glymo + THTD	0.00
MCM-41	Glymo + THTD	0.00
SBA-15	Glymo + THTD	0.00
HMS	Glymo + THTD	0.00
	Average %	0.00
Si-gel (60Å)	Glymo + THTUD	0.00
MCM-41	Glymo + THTUD	0.00
SBA-15	Glymo + THTUD	0.00
HMS	Glymo + THTUD	0.00
	Average %	0.00

Sr(II) extraction at pH 5.9

Accuracy	Certified std value	24.68
	Analysed	24.81
	% Deviation	0.53

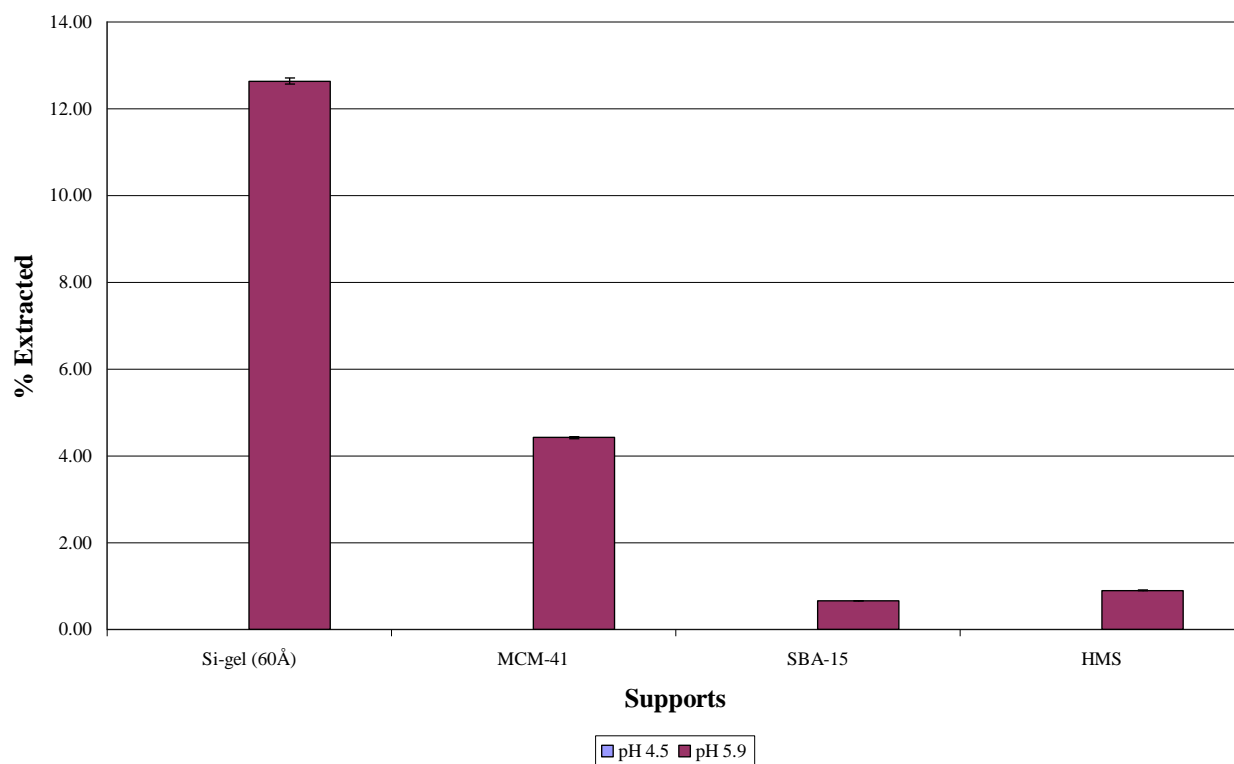
Standard Solution (ppm)	Support	Ligand	Extracted ppb		% Extracted
916.65	Si-gel (60Å)	15-k-5	800.86	115.79	12.63
		18-k-6	828.95	87.70	9.57
		Glymo + 15-k-5	683.90	232.75	25.39
		Glymo + 18-k-6	836.06	80.59	8.79
		Glymo + THTD	885.50	31.15	3.40
		Glymo + THTUD	916.16	0.49	0.05
		Average %			9.97
	MCM-41	15-k-5	876.13	40.52	4.42
		18-k-6	877.09	39.56	4.32
		Glymo + 15-k-5	917.38	0.00	0.00
		Glymo + 18-k-6	691.81	224.84	24.53
		Glymo + THTD	806.21	110.44	12.05
		Glymo + THTUD	834.87	81.78	8.92
		Average %			9.04
	SBA-15	15-k-5	910.65	6.00	0.65
		18-k-6	926.86	0.00	0.00
		Glymo + 15-k-5	891.92	24.73	2.70
		Glymo + 18-k-6	892.96	23.69	2.58
		Glymo + THTD	926.88	0.00	0.00
		Glymo + THTUD	939.61	0.00	0.00
		Average %			0.99
	HMS	15-k-5	908.42	8.23	0.90
		18-k-6	639.75	276.90	30.21
		Glymo + 15-k-5	834.03	82.62	9.01
		Glymo + 18-k-6	905.04	11.61	1.27
		Glymo + THTD	904.07	12.58	1.37
		Glymo + THTUD	922.05	0.00	0.00
		Average %			7.13

Sr(II) extraction at pH 5.9

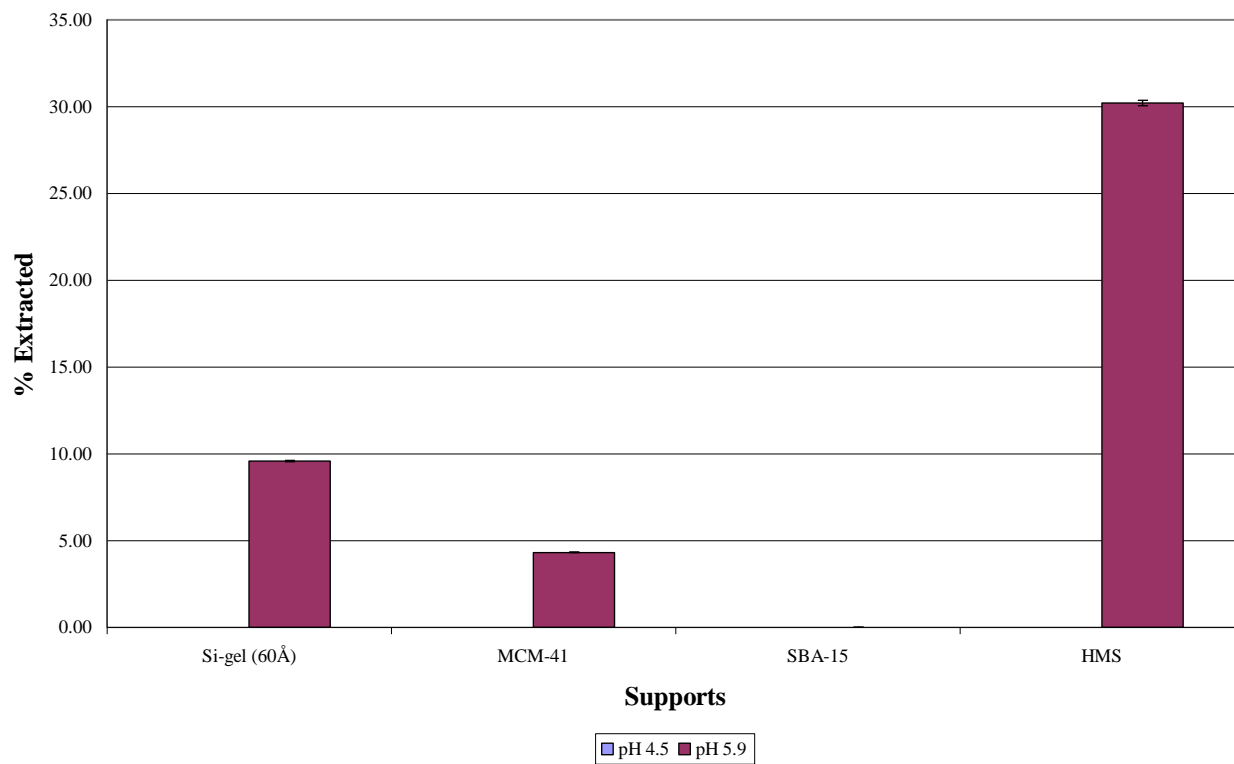
Accuracy	Certified std value	24.68
	Analysed	24.81
	% Deviation	0.53

Support	Ligand	% Extracted
Si-gel (60Å)	15-k-5	12.63
MCM-41	15-k-5	4.42
SBA-15	15-k-5	0.65
HMS	15-k-5	0.90
	Average %	4.65
Si-gel (60Å)	18-k-6	9.57
MCM-41	18-k-6	4.32
SBA-15	18-k-6	0.00
HMS	18-k-6	30.21
	Average %	11.02
Si-gel (60Å)	Glymo + 15-k-5	25.39
MCM-41	Glymo + 15-k-5	0.00
SBA-15	Glymo + 15-k-5	2.70
HMS	Glymo + 15-k-5	9.01
	Average %	9.28
Si-gel (60Å)	Glymo + 18-k-6	8.79
MCM-41	Glymo + 18-k-6	24.53
SBA-15	Glymo + 18-k-6	2.58
HMS	Glymo + 18-k-6	1.27
	Average %	9.29
Si-gel (60Å)	Glymo + THTD	3.40
MCM-41	Glymo + THTD	12.05
SBA-15	Glymo + THTD	0.00
HMS	Glymo + THTD	1.37
	Average %	4.20
Si-gel (60Å)	Glymo + THTUD	0.05
MCM-41	Glymo + THTUD	8.92
SBA-15	Glymo + THTUD	0.00
HMS	Glymo + THTUD	0.00
	Average %	2.24

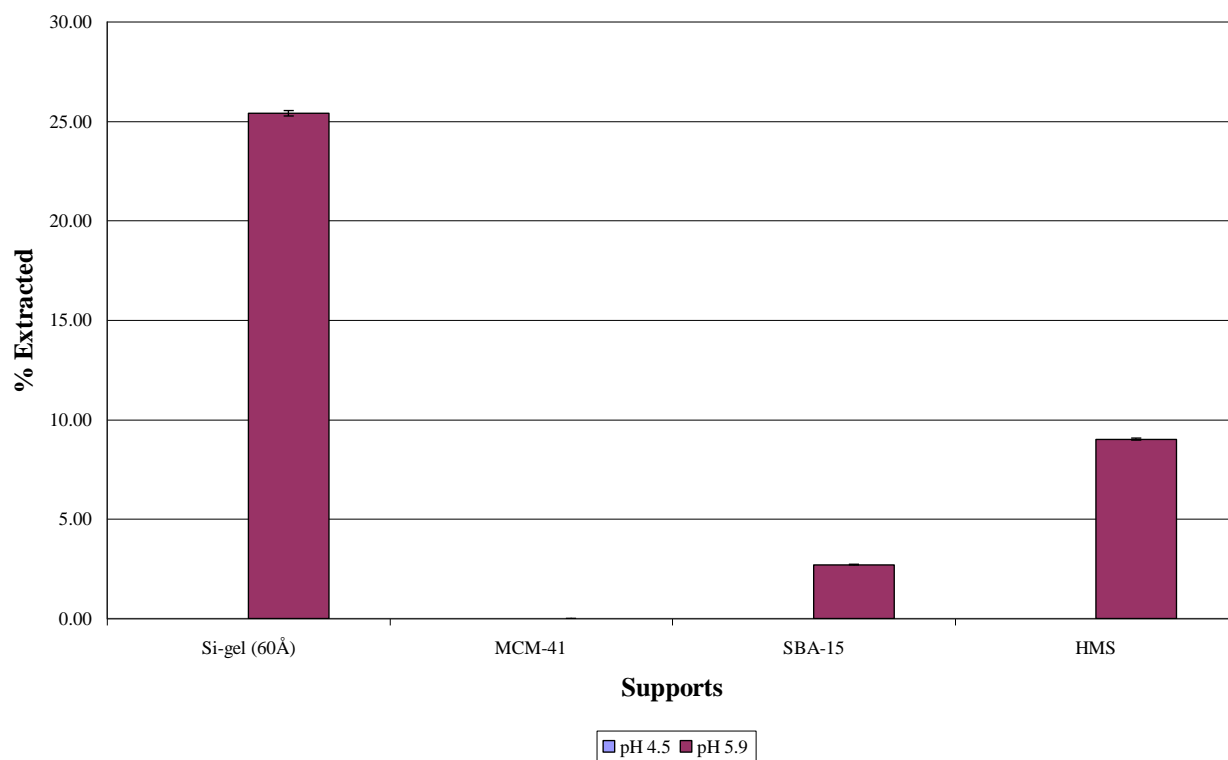
Extraction of Sr(II) with 15-c-5 Immobilized Directly on Different Supports



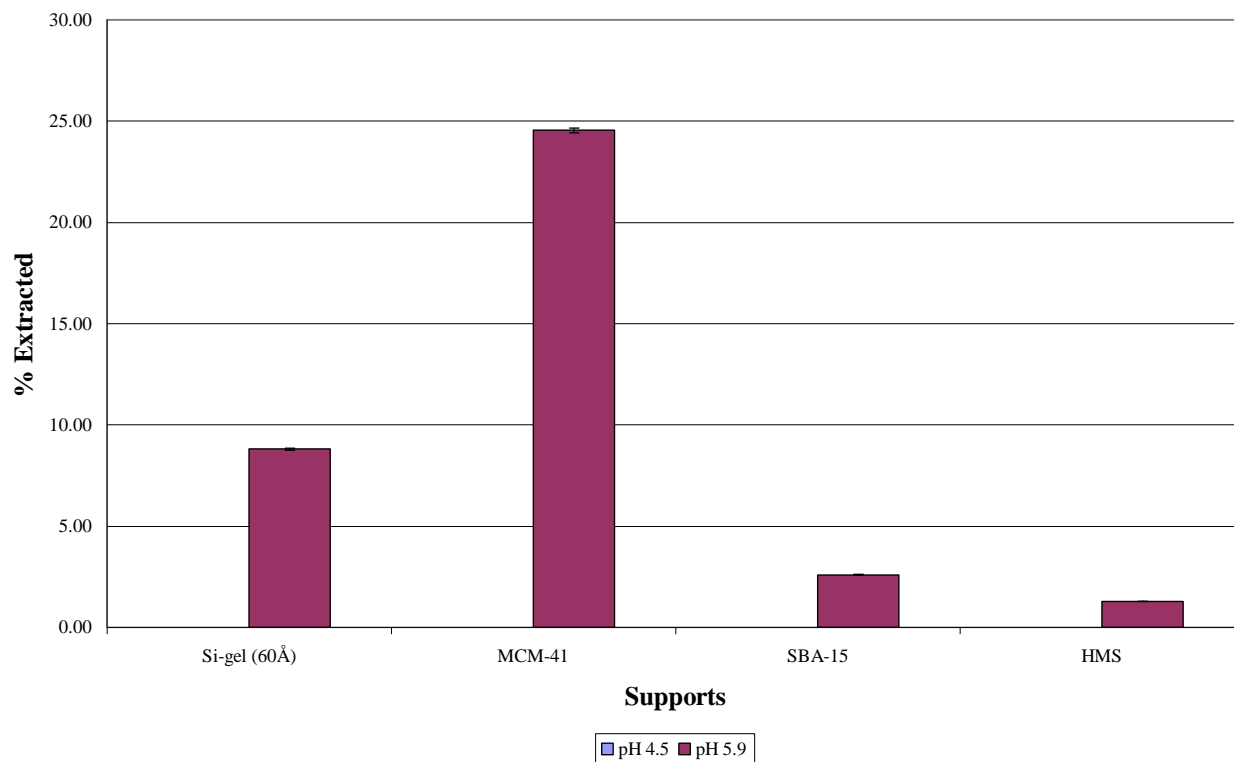
Extraction of Sr(II) with 18-c-6 Immobilized Directly on MCM-41



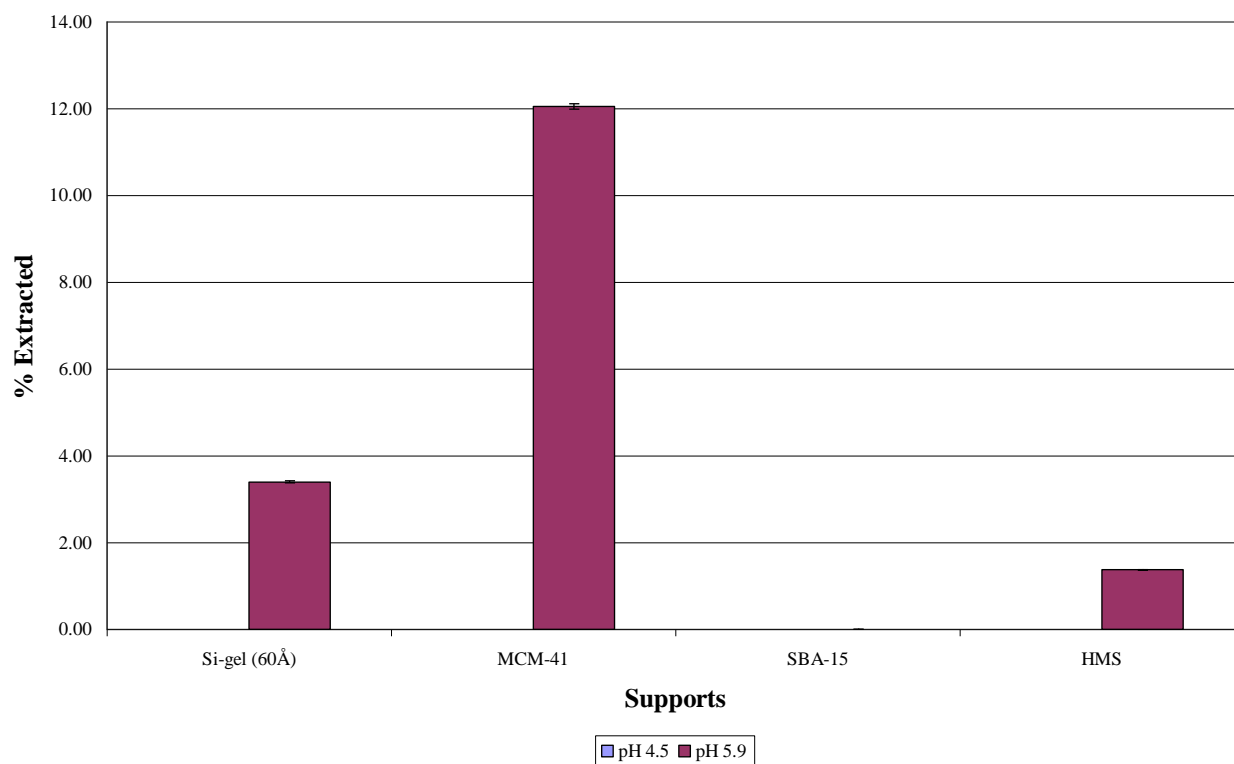
Extraction of Sr(II) with 15-c-5 Immobilized with Glymo on Different Supports



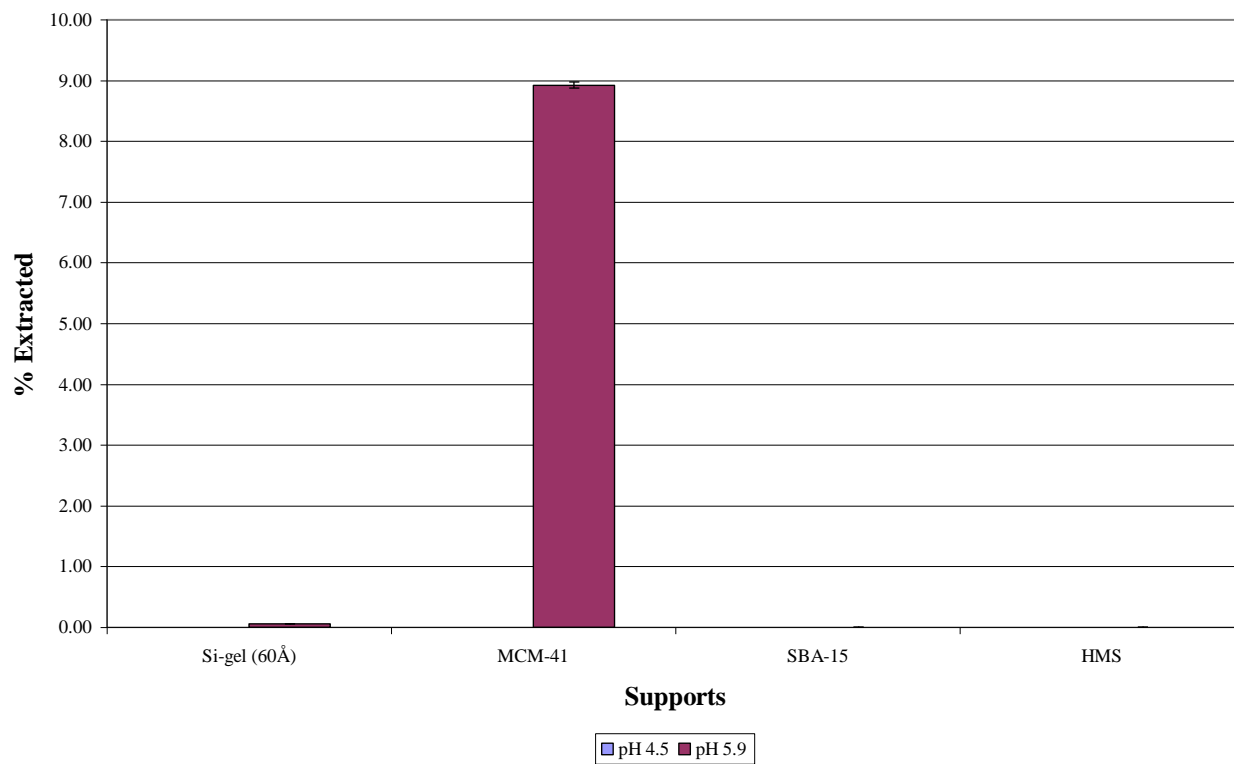
Extraction of Sr(II) with 18-c-6 Immobilized with Glymo on Different supports



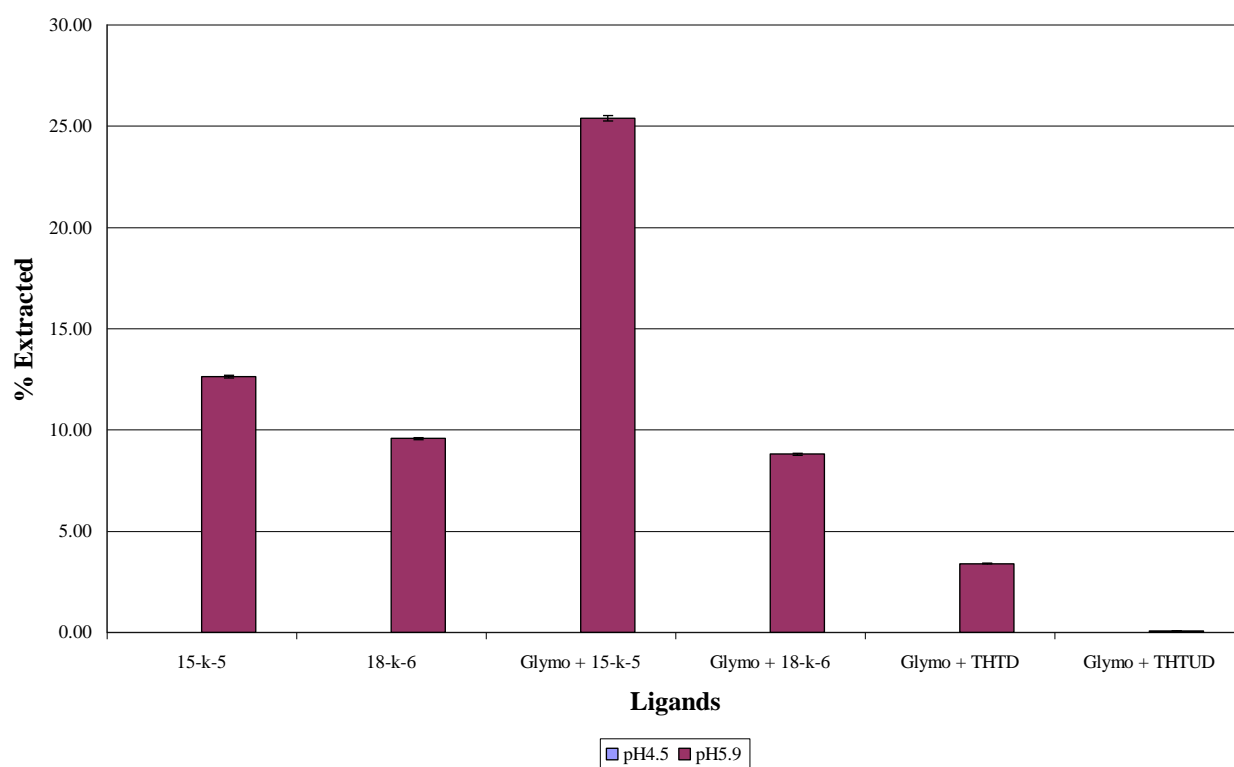
Extraction of Sr(II) with THTD Immobilized on Different Supports



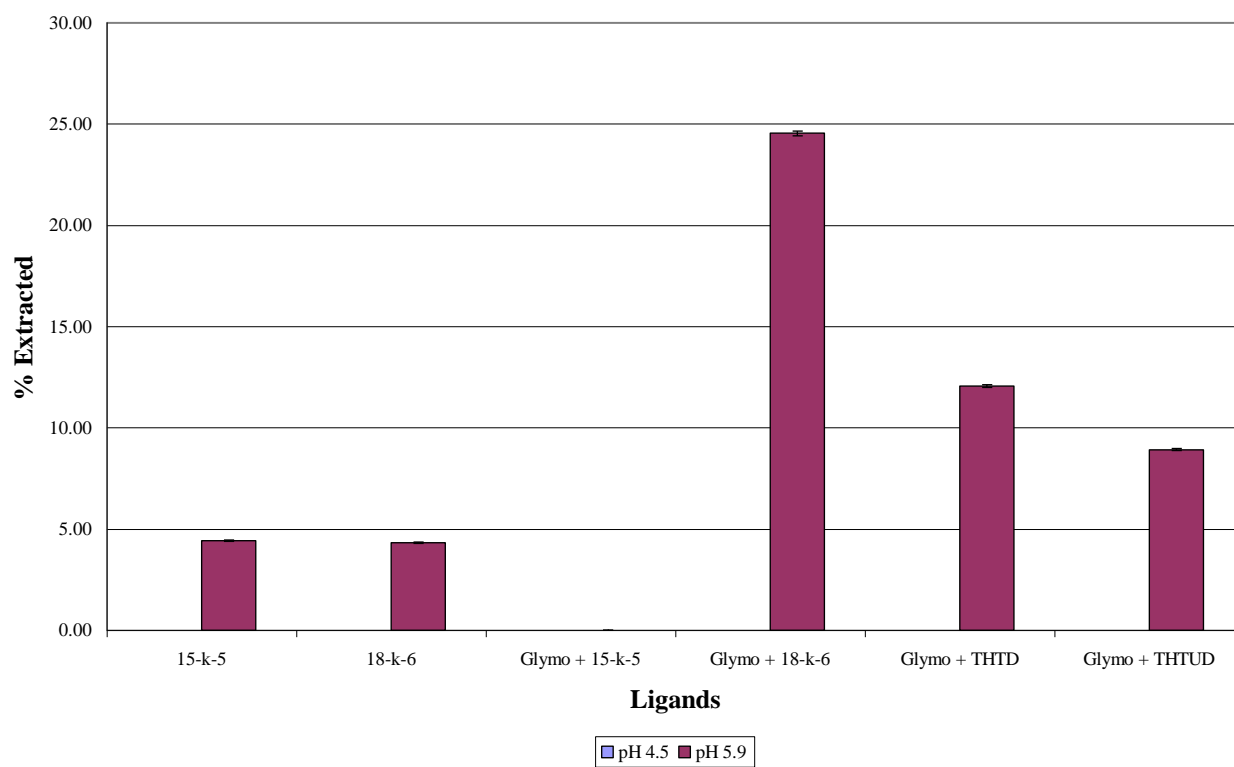
Extraction of Sr(II) with THTUD Immobilized on Different Supports



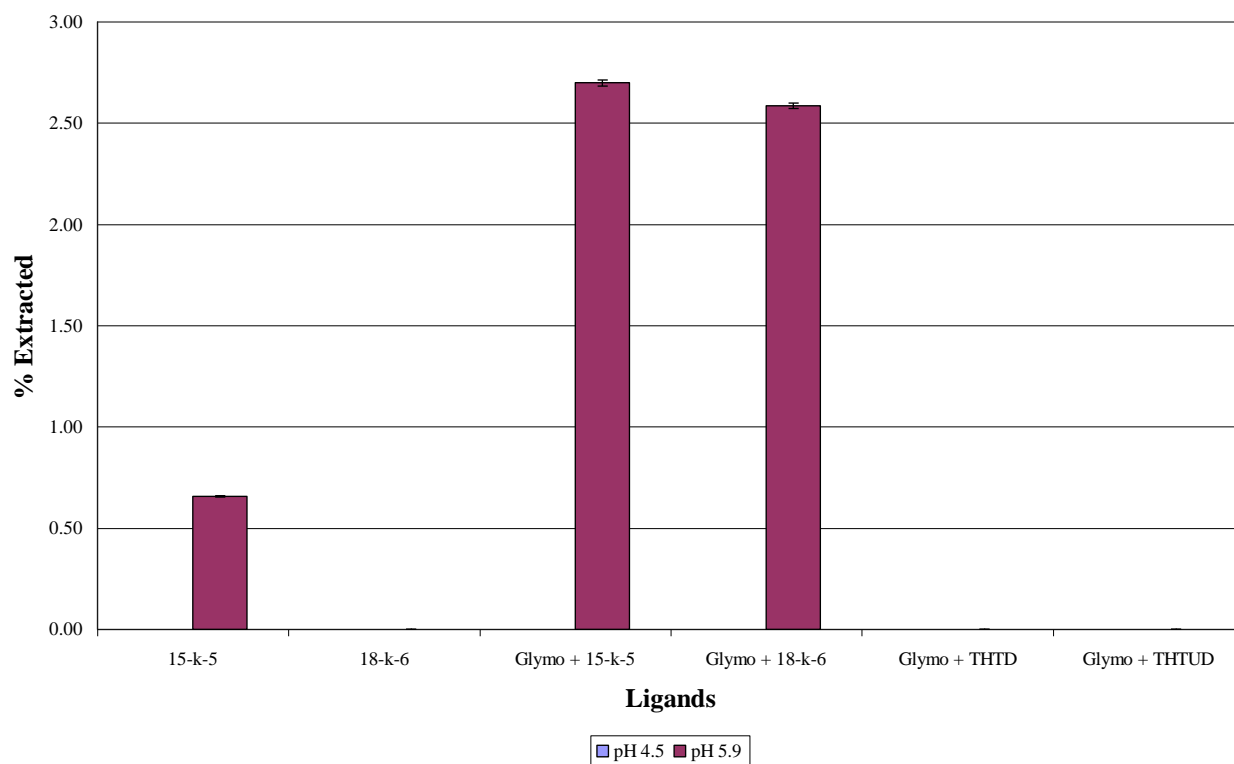
Extraction of Sr(II) with Different Ligands Immobilized on Si gel (60 Å)



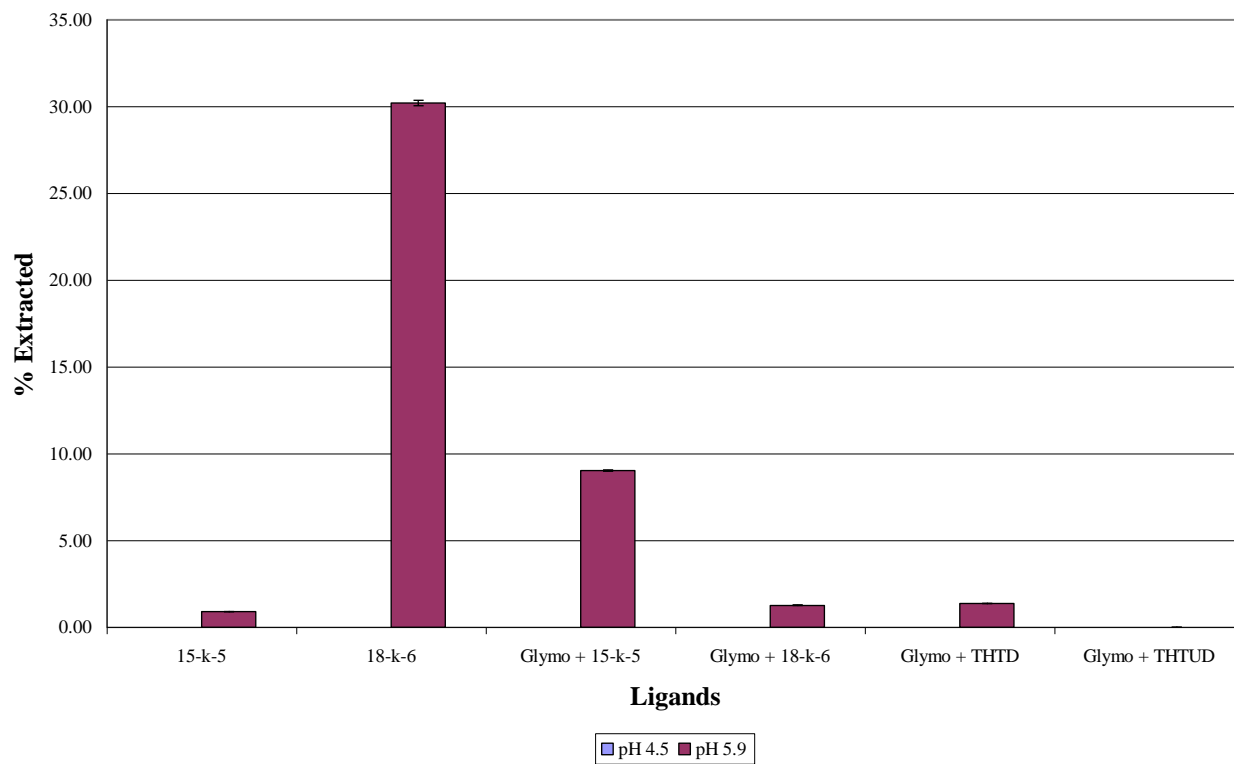
Extraction of Sr(II) with Different Ligands Immobilized on MCM-41



Extraction of Sr(II) with Different Ligands Immobilized on SBA-15



Extraction of Sr(II) with Different Ligands Immobilized on HMS



Cd(II) extraction at pH 4.5

Accuracy	Certified std value	11.60
	Analysed	11.71
	% Deviation	0.94

Standard Solution (ppm)	Support	Ligand	Extracted ppm		% Extracted
117.073	Si-gel (60Å)	15-c-5	118.29	0.00	0.00
		18-c-6	121.62	0.00	0.00
		Glymo + 15-c-5	121.93	0.00	0.00
		Glymo + 18-c-6	117.20	0.00	0.00
		Glymo + THTD	115.37	1.45	1.70
		Glymo + THTUD	118.69	0.00	0.00
					Average %
					0.28
	MCM-41	15-c-5	117.35	0.00	0.00
		18-c-6	116.61	0.40	0.47
		Glymo + 15-c-5	114.41	2.28	2.66
		Glymo + 18-c-6	119.48	0.00	0.00
		Glymo + THTD	115.37	1.45	1.70
		Glymo + THTUD	119.26	0.00	0.00
					Average %
					0.81
	SBA-15	15-c-5	117.11	0.00	0.00
		18-c-6	121.16	0.00	0.00
		Glymo + 15-c-5	117.61	0.00	0.00
		Glymo + 18-c-6	118.04	0.00	0.00
		Glymo + THTD	115.33	1.49	1.74
		Glymo + THTUD	121.19	0.00	0.00
					Average %
					0.29
	HMS	15-c-5	116.80	0.23	0.27
		18-c-6	117.13	0.00	0.00
		Glymo + 15-c-5	117.06	0.01	0.02
		Glymo + 18-c-6	116.17	0.78	0.91
		Glymo + THTD	117.72	0.00	0.00
		Glymo + THTUD	118.41	0.00	0.00
					Average %
					0.20

Cd(II) extraction at pH 4.5

Accuracy	Certified std value	11.60
	Analysed	11.71
	% Deviation	0.94

Support	Ligand	% Extracted
Si-gel (60Å)	15-c-5	0.00
MCM-41	15-c-5	0.00
SBA-15	15-c-5	0.00
HMS	15-c-5	0.27
	Average %	0.07
Si-gel (60Å)	18-c-6	0.00
MCM-41	18-c-6	0.47
SBA-15	18-c-6	0.00
HMS	18-c-6	0.00
	Average %	0.12
Si-gel (60Å)	Glymo + 15-c-5	0.00
MCM-41	Glymo + 15-c-5	2.66
SBA-15	Glymo + 15-c-5	0.00
HMS	Glymo + 15-c-5	0.02
	Average %	0.67
Si-gel (60Å)	Glymo + 18-c-6	0.00
MCM-41	Glymo + 18-c-6	0.00
SBA-15	Glymo + 18-c-6	0.00
HMS	Glymo + 18-c-6	0.91
	Average %	0.23
Si-gel (60Å)	Glymo + THTD	1.70
MCM-41	Glymo + THTD	1.70
SBA-15	Glymo + THTD	1.74
HMS	Glymo + THTD	0.00
	Average %	1.29
Si-gel (60Å)	Glymo + THTUD	0.00
MCM-41	Glymo + THTUD	0.00
SBA-15	Glymo + THTUD	0.00
HMS	Glymo + THTUD	0.00
	Average %	0.00

Cd(II) extraction at pH 5.9

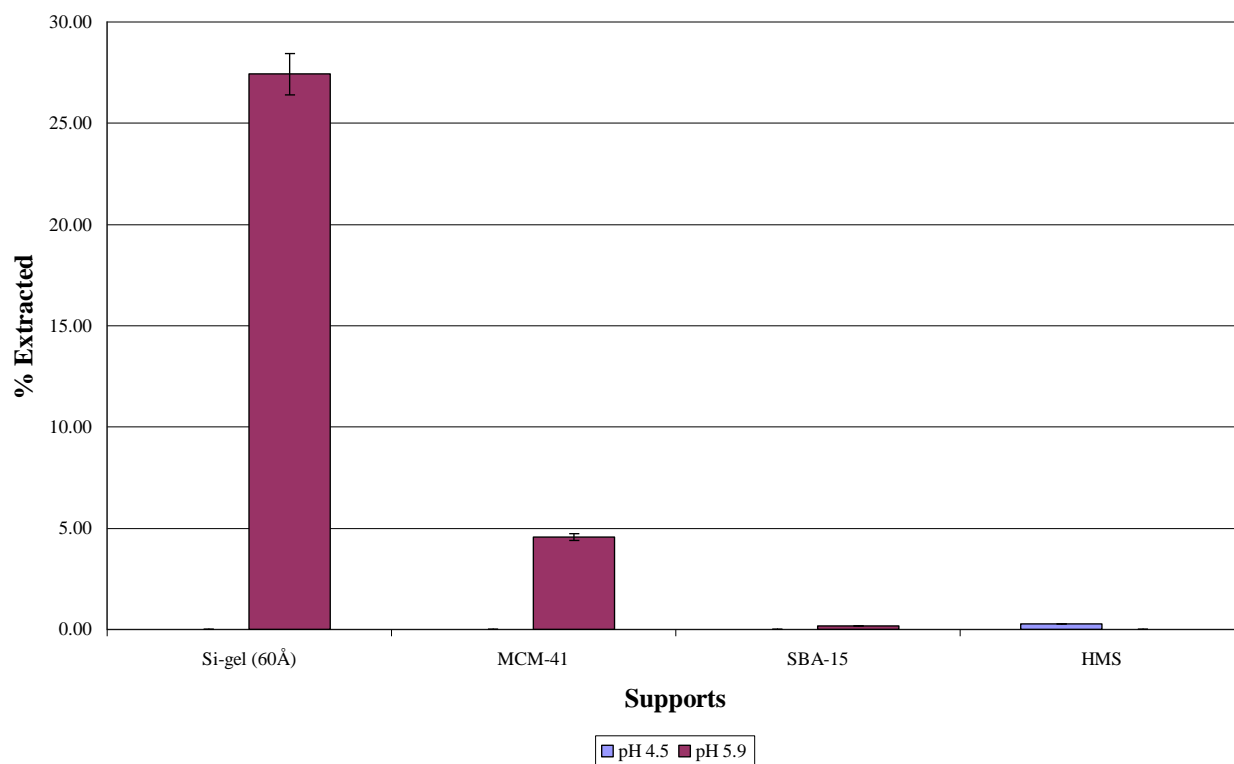
Accuracy	Certified std value	9.87
	Analysed	10.24
	% Deviation	3.73

Standard Solution (ppm)	Support	Ligand		Extracted ppb	% Extracted
1300.20	Si-gel (60Å)	15-c-5	943.84	356.36	27.41
		18-c-6	1390.89	0.00	0.00
		Glymo + 15-c-5	1444.46	0.00	0.00
		Glymo + 18-c-6	835.70	464.50	35.73
		Glymo + THTD	1041.77	258.43	19.88
		Glymo + THTUD	1193.91	106.29	8.17
					Average %
					15.20
	MCM-41	15-c-5	1241.06	59.14	4.55
		18-c-6	1374.62	0.00	0.00
		Glymo + 15-c-5	1286.40	13.80	1.06
		Glymo + 18-c-6	1282.35	17.85	1.37
		Glymo + THTD	1286.90	13.30	1.02
		Glymo + THTUD	1280.48	19.72	1.52
					Average %
					1.59
	SBA-15	15-c-5	1297.96	2.24	0.17
		18-c-6	833.42	466.78	35.90
		Glymo + 15-c-5	1105.35	194.85	14.99
		Glymo + 18-c-6	1211.71	88.49	6.81
		Glymo + THTD	1258.66	41.54	3.19
		Glymo + THTUD	1313.60	0.00	0.00
					Average %
					10.18
	HMS	15-c-5	1335.34	0.00	0.00
		18-c-6	1340.56	0.00	0.00
		Glymo + 15-c-5	1361.39	0.00	0.00
		Glymo + 18-c-6	1323.01	0.00	0.00
		Glymo + THTD	1303.46	0.00	0.00
		Glymo + THTUD	1307.04	0.00	0.00
					Average %
					0.00

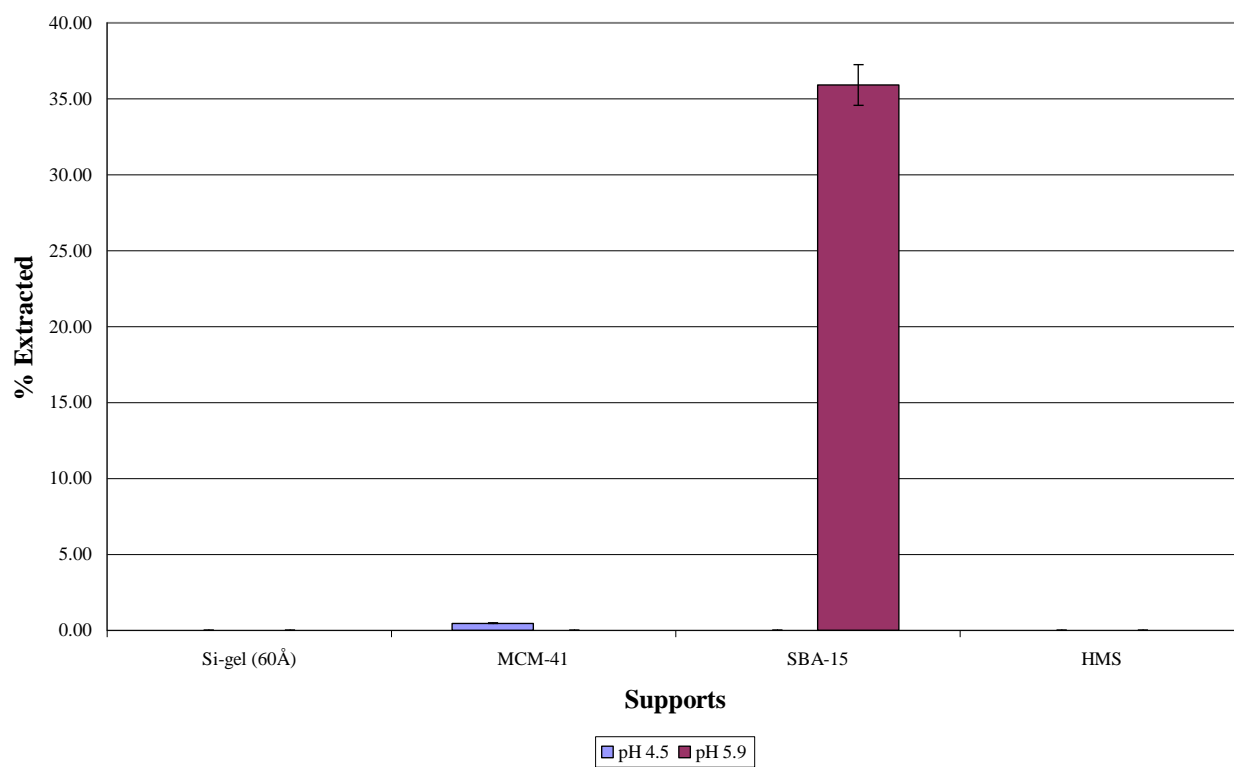
Cd(II) extraction at pH 5.9

Accuracy	Certified std value	9.87	
	Analysed	10.24	
	% Deviation	3.73	
Support	Ligand		% Extracted
Si-gel (60Å)	15-c-5		27.41
MCM-41	15-c-5		4.55
SBA-15	15-c-5		0.17
HMS	15-c-5		0.00
		Average %	8.03
Si-gel (60Å)	18-c-6		0.00
MCM-41	18-c-6		0.00
SBA-15	18-c-6		35.90
HMS	18-c-6		0.00
		Average %	8.98
Si-gel (60Å)	Glymo + 15-c-5		0.00
MCM-41	Glymo + 15-c-5		1.06
SBA-15	Glymo + 15-c-5		14.99
HMS	Glymo + 15-c-5		0.00
		Average %	4.01
Si-gel (60Å)	Glymo + 18-c-6		35.73
MCM-41	Glymo + 18-c-6		1.37
SBA-15	Glymo + 18-c-6		6.81
HMS	Glymo + 18-c-6		0.00
		Average %	10.98
Si-gel (60Å)	Glymo + THTD		19.88
MCM-41	Glymo + THTD		1.02
SBA-15	Glymo + THTD		3.19
HMS	Glymo + THTD		0.00
		Average %	6.02
Si-gel (60Å)	Glymo + THTUD		8.17
MCM-41	Glymo + THTUD		1.52
SBA-15	Glymo + THTUD		0.00
HMS	Glymo + THTUD		0.00
		Average %	2.42

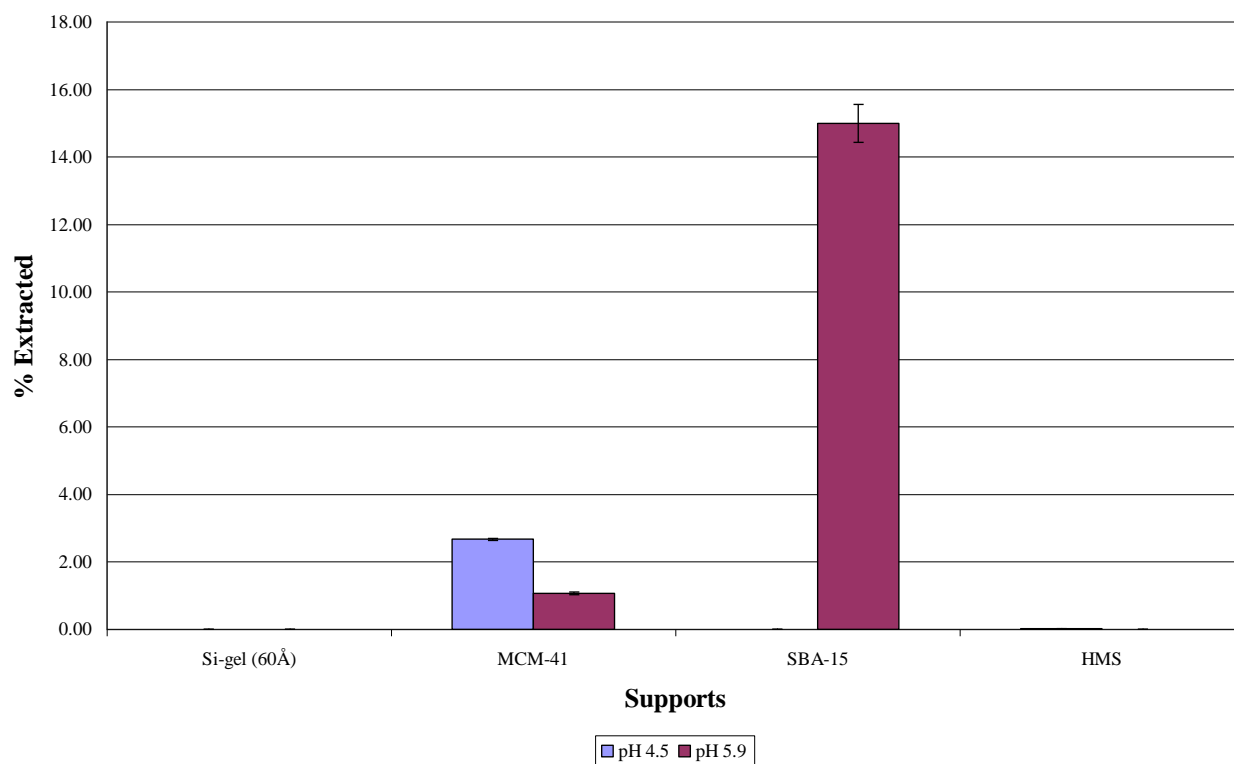
Extraction of Cd(II) with 15-c-5 Immobilized Directly on Different Supports



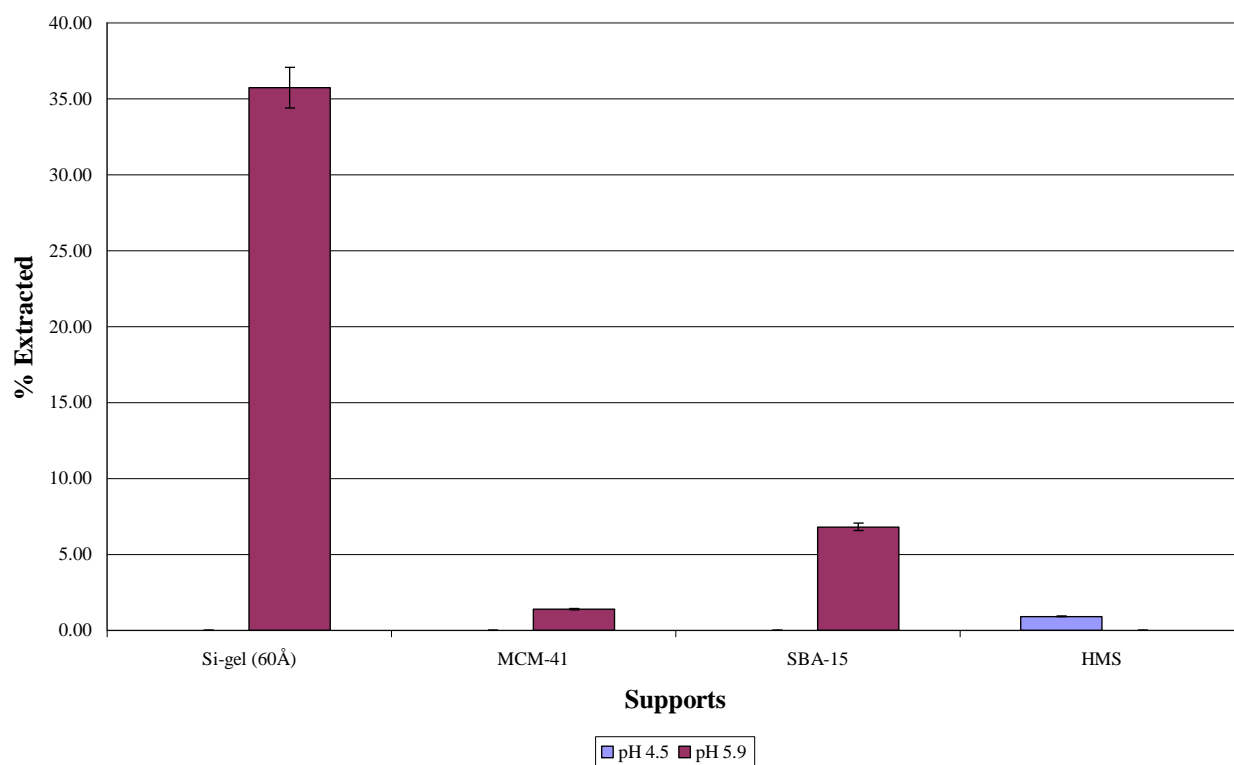
Extraction of Cd(II) with 18-c-6 Immobilized Directly on Different Supports



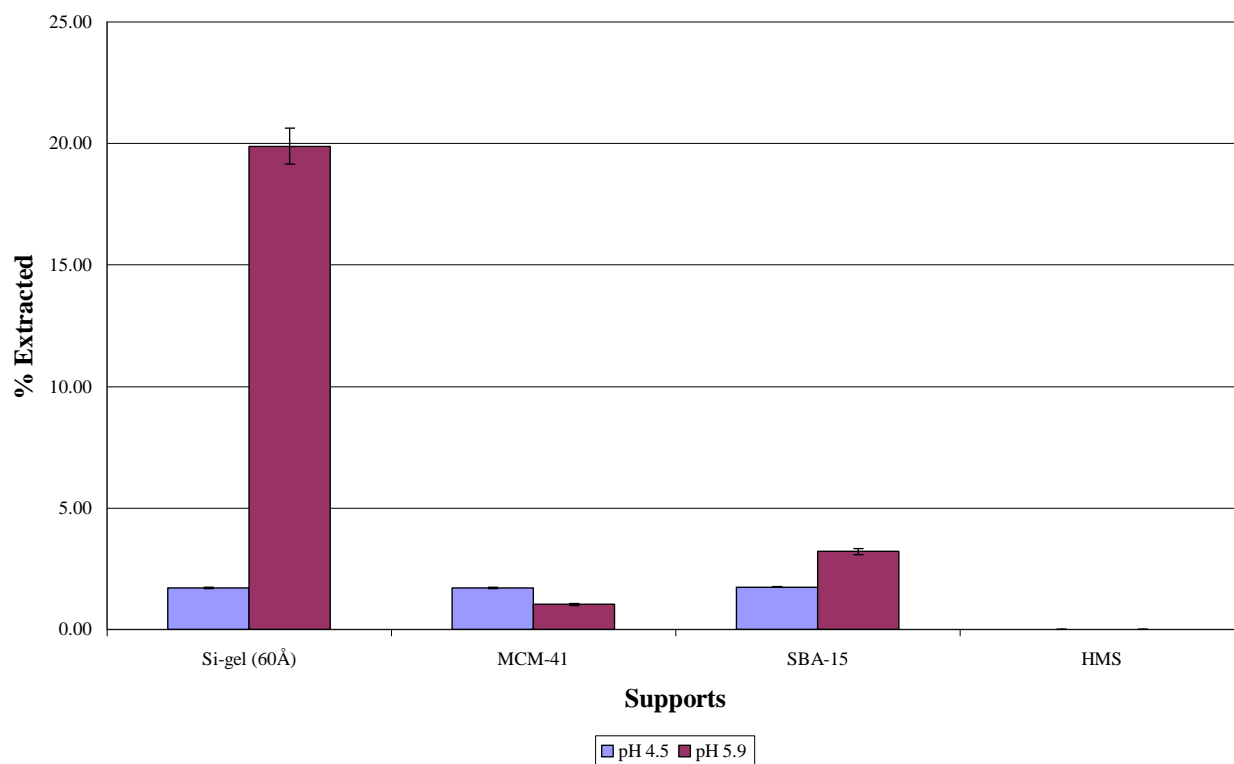
Extraction of Cd(II) with 15-c-5 Immobilized with Glymo on Different Supports



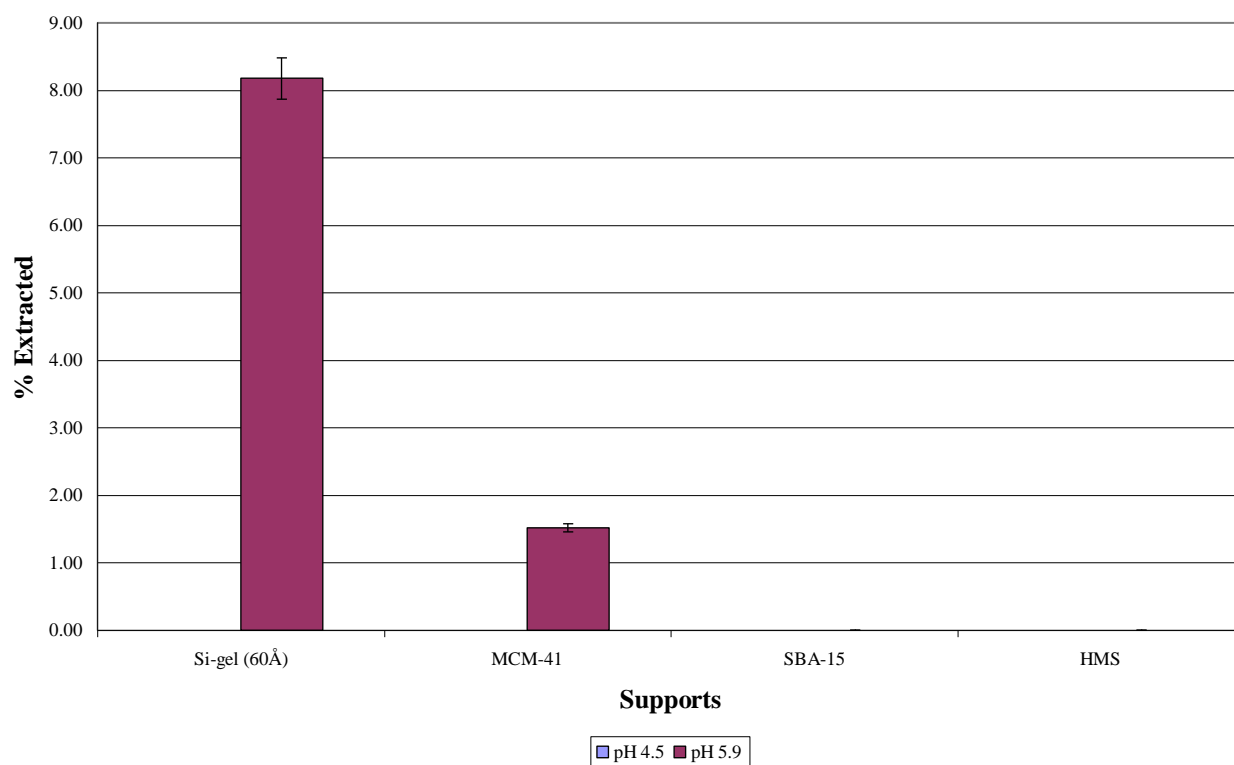
Extraction of Cd(II) with 18-c-6 Immobilized with Glymo on Different Supports



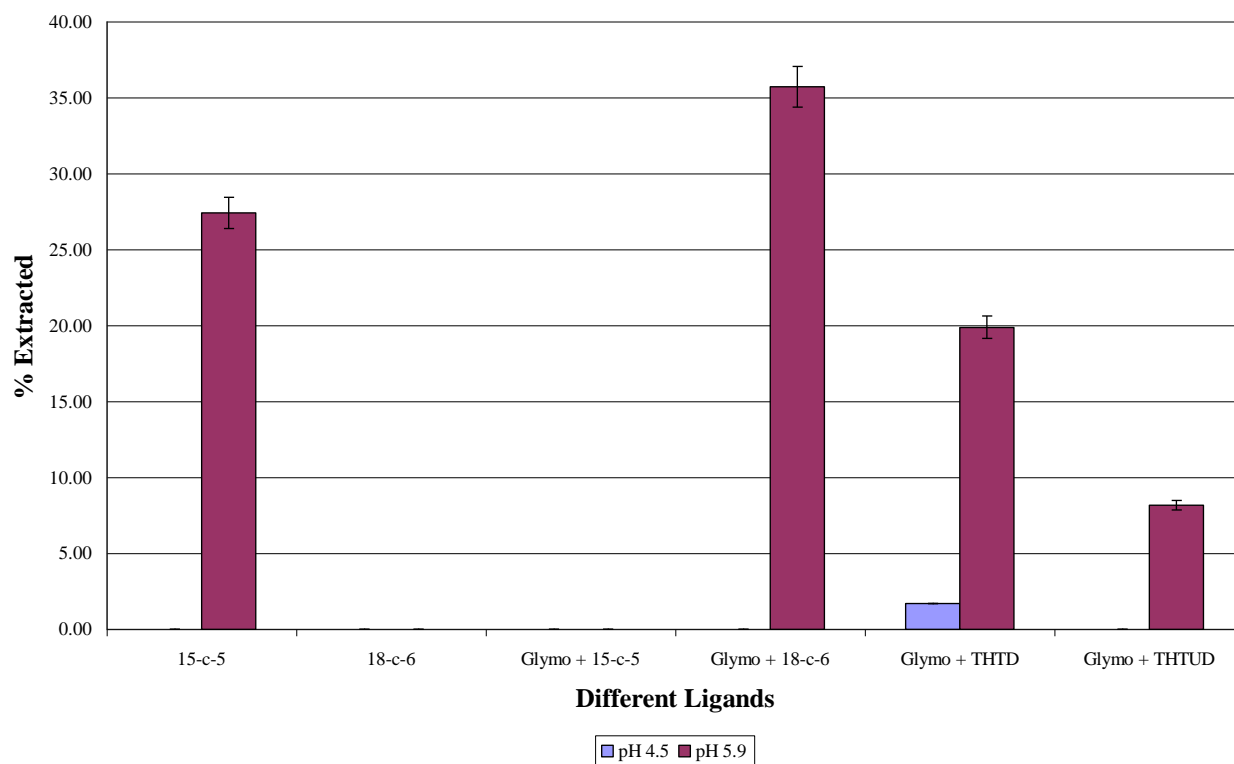
Extraction Of Cd(II) with THTD Immobilized on Different Supports



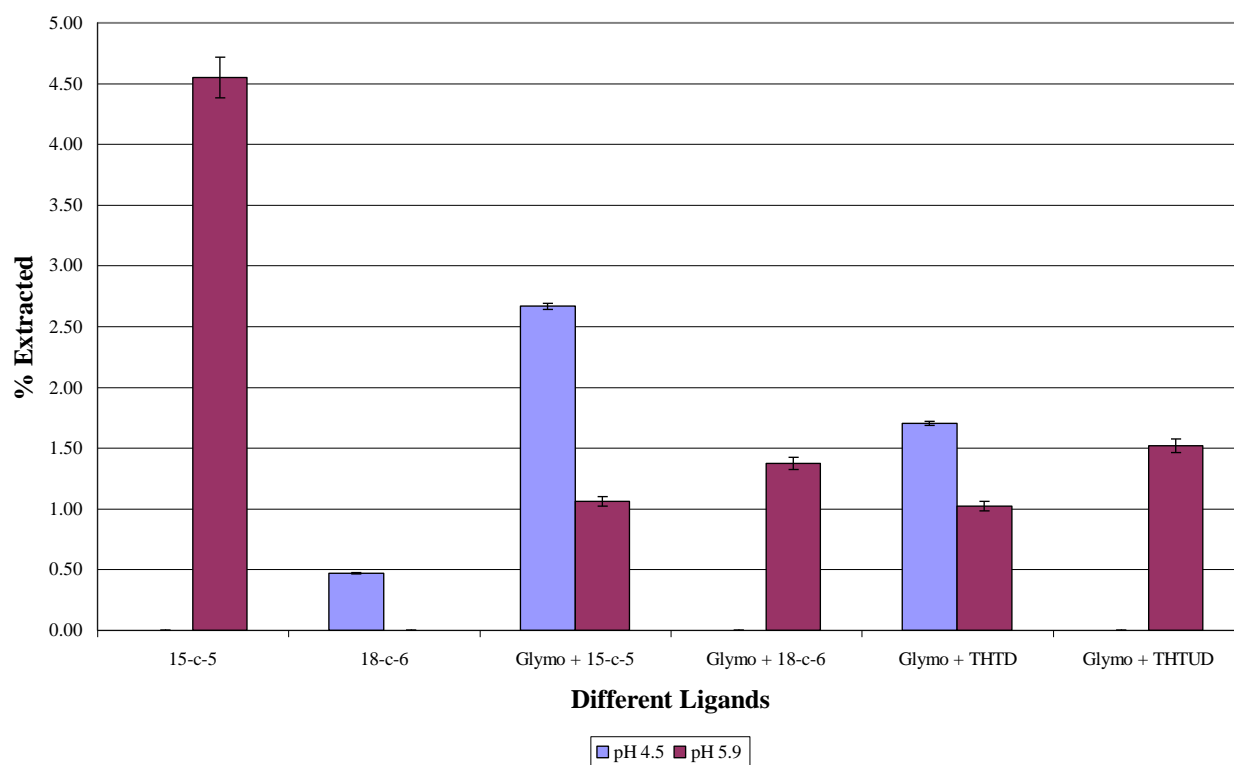
Extraction of Cd(II) with THTUD Immobilized on Different Supports



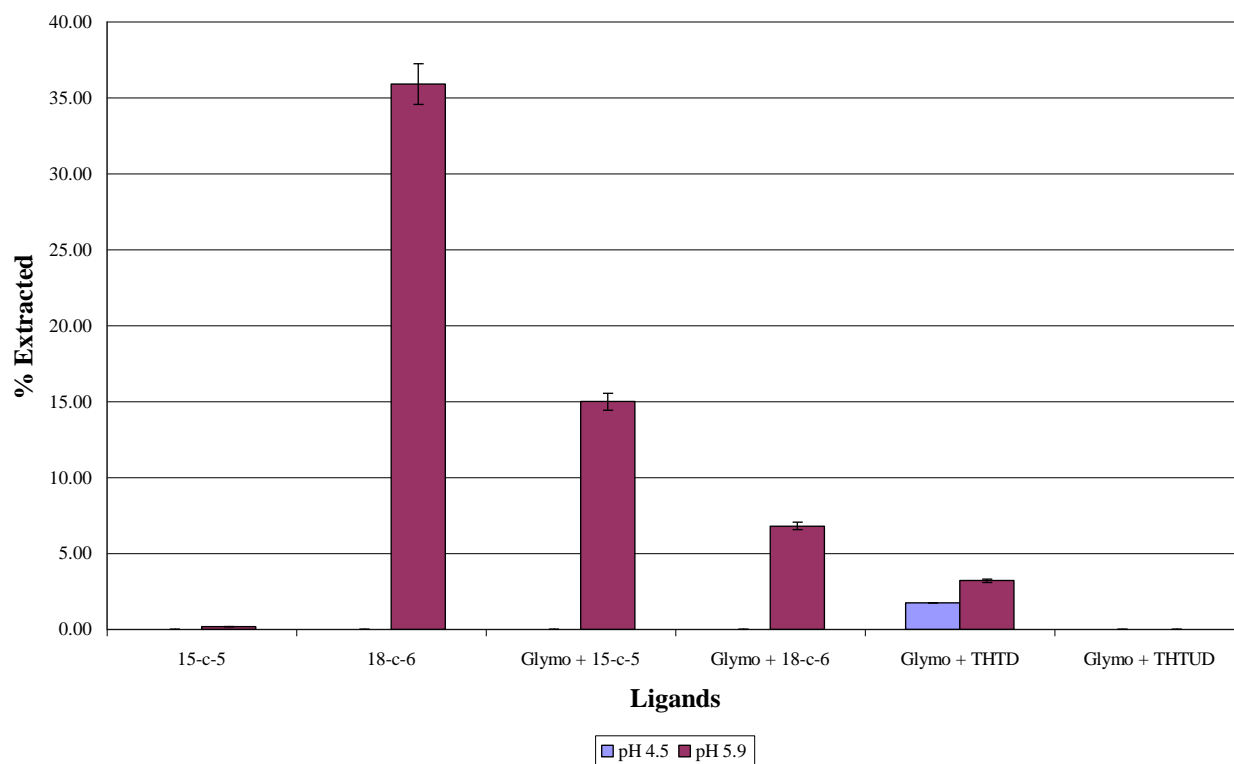
Extraction of Cd(II) with Different Ligands Immobilized on Si gel (60 Å)



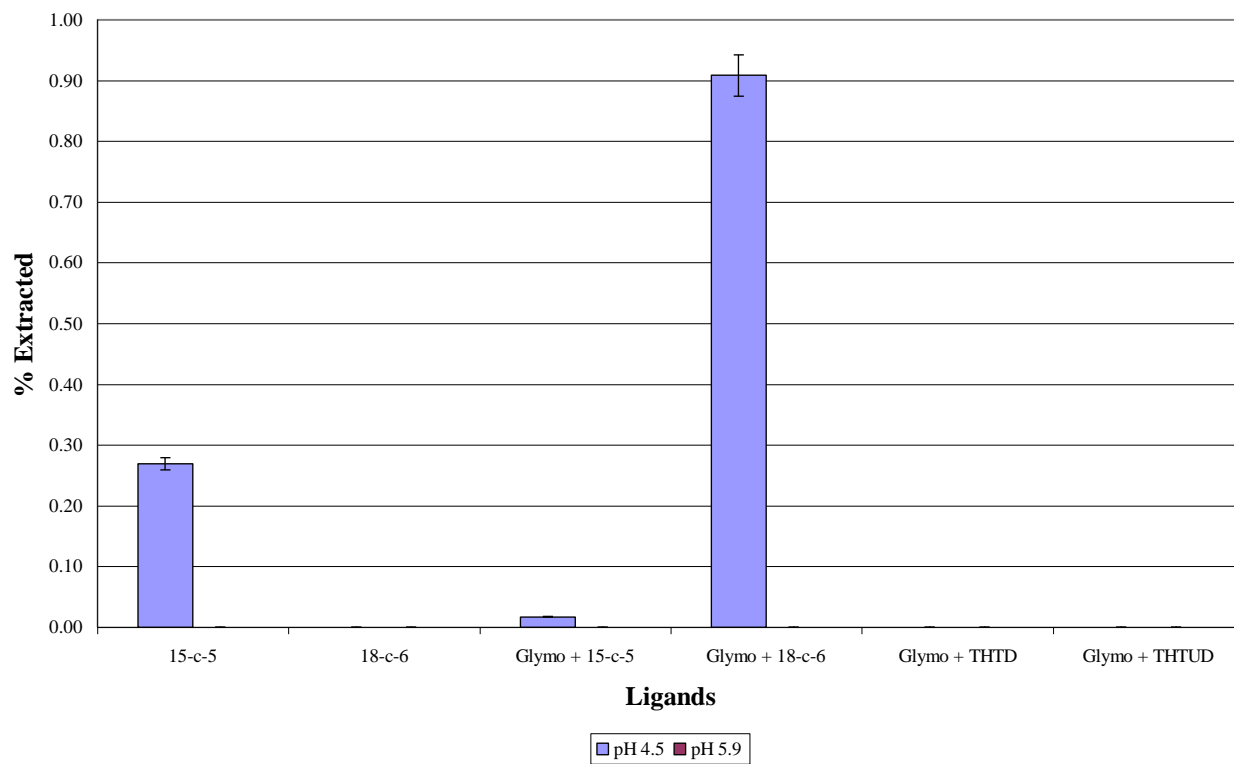
Extraction of Cd(II) with Different Ligands Immobilized on MCM-41



Extraction of Cd(II) with Different Ligands Immobilized on SBA-15



Extraction of Cd(II) with Different Ligands Immobilized on HMS



Hg(II) extraction at pH 5.9

Accuracy	Certified std value	5.00
	Analysed	5.26
	% Deviation	5.24

Standard Solution (ppb)	Support	Ligand		Extracted ppb	% Extracted
201.832	Si-gel (60Å)	15-k-5	204.496	0.00	0.00
		18-k-6	223.538	0.00	0.00
		Glymo + 15-k-5	280.18	0.00	0.00
		Glymo + 18-k-6	302.376	0.00	0.00
		Glymo + THTD	224.66	0.00	0.00
		Glymo + THTUD	289.414	0.00	0.00
				Average %	0.00
	MCM-41	15-k-5	269.98	0.00	0.00
		18-k-6	226.414	0.00	0.00
		Glymo + 15-k-5	230.9	0.00	0.00
		Glymo + 18-k-6	214.692	0.00	0.00
		Glymo + THTD	205.98	0.00	0.00
		Glymo + THTUD	260.964	0.00	0.00
				Average %	0.00
	SBA-15	15-k-5	236.646	0.00	0.00
		18-k-6	219.386	0.00	0.00
		Glymo + 15-k-5	212.748	0.00	0.00
		Glymo + 18-k-6	217.252	0.00	0.00
		Glymo + THTD	215.984	0.00	0.00
		Glymo + THTUD	277.336	0.00	0.00
				Average %	0.00
	HMS	15-k-5	249.414	0.00	0.00
		Glymo + 15-k-5	233.79	0.00	0.00
		Glymo + 18-k-6	232.686	0.00	0.00
		Glymo + THTD	236.426	0.00	0.00
		Glymo + THTUD	302.812	0.00	0.00
				Average %	0.00

U(VI) extraction at pH 5.9

Accuracy
Certified std value
Analysed
% Deviation

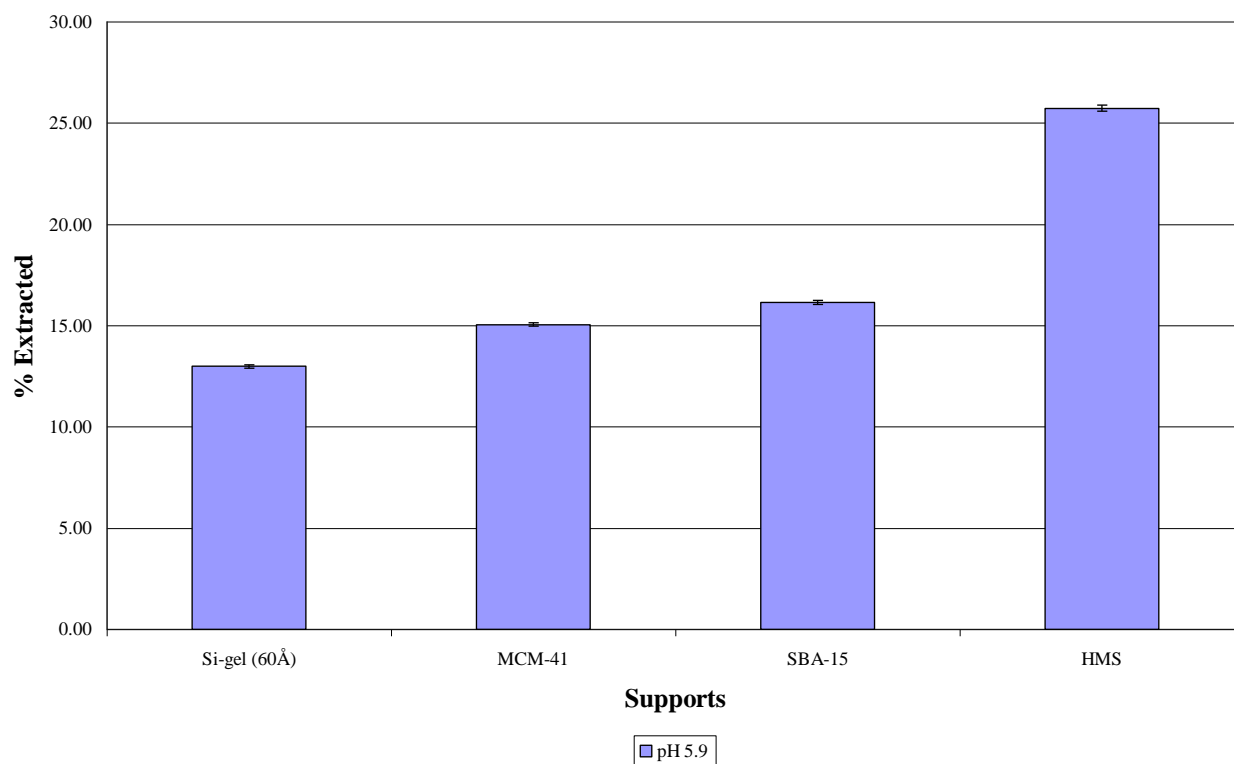
4.85
 4.82
 0.58

Standard Solution (ppb)	Support	Ligand	Extracted ppb		% Extracted
9.86	Si-gel (60Å)	15-k-5	8.58	1.28	12.98
		18-k-6	8.33	1.53	15.54
		Glymo + 15-k-5	8.42	1.44	14.61
		Glymo + 18-k-6	8.39	1.47	14.88
		Glymo + THTD	8.46	1.40	14.22
		Glymo + THTUD	8.77	1.09	11.10
		Average %			13.89
	MCM-41	15-k-5	8.38	1.48	15.05
		18-k-6	8.46	1.40	14.22
		Glymo + 15-k-5	8.67	1.19	12.08
		Glymo + 18-k-6	8.78	1.08	10.92
		Glymo + THTD	8.73	1.13	11.45
		Glymo + THTUD	8.48	1.38	14.02
		Average %			12.96
	SBA-15	15-k-5	8.27	1.59	16.13
		18-k-6	8.23	1.63	16.55
		Glymo + 15-k-5	9.10	0.76	7.71
		Glymo + 18-k-6	8.83	1.03	10.45
		Glymo + THTD	8.29	1.57	15.97
		Glymo + THTUD	8.17	1.69	17.12
		Average %			13.99
	HMS	15-k-5	7.32	2.54	25.72
		18-k-6	8.53	1.33	13.46
		Glymo + 15-k-5	7.97	1.89	19.20
		Glymo + 18-k-6	8.76	1.10	11.20
		Glymo + THTD	8.15	1.71	17.32
		Glymo + THTUD	8.67	1.19	12.11
		Average %			16.50

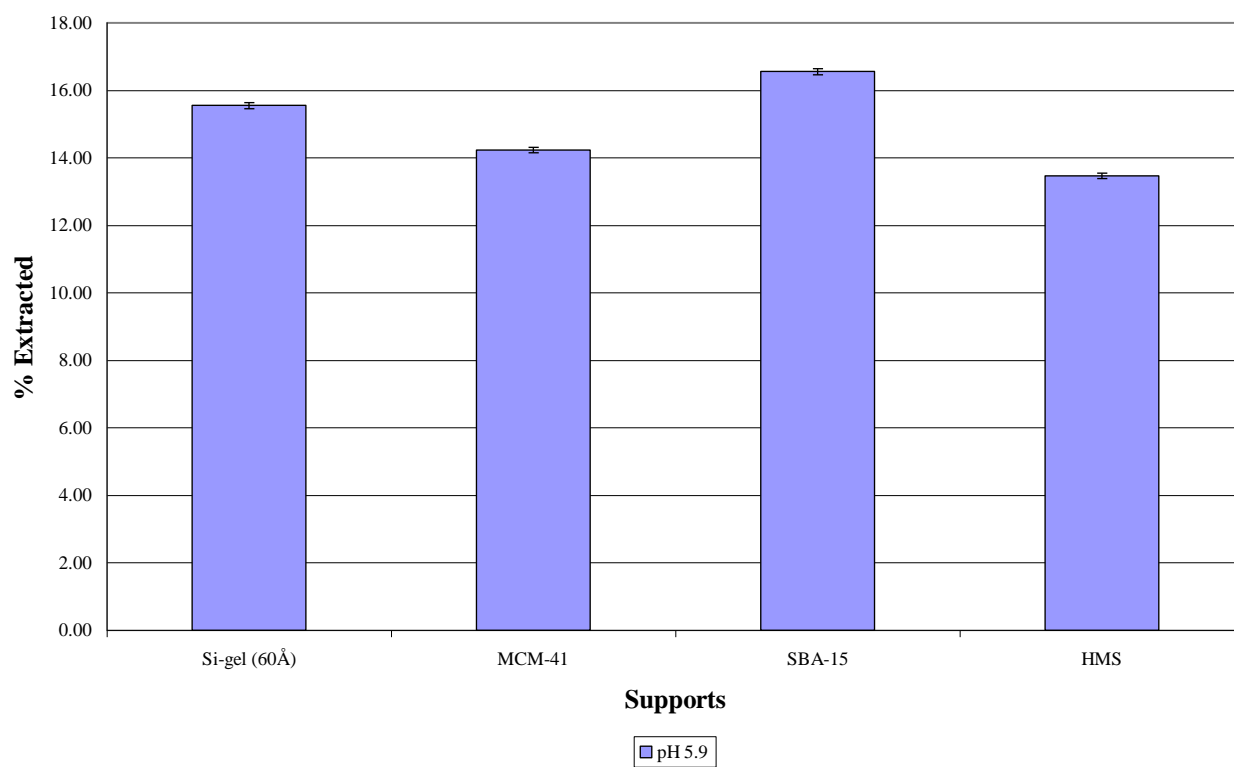
U(VI) extraction at pH 5.9

Accuracy	Certified std value	4.85
	Analysed	4.82
	% Deviation	0.58
Support	Ligand	% Extracted
Si-gel (60Å)	15-k-5	12.98
MCM-41	15-k-5	15.05
SBA-15	15-k-5	16.13
HMS	15-k-5	25.72
	Average %	17.47
Si-gel (60Å)	18-k-6	15.54
MCM-41	18-k-6	14.22
SBA-15	18-k-6	16.55
HMS	18-k-6	13.46
	Average %	14.94
Si-gel (60Å)	Glymo + 15-k-5	14.61
MCM-41	Glymo + 15-k-5	12.08
SBA-15	Glymo + 15-k-5	7.71
HMS	Glymo + 15-k-5	19.20
	Average %	13.40
Si-gel (60Å)	Glymo + 18-k-6	14.88
MCM-41	Glymo + 18-k-6	10.92
SBA-15	Glymo + 18-k-6	10.45
HMS	Glymo + 18-k-6	11.20
	Average %	11.86
Si-gel (60Å)	Glymo + THTD	14.22
MCM-41	Glymo + THTD	11.45
SBA-15	Glymo + THTD	15.97
HMS	Glymo + THTD	17.32
	Average %	14.74
Si-gel (60Å)	Glymo + THTUD	11.10
MCM-41	Glymo + THTUD	14.02
SBA-15	Glymo + THTUD	17.12
HMS	Glymo + THTUD	12.11
	Average %	13.59

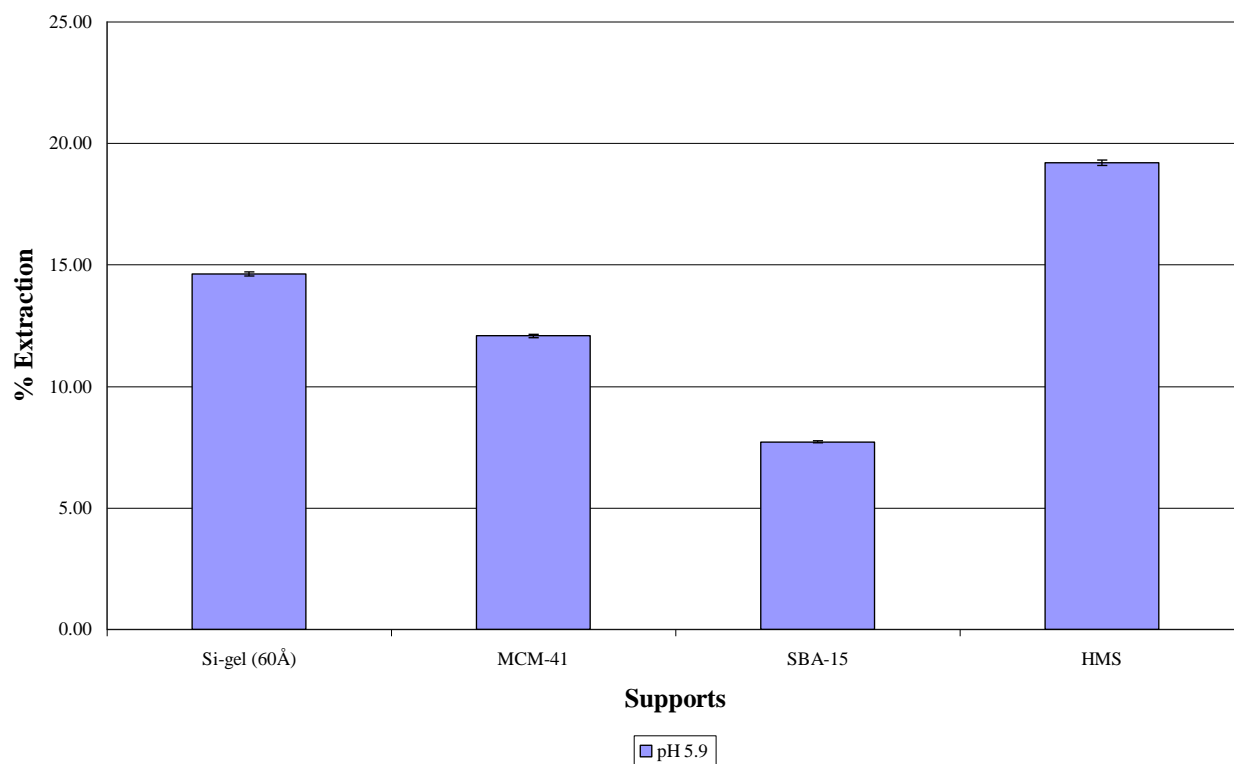
Extraction of U(VI) with 15-c-5 Immobilized Directly on Various Supports



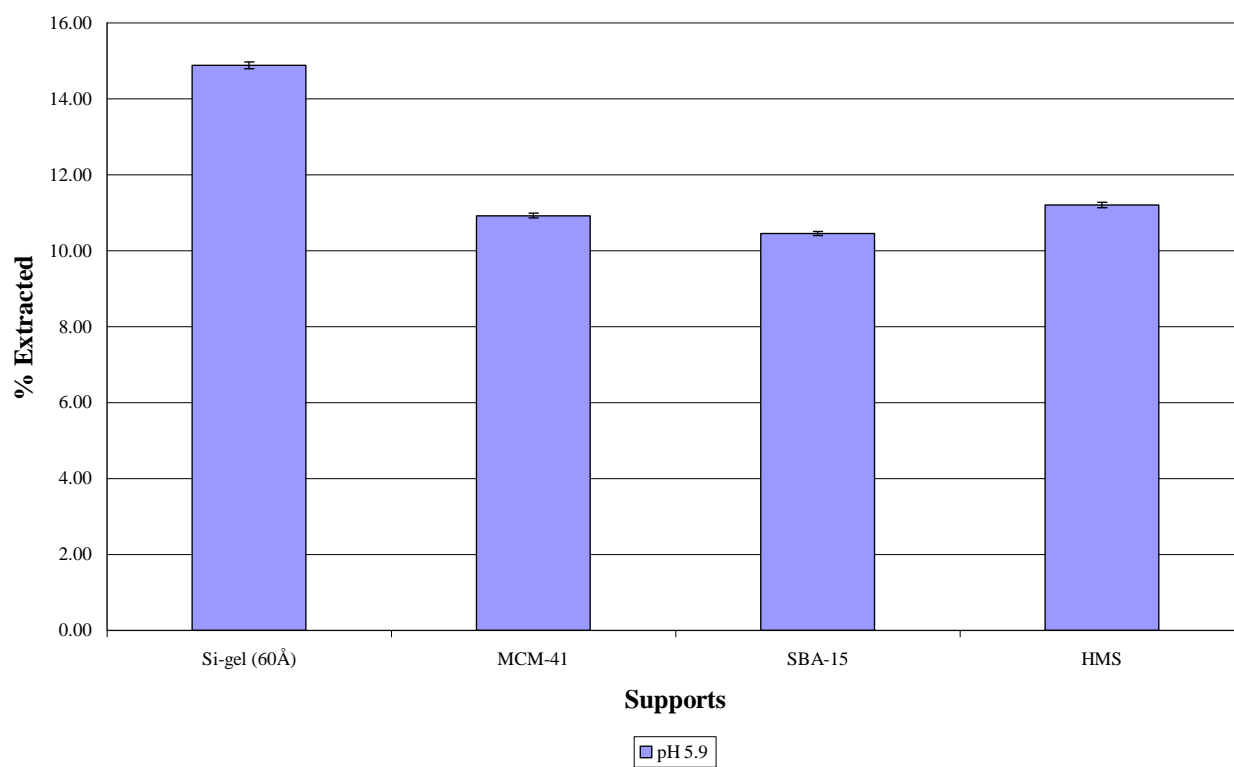
Extraction of U(VI) with 18-c-6 Immobilized Directly on Various Supports



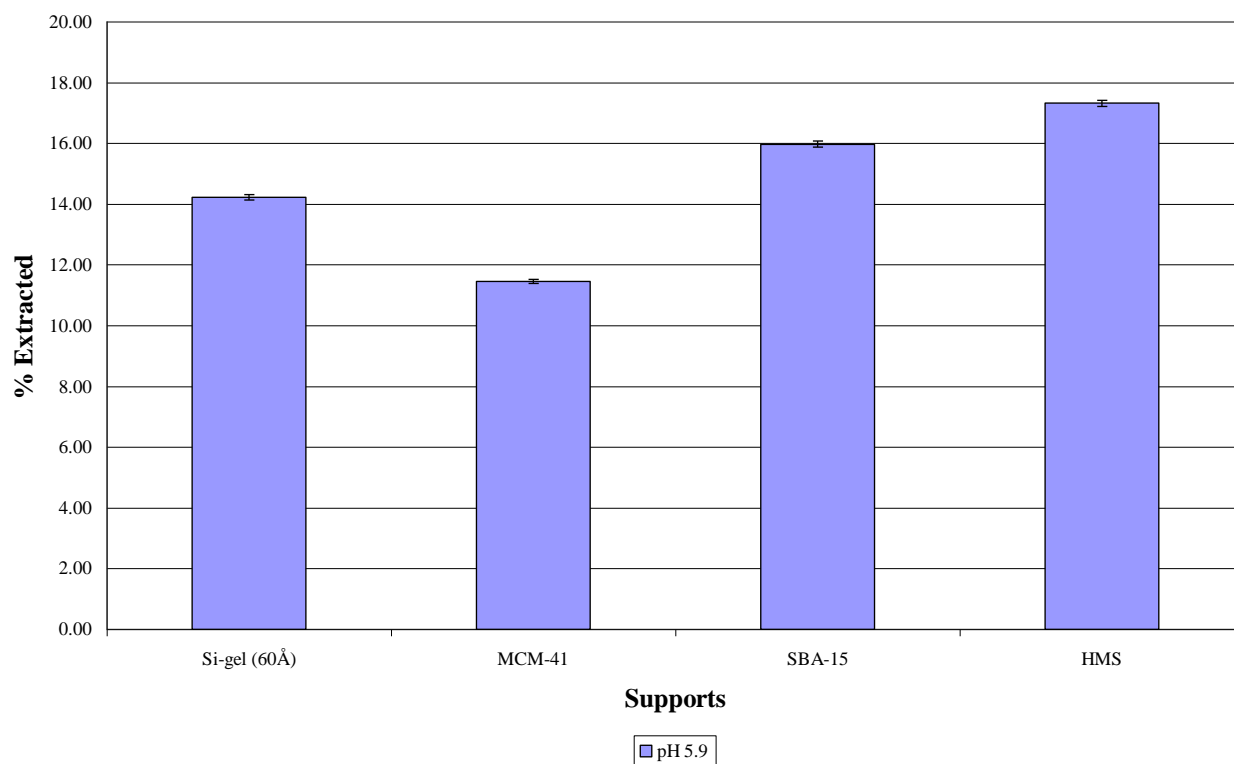
Extraction of U(VI) with 15-c-5 Immobilized with Glymo on Various Supports



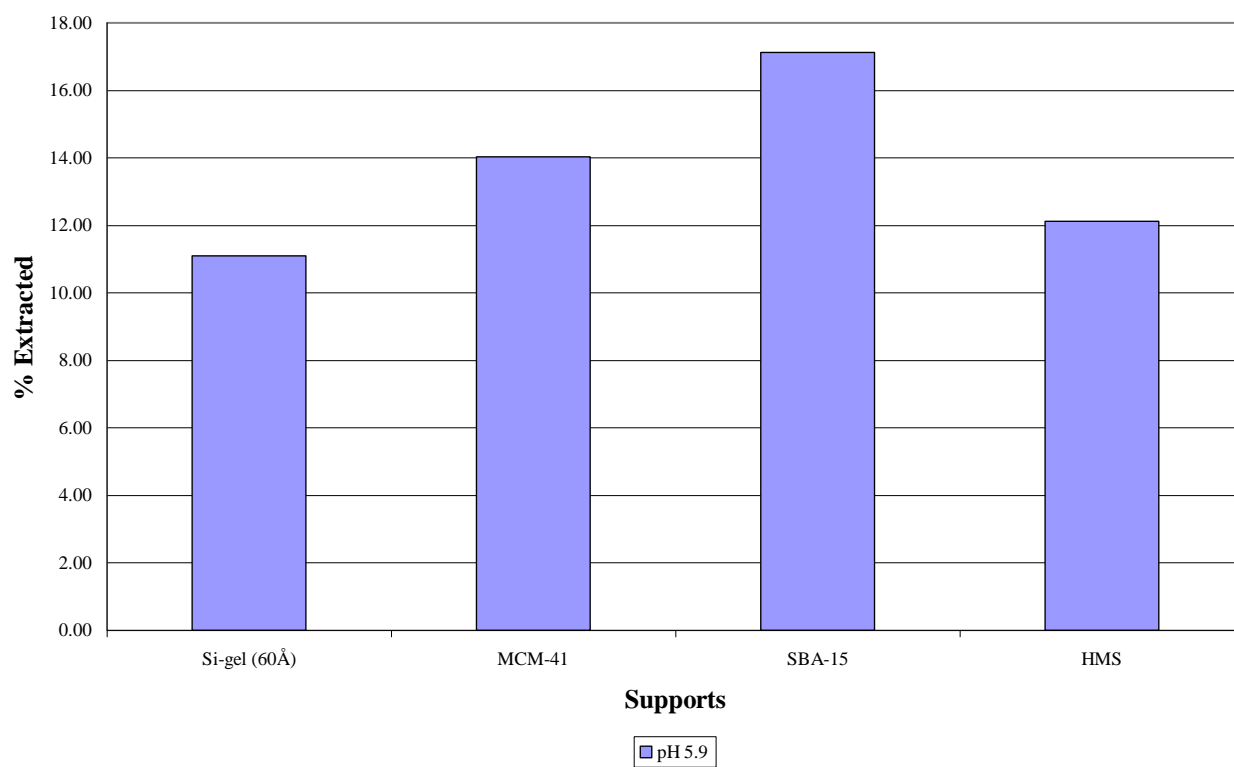
Extraction of U(VI) with 18-c-6 Immobilized with Glymo on Various Supports



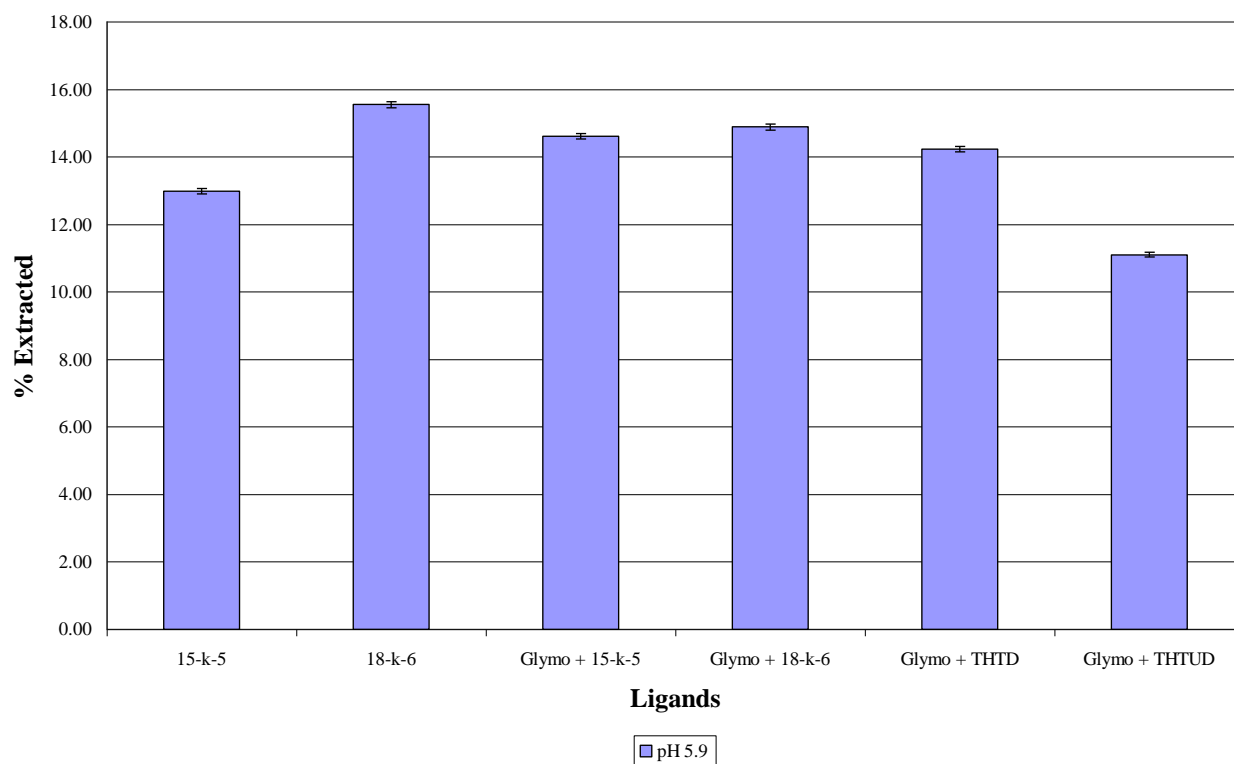
Extraction of U(VI) with THTD Immobilized on Various Supports



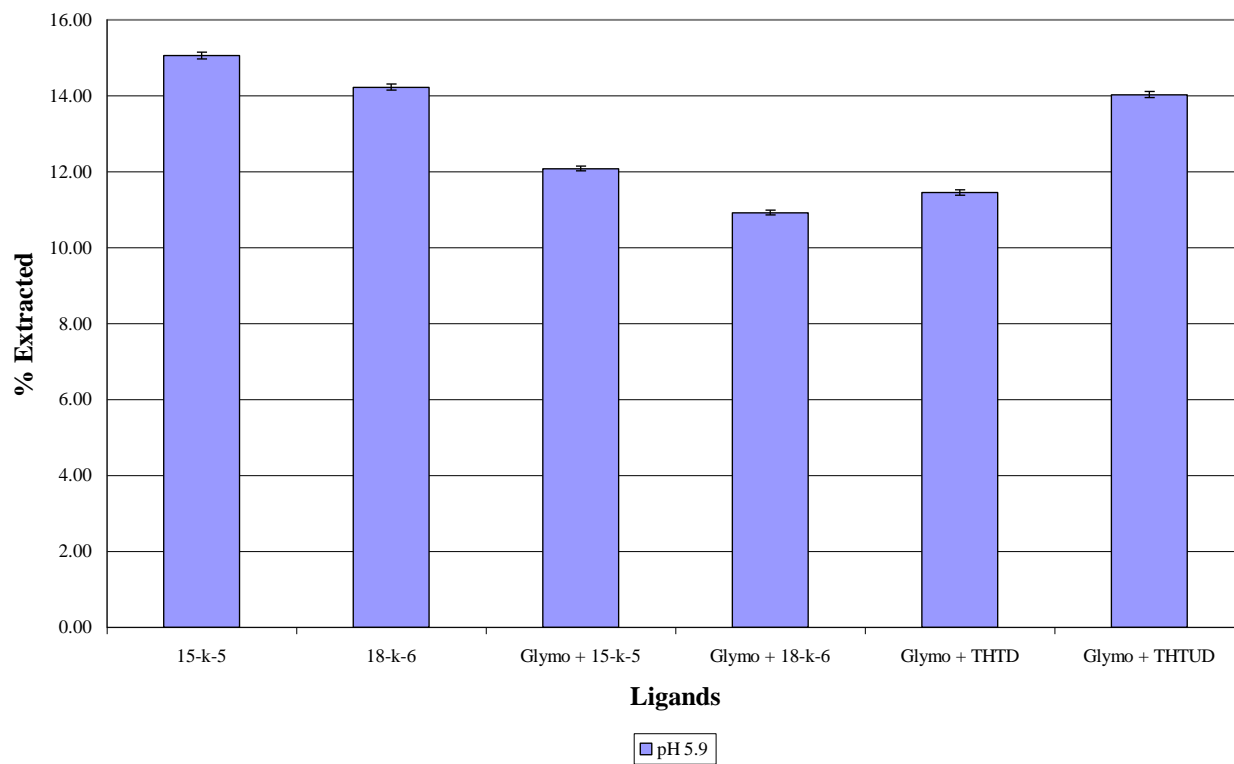
Extraction of U(VI) with THTUD Immobilized on Various Supports



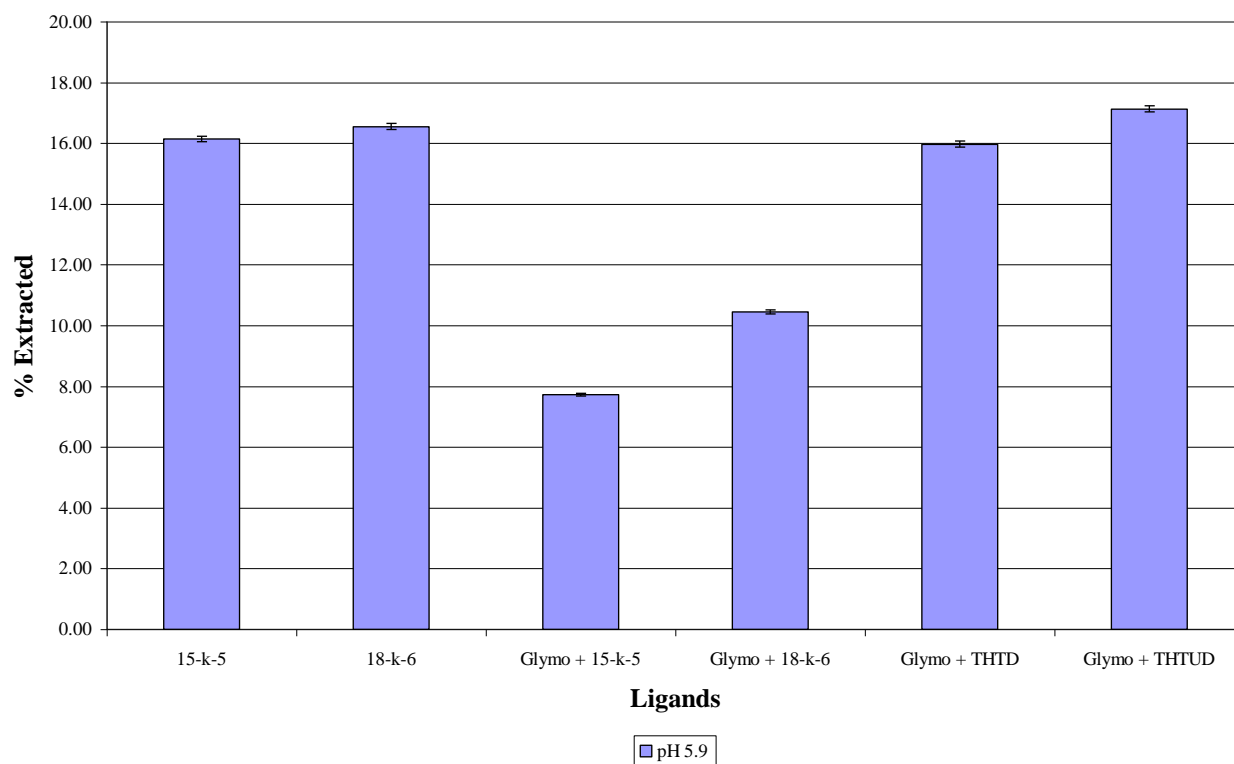
Extraction of U(VI) with Various Ligands Immobilized on Si gel (60 Å)



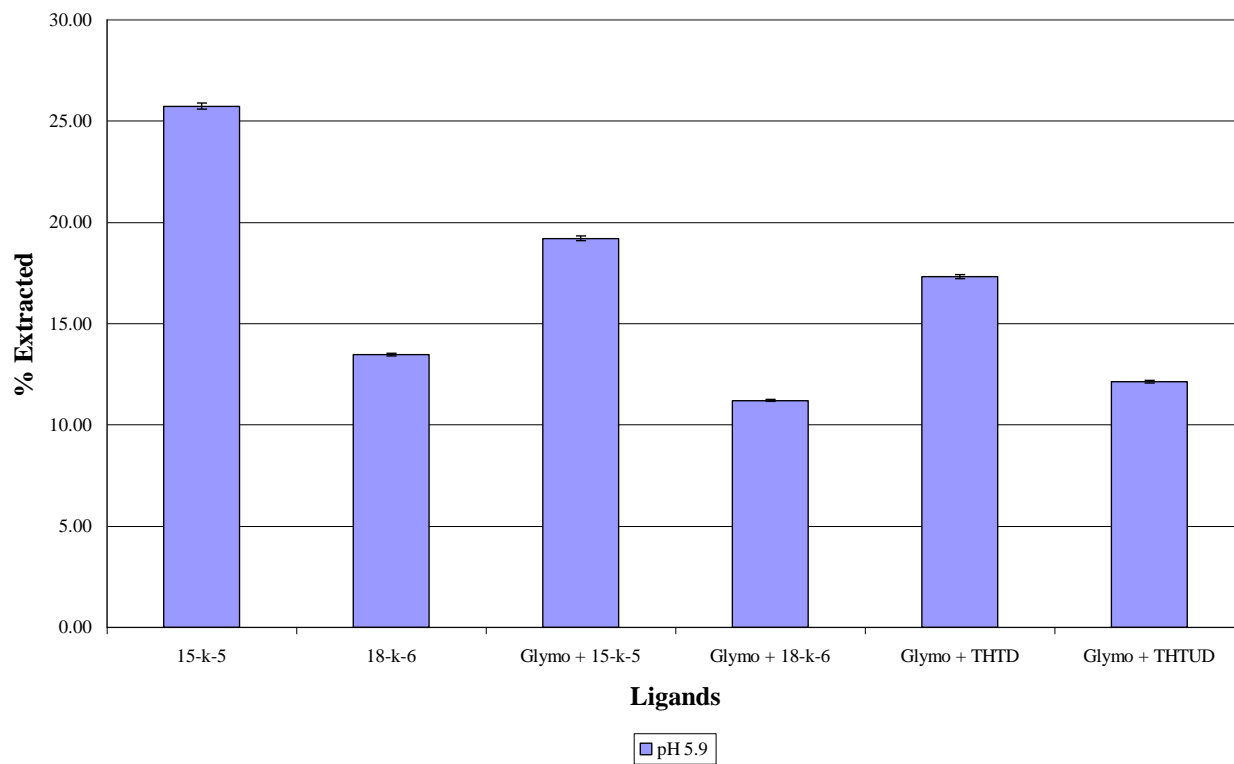
Extraction of U(VI) with Various Ligands Immobilized on MCM-41



Extraction of U(VI) with Various Ligands Immobilized on SBA-15



Extraction of U(VI) with Various Ligands Immobilized on HMS



Combination extraction of two metal ions at pH 5.9 [Hg(II)]

Accuracy	Certified std value	Hg	U
	Analysed	5.00	4.85
	% Deviation	5.26	4.82
		5.24	0.58

Standard Solution (ppb)		Support	Ligand	Extracted ppb		% Extracted
Hg	10.37	Si-gel (60Å)	15-k-5	17.68	0.00	0.00
			18-k-6	14.44	0.00	0.00
			Glymo + 15-k-5	20.20	0.00	0.00
			Glymo + 18-k-6	19.88	0.00	0.00
			Glymo + THTD	12.92	0.00	0.00
			Glymo + THTUD	16.57	0.00	0.00
			Average %			0.00
		MCM-41	15-k-5	14.09	0.00	0.00
			18-k-6	12.28	0.00	0.00
			Glymo + 15-k-5	13.43	0.00	0.00
			Glymo + 18-k-6	12.31	0.00	0.00
			Glymo + THTD	14.02	0.00	0.00
			Glymo + THTUD	14.51	0.00	0.00
			Average %			0.00
		SBA-15	15-k-5	12.19	0.00	0.00
			18-k-6	11.54	0.00	0.00
			Glymo + 15-k-5	12.28	0.00	0.00
			Glymo + 18-k-6	11.59	0.00	0.00
			Glymo + THTD	14.08	0.00	0.00
			Glymo + THTUD	17.26	0.00	0.00
			Average %			0.00
		HMS	15-k-5	14.12	0.00	0.00
			18-k-6	12.70	0.00	0.00
			Glymo + 15-k-5	11.72	0.00	0.00
			Glymo + 18-k-6	12.75	0.00	0.00
			Glymo + THTD	14.81	0.00	0.00
			Glymo + THTUD	16.74	0.00	0.00
			Average %			0.00

Combination extraction of two metal ions at pH 5.9 [Hg(II)]

		Hg	U
Accuracy	Certified std value	5.00	4.85
	Analysed	5.26	4.82
	% Deviation	5.24	0.58

Support	Ligand		% Extracted
Si-gel (60Å)	15-k-5		0.00
MCM-41	15-k-5		0.00
SBA-15	15-k-5		0.00
HMS	15-k-5		0.00
		Average %	0.00
Si-gel (60Å)	18-k-6		0.00
MCM-41	18-k-6		0.00
SBA-15	18-k-6		0.00
HMS	18-k-6		0.00
		Average %	0.00
Si-gel (60Å)	Glymo + 15-k-5		0.00
MCM-41	Glymo + 15-k-5		0.00
SBA-15	Glymo + 15-k-5		0.00
HMS	Glymo + 15-k-5		0.00
		Average %	0.00
Si-gel (60Å)	Glymo + 18-k-6		0.00
MCM-41	Glymo + 18-k-6		0.00
SBA-15	Glymo + 18-k-6		0.00
HMS	Glymo + 18-k-6		0.00
		Average %	0.00
Si-gel (60Å)	Glymo + THTD		0.00
MCM-41	Glymo + THTD		0.00
SBA-15	Glymo + THTD		0.00
HMS	Glymo + THTD		0.00
		Average %	0.00
Si-gel (60Å)	Glymo + THTUD		0.00
MCM-41	Glymo + THTUD		0.00
SBA-15	Glymo + THTUD		0.00
HMS	Glymo + THTUD		0.00
		Average %	0.00

Combination extraction of two metal ions at pH 5.9 [U(VI)]

Accuracy	Certified std value	Hg	U
	Analysed	5.00	4.85
	% Deviation	5.26	4.82
		5.24	0.58

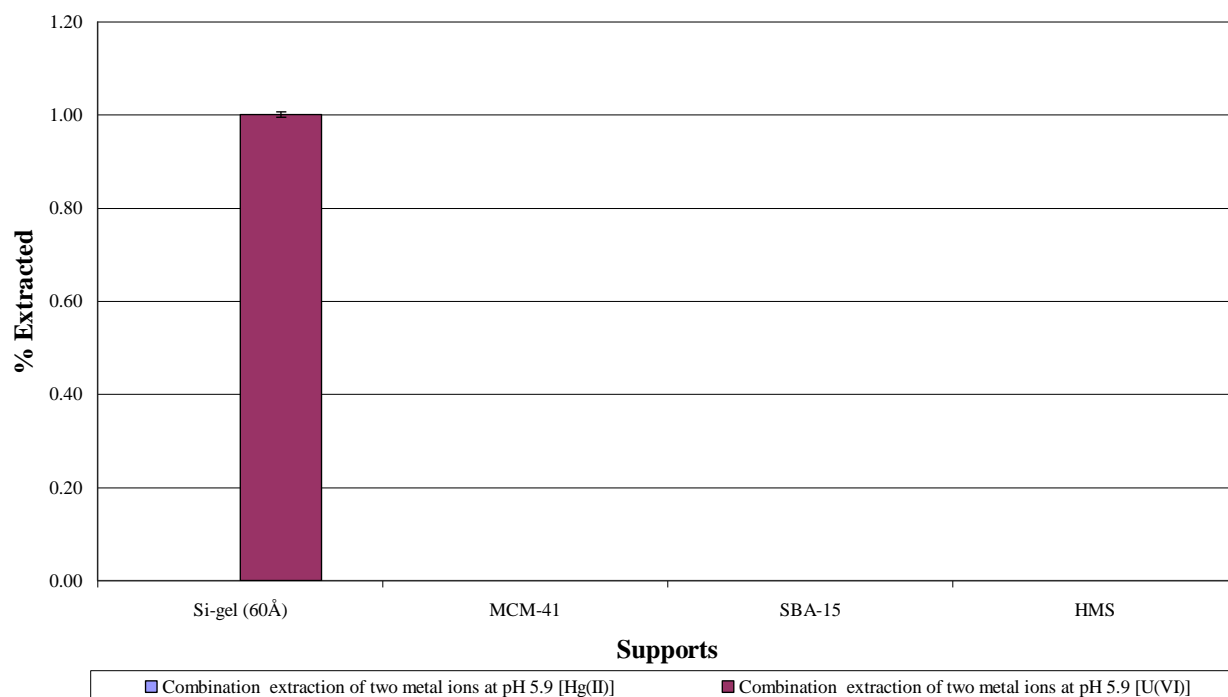
Standard Solution (ppb)		Support	Ligand		Extracted ppb	% Extracted
U	10.17	Si-gel (60Å)	15-k-5	9.27	17.96	8.83
			18-k-6	8.79	27.62	13.58
			Glymo + 15-k-5	9.31	17.27	8.49
			Glymo + 18-k-6	9.44	14.57	7.16
			Glymo + THTD	9.89	5.62	2.76
			Glymo + THTUD	8.71	29.24	14.38
					Average %	9.20
		MCM-41	15-k-5	9.34	16.66	8.19
			18-k-6	9.54	12.59	6.19
			Glymo + 15-k-5	9.67	9.98	4.91
			Glymo + 18-k-6	9.26	18.10	8.90
			Glymo + THTD	9.61	11.27	5.54
			Glymo + THTUD	9.43	14.76	7.26
					Average %	6.83
		SBA-15	15-k-5	9.32	17.04	8.38
			18-k-6	9.16	20.22	9.94
			Glymo + 15-k-5	9.45	14.38	7.07
			Glymo + 18-k-6	9.92	5.07	2.49
			Glymo + THTD	9.64	10.58	5.20
			Glymo + THTUD	9.74	8.49	4.17
					Average %	6.21
		HMS	15-k-5	8.81	27.19	13.37
			18-k-6	9.82	6.98	3.43
			Glymo + 15-k-5	9.34	16.55	8.13
			Glymo + 18-k-6	9.85	6.29	3.09
			Glymo + THTD	9.66	10.09	4.96
			Glymo + THTUD	9.67	9.97	4.90
					Average %	6.32

Combination extraction of two metal ions at pH 5.9 [U(VI)]

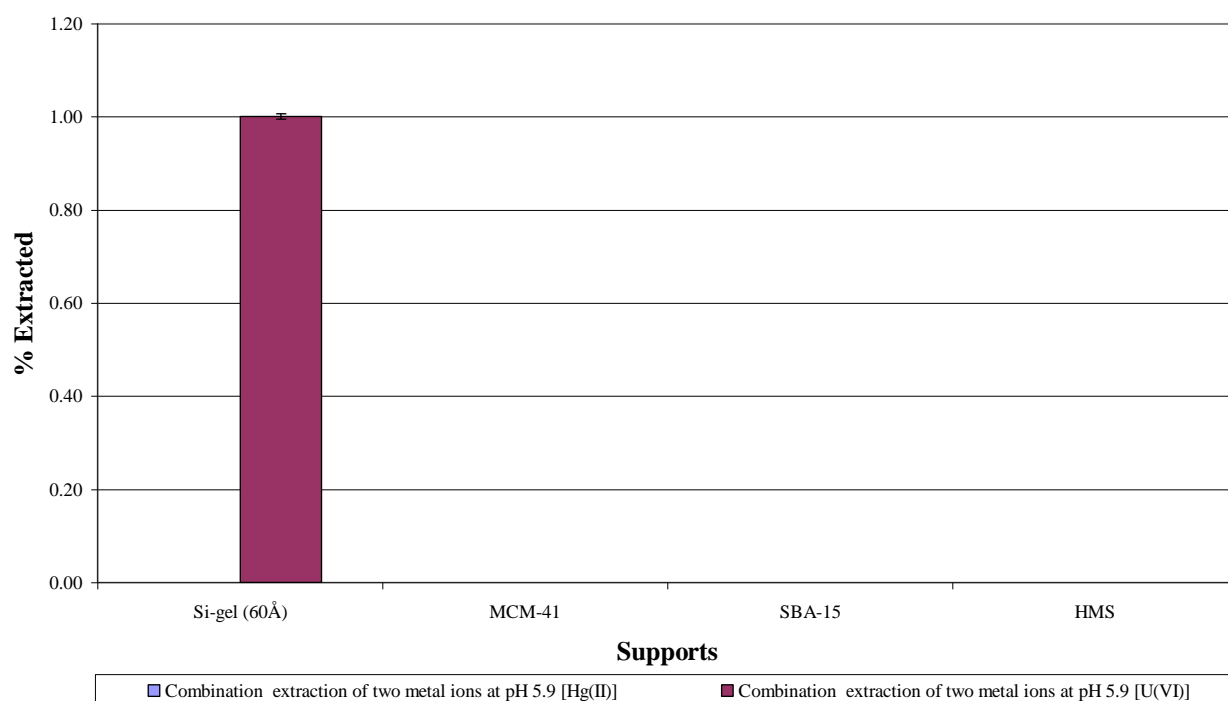
		Hg	U
Accuracy	Certified std value	5.00	4.85
	Analysed	5.26	4.82
	% Deviation	5.24	0.58

Support	Ligand	% Extracted	
Si-gel (60Å)	15-k-5		8.83
MCM-41	15-k-5		8.19
SBA-15	15-k-5		8.38
HMS	15-k-5		13.37
		Average %	9.69
Si-gel (60Å)	18-k-6		13.58
MCM-41	18-k-6		6.19
SBA-15	18-k-6		9.94
HMS	18-k-6		3.43
		Average %	8.28
Si-gel (60Å)	Glymo + 15-k-5		8.49
MCM-41	Glymo + 15-k-5		4.91
SBA-15	Glymo + 15-k-5		7.07
HMS	Glymo + 15-k-5		8.13
		Average %	7.15
Si-gel (60Å)	Glymo + 18-k-6		7.16
MCM-41	Glymo + 18-k-6		8.90
SBA-15	Glymo + 18-k-6		2.49
HMS	Glymo + 18-k-6		3.09
		Average %	5.41
Si-gel (60Å)	Glymo + THTD		2.76
MCM-41	Glymo + THTD		5.54
SBA-15	Glymo + THTD		5.20
HMS	Glymo + THTD		4.96
		Average %	4.62
Si-gel (60Å)	Glymo + THTUD		14.38
MCM-41	Glymo + THTUD		7.26
SBA-15	Glymo + THTUD		4.17
HMS	Glymo + THTUD		4.90
		Average %	7.68

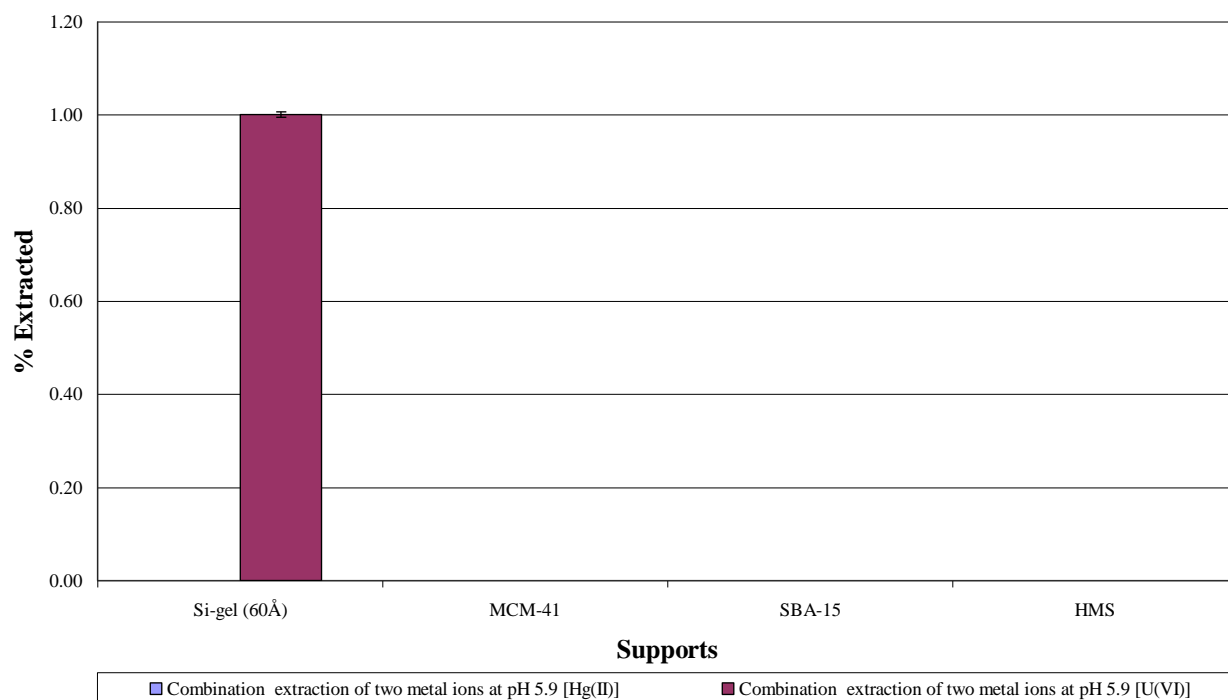
Competition Between 2 Metal Ions Extracted by 15-c-5 Immobilized on Different Supports



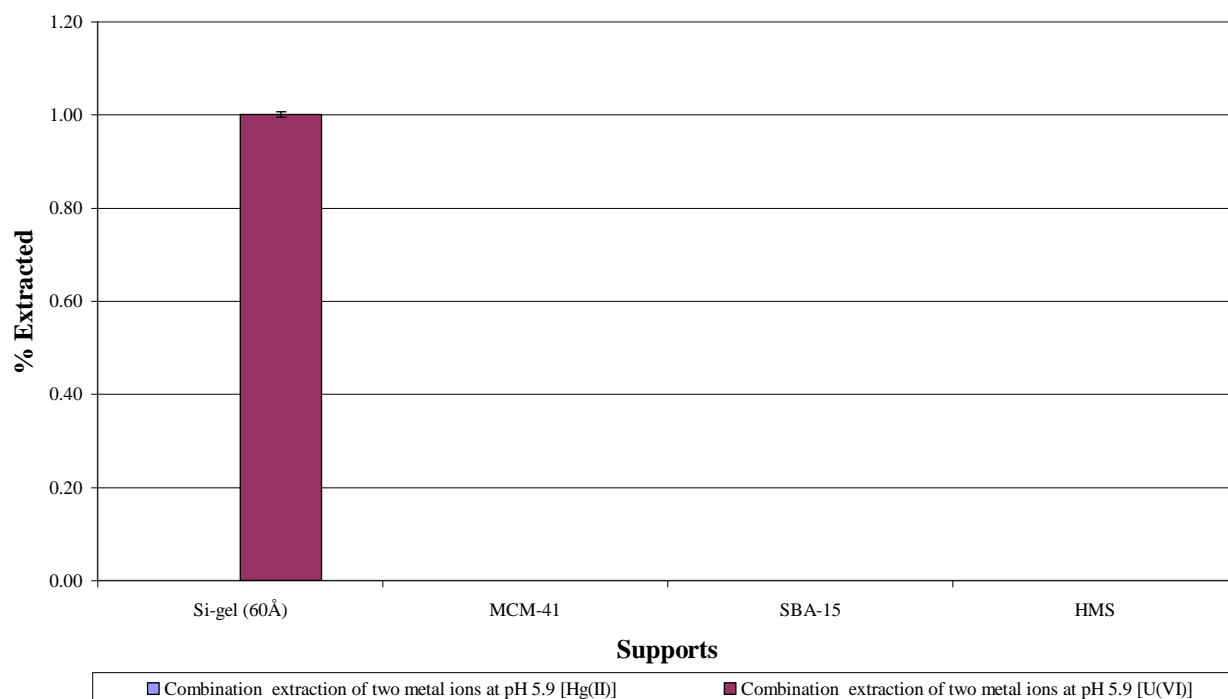
Competition Between 2 Metal Ions Extracted by 18-c-6 Immobilized on Different Supports



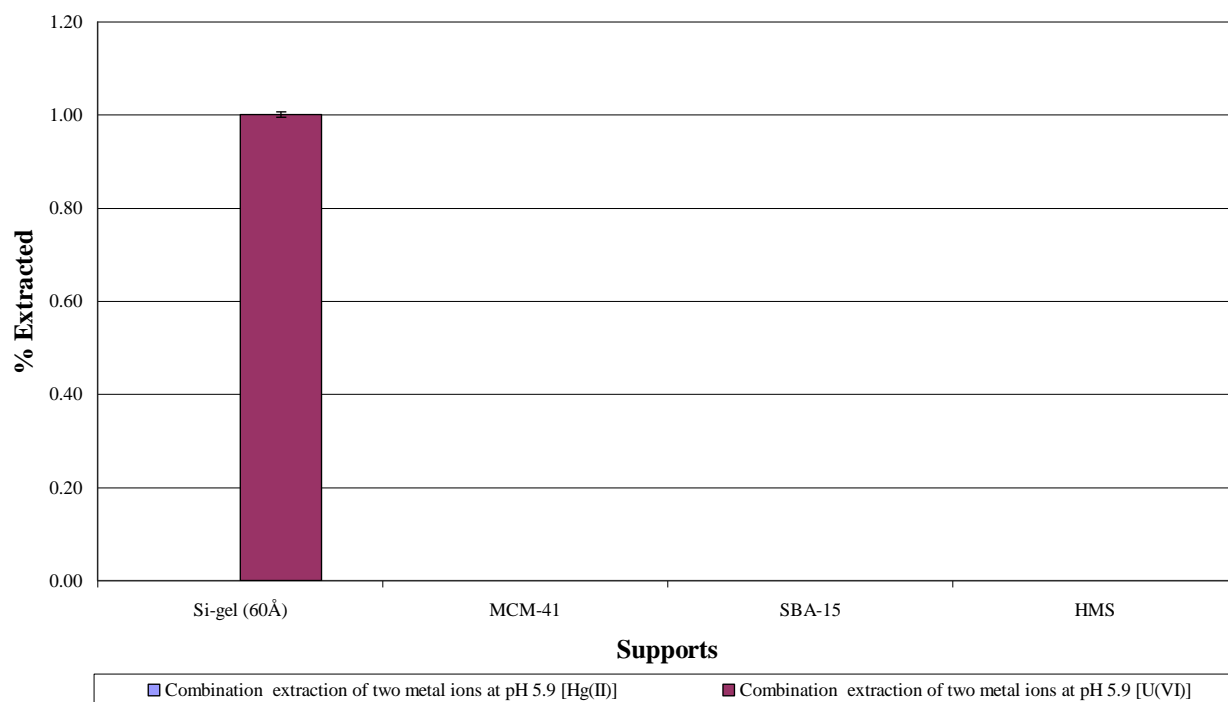
Competition Between 2 Metal Ions Extracted by 15-c-5 Immobilized by Glymo on Different Supports



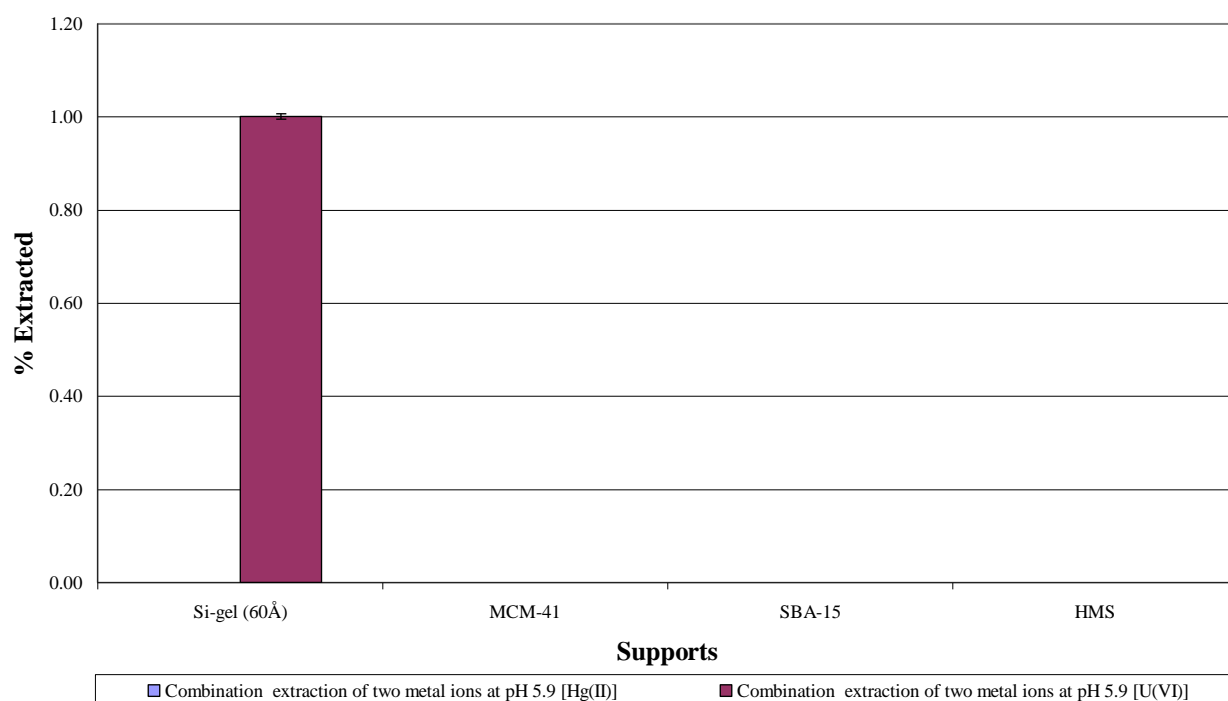
Competition Between 2 Metal Ions Extracted by 18-c-6 Immobilized by Glymo on Different Supports



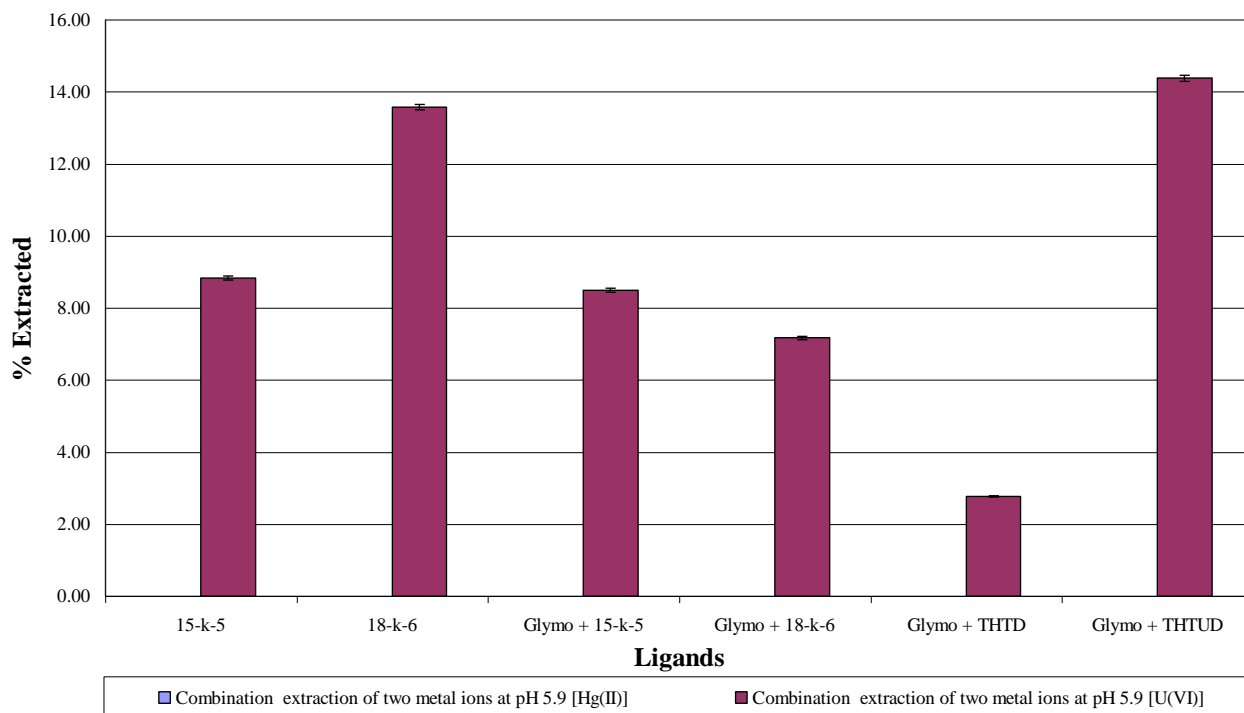
Competition Between 2 Metal Ions Extracted by THTD Immobilized on Different Supports



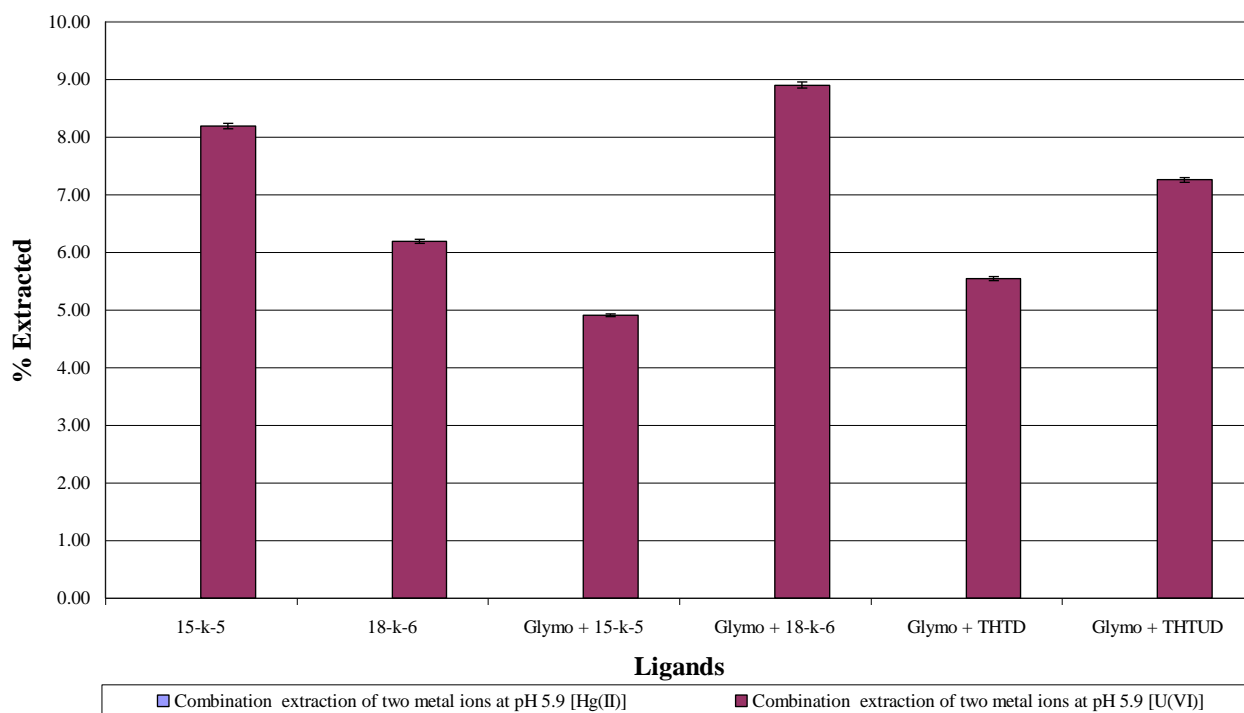
Competition Between 2 Metal Ions Extracted by THTUD Immobilized on Different Supports



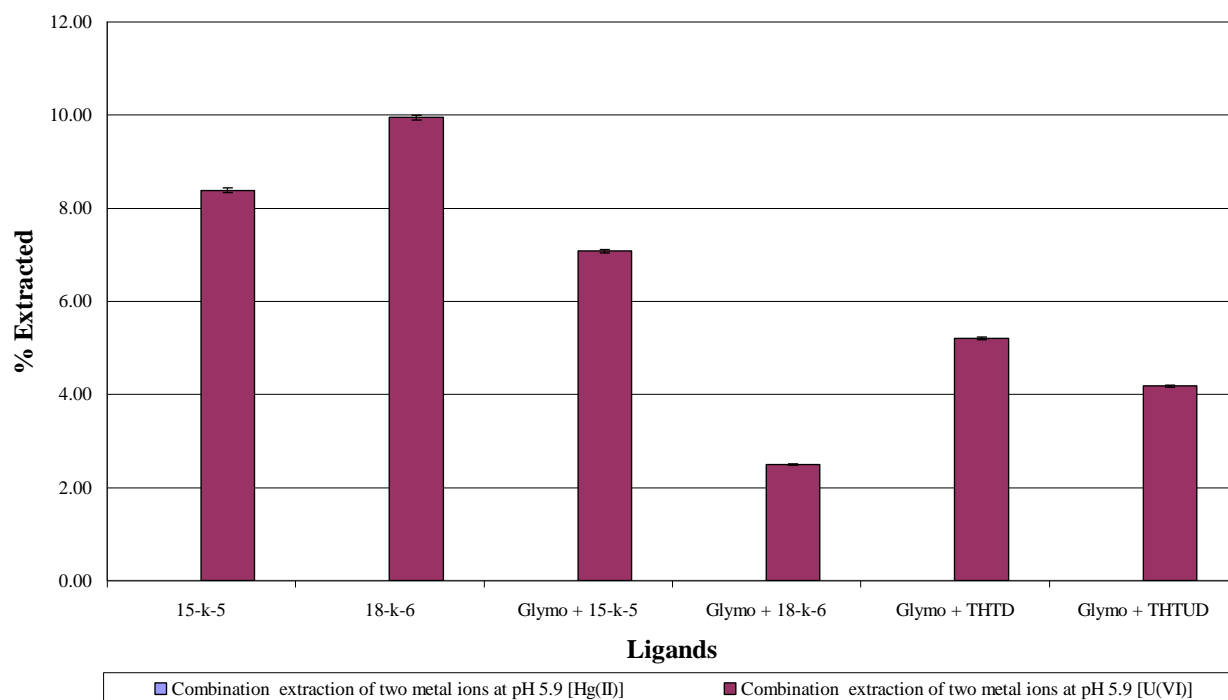
Competition Between 2 Metal Ions Extracted by Different Ligands Immobilized on Si gel (60 Å)



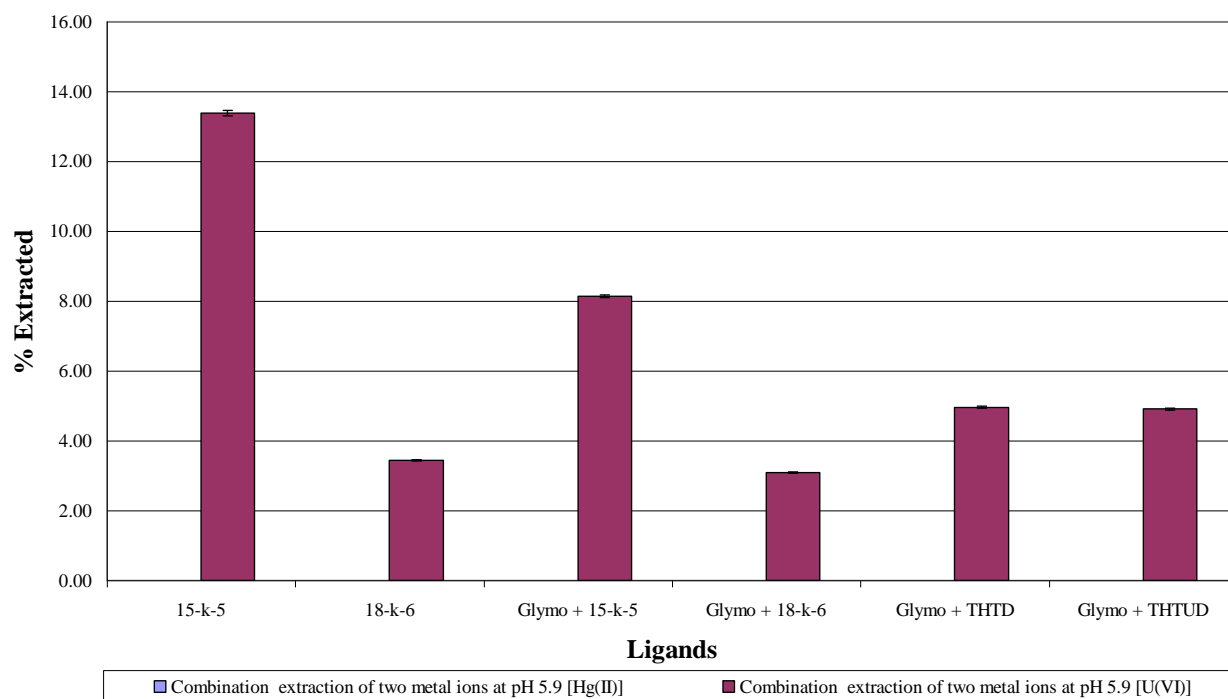
Competition Between 2 Metal Ions Extracted by Different Ligands Immobilized on MCM-41



Comptions Between 2 Metal Ions Extracted by Different Ligands Immobilized on SBA-15



Competition Between 2 Metal Ions Extracted by Different Ligands Immobilized on HMS



Competition extraction of 4 different metal ions at pH 4.5 [As(V)]

		As	Cd	Cr	Sr
Accuracy	Certified std value	2.47	0.97	0.97	0.97
	Analysed	2.25	0.96	0.97	1.00
	% Deviation	8.91	1.16	0.27	3.04

Standard Solution (ppm)

				As		
		Support	Ligand		Extracted ppm	% Extracted
As	66.43	Si-gel (60Å)	15-k-5	66.35	0.08	0.12
			18-k-6	66.34	0.09	0.14
			Glymo + 15-k-5	64.56	1.87	2.81
			Glymo + 18-k-6	64.33	2.10	3.17
			Glymo + THTD	65.30	1.13	1.69
			Glymo + THTUD	63.76	2.67	4.01
			Average %		1.99	
		MCM-41	15-k-5	65.66	0.77	1.16
			18-k-6	66.38	0.05	0.07
			Glymo + 15-k-5	66.82	0.00	0.00
			Glymo + 18-k-6	66.75	0.00	0.00
			Glymo + THTD	65.83	0.60	0.90
			Glymo + THTUD	65.30	1.13	1.70
			Average %		0.64	
		SBA-15	15-k-5	67.24	0.00	0.00
			18-k-6	67.92	0.00	0.00
			Glymo + 15-k-5	67.09	0.00	0.00
			Glymo + 18-k-6	65.87	0.56	0.84
			Glymo + THTD	61.30	5.13	7.73
			Glymo + THTUD	67.15	0.00	0.00
			Average %		1.43	
		HMS	15-k-5	66.87	0.00	0.00
			18-k-6	65.93	0.50	0.76
			Glymo + 15-k-5	63.80	2.63	3.97
			Glymo + 18-k-6	65.25	1.18	1.77
			Glymo + THTD	65.30	1.13	1.70
			Glymo + THTUD	66.54	0.00	0.00
			Average %		1.37	

Competition extraction of 4 different metal ions at pH 4.5 [Cd(II)]

		As	Cd	Cr	Sr
Accuracy	Certified std value	2.47	0.97	0.97	0.97
	Analysed	2.25	0.96	0.97	1.00
	% Deviation	8.91	1.16	0.27	3.04

Standard Solution (ppm)

		Cd				
		Support	Ligand		Extracted ppm	Extracted %
Cd	96.46	Si-gel (60Å)	15-k-5	94.46	2.00	2.07
			18-k-6	97.10	0.00	0.00
			Glymo + 15-k-5	95.86	0.61	0.63
			Glymo + 18-k-6	93.81	2.65	2.75
			Glymo + THTD	96.14	0.32	0.33
			Glymo + THTUD	97.44	0.00	0.00
			Average %		0.96	
		MCM-41	15-k-5	97.06	0.00	0.00
			18-k-6	96.38	0.08	0.08
			Glymo + 15-k-5	98.67	0.00	0.00
			Glymo + 18-k-6	96.27	0.19	0.20
			Glymo + THTD	95.50	0.96	1.00
			Glymo + THTUD	95.30	1.16	1.20
			Average %		0.41	
		SBA-15	15-k-5	96.30	0.16	0.16
			18-k-6	96.05	0.41	0.43
			Glymo + 15-k-5	95.74	0.72	0.75
			Glymo + 18-k-6	96.14	0.32	0.33
			Glymo + THTD	97.79	0.00	0.00
			Glymo + THTUD	100.05	0.00	0.00
			Average %		0.28	
		HMS	15-k-5	97.90	0.00	0.00
			18-k-6	96.81	0.00	0.00
			Glymo + 15-k-5	97.05	0.00	0.00
			Glymo + 18-k-6	98.00	0.00	0.00
			Glymo + THTD	97.06	0.00	0.00
			Glymo + THTUD	96.28	0.19	0.19
			Average %		0.03	0.03

Competition extraction of 4 different metal ions at pH 4.5 [Cr(VI)]

		As	Cd	Cr	Sr
Accuracy	Certified std value	2.47	0.97	0.97	0.97
	Analysed	2.25	0.96	0.97	1.00
	% Deviation	8.91	1.16	0.27	3.04

Standard Solution (ppm)				Cr	
Cr		Support	Ligand	Extracted ppm	Extracted %
51.22	Si-gel (60Å)		15-k-5	45.96	10.27
			18-k-6	46.93	8.38
			Glymo + 15-k-5	41.22	19.53
			Glymo + 18-k-6	38.99	23.89
			Glymo + THTD	37.15	27.47
			Glymo + THTUD	33.28	35.02
			Average %		20.76
	MCM-41		15-k-5	47.15	7.94
			18-k-6	47.50	7.26
			Glymo + 15-k-5	47.61	7.04
			Glymo + 18-k-6	45.30	11.56
			Glymo + THTD	44.20	13.72
			Glymo + THTUD	46.95	8.34
			Average %		9.31
	SBA-15		15-k-5	46.74	8.75
			18-k-6	46.37	9.46
			Glymo + 15-k-5	47.02	8.21
			Glymo + 18-k-6	46.81	8.61
			Glymo + THTD	27.91	45.52
			Glymo + THTUD	51.10	0.23
			Average %		13.46
	HMS		15-k-5	50.91	0.61
			18-k-6	51.55	0.00
			Glymo + 15-k-5	40.53	20.88
			Glymo + 18-k-6	34.71	32.23
			Glymo + THTD	45.39	11.39
			Glymo + THTUD	44.96	12.22
			Average %		12.89

Competition extraction of 4 different metal ions at pH 4.5 [Sr(II)]

		As	Cd	Cr	Sr
Accuracy	Certified std value	2.47	0.97	0.97	0.97
	Analysed	2.25	0.96	0.97	1.00
	% Deviation	8.91	1.16	0.27	3.04

Standard Solution (ppm)

		Sr				
		Support	Ligand		Extracted ppm	Extracted %
Sr	75.40	Si-gel (60Å)	15-k-5	79.14	0.00	0.00
			18-k-6	79.92	0.00	0.00
			Glymo + 15-k-5	78.16	0.00	0.00
			Glymo + 18-k-6	79.59	0.00	0.00
			Glymo + THTD	79.70	0.00	0.00
			Glymo + THTUD	79.04	0.00	0.00
			Average %			0.00
		MCM-41	15-k-5	80.15	0.00	0.00
			18-k-6	80.07	0.00	0.00
			Glymo + 15-k-5	82.17	0.00	0.00
			Glymo + 18-k-6	79.42	0.00	0.00
			Glymo + THTD	79.00	0.00	0.00
			Glymo + THTUD	79.76	0.00	0.00
			Average %			0.00
		SBA-15	15-k-5	79.76	0.00	0.00
			18-k-6	80.60	0.00	0.00
			Glymo + 15-k-5	80.41	0.00	0.00
			Glymo + 18-k-6	79.63	0.00	0.00
			Glymo + THTD	78.81	0.00	0.00
			Glymo + THTUD	80.89	0.00	0.00
			Average %			0.00
		HMS	15-k-5	80.78	0.00	0.00
			18-k-6	78.48	0.00	0.00
			Glymo + 15-k-5	78.17	0.00	0.00
			Glymo + 18-k-6	78.88	0.00	0.00
			Glymo + THTD	79.31	0.00	0.00
			Glymo + THTUD	78.75	0.00	0.00
			Average %			0.00

Competition extraction of 4 different metal ions at pH 5.9 [As(V)]

		As	Cd	Cr	Sr
Accuracy	Certified std value	24.68	24.68	24.68	9.87
	Analysed	24.99	25.23	24.81	10.24
	% Deviation	1.27	2.23	0.53	3.73

Standard Solution (ppb)		As				
		Support	Ligand		Extracted ppb	% Extracted
As	649.31	Si-gel (60Å)	15-k-5	611.18	38.13	5.87
			18-k-6	665.81	0.00	0.00
			Glymo + 15-k-5	647.34	1.97	0.30
			Glymo + 18-k-6	651.36	0.00	0.00
			Glymo + THTD	651.87	0.00	0.00
			Glymo + THTUD	650.60	0.00	0.00
			Average %			1.03
		MCM-41	15-k-5	662.62	0.00	0.00
			18-k-6	663.51	0.00	0.00
			Glymo + 15-k-5	659.91	0.00	0.00
			Glymo + 18-k-6	641.59	7.71	1.19
			Glymo + THTD	660.42	0.00	0.00
			Glymo + THTUD	799.54	0.00	0.00
			Average %			0.20
		SBA-15	15-k-5	646.91	2.39	0.37
			18-k-6	686.07	0.00	0.00
			Glymo + 15-k-5	662.01	0.00	0.00
			Glymo + 18-k-6	655.44	0.00	0.00
			Glymo + THTD	634.73	14.57	2.24
			Glymo + THTUD	662.24	0.00	0.00
			Average %			0.44
		HMS	15-k-5	646.02	3.28	0.51
			18-k-6	639.37	9.94	1.53
			Glymo + 15-k-5	652.56	0.00	0.00
			Glymo + 18-k-6	626.03	23.28	3.59
			Glymo + THTD	628.24	21.06	3.24
			Glymo + THTUD	629.85	19.46	3.00
			Average %			1.98

Competition extraction of 4 different metal ions at pH 5.9 [Cd(II)]

		As	Cd	Cr	Sr
Accuracy	Certified std value	24.68	24.68	24.68	9.87
	Analysed	24.99	25.23	24.81	10.24
	% Deviation	1.27	2.23	0.53	3.73

Standard Solution (ppb)		Cd				
		Support	Ligand	Extracted ppb	Extracted %	
Cd	1056.14	Si-gel (60Å)	15-k-5	1066.55	0.00	0.00
			18-k-6	1150.25	0.00	0.00
			Glymo + 15-k-5	1049.80	6.34	0.60
			Glymo + 18-k-6	1060.93	0.00	0.00
			Glymo + THTD	1017.33	38.81	3.67
			Glymo + THTUD	1039.09	17.04	1.61
			Average %			0.98
		MCM-41	15-k-5	1110.25	0.00	0.00
			18-k-6	1054.66	1.48	0.14
			Glymo + 15-k-5	1045.07	11.07	1.05
			Glymo + 18-k-6	1040.65	15.49	1.47
			Glymo + THTD	1039.27	16.87	1.60
			Glymo + THTUD	1041.43	14.71	1.39
			Average %			0.94
		SBA-15	15-k-5	1049.42	6.72	0.64
			18-k-6	872.40	183.73	17.40
			Glymo + 15-k-5	1109.30	0.00	0.00
			Glymo + 18-k-6	1043.54	12.60	1.19
			Glymo + THTD	996.21	59.93	5.67
			Glymo + THTUD	1042.79	13.35	1.26
			Average %			4.36
		HMS	15-k-5	1027.44	28.70	2.72
			18-k-6	1052.96	3.18	0.30
			Glymo + 15-k-5	1026.43	29.71	2.81
			Glymo + 18-k-6	1023.10	33.04	3.13
			Glymo + THTD	1004.43	51.70	4.90
			Glymo + THTUD	1034.91	21.23	2.01
			Average %			2.64

Competition extraction of 4 different metal ions at pH 5.9 [Cr(VI)]

		As	Cd	Cr	Sr
Accuracy	Certified std value	24.68	24.68	24.68	9.87
	Analysed	24.99	25.23	24.81	10.24
	% Deviation	1.27	2.23	0.53	3.73

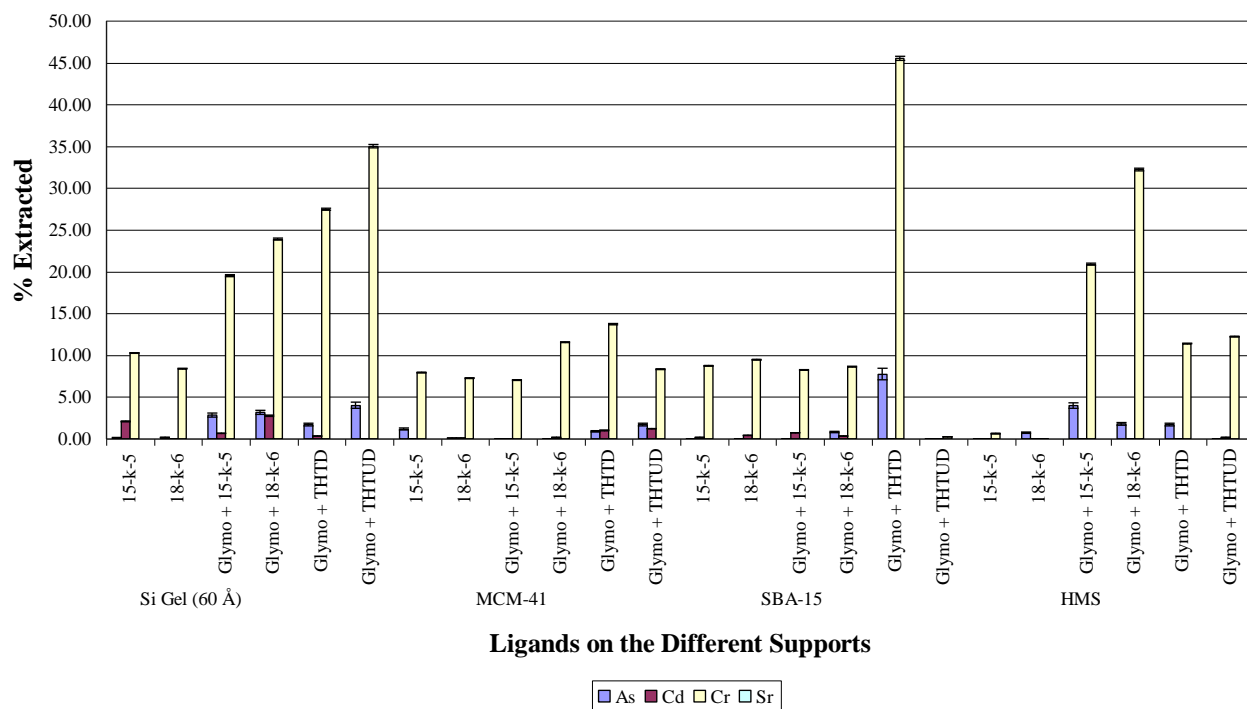
Standard Solution (ppb)		Cr				
		Support	Ligand		Extracted ppb	Extracted %
Cr	485.57	Si-gel (60Å)	15-k-5	453.28	32.29	6.65
			18-k-6	483.37	2.20	0.45
			Glymo + 15-k-5	466.55	19.02	3.92
			Glymo + 18-k-6	467.48	18.09	3.73
			Glymo + THTD	350.86	134.71	27.74
			Glymo + THTUD	420.72	64.85	13.36
					Average %	9.31
		MCM-41	15-k-5	499.62	0.00	0.00
			18-k-6	509.19	0.00	0.00
			Glymo + 15-k-5	494.14	0.00	0.00
			Glymo + 18-k-6	470.30	15.27	3.15
			Glymo + THTD	475.11	10.46	2.15
			Glymo + THTUD	576.15	0.00	0.00
					Average %	0.88
		SBA-15	15-k-5	476.49	9.08	1.87
			18-k-6	513.90	0.00	0.00
			Glymo + 15-k-5	504.52	0.00	0.00
			Glymo + 18-k-6	490.05	0.00	0.00
			Glymo + THTD	419.09	66.48	13.69
			Glymo + THTUD	475.74	9.84	2.03
					Average %	2.93
		HMS	15-k-5	474.14	11.43	2.35
			18-k-6	377.94	107.63	22.17
			Glymo + 15-k-5	476.52	9.05	1.86
			Glymo + 18-k-6	371.06	114.51	23.58
			Glymo + THTD	364.58	120.99	24.92
			Glymo + THTUD	414.92	70.65	14.55
					Average %	14.91

Competition extraction of 4 different metal ions at pH 5.9 [Sr(II)]

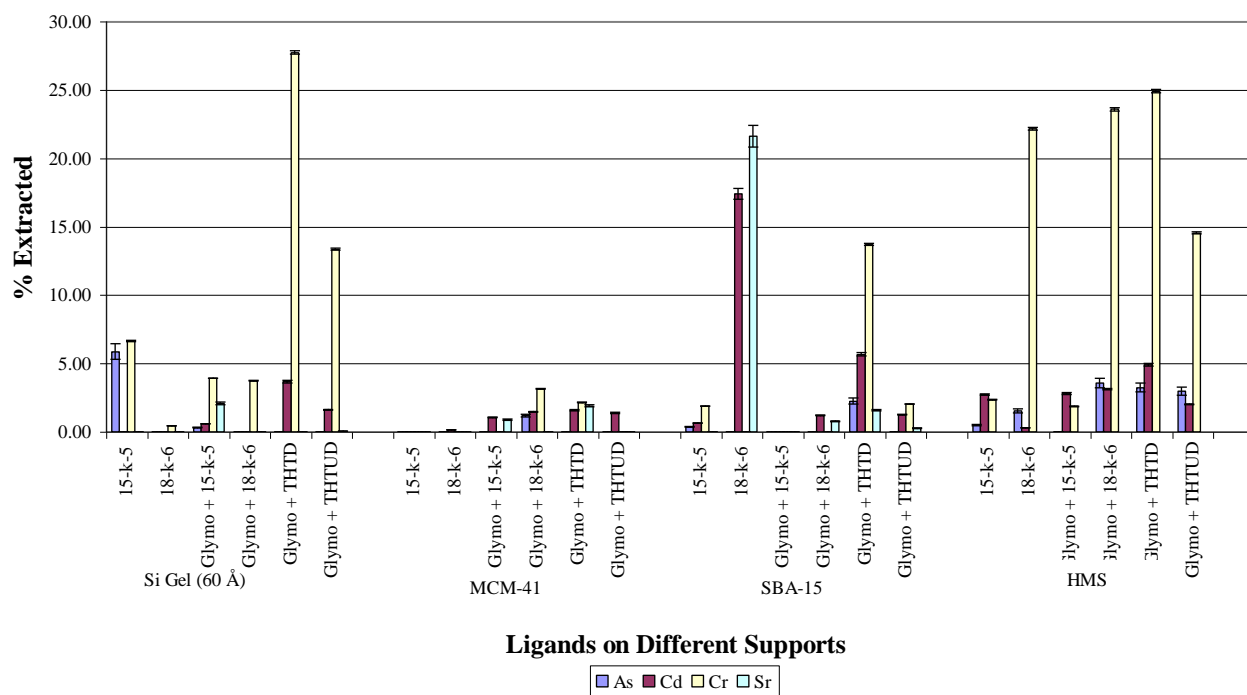
		As	Cd	Cr	Sr
Accuracy	Certified std value	24.68	24.68	24.68	9.87
	Analysed	24.99	25.23	24.81	10.24
	% Deviation	1.27	2.23	0.53	3.73

Standard Solution (ppb)				Sr		
Sr		Support	Ligand	Extracted ppb	Extracted %	
843.61		Si-gel (60Å)	15-k-5	886.94	0.00	0.00
			18-k-6	931.08	0.00	0.00
			Glymo + 15-k-5	826.03	17.58	2.08
			Glymo + 18-k-6	854.47	0.00	0.00
			Glymo + THTD	853.03	0.00	0.00
			Glymo + THTUD	843.35	0.26	0.03
		MCM-41	Average %		0.35	
			15-k-5	910.76	0.00	0.00
			18-k-6	853.18	0.00	0.00
			Glymo + 15-k-5	836.08	7.53	0.89
			Glymo + 18-k-6	845.55	0.00	0.00
			Glymo + THTD	827.65	15.97	1.89
			Glymo + THTUD	847.61	0.00	0.00
		SBA-15	Average %		0.46	
			15-k-5	844.08	0.00	0.00
			18-k-6	661.25	182.37	21.62
			Glymo + 15-k-5	909.08	0.00	0.00
			Glymo + 18-k-6	837.12	6.50	0.77
			Glymo + THTD	830.19	13.42	1.59
			Glymo + THTUD	841.33	2.28	0.27
		HMS	Average %		4.04	
			15-k-5	840.60	3.01	0.36
			18-k-6	854.36	0.00	0.00
			Glymo + 15-k-5	856.24	0.00	0.00
			Glymo + 18-k-6	834.38	9.23	1.09
			Glymo + THTD	832.62	10.99	1.30
			Glymo + THTUD	839.28	4.34	0.51
			Average %		0.54	

Competition Between 4 Metal Ions with Varions Ligands Immobilized on Different Supports (pH 4.5)



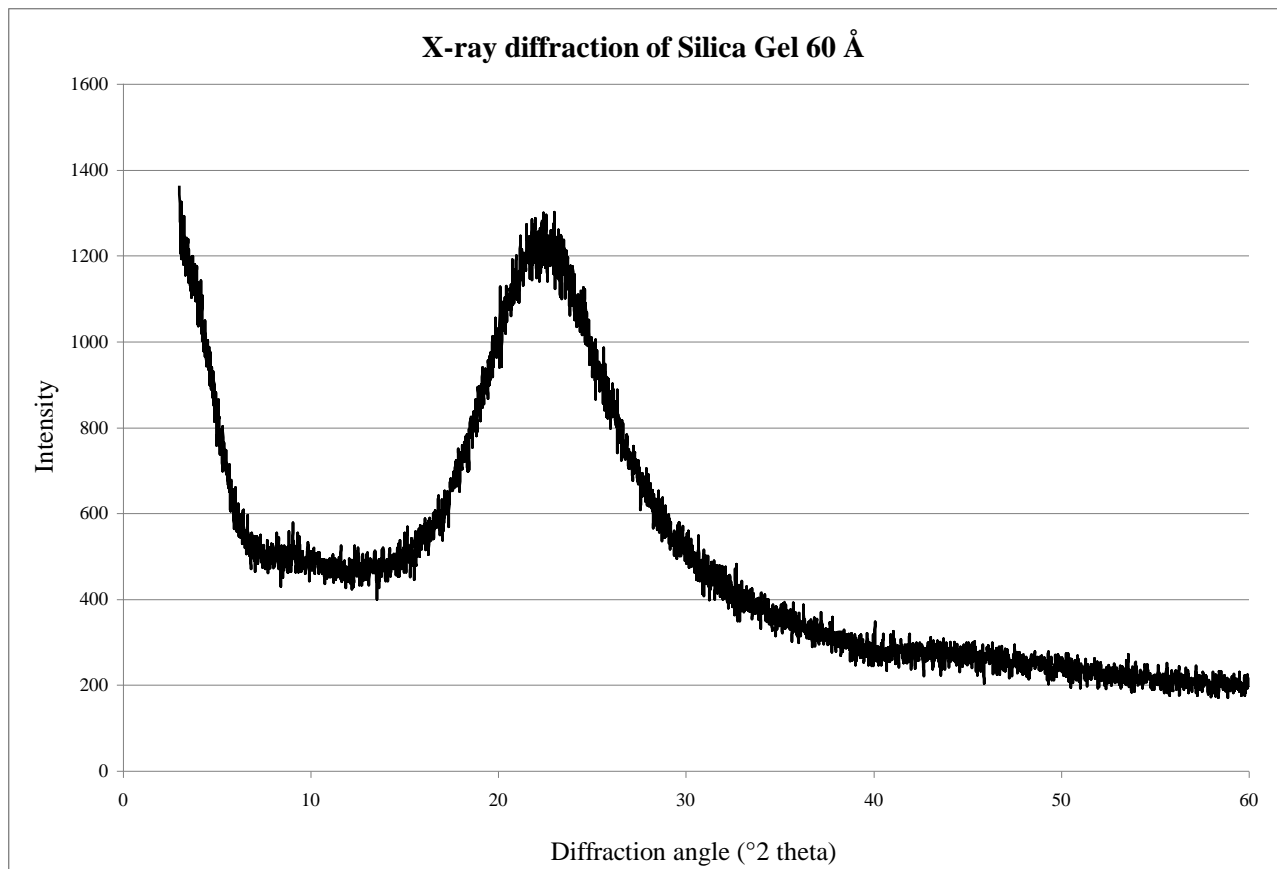
Competition between 4 Metal Ions Extracted by Various Ligands Immobilized on Different Supports (pH 5.9)



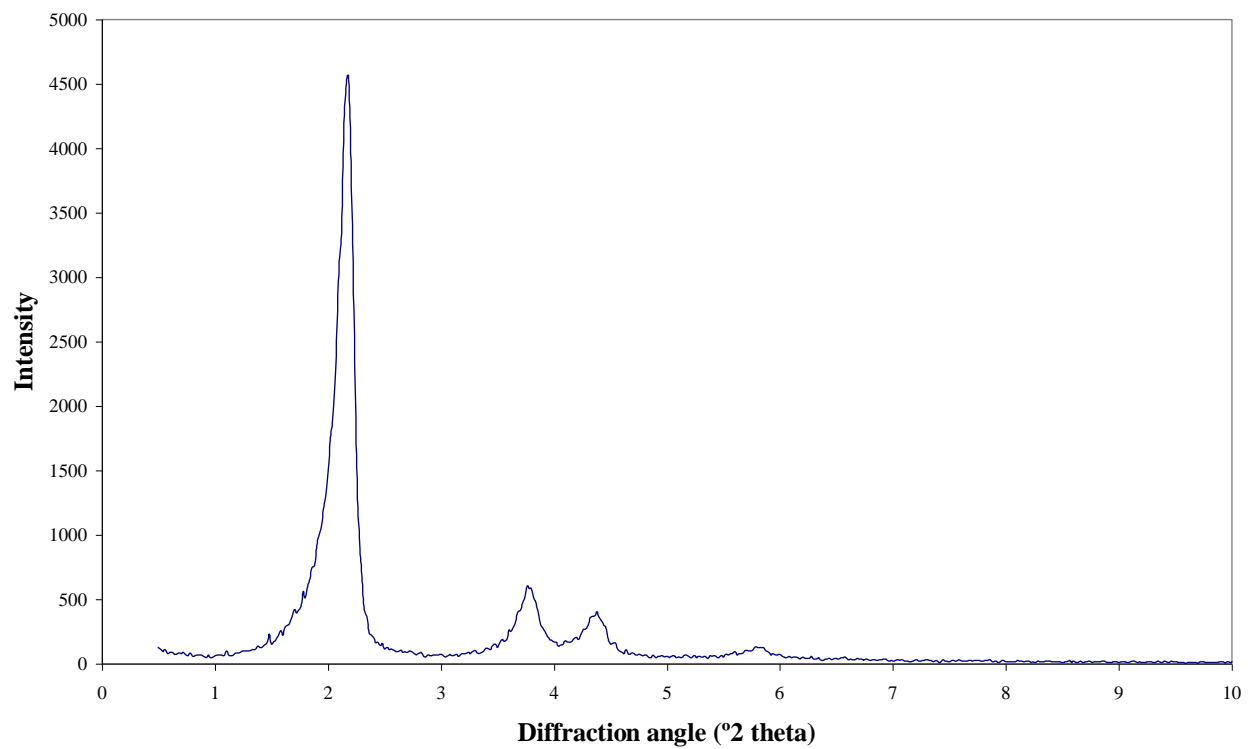
ADDENDUM D

Low Angle X-Ray Diffraction of the Various Silica Support

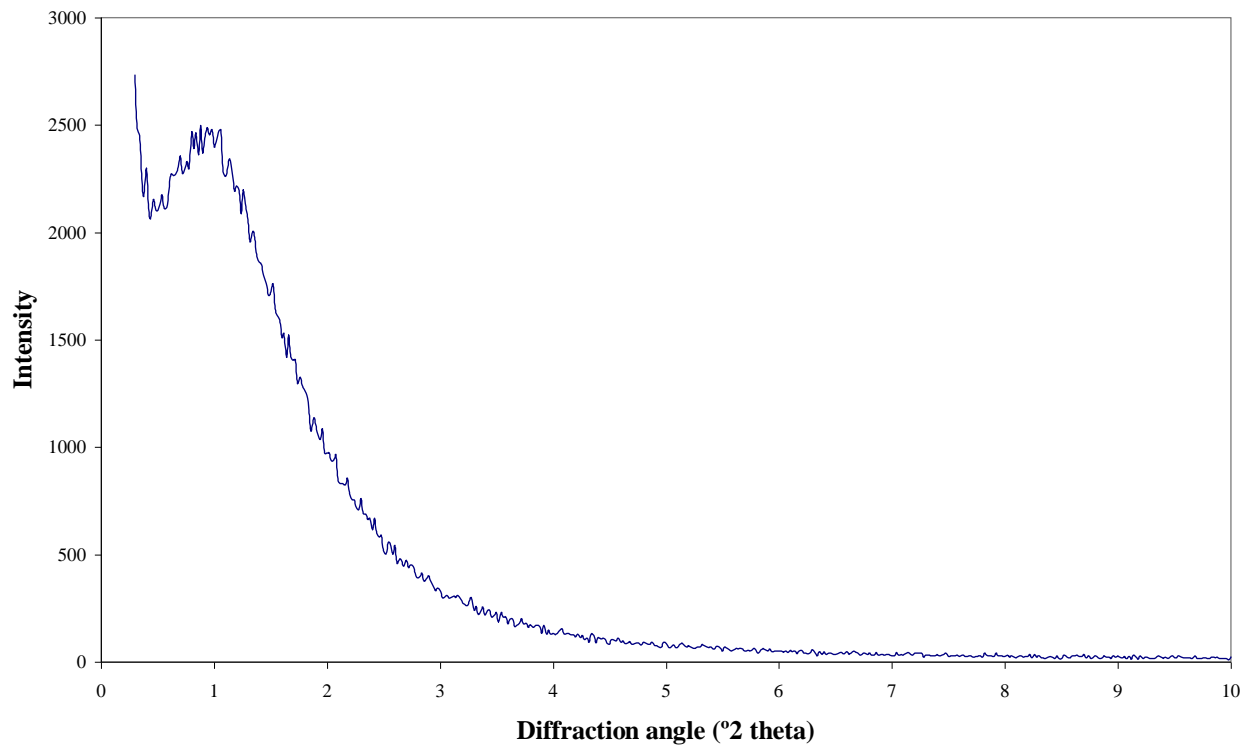
1. Si gel (60 Å).....	XCI
2. MCM-41.....	XCI
3. SBA-15.....	XCII
4. HMS	XCII



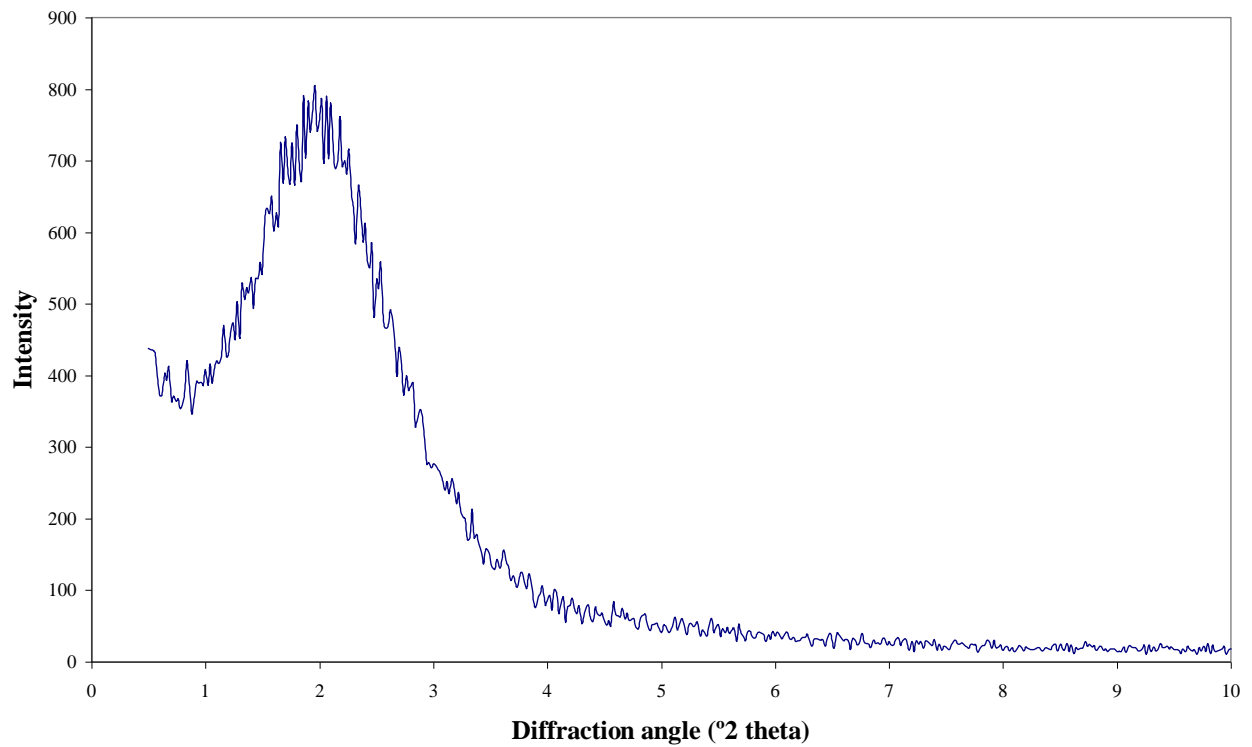
MCM-41



SBA-15



HMS



ADDENDUM E

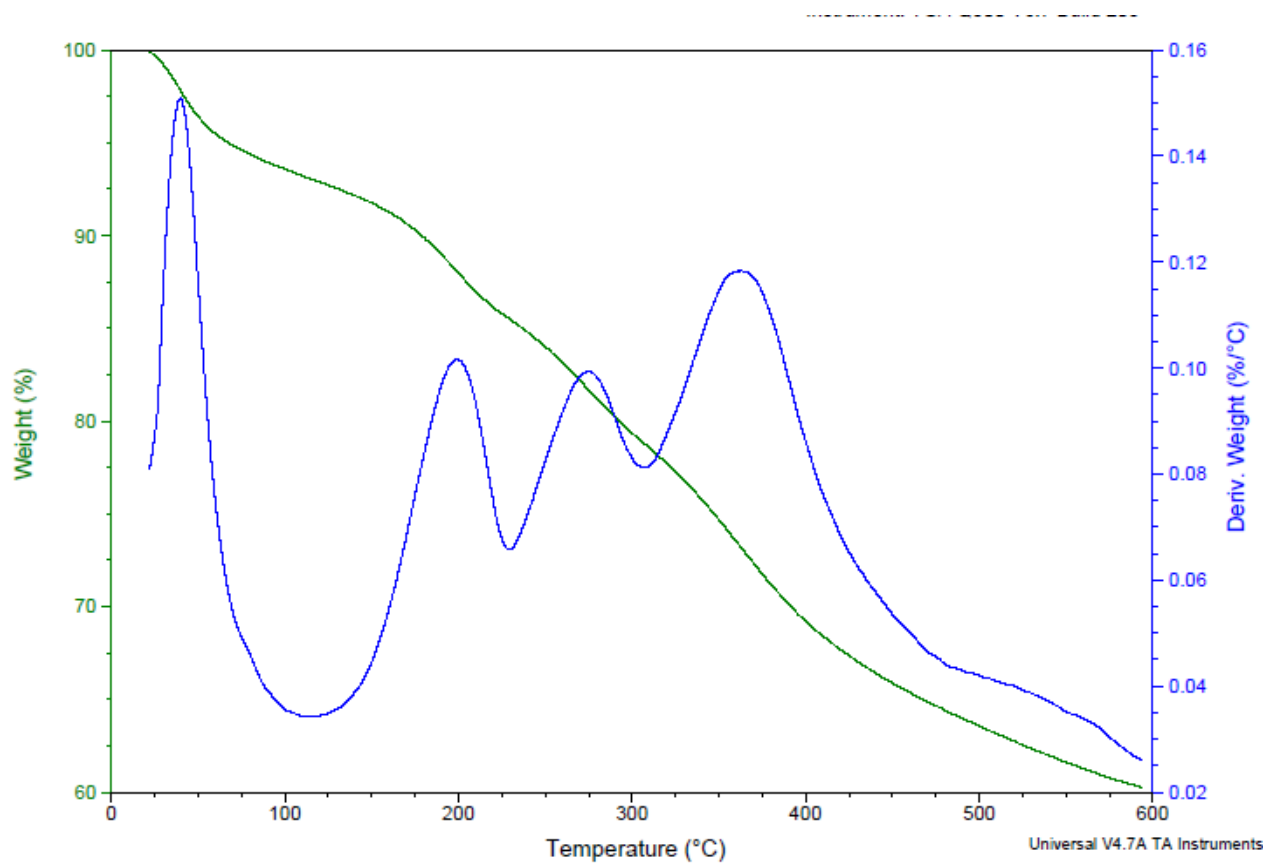
BET Analysis

Electronically available

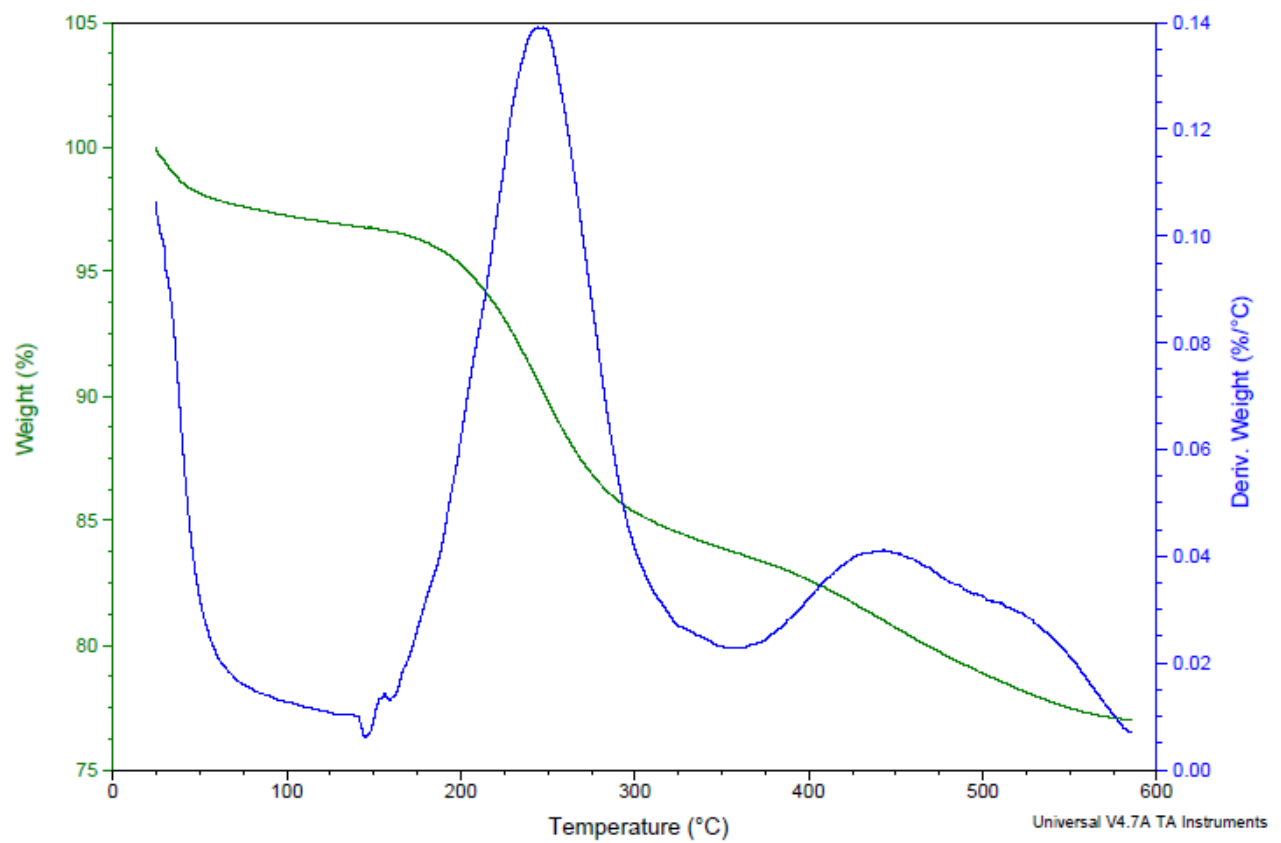
ADDENDUM F

TGA Analysis

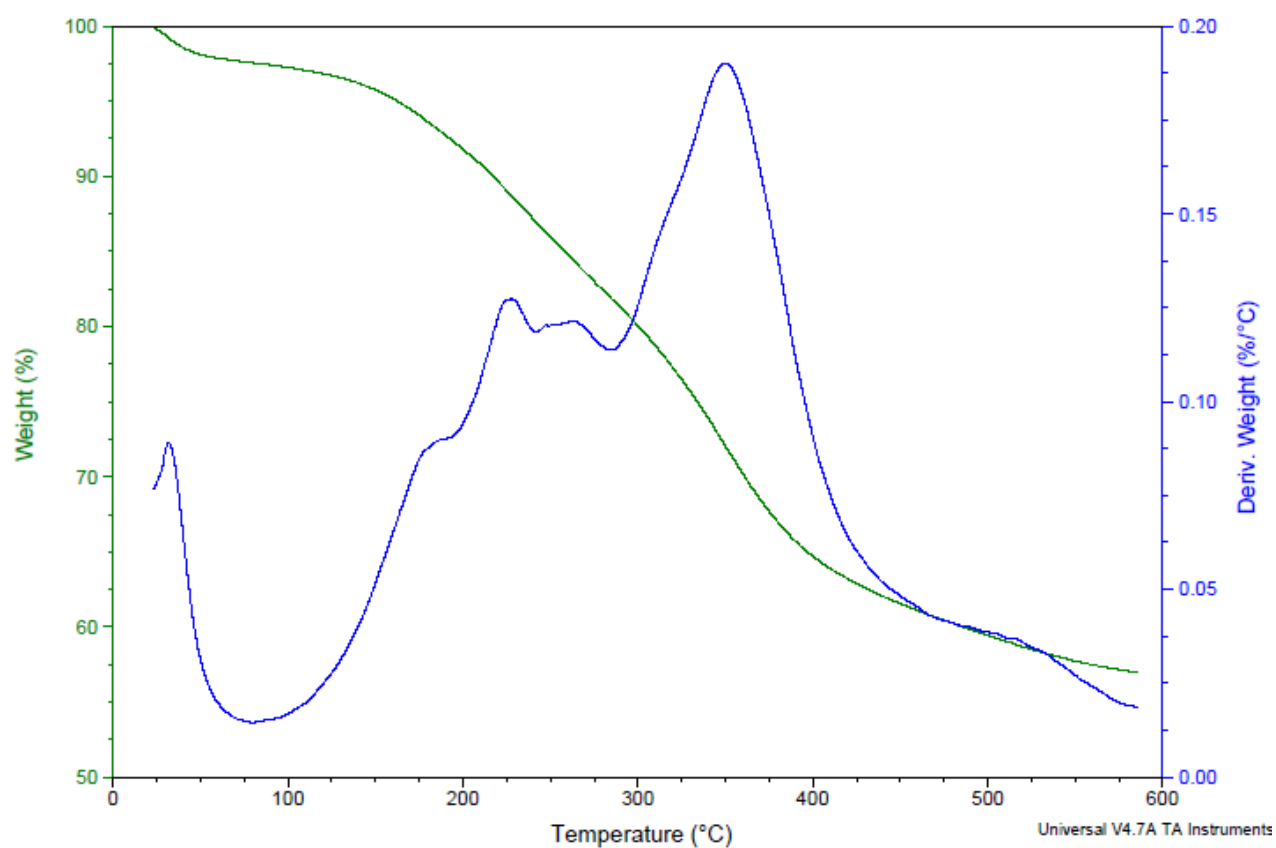
1. 15-c-5 immobilized directly on the silica supportXCIV
2. 18-c-6 immobilized directly on the silica supportXCIV
3. 15-c-5 immobilized with the glymo spacer on the silica support XCV
4. 18-c-6 immobilized with the glymo spacer on the silica support XCV
5. THTD immobilized with the glymo spacer on the silica supportXCVI
6. THTUD immobilized with the glymo spacer on the silica supportXCVI



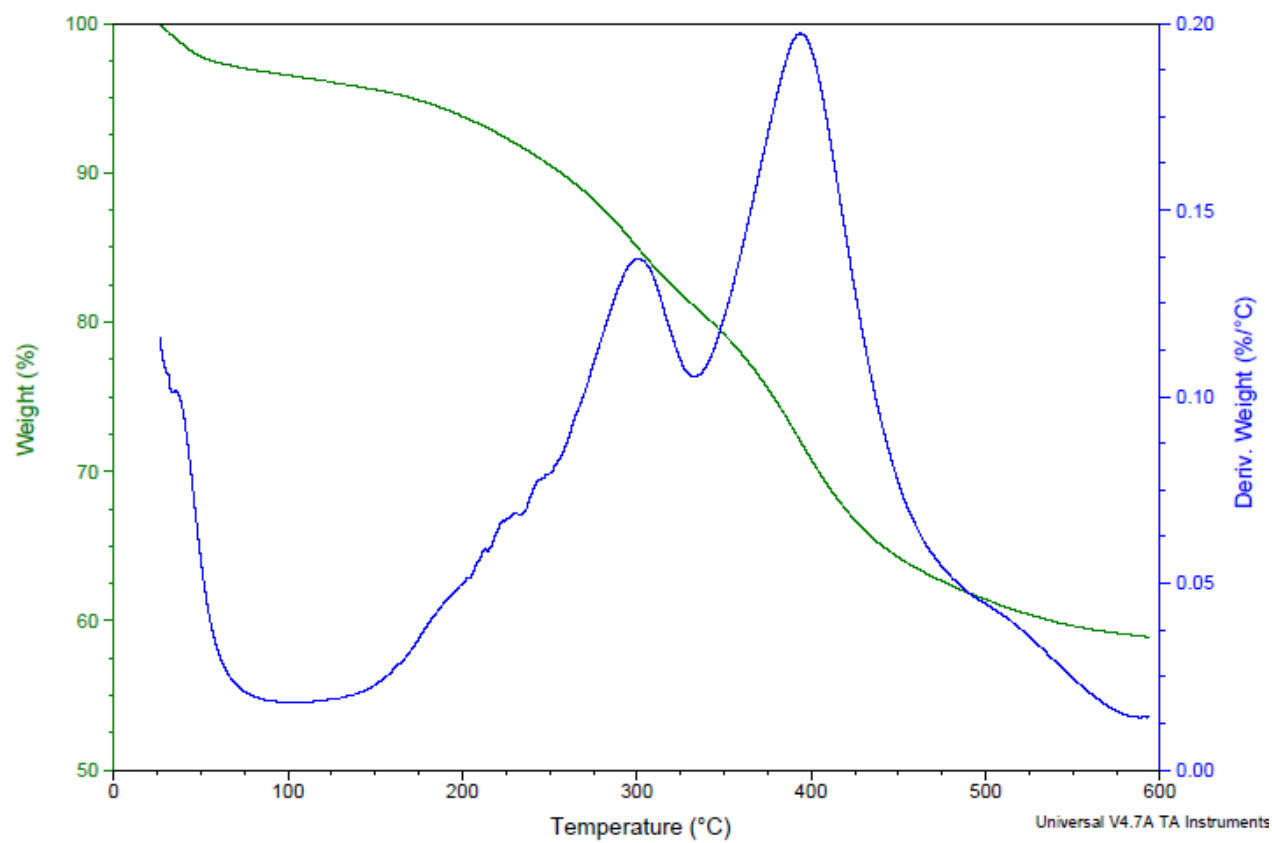
15-c-5 immobilized directly on the silica support



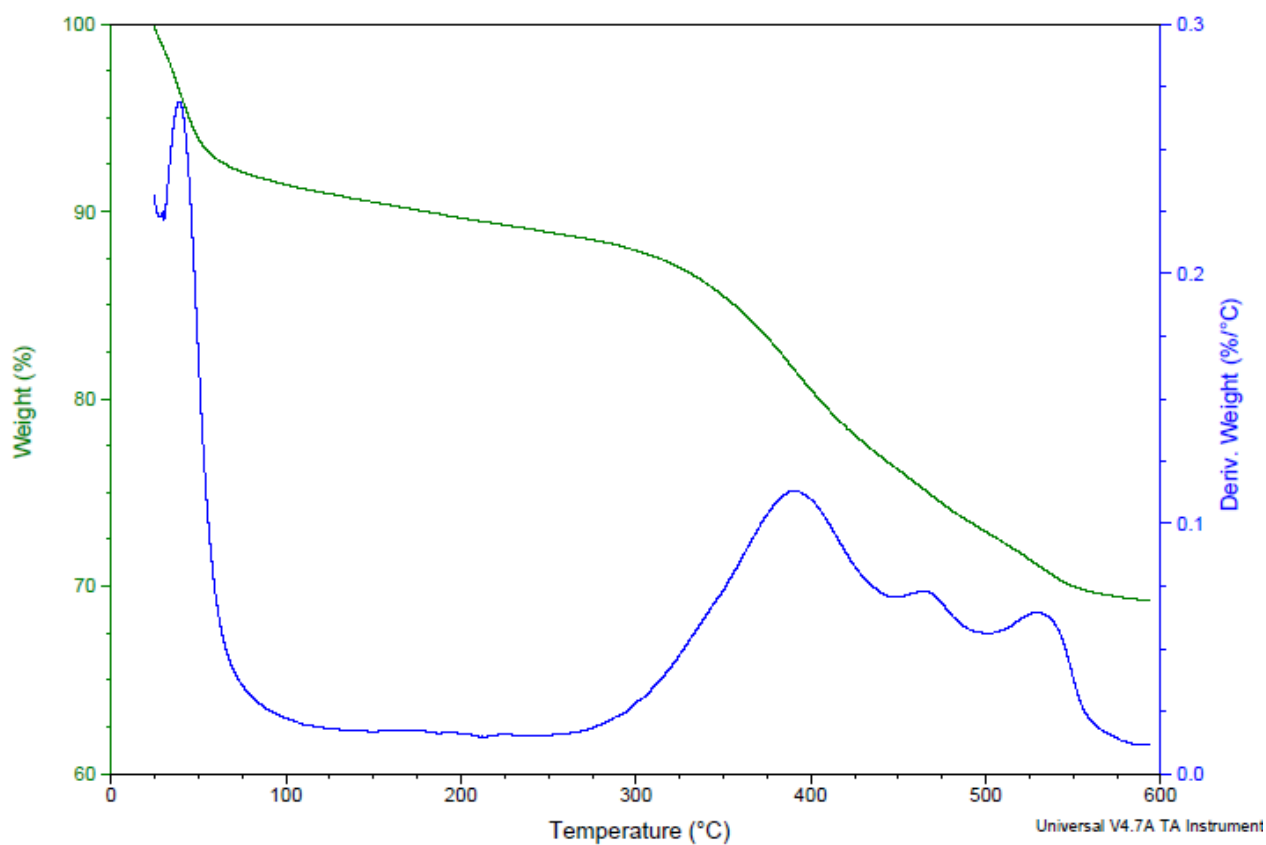
18-c-6 immobilized directly on the silica support



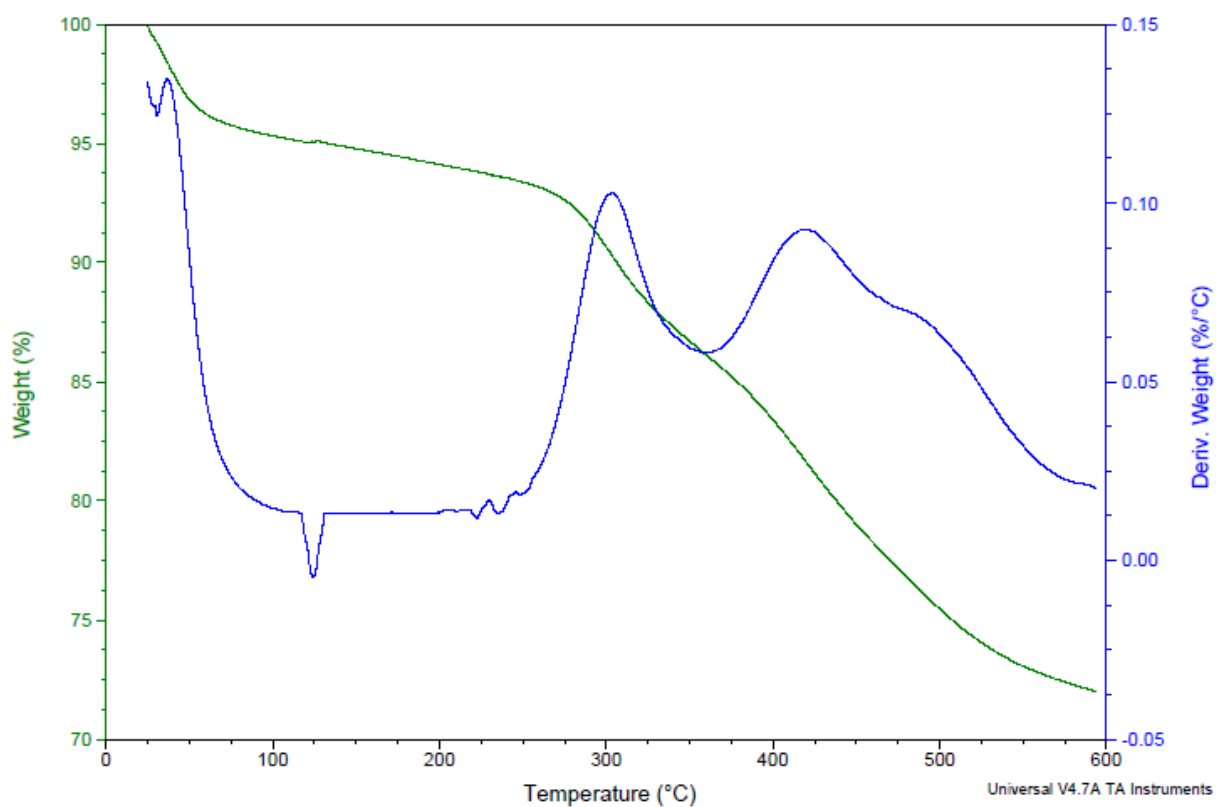
15-c-5 immobilized with the glymo spacer on the silica support



18-c-6 immobilized with the glymo spacer on the silica support



THTD immobilized with the glymo spacer on the silica support



THTUD immobilized with the glymo spacer on the silica support